2016

# Establishing Chemical Mechanisms And Estimating Phase State Of Secondary Organic Aerosol From Atmospherically Relevant Organic Precursors

Shashank Jain
*University of Vermont*

Follow this and additional works at: http://scholarworks.uvm.edu/graddis
Part of the Analytical Chemistry Commons

ESTABLISHING CHEMICAL MECHANISMS AND ESTIMATING PHASE
STATE OF SECONDARY ORGANIC AEROSOL FROM
ATMOSPHERICALLY RELEVANT ORGANIC PRECURSORS


A Dissertation Presented


by

Shashank Jain

to

The Faculty of the Graduate College

of

The University of Vermont

In Partial Fulfillment of the Requirements
for the Degree of Doctor of Philosophy
Specializing in Chemistry

October, 2016


Defense Date:  June 9th, 2016
Dissertation Examination Committee:

Giuseppe A. Petrucci, Ph.D., Advisor
Britt Holmen Ph.D., Chairperson
Matthias Brewer, Ph.D.
Joel Goldberg, Ph.D.
Cynthia J. Forehand, Ph.D., Dean of the Graduate College

# ABSTRACT

Organic aerosol (OA) is a ubiquitous component of atmospheric particulate that influences both human health and global climate. A large fraction of OA is secondary in nature (SOA), being produced by oxidation of volatile organic compounds (VOCs) emitted by biogenic and anthropogenic sources. Despite the integral role of SOA in atmospheric processes, there remains a limited scientific understanding of the chemical and physical changes induced in SOA as it ages in the atmosphere. This thesis describes work done to increase the knowledge of processes and properties of atmospherically relevant SOA.

In the work presented in this thesis, I have worked on improving an existing innovative, soft ionization aerosol mass spectrometer and utilized it to establish chemical mechanisms for oxidation of atmospherically relevant organic precursors (i.e., Green Leaf Volatiles). I discovered that SOA formation from *cis*-3-hexen-1-ol is dominated by oligomer and higher molecular weight products, whereas the acetate functionality in *cis*-3-hexenylacetate inhibited oligomer formation, resulting in SOA that is dominated by low molecular weight products.

One of the most important factors contributing to uncertainties in our estimations of SOA mass in the atmosphere, remains our basic assumption that atmospheric SOA is liquid-like, which we have found to be untrue. Hence, I developed a methodology to estimate the phase state of SOA and identified new parameters that can have significant influence on the phase state of atmospheric aerosol. This simplified method eliminates the need for a Scanning Mobility Particle Sizer (SMPS) and directly measures Bounce Factor (BF) of polydisperse SOA using only one multi-stage cascade Electrostatic Low Pressure Impactor (ELPI). The novel method allows for the real time determination of SOA phase state, permitting studies of the relationship between SOA phase, oxidative formation and chemical aging in the atmosphere. I demonstrated that SOA mass loading ($C_{SOA}$) influences the phase state significantly. Results show that under nominally identical conditions, the maximum BF decreases by approximately 30% at higher $C_{SOA}$ and suggests that extrapolation of experiments not conducted at atmospherically relevant SOA levels to simulate the chemical properties may not yield results that are relevant to our natural environment.

My work has provided a better understanding of the mechanisms of aerosol formation at atmospheric concentrations, which is necessary to understand its physical properties. This improved understanding is fundamental to accurately model aerosol formation in the atmosphere, and subsequently evaluate their large-scale effect on human health and environment.

## CITATIONS

Material from this dissertation has been published in the following form:

- **Jain, S.**, Zahardis, J., Petrucci, G. A.. (2014). Soft Ionization Chemical Analysis of Secondary Organic Aerosol from Green Leaf Volatiles Emitted by Turf Grass. Environ. Sci. Technol. 48:4835-4843.

- **Jain, S**. and Petrucci, G. A.. (2015) A New Method to Measure Aerosol Particle Bounce Using a Cascade Electrical Low Pressure Impactor. Aerosol Sci. Technol. 49:390-399.

- Harvey, R. M., Bateman, A. P., **Jain, S**., Li, Y. J., Martin, S., Petrucci, G. A.. (2016). Optical Properties of Secondary Organic Aerosol from cis-3-Hexenol and cis-3-Hexenyl Acetate: Effect of Chemical Composition, Humidity, and Phase. Environ Sci. Technol. 50:4997-5006.

Material from this dissertation has been submitted for review to Aerosol Science and Technology on May 6th, 2016 in the following form:

- **Jain, S**. and Petrucci, G. A.. (2016) The influence of absolute mass loading of secondary organic aerosols on their phase state. Aerosol Sci. Technol.

# ACKNOWLEDGEMENTS

I still remember the day I received the acceptance letter from UVM and looking back at my years at UVM, I feel blessed every step along the way. It has been such an amazing journey, mainly because of all the great science and wonderful people that I got to know and become friends with.

I am heartily thankful to my advisor, Dr. Giuseppe Petrucci (Joe), whose encouragement, trust, guidance and support from the initial to the final level helped me to complete my research.  I could not have asked for a better advisor. Joe's help as an advisor throughout my research has been invaluable. I really appreciate his invariably positive attitude, open door policy and open mind towards research, combined with a great amount of friendliness and patience. Thank you Joe for letting me do research in your lab.

I would also like to thank my committee members Dr. Brewer, Dr. Goldberg and Dr. Holmen for their continuous support and guidance during the past 5 years and helping me stay on track during my journey as a grad student. I am also thankful to the Chemistry Department at UVM for providing me with funds to complete my education and for a great learning and teaching experience.

I have been very fortunate to have such a supportive, friendly, and fun collogue. Dr. Rebecca Harvey (Red), thanks for all your support during the past 5 years. Thank you for tolerating me and listening to my crap when things didn't work. Also thanks for having many meaningful conversations about work and life.

This thesis would not have been possible without the support of my family. Even though I am thousands of miles away from home, my family on the other side of the ocean

# TABLE OF CONTENTS

# LIST OF FIGURES

# LIST OF TABLES

# LIST OF ABBREVIATIONS

| | |
|---|---|
| OA | Organic Aerosol |
| SOA | Secondary Organic Aerosol |
| VOC | Volatile Organic Compound |
| SMPS | Scanning Mobility Particle Sizer |
| ELPI | Electrostatic Low Pressure Impactor |
| $C_{SOA}$ | SOA mass loading |
| PM | Particulate Matter |
| POA | Primary Organic Aerosol |
| AVOC | Anthropogenic Volatile Organic Compound |
| BVOC | Biogenic Volatile Organic Compound |
| NIR-LDI-AMS | Near Infrared Laser Desorption Ionization Aerosol Mass Spectrometer |
| GLV | Green Leaf Volatile |
| nm | Nanometer |
| μm | Micrometer |
| CI* | Excited Criegee Intermediate |
| SCI | Stabilized Criegee Intermediate |
| CCN | Cloud Condensation Nuclei |
| IN | Ice Nuclei |
| MS | Mass Spectrometry |
| AMS | Aerosol Mass Spectrometer |
| TOF | Time of Flight |
| CI | Chemical Ionization |
| LDI | Laser Desorption Ionization |
| LOD | Limit of Detection |
| OL | Oleic Acid |
| Li | Lithium |

| | |
|---|---|
| Mg | Magnesium |
| Al | Aluminum |
| Ag | Silver |
| Cu | Copper |
| W | Tungsten |
| LDR | Linear Dynamic Range |
| LDI | Laser Desorption Ionization |
| ORVOC | Other Reactive Volatile Organic Compound |
| CHA | *cis*-3-hexenylacetate |
| HXL | *cis*-3-hexen-1-ol |
| RH | Relative Humidity |
| UVMEC | University of Vermont Environmental Chamber |
| TD-GC-MS | Thermal Desorption Gas Chromatography Mass Spectrometer |
| SVOC | Semi Volatile Organic Compound |
| 3HPA | 3-hydroxypropanal |
| BF | Bounce Factor |
| AS | Ammonium sulfate |
| DOS | Dioctyl Sebacate |
| GMD | Geometric Mean Diameter |

# CHAPTER 1: INTRODUCTION & OUTLINE OF THESIS

By definition, an aerosol is a mixture of solid or liquid particles suspended in a gas with particle diameters in the range of $10^{-10}$–$10^{-6}$ m.[1] Traditionally, the term aerosol refers to suspended particles in air that contain a large proportion of condensed matter other than water.[2] Common examples of such aerosol include crystal particles of dusts lofted by wind, smoke from incomplete combustion of fossil fuels, suspended bacterial cells, salt particles from ocean spray, etc. Tropospheric aerosol particles are typically comprised of inorganic and organic matter. In general, the predominant chemical components of air particulate matter (PM) are sulfate, nitrate, ammonium, sea salt, mineral dust, organic compounds, and black or elemental carbon, each of which typically contributes about 10–30% of the overall mass load. These can be emitted directly to the atmosphere as primary emission or can be formed through various atmospheric process (secondary formation). The concentration, composition, and size distributions of atmospheric aerosol particles are temporally and spatially highly variable; however, in the lower atmosphere (troposphere) the total particle number and mass concentrations typically vary in the range of about $10^2$ – $10^5$ cm$^{-3}$ and 1–100 µg m$^{-3}$, respectively.[3, 4] Thus we are surrounded by aerosol. It is important to note that the term aerosol and particles are often interchanged in the atmospheric community and from this point on, the term aerosol will be used to refer specifically to the particulate component of atmospheric aerosol.

## 1.1 Motivation

Aerosol are ubiquitous in the atmosphere and play critical but poorly understood roles in the Earth's climate forcing.[5] Atmospheric aerosol are produced from a variety of sources and have a tendency to either scatter or absorb solar radiation, depending on their chemical composition, as well as other factors, such as phase, optical properties, size distribution, etc.[6] Moreover, aerosol particles can have significant effects on human health, air quality and global climate.[7, 8] Black carbon has the potential to heat the atmosphere by absorption of solar radiation, whereas most organic aerosol components cool the Earth's atmosphere. Fine aerosol (i.e. the particle size that concerns us the most) have sizes close to wavelengths in the visible and are thus expected to have a greater climatic impact than larger particles.[9]

Organic aerosol, which contribute about 20-90% of total fine aerosol mass in the atmosphere, can be classified into two main categories according to their formation processes. Primary organic aerosol (POA) are emitted directly as particles in the atmosphere from different sources, such as combustion of diesel or biomass burning, etc., while the oxidation of volatile organic compounds (VOCs) leads to the formation of low-volatility products that partition to the condensed phase and result in the formation of secondary organic aerosol (SOA). The chemical diversity of SOA composition in the atmosphere reflects the large number of SOA precursors and processes that act on them during their atmospheric lifetime. Thus, studies involving SOA have received considerable attention in the last two decades from the atmospheric sciences community.

Major classes of SOA precursors include volatile and semi-volatile alkanes, alkenes, aromatic hydrocarbons, and oxygenated compounds from both anthropogenic [10] (AVOC) and biogenic[11] (BVOC) sources. Anthropogenic sources contribute only about 2 percent of SOA by mass; the remainder being produced by biogenic sources. Despite the significance and abundance of SOA, their sources, sinks, rates of formation, chemical and physical properties in the atmosphere are poorly understood, owing largely to their chemical complexity.[12, 13] As a result, there persists a significant gap between ambient SOA mass measurements, and predictions by regional and global models.[14, 15]

The scope of this thesis is to study the chemical and physical properties of SOA from various biogenic precursors, with the aim of reducing the existing gaps in knowledge. Selected atmospherically relevant systems were experimentally investigated with emphasis on their chemical composition and physical properties, such as phase or viscosity. Focus of this work is to optimize the Near Infrared Laser Desorption Ionization Aerosol Mass Spectrometer (NIR-LDI-AMS) for SOA measurements, including fundamental studies of laser/probe metal interactions, to better understand the chemical mechanism involved during ozonolysis of atmospherically relevant chemical systems and develop a new methodology to provide a nascent understanding of particle phase and its changes involved in both the formation and aging of SOA.

## 1.2 Research Questions

*In this thesis, I have made the following contributions: I worked towards increasing the sensitivity of our custom built NIR-LDI-AMS by modifying the OA collection probe so that we could sample both liquid and solid particles. I utilized this*

*improved NIR-LDI-AMS to study SOA derived from grass clippings emissions and elucidate the operative chemical mechanisms in its formation and aging. I developed a simplified method to estimate the SOA bounce factor to gain a nascent understanding of the phase state of atmospheric SOA. Lastly, I utilized the developed methodology to study the influence of total SOA mass loading and time on the phase state of SOA.*

The following list summarizes the research questions driving each chapter in this thesis.

1. How can we improve the existing NIR-LDI-AMS such that we can sample both liquid and solid aerosol? (Chapter 3)

2. What are the primary precursors of SOA from grass clippings? (Chapter 4)

   a. What is (are) the chemical mechanism (s) leading to the formation of SOA by ozonolysis of various GLVs?

   b. Can a single precursor be used to describe SOA formation for this complex chemical system?

3. How can we estimate the phase state of atmospheric aerosol in the most simplified way? (Chapter 5)

4. What are the parameters that can have an impact on the phase state of atmospheric aerosol? (Chapter 6)

**1.3 Thesis outline**

Chapter 2 details a broad literature review that has informed the writing of this thesis and the research questions it poses. It contains an introduction to atmospheric chemistry with respect to organic aerosol formation, placing this work into a wider context.

Chapter 3 of the thesis explains in detail the functioning of our custom aerosol mass spectrometer (NIR-LDI-AMS). Herein I present results obtained for various modifications of the collection probe (i.e., changing the material of the collection probe or physical modifications to the collection probe) to improve the instrumental analytical figures of merit, as well as enhance the collection efficiency for both liquid and solid aerosol. To demonstrate the application of the optimized NIR-LDI-AMS, soft ionization chemical analysis of SOA generated by ozonolysis of monoterpenes, such as limonene, was studied. Also I present preliminary results showing the impact of order of introduction of VOC or ozone on the chemical composition of generated SOA.

In **chapter 4**, I utilize the NIR-LDI-AMS to chemically analyze SOA from GLVs emitted by turf grass. In this chapter the rather complex mass spectra of various GLVs was deconvoluted by establishing and discussing the chemical mechanisms involved in generation of SOA from GLVs, thus providing a better understanding of an underlying question: i.e., whether a single precursor can be used to quantitatively predict and determine SOA formation for a complex chemical system.

To more fully understand the impact of SOA from GLVs on climate, it is essential also to understand SOA phase state. In order to do so, a method was developed to estimate the phase of aerosol. In **Chapter 5**, I present a relatively simple and direct method to

estimate SOA bounce factor, which we argue may be used as a surrogate for particle viscosity (or phase). This newly developed method overcomes the limitations of some of the existing methods and provides the temporal resolution necessary to measure phase changes in a continuously evolving SOA parcel. This method was validated by using solid and liquid reference aerosol.

Some interesting results from the work presented in **Chapter 5** also raised questions as to the influence of a variety of factors, such as temperature and maximum SOA mass loading, on the phase of atmospheric aerosol. In **Chapter 6**, I present and discuss results showing that SOA mass loading is an important parameter that has a significant impact on the phase state of aerosol. Hopefully the results from this work will help to reduce the consistent disparity between measured and observed SOA levels.

Lastly, **Chapter 7** summarizes the main conclusions of this work and highlights possible directions for future research. It also presents a more general discussion of how the various results obtained in this thesis fit into the wider perspective of atmospheric chemistry.

## 1.4 References

1.      Hinds, W. C., *Aerosol Technology: Properties, Behavior, and Measurements or Airborne Particles*. 2 ed.; John Wiley & Sons, Inc.: New york, 1999; p 483.
2.      Poschl, U., Atmospheric aerosols: Composition, transformation, climate and health effects. *Angew Chem Int Edit* **2005,** *44*, (46), 7520-7540.
3.      Raes, F.; Van Dingenen, R.; Vignati, E.; Wilson, J.; Putaud, J. P.; Seinfeld, J. H.; Adams, P., Formation and cycling of aerosols in the global troposphere. *Atmospheric Environment* **2000,** *34*, (25), 4215-4240.
4.      Krejci, R.; Strom, J.; de Reus, M.; Williams, J.; Fischer, H.; Andreae, M. O.; Hansson, H. C., Spatial and temporal distribution of atmospheric aerosols in the lowermost troposphere over the Amazonian tropical rainforest. *Atmospheric Chemistry and Physics* **2005,** *5*, 1527-1543.
5.      Myhre, G.; Samset, B. H.; Schulz, M.; Balkanski, Y.; Bauer, S.; Berntsen, T. K.; Bian, H.; Bellouin, N.; Chin, M.; Diehl, T.; Easter, R. C.; Feichter, J.; Ghan, S. J.; Hauglustaine, D.; Iversen, T.; Kinne, S.; Kirkevag, A.; Lamarque, J. F.; Lin, G.; Liu, X.; Lund, M. T.; Luo, G.; Ma, X.; van Noije,

T.; Penner, J. E.; Rasch, P. J.; Ruiz, A.; Seland, O.; Skeie, R. B.; Stier, P.; Takemura, T.; Tsigaridis, K.; Wang, P.; Wang, Z.; Xu, L.; Yu, H.; Yu, F.; Yoon, J. H.; Zhang, K.; Zhang, H.; Zhou, C., Radiative forcing of the direct aerosol effect from AeroCom Phase II simulations. *Atmospheric Chemistry and Physics* **2013,** *13*, (4), 1853-1877.

6.      Yu, H.; Kaufman, Y. J.; Chin, M.; Feingold, G.; Remer, L. A.; Anderson, T. L.; Balkanski, Y.; Bellouin, N.; Boucher, O.; Christopher, S.; DeCola, P.; Kahn, R.; Koch, D.; Loeb, N.; Reddy, M. S.; Schulz, M.; Takemura, T.; Zhou, M., A review of measurement-based assessments of the aerosol direct radiative effect and forcing. *Atmos Chem Phys* **2006,** *6*, 613-666.

7.      Poschl, U., Atmospheric aerosols: Composition, transformation, climate and health effects. *Angew Chem Int Edit* **2005,** *44*, (46), 7520-7540.

8.      Pope, C. A.; Dockery, D. W., Health effects of fine particulate air pollution: Lines that connect. *J Air Waste Manage* **2006,** *56*, (6), 709-742.

9.      Kanakidou, M.; Seinfeld, J. H.; Pandis, S. N.; Barnes, I.; Dentener, F. J.; Facchini, M. C.; Van Dingenen, R.; Ervens, B.; Nenes, A.; Nielsen, C. J.; Swietlicki, E.; Putaud, J. P.; Balkanski, Y.; Fuzzi, S.; Horth, J.; Moortgat, G. K.; Winterhalter, R.; Myhre, C. E. L.; Tsigaridis, K.; Vignati, E.; Stephanou, E. G.; Wilson, J., Organic aerosol and global climate modelling: a review. *Atmospheric Chemistry and Physics* **2005,** *5*, 1053-1123.

10.     Farina, S. C.; Adams, P. J.; Pandis, S. N., Modeling global secondary organic aerosol formation and processing with the volatility basis set: Implications for anthropogenic secondary organic aerosol. *J Geophys Res-Atmos* **2010,** *115*.

11.     Scott, C. E.; Rap, A.; Spracklen, D. V.; Forster, P. M.; Carslaw, K. S.; Mann, G. W.; Pringle, K. J.; Kivekäs, N.; Kulmala, M.; Lihavainen, H.; Tunved, P., The direct and indirect radiative effects of biogenic secondary organic aerosol. *Atmos. Chem. Phys. Discuss.* **2013,** *13*, (6), 16961-17019.

12.     Hallquist, M.; Wenger, J. C.; Baltensperger, U.; Rudich, Y.; Simpson, D.; Claeys, M.; Dommen, J.; Donahue, N. M.; George, C.; Goldstein, A. H.; Hamilton, J. F.; Herrmann, H.; Hoffmann, T.; Iinuma, Y.; Jang, M.; Jenkin, M. E.; Jimenez, J. L.; Kiendler-Scharr, A.; Maenhaut, W.; McFiggans, G.; Mentel, T. F.; Monod, A.; Prevot, A. S. H.; Seinfeld, J. H.; Surratt, J. D.; Szmigielski, R.; Wildt, J., The formation, properties and impact of secondary organic aerosol: current and emerging issues. *Atmos Chem Phys* **2009,** *9*, (14), 5155-5236.

13.     De Gouw, J.; Jimenez, J. L., Organic Aerosols in the Earth's Atmosphere. *Environ Sci Technol* **2009,** *43*, (20), 7614-7618.

14.     Volkamer, R.; Jimenez, J. L.; San Martini, F.; Dzepina, K.; Zhang, Q.; Salcedo, D.; Molina, L. T.; Worsnop, D. R.; Molina, M. J., Secondary organic aerosol formation from anthropogenic air pollution: Rapid and higher than expected. *Geophys Res Lett* **2006,** *33*, (17).

15.     Heald, C. L.; Kroll, J. H.; Jimenez, J. L.; Docherty, K. S.; DeCarlo, P. F.; Aiken, A. C.; Chen, Q.; Martin, S. T.; Farmer, D. K.; Artaxo, P., A simplified description of the evolution of organic aerosol composition in the atmosphere. *Geophys Res Lett* **2010,** *37*.

## CHAPTER 2: BACKGROUND AND REVIEW

### 2.1 Atmospheric aerosols in general

The term "atmospheric aerosol" refers to a suspension of condensed phase particles (solid or liquid) in a gaseous medium[1] and encompasses a wide range of particle types having different compositions, sizes and shapes. Atmospheric aerosol are ubiquitous in air and are most commonly observed as clouds, dust, smoke, and haze. Such aerosol and clouds play significant roles in shaping conditions at the earth's surface and in the lower atmosphere.[2]

Atmospheric aerosol are generally considered to be particles that range in size from a few nanometers (nm) to tens of micrometers (µm) in diameter. Submicron particles are the most important for our climate as they have the longest atmospheric lifetimes relative to larger particles and can be transported over long distances.[3] The variation in aerosol chemical composition in the atmosphere reveals a large number of sources of particles and processes that act on them during their lifetime.[4] Accurate determination of the chemical composition of aerosol is a formidable analytical task. Depending on the mixing state, atmospheric aerosol are either considered externally mixed, if they arise from different sources and have different chemical composition, or internally mixed if all particles of a given size contain a uniform mixture of components.[5] The real mixed state can be expected to lie somewhere in between the above two cases. Once airborne, the composition and size of individual particles can be fairly uniform, such as for internally mixed aerosol, or very different for externally mixed aerosol, depending on the particle sources and atmospheric aging processes involved, including coagulation, gas – particle partitioning or chemical reactions.[6]

Within the submicron size fraction, aerosols consist primarily of an organic or an inorganic fraction, either of which can dominate particle mass depending on geographical location, source, and chemistry. In brief, the inorganic fraction is comprised of salts and major ions (such as: $NH_4^+$, $Na^+$, $K^+$, $Mg^{2+}$, $Ca^{2+}$, $NO_3^-$, and $Cl^-$) and its sources and mechanisms of formation are relatively well-understood.[7] The organic fraction, on the other hand, has a large uncertainty associated with its mass (20-90%), due to the chemical complexity and plethora of sources.[8] Hence, only a little is known about the sources, properties, and the mechanisms that lead to its formation and ageing, thereby limiting our understanding of its role in atmospheric chemistry, making it an important area for study.[9-11]

## 2.2 Organic aerosols (precursors to Secondary organic aerosols)

Organic aerosol (OA) are a major component of fine-particle mass in the atmosphere,[12] contributing up to ~20–50% to the total fine particle mass at continental mid-latitudes and as high as 90% in tropical forested areas.[13, 14]  Traditionally, OA have been split into two broad classes based on how it is introduced to the atmosphere: primary organic aerosol (POA) and secondary organic aerosols (SOA). Organic compounds that are emitted directly in particulate form from sources such as motor vehicles, forest fires, etc. are referred to as POA.[12] On the other hand, volatile organic compounds that transfer to the aerosol phase from the gas phase as a result of gas-phase oxidation of parent volatile organic compounds (VOC) are referred to as SOA.[15] Depending on the location, time and specific source regions, SOA can be produced from both anthropogenic (AVOC)[16] and biogenic volatile organic compounds (BVOC)[17]. While recent assessments indicate that,

on a global basis, VOCs from biogenic sources exceed anthropogenic emissions, there is also a great uncertainty in the global estimates of SOA precursors in general.[12, 18]

*AVOC emissions* include a wide range of compounds, such as hydrocarbons (alkanes, alkenes and aromatics), halocarbons (e.g., trichloroethylene) and oxygenates (alcohols, aldehydes, and ketones). However, because biogenic sources are a much greater contributor to SOA, work in this thesis will primarily focus on BVOC emissions and their sources.
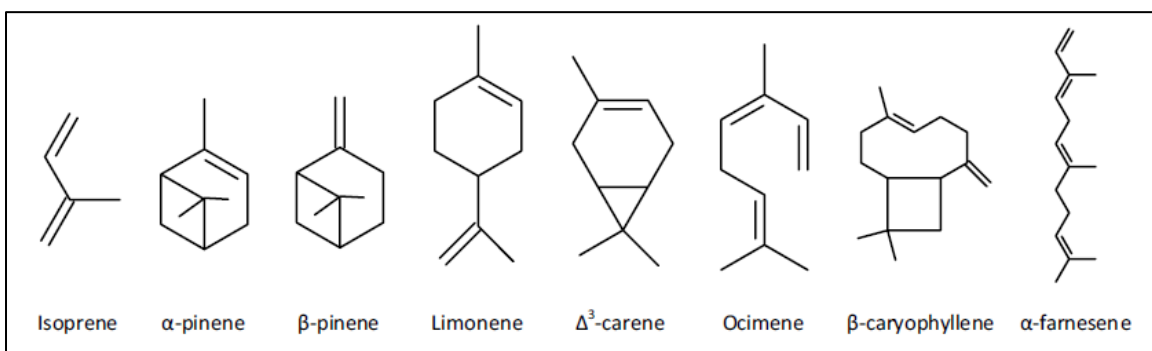


*Figure 2.1 Chemical structures of typical BVOCs*

*BVOC emissions* (Figure 2.1) consist primarily of alkenes, with an estimated mean annual total BVOC emission of 750-1000 TgC/year. The majority of this total can be allocated to isoprene (70 %), monoterpenes (11 %), methanol (6 %), acetone (3 %), sesquiterpenes (2.5 %) and other BVOC species (each contributing less than 2 %). [11, 19, 20] Isoprene is the single most important source of BVOC in the atmosphere, with global mean emissions of $594 \pm 34$ TgC/year. However, isoprene is generally not considered as a major producer of SOA. Only a very small (0.2%) fraction of all isoprene may be getting converted into SOA, which corresponds to ~2 TgC/year emissions.[21] The monoterpenes comprise two isoprene units and may contain multiple double bonds, or in some cases oxygenated functional groups. Depending on the number of isoprene units, the terpene is

called a hemiterpene (C5), monoterpene (C10) or a sesquiterpenes (C15). More than 40,000 different terpenes are known, of which the hemiterpenes, monoterpenes and sesquiterpenes account for almost 40-80 % of total terpene emissions.[11, 19, 20] Another factor that makes terpenes important besides the emission amount is the conversion yield, i.e., terpene potential to form SOA. In other words, a given terpene may constitute only a small fraction of the BVOC mass, but due to a large conversion yield (for example SOA yields can approach 100% for some sesquiterpenes[22]), that same terpene would make a greater than expected contribution to the SOA mass. Recent top-down/bottom-up hybrid approaches to modeling SOA estimate a net BSOA production rate of only approximately 80−90 TgC/year,[11, 12, 23] in sharp contrast to the measured SOA masses described above.

BVOCs are removed from the atmosphere by various oxidative chemical reactions. The chemical lifetime of these VOCs depends largely on their reactivity. In addition to the chemical structure and the presence of oxidants, such as ozone, $NO_x$ or OH radicals, physical factors like temperature and humidity can also play an important role in their reactivity. Reactive, terpenes with varying lifetimes (minutes to hours) and chemical behavior have been observed in the atmosphere. Several of the products formed in these reactions will take part in further reactions, and are usually referred to as first and second generation products. The next section of the thesis helps in understanding the oxidative processing of VOCs and mechanisms that lead to formation of SOA.

## 2.3 Atmospheric oxidation mechanisms leading to SOA formation

The most prevalent atmospheric oxidants in the troposphere are ozone ($O_3$), OH radicals (day-time) and $NO_x$-radicals (night-time). In general, ozone and OH are the most important oxidants, while $NO_x$ chemistry is considered significant only during night-

time.[24] SOA is generally formed from the gas phase, homogeneous oxidation of VOCs to produce oxygenated compounds, which are sufficiently low in volatility to be able to transfer from the gas phase into the particle phase. Work in this thesis primarily focuses on ozonolysis of the VOCs because: 1) ozone is a predominant daytime oxidant, 2) ozone can be readily produced and quantified in the lab and 3) most BVOCs are chemically unsaturated and are reactive with ozone.

**2.3.1 Oxidation by ozone**
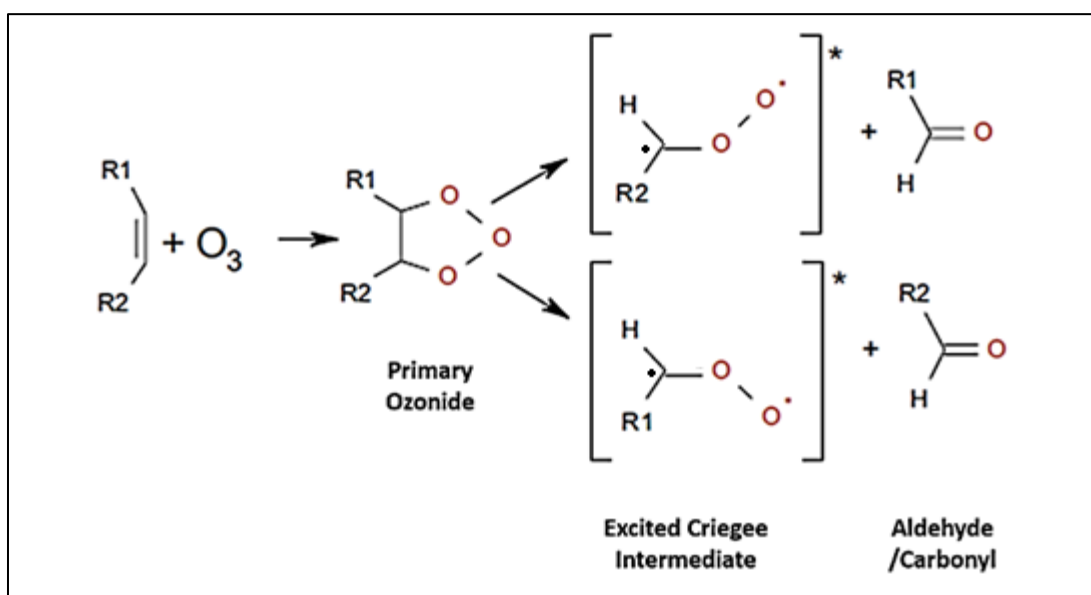


*Figure 2.2 Initial mechanism of the ozonolysis of alkenes.*

The main source of ozone in the atmosphere is the photolysis of $NO_2$ resulting in formation of the atomic oxygen radical, which reacts with molecular oxygen to form ozone.[25] The typical mixing ratios of ozone in the northern hemisphere are between 20-45 ppb, while in highly polluted megacities such as Mexico City and Beijing, up to hundreds of ppb have been measured.[26] Atmospheric alkenes react readily with ozone due to the presence of a double bond, resulting in formation of SOA. Briefly, as shown in Figure 2.2, oxidation of alkenes is initiated by electrophilic addition of ozone across the double bond,

resulting in the formation of a primary ozonide. This ozonide is unstable and readily decomposes to produce two carbonyl compounds (aldehydes or ketones) and two excited Criegee intermediates (CI*). Criegee chemistry has been discussed extensively in the literature[27-30] and more elaborate mechanisms, as they pertain directly to this work, will be presented in Chapter 4 of this thesis. The CI* has two fates: 1) formation of a Stabilized Criegee Intermediate (SCI), where the excited CI* is quenched to form a stabilized CI that can react with water or oxygenated organics, and 2) the CI* rearranges to form a vinyl hydroperoxide (hence, this path is called the hydroperoxide channel) that rapidly decomposes to generate hydroxyl (OH) and alkyl radicals (R•). The R• then reacts rapidly with molecular oxygen to form an alkylperoxy radical (RO$_2$•), which plays an important role in the production of lower-volatility products.[10, 31] The relative importance of the two reaction paths (i.e., SCI vs hydroperoxide channel) is dependent on the molecular structure of the parent alkene. Chemical products from both channels have been identified in aerosol and often appear together, indicating that both mechanisms are operative, although one or the other may be dominant.

**2.3.2 Oxidation by OH radicals**

Radicals are important in atmospheric oxidation and as mentioned in the previous section, ozonolysis of VOCs could also result in formation of OH radicals and hence it is important to incorporate OH radical oxidation mechanisms to understand overall SOA formation mechanisms.

The reaction between VOC and OH radicals starts either by attack at the double bond (major pathway, 85%, Figure 2.3), or by the abstraction of an H-atom to form a β– hydroxy alkyl radical (R$^.$) and water. This is followed by a fast addition of O$_2$, generating

a β– hydroxy alkyl peroxy radical ($RO_2$), which can further react to form a variety of low volatility products and isomers.[11]
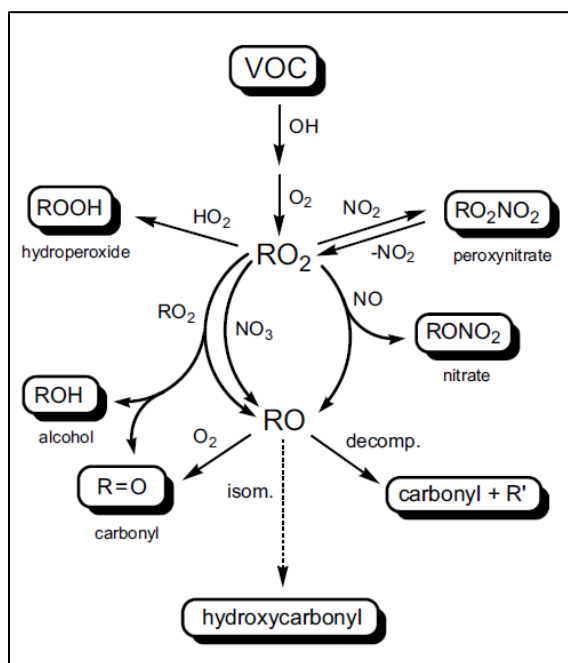


*Figure 2.3 Initial mechanism of oxidation of alkenes by OH radicals.[11]*

Even though OH radical-initiated oxidation experiments were not performed in this work, a portion of the above mechanism had to be invoked to understand products formed during the ozonolysis of certain BVOC. Also, a few experiments were performed utilizing OH scrubbers (cyclohexane and butanol) to eliminate OH radicals during ozonolysis.

**2.4 Secondary organic aerosols (SOA)**

Gas phase oxidation reactions of organic precursor compounds result in formation of organic species with varying volatility. These organic species could either have higher volatility than the parent VOC, such as $CO_2$, $CH_2O$, or be of sufficiently low vapor pressure to condense to the particle phase. The vapor pressure of a molecule is determined largely by its polarity and size. As a result, a key determinant of the volatility of an oxidation product is the importance of reactions that add polar functional groups relative to those that

break the carbon skeleton. These low vapor pressure semi-volatile products can undergo gas to particle conversion either by heterogeneous or homogenous nucleation. Heterogeneous nucleation occurs by condensation of the semi-volatile products onto pre-existing nuclei (e.g., ion clusters), while homogenous nucleation involves the formation of particles due to intra molecular attractive forces (e.g., van der Waal forces) present in all gases. Again, the process of gas-to-particle conversion depends largely on vapor pressure. Extremely low vapor pressures would initiate self-nucleation/homogeneous nucleation, whereas more semi-volatile compounds will not self-nucleate but will partition onto existing particle surfaces via heterogeneous nucleation.[32] After the initial formation of particles, the SOA can undergo heterogeneous/ multiphase reactions with time, often referred to as aerosol aging. Further oxidation of the SOA to form second generation products (and third, fourth and so on) can result in new products with even lower volatility and higher molecular weights, such as oligomers (Figure 2.4)[11].

Our understanding of the qualitative and quantitative impacts of aerosol on climate and health remains far from complete, although significant advances are being made. In this project, our focus was to gain an improved understanding of the chemistry of SOA chemical formation and its influence on particle properties, such as phase, which are important in radiative forcing and global change.
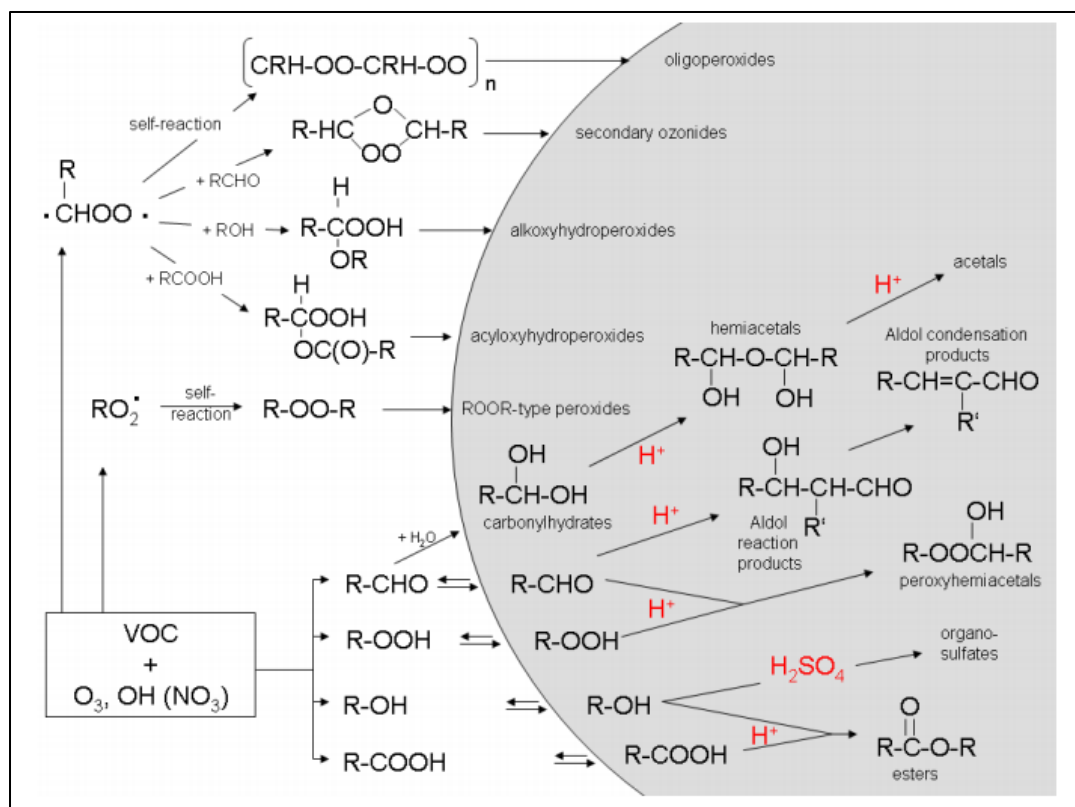
*Figure 2.4 Possible chemical reaction pathways for the formation of oligomers and other higher-MW products observed in SOA[11]*

### 2.4.1 Impact on human health

The health risk of aerosols is determined by particle size, surface area and chemical composition. Epidemiological studies in humans and laboratory animals have consistently provided evidence that both short- and long-term exposure to fine and ultrafine particulate air pollution is related to acute and chronic health effects, such as respiratory and cardiovascular diseases.[33-35] Some recent studies have investigated the health impact of biogenic SOA[36, 37] however, for studies in which humans were subjected to ambient SOA, no specific correlation between health effects and SOA (both biogenic and anthropogenic) has been demonstrated, although there was a relation with POA.[38] It is therefore possible that the health impact of fine PM is highly dependent on composition. Considering the adverse health effects of exposure to the PM, the complex composition of particles makes

it inherently difficult to identify with any surety which components are culpable for adverse health effects.[39]

## 2.4.2 Impact on climate

The global average temperature has increased by about 0.85 ∘C over the period 1880 to 2012, most probably due to anthropogenic forcing by greenhouse gases. Aerosol can also affect climate by processes that are generally classified as direct or indirect with respect to radiative forcing of the climate system. Radiative forcing describes changes in the energy fluxes of solar radiation (maximum intensity in the spectral range of visible light) and terrestrial radiation (maximum intensity in the infrared spectral range) in the atmosphere induced by anthropogenic or natural changes in atmospheric composition, Earth surface properties, or solar activity.[40] Figure 2.5 depicts a simplistic distinction between direct and indirect aerosol effects and some major feedback loops in the climate system.



**Natural and Anthropogenic Emissions of Particles and Precursor Gases**
• soil, mineral and road dust; sea spray; soot and ashes; POA and VOC, $SO_2$, etc.

**Direct Effects**

**Atmospheric Aerosols**
• optical properties
• CCN and IN activity
• chem. and biol. activity

**Indirect Effects**

**Radiation and Temperature**
• absorption and scattering (reflection)
• solar (UV/VIS) and terrestrial (IR)

**Clouds and Precipitations**
• water droplets and ice crystals
• formation, evaporation, deposition

**Atmospheric and Oceanic Circulation, Biogeochemical Cycles**
• mass and heat transport, horizontal and vertical transport, extreme weather events
• water cycle: surface and ground water, snow and ice, evapotranspiration
• carbon and sulfur cycle: photosynthesis and decay of biomass, biological metabolisms, biomass burning and fossil fuel combustion, volcanism, etc.

*Figure 2.5 Direct and indirect effect of aerosol on climate [40]*

*2.4.2.1 Direct effect*

Direct effects refer to the scattering, reflection and absorption of incoming solar radiation and outgoing terrestrial radiation by particles, or their deposition on snow/ice lowering the reflection coefficient (albedo), i.e., the reflecting power of Earth surface. By scattering and reflecting light, aerosols provide an overall cooling effect, because they reflect part of the incoming sunlight back into space. However, aerosol such as black carbon, which is a strong broadband absorber, can also absorb part of the incoming solar radiation and outgoing terrestrial radiation, and thereby contributing to global warming.[40, 41]

*2.4.2.2 Indirect effect*

The indirect effect is more complex, and is caused by the ability of aerosol particles to serve as cloud seeds, i.e., cloud condensation nuclei (CCN) or ice nuclei (IN) activity (influence on clouds and precipitation).[42] Depending on the type of cloud and where it is found in the atmosphere, cloud water can be in the form of liquid droplets, solid ice crystals, or a mix of the two. The phase, composition, size and shape of cloud water play important roles in determining the effect of clouds on climate. Higher CCN numbers lead to clouds with a higher cloud droplet density, which have a higher albedo, and therefore cool the atmosphere more effectively. Higher IN numbers also contribute to overall cooling by reflecting solar radiation into space, however, ice clouds can also trap longwave radiation emitted by the earth back towards its surface and produce a warming effect.[23]

## 2.5 Phase of SOA

Despite the integral role of SOA in atmospheric processes, there remains a limited understanding of the chemical and physical changes induced in SOA as it ages in the atmosphere. Understanding the phase of SOA is especially important, as it can provide

insight into its sources and formation, and also its subsequent growth, reactivity and atmospheric impacts.[43, 44] The physical state of particles can  affect particulate phase chemical reactions, and, thus, the growth rates of newly formed atmospheric aerosol.[45] The phase state is also an important factor for the lifetime consideration of particles because the chemical reactions in the particle can become diffusion limited to the surface of solid particles. This may increase the lifetime of organic aerosols markedly, as the oxidation caused by atmospheric ozone and other oxidants is confined only to the surface.[43] Thus, verifying the physical phase state of SOA particles can provide us with new and important insight into their formation, subsequent growth and, consequently, potential atmospheric impacts.[45]

Furthermore, a disparity exists between modeled and observed atmospheric SOA levels, which has stimulated several efforts focused on improving the understanding of SOA sources and formation yields.[18, 46, 47] Present models assume that SOA particles remain liquid-like throughout their lifetime and an equilibrium exists between the particle and gas phase due to rapid evaporation and condensation.[46, 48, 49] However, recent work suggests otherwise, where researchers [46, 50] found that evaporation of α-pinene SOA at room temperature was orders of magnitude slower than expected from well-mixed liquid droplets. Models further assume that SOA particles have low viscosity, resulting in rapid diffusion and mixing throughout the particles; however, recent studies provide surmounting evidence to challenge this long-held fundamental assumption.[44, 51-53]

## 2.6 Characterization methods of SOA

Considerable effort has been expended to gain a more detailed understanding of the formation and growth of SOA, and this still remains an area of great interest as it presents

significant challenges in identifying SOA precursors and individual chemical components of a SOA parcel. Quantitatively addressing the molecular composition of SOA is a formidable challenge because ambient SOA in a typical air parcel is often comprised of hundreds or more compounds from diverse chemical classes, which are constantly changing.[23] Even a single precursor, for example limonene, could yield over 1000 products in the gas and aerosol phase, most of them not identified yet.[54] To quantitatively address the molecular composition of SOA, a number of on-line analysis techniques involving mass spectrometry (MS) have been developed.[55-57] Critical advantages of the online techniques are simultaneous measurements of particle composition, as well as size, high temporal resolution, and the ability to distinguish between internally and externally mixed particle components. MS techniques have an overall versatility of sensitive detection of a range of chemical species, providing high-throughput qualitative and semi-quantitative data on chemical properties of aerosols in laboratory, test facilities, and field studies.[56]

On-line analysis of atmospheric aerosols can be performed using Aerosol Mass Spectrometry (AMS), which differs from conventional mass spectrometry in its method of sample introduction. In AMS, aerosol sampling is typically achieved by an aerodynamic lens system or particle inlet. Once particles are sampled into the mass spectrometer, most AMS techniques use hard (or energetic) ionization methods that produce mostly fragments of the organic compounds, thereby losing the majority of the molecular information and making the MS spectra of complex mixtures difficult to interpret. Recently, a new class of AMS instruments utilizing soft ionization has been developed. Instruments employing soft ionization sources may be considered a niche within the aerosol MS field, however, their

mass spectral simplicity continues to provide unprecedented molecular level detail of the chemistry of SOA, greatly facilitating chemical interpretation of the complex mixtures.

In my research at UVM, I have utilized a custom built, state of the art soft ionization AMS for analysis of SOA that provided me with negligible molecular fragmentation, while affording an unprecedented sensitivity to organic constituents of aerosol at atmospherically relevant conditions. The instrument is highly sensitive to oxygenated organics (e.g., organic acids), permitting near real-time chemical analysis of SOA in chamber experiments at realistic SOA loadings (i.e., $C_{OA}$~0.1-10 $\mu g\ m^{-3}$). All condensed phase chemical products are measured exclusively as their $[M-H]^-$ pseudo-molecular anion. The instrumental details are described in Chapter 3.

## 2.7 References

1.      Hinds, W. C., *Aerosol Technology: Properties, Behavior, and Measurements or Airborne Particles*. 2 ed.; John Wiley & Sons, Inc.: New york, 1999; p 483.
2.      Ginzburg, A. S.; Gubanova, D. P.; Minashkin, V. M., Influence of natural and anthropogenic aerosols on global and regional climate. *Russ J Gen Chem+* **2009,** *79*, (9), 2062-2070.
3.      Finlayson-Pitts, B. J.; Pitts Jr, J. N., Preface. In *Chemistry of the Upper and Lower Atmosphere*, Academic Press: San Diego, 2000; pp xvii-xviii.
4.      Prather, K. A.; Hatch, C. D.; Grassian, V. H., Analysis of Atmospheric Aerosols. *Annu Rev Anal Chem* **2008,** *1*, 485-514.
5.      Lesins, G.; Chylek, P.; Lohmann, U., A study of internal and external mixing scenarios and its effect on aerosol optical properties and direct radiative forcing. *J Geophys Res-Atmos* **2002,** *107*, (D10).
6.      Poschl, U., Atmospheric aerosols: Composition, transformation, climate and health effects. *Angew Chem Int Edit* **2005,** *44*, (46), 7520-7540.
7.      Wexler, A. S.; Clegg, S. L., Atmospheric aerosol models for systems including the ions H+, NH4+, Na+, SO42-, NO3-,Cl-, Br-, and H2O. *J Geophys Res-Atmos* **2002,** *107*, (D14).
8.      Seinfeld, J. H.; Pandis, S. N., *Atmospheric chemistry and physics: from air pollution to climate change*. Wiley: 1998.
9.      Carlton, A. G.; Wiedinmyer, C.; Kroll, J. H., A review of Secondary Organic Aerosol (SOA) formation from isoprene. *Atmos Chem Phys* **2009,** *9*, (14), 4987-5005.
10.     Kroll, J. H.; Seinfeld, J. H., Chemistry of secondary organic aerosol: Formation and evolution of low-volatility organics in the atmosphere. *Atmos Environ* **2008,** *42*, (16), 3593-3624.
11.     Hallquist, M.; Wenger, J. C.; Baltensperger, U.; Rudich, Y.; Simpson, D.; Claeys, M.; Dommen, J.; Donahue, N. M.; George, C.; Goldstein, A. H.; Hamilton, J. F.; Herrmann, H.; Hoffmann, T.; Iinuma, Y.; Jang, M.; Jenkin, M. E.; Jimenez, J. L.; Kiendler-Scharr, A.; Maenhaut,

W.; McFiggans, G.; Mentel, T. F.; Monod, A.; Prevot, A. S. H.; Seinfeld, J. H.; Surratt, J. D.; Szmigielski, R.; Wildt, J., The formation, properties and impact of secondary organic aerosol: current and emerging issues. *Atmos Chem Phys* **2009,** *9*, (14), 5155-5236.

12.    Kanakidou, M.; Seinfeld, J. H.; Pandis, S. N.; Barnes, I.; Dentener, F. J.; Facchini, M. C.; Van Dingenen, R.; Ervens, B.; Nenes, A.; Nielsen, C. J.; Swietlicki, E.; Putaud, J. P.; Balkanski, Y.; Fuzzi, S.; Horth, J.; Moortgat, G. K.; Winterhalter, R.; Myhre, C. E. L.; Tsigaridis, K.; Vignati, E.; Stephanou, E. G.; Wilson, J., Organic aerosol and global climate modelling: a review. *Atmospheric Chemistry and Physics* **2005,** *5*, 1053-1123.

13.    Putaud, J.-P.; Raes, F.; Van Dingenen, R.; Brüggemann, E.; Facchini, M. C.; Decesari, S.; Fuzzi, S.; Gehrig, R.; Hüglin, C.; Laj, P.; Lorbeer, G.; Maenhaut, W.; Mihalopoulos, N.; Müller, K.; Querol, X.; Rodriguez, S.; Schneider, J.; Spindler, G.; Brink, H. t.; Tørseth, K.; Wiedensohler, A., A European aerosol phenomenology—2: chemical characteristics of particulate matter at kerbside, urban, rural and background sites in Europe. *Atmos Environ* **2004,** *38*, (16), 2579-2595.

14.    Andreae, M. O.; Crutzen, P. J., Atmospheric aerosols: Biogeochemical sources and role in atmospheric chemistry. *Science* **1997,** *276*, (5315), 1052-1058.

15.    Baltensperger, U.; Kalberer, M.; Dommen, J.; Paulsen, D.; Alfarra, M. R.; Coe, H.; Fisseha, R.; Gascho, A.; Gysel, M.; Nyeki, S.; Sax, M.; Steinbacher, M.; Prevot, A. S. H.; Sjogren, S.; Weingartner, E.; Zenobi, R., Secondary organic aerosols from anthropogenic and biogenic precursors. *Faraday Discuss* **2005,** *130*, 265-278.

16.    Farina, S. C.; Adams, P. J.; Pandis, S. N., Modeling global secondary organic aerosol formation and processing with the volatility basis set: Implications for anthropogenic secondary organic aerosol. *J Geophys Res-Atmos* **2010,** *115*.

17.    Scott, C. E.; Rap, A.; Spracklen, D. V.; Forster, P. M.; Carslaw, K. S.; Mann, G. W.; Pringle, K. J.; Kivekas, N.; Kulmala, M.; Lihavainen, H.; Tunved, P., The direct and indirect radiative effects of biogenic secondary organic aerosol. *Atmos Chem Phys* **2014,** *14*, (1), 447-470.

18.    Robinson, A. L.; Donahue, N. M.; Shrivastava, M. K.; Weitkamp, E. A.; Sage, A. M.; Grieshop, A. P.; Lane, T. E.; Pierce, J. R.; Pandis, S. N., Rethinking organic aerosols: Semivolatile emissions and photochemical aging. *Science* **2007,** *315*, (5816), 1259-1262.

19.    Guenther, A.; Hewitt, C. N.; Erickson, D.; Fall, R.; Geron, C.; Graedel, T.; Harley, P.; Klinger, L.; Lerdau, M.; Mckay, W. A.; Pierce, T.; Scholes, B.; Steinbrecher, R.; Tallamraju, R.; Taylor, J.; Zimmerman, P., A Global-Model of Natural Volatile Organic-Compound Emissions. *J Geophys Res-Atmos* **1995,** *100*, (D5), 8873-8892.

20.    Sindelarova, K.; Granier, C.; Bouarar, I.; Guenther, A.; Tilmes, S.; Stavrakou, T.; Muller, J. F.; Kuhn, U.; Stefani, P.; Knorr, W., Global data set of biogenic VOC emissions calculated by the MEGAN model over the last 30 years. *Atmospheric Chemistry and Physics* **2014,** *14*, (17), 9317-9341.

21.    Claeys, M.; Graham, B.; Vas, G.; Wang, W.; Vermeylen, R.; Pashynska, V.; Cafmeyer, J.; Guyon, P.; Andreae, M. O.; Artaxo, P.; Maenhaut, W., Formation of secondary organic aerosols through photooxidation of isoprene. *Science* **2004,** *303*, (5661), 1173-1176.

22.    Hoffmann, T.; Odum, J. R.; Bowman, F.; Collins, D.; Klockow, D.; Flagan, R. C.; Seinfeld, J. H., Formation of organic aerosols from the oxidation of biogenic hydrocarbons. *J Atmos Chem* **1997,** *26*, (2), 189-222.

23.    Goldstein, A.; Galbally, I., Known and unexplored organic constituents in the earth's atmosphere. *Environ Sci Technol* **2007,** *41*, (5), 1514–1521.

24.    Brown, S. S.; Stutz, J., Nighttime radical observations and chemistry. *Chem Soc Rev* **2012,** *41*, (19), 6405-6447.

25.    Finlayson-Pitts, B. J.; Pitts Jr, J. N., CHAPTER 5 - Kinetics and Atmospheric Chemistry. In *Chemistry of the Upper and Lower Atmosphere*, Academic Press: San Diego, 2000; pp 130-178.

26.     Vingarzan, R., A review of surface ozone background levels and trends. *Atmospheric Environment* **2004,** *38*, (21), 3431-3442.

27.     Grosjean, E.; Grosjean, D., The gas-phase reaction of alkenes with ozone: formation yields of carbonyls from biradicals in ozone–alkene–cyclohexane experiments. *Atmos Environ* **1998,** *32*, (20), 3393-3402.

28.     Grosjean, E.; Grosjean, D., The gas phase reaction of unsaturated oxygenates with ozone: Carbonyl products and comparison with the alkene-ozone reaction. *J Atmos Chem* **1997,** *27*, (3), 271-289.

29.     Horie, O.; Moortgat, G. K., Gas phase ozonolysis of alkenes. Recent advances in mechanistic investigations. *Accounts Chem Res* **1998,** *31*, (7), 387-396.

30.     Grosjean, E.; DeAndrade, J. B.; Grosjean, D., Carbonyl products of the gas-phase reaction of ozone with simple alkenes. *Environ Sci Technol* **1996,** *30*, (3), 975-983.

31.     Ziemann, P. J.; Atkinson, R., Kinetics, products, and mechanisms of secondary organic aerosol formation. *Chem Soc Rev* **2012,** *41*, (19), 6582-6605.

32.     Kamens, R.; Jang, M.; Chien, C. J.; Leach, K., Aerosol formation from the reaction of alpha-pinene and ozone using a gas-phase kinetics aerosol partitioning model. *Environ Sci Technol* **1999,** *33*, (9), 1430-1438.

33.     Brook, R. D.; Rajagopalan, S., Particulate Matter Air Pollution and Atherosclerosis. *Curr Atheroscler Rep* **2010,** *12*, (5), 291-300.

34.     Ruckerl, R.; Schneider, A.; Breitner, S.; Cyrys, J.; Peters, A., Health effects of particulate air pollution: A review of epidemiological evidence. *Inhal Toxicol* **2011,** *23*, (10), 555-592.

35.     Anenberg, S. C.; West, J. J.; Horowitz, L. W.; Tong, D. Q., The Global Burden of Air Pollution on Mortality response. *Environ Health Persp* **2010,** *118*, (10), A424-A425.

36.     McDonald, J. D.; Doyle-Eisele, M.; Campen, M. J.; Seagrave, J.; Holmes, T.; Lund, A.; Surratt, J. D.; Seinfeld, J. H.; Rohr, A. C.; Knipping, E. M., Cardiopulmonary response to inhalation of biogenic secondary organic aerosol. *Inhal Toxicol* **2010,** *22*, (3), 253-265.

37.     Gaschen, A.; Lang, D.; Kalberer, M.; Savi, M.; Geiser, T.; Gazdhar, A.; Lehr, C. M.; Bur, M.; Dommen, J.; Baltensperger, U.; Geiser, M., Cellular Responses after Exposure of Lung Cell Cultures to Secondary Organic Aerosol Particles. *Environ Sci Technol* **2010,** *44*, (4), 1424-1430.

38.     Rohr, A. C., The health significance of gas- and particle-phase terpene oxidation products: A review. *Environ Int* **2013,** *60*, 145-162.

39.     Oberdorster, G.; Oberdorster, E.; Oberdorster, J., Nanotoxicology: An emerging discipline evolving from studies of ultrafine particles. *Environ Health Persp* **2005,** *113*, (7), 823-839.

40.     Poschl, U., Atmospheric aerosols: Composition, transformation, climate and health effects. *Angew Chem Int Edit* **2005,** *44*, (46), 7520-7540.

41.     Seinfeld, J. H.; Pandis, S. N., *Atmospheric Chemistry and Physics: From Air Pollution to Climate Change*. Wiley: 2006.

42.     Scott, C. E.; Rap, A.; Spracklen, D. V.; Forster, P. M.; Carslaw, K. S.; Mann, G. W.; Pringle, K. J.; Kivekäs, N.; Kulmala, M.; Lihavainen, H.; Tunved, P., The direct and indirect radiative effects of biogenic secondary organic aerosol. *Atmos. Chem. Phys. Discuss.* **2013,** *13*, (6), 16961-17019.

43.     Saukko, E.; Kuuluvainen, H.; Virtanen, A., A method to resolve the phase state of aerosol particles. *Atmos Meas Tech* **2012,** *5*, (1), 259-265.

44.     Virtanen, A.; Joutsensaari, J.; Koop, T.; Kannosto, J.; Yli-Pirila, P.; Leskinen, J.; Makela, J. M.; Holopainen, J. K.; Poschl, U.; Kulmala, M.; Worsnop, D. R.; Laaksonen, A., An amorphous solid state of biogenic secondary organic aerosol particles. *Nature* **2010,** *467*, (7317), 824-827.

45.     Virtanen, A.; Kannosto, J.; Joutsensaari, J.; Saukko, E.; Kuuluvainen, H.; Hao, L.; Yli-Pirilä, P.; Tiitta, P.; Holopainen, J. K.; Worsnop, D. R.; Smith, J. N.; Laaksonen, A., Bounce behavior of

freshly nucleated biogenic secondary organic aerosol particles. *Atmospheric Chemistry and Physics Discussions* **2011,** *11*, (3), 9313-9334.

46.      Vaden, T. D.; Imre, D.; Beranek, J.; Shrivastava, M.; Zelenyuk, A., Evaporation kinetics and phase of laboratory and ambient secondary organic aerosol. *Proc. Natl. Acad. Sci. USA* **2011,** *108*, (6), 2190-2195.

47.      Pye, H. O. T.; Seinfeld, J. H., A global perspective on aerosol from low-volatility organic compounds. *Atmos Chem Phys* **2010,** *10*, (9), 4377-4401.

48.      Pankow, J. F., An Absorption-Model of Gas-Particle Partitioning of Organic-Compounds in the Atmosphere. *Atmos Environ* **1994,** *28*, (2), 185-188.

49.      Chan, A. W. H.; Kroll, J. H.; Ng, N. L.; Seinfeld, J. H., Kinetic modeling of secondary organic aerosol formation: effects of particle- and gas-phase reactions of semivolatile products. *Atmos Chem Phys* **2007,** *7*, (15), 4135-4147.

50.      Abramson, E.; Imre, D.; Beranek, J.; Wilson, J.; Zelenyuk, A., Experimental determination of chemical diffusion within secondary organic aerosol particles. *Phys Chem Chem Phys* **2013,** *15*, (8), 2983-2991.

51.      Kannosto, J.; Yli-Pirila, P.; Hao, L. Q.; Leskinen, J.; Jokiniemi, J.; Makela, J. M.; Joutsensaari, J.; Laaksonen, A.; Worsnop, D. R.; Keskinen, J.; Virtanen, A., Bounce characteristics of alpha-pinene-derived SOA particles with implications to physical phase. *Boreal Environ Res* **2013,** *18*, (3-4), 329-340.

52.      Virtanen, A.; Kannosto, J.; Kuuluvainen, H.; Arffman, A.; Joutsensaari, J.; Saukko, E.; Hao, L.; Yli-Pirila, P.; Tiitta, P.; Holopainen, J. K.; Keskinen, J.; Worsnop, D. R.; Smith, J. N.; Laaksonen, A., Bounce behavior of freshly nucleated biogenic secondary organic aerosol particles. *Atmos Chem Phys* **2011,** *11*, (16), 8759-8766.

53.      Cappa, C. D.; Wilson, K. R., Evolution of organic aerosol mass spectra upon heating: implications for OA phase and partitioning behavior. *Atmos Chem Phys* **2011,** *11*, (5), 1895-1911.

54.      Kundu, S.; Fisseha, R.; Putman, A. L.; Rahn, T. A.; Mazzoleni, L. R., High molecular weight SOA formation during limonene ozonolysis: insights from ultrahigh-resolution FT-ICR mass spectrometry characterization. *Atmos Chem Phys* **2012,** *12*, (12), 5523-5536.

55.      Zahardis, J.; Geddes, S.; Petrucci, G. A., Improved understanding of atmospheric organic aerosols via innovations in soft ionization aerosol mass spectrometry. *Analytical chemistry* **2011,** *83*, (7), 2409-15.

56.      Laskin, A.; Laskin, J.; Nizkorodov, S. A., Mass spectrometric approaches for chemical characterisation of atmospheric aerosols: critical review of the most recent advances. *Environ Chem* **2012,** *9*, (3), 163-189.

57.      Yu, J. Z., Editorial: mass spectrometric approaches for chemical characterisation of atmospheric aerosols. *Environ Chem* **2012,** *9*, (3), I-Ii.

# CHAPTER 3: NEAR INFRARED LASER DESORPTION IONIZATION AEROSOL MASS SPECTROMETRY (NIR-LDI-AMS)

One of the most demanding areas of aerosol analysis is to understand the chemistry of complex organic compounds within the aerosol phases.[1] Recently, there has been a great interest in developing technologies that allow one to measure aerosol chemical composition, sizes, aerosol mixing state, aging, and multiphase reactions as a function of location and time.[1] Single aerosol particles are a complex mixture containing on the order of $\sim 10^2$ to $10^{15}$ molecules per particle, translating to masses on the order of $\sim 10^{-20}$ to $10^{-6}$ g/particle. Typical PM2.5 mass concentrations in the atmosphere range from $\sim 1$ to 50 $\mu g/m^3$ in rural locations to up to $\sim 200$ $\mu g/m^3$ in highly polluted urban areas.[2] In addition to primary emission of particles, SOA is also formed, which can be chemically complex, consisting of >10,000 organic compounds, and comprise a significant fraction of organic aerosol mass. Thus, the measurement of chemical composition of atmospheric particles represents a significant analytical challenge.[3] Comprehensive analysis of diverse mixtures of aerosol requires multi-dimensional measurements and applications of complementary analytical methods that provide experimental data ranging from bulk measurements, such as mass loadings of simplified aerosol classes to in-depth properties of individual particles and advanced molecular-level characterization of complex molecules comprising organic particulate matter.[1, 4] No single instrument can perform all these tasks and overcome the challenges.

## 3.1 Aerosol Mass spectrometry (AMS)

Mass spectrometry (MS) techniques have an overall versatility of sensitive detection of a range of chemical species, providing high-throughput qualitative and

quantitative data on physicochemical properties of aerosols in laboratory, test facilities, and field studies.[4] Owing to a broad range of MS analytical capabilities, with variations in sample introduction approaches, ionization techniques and mass detectors, a field of 'Mass Spectrometry of Atmospheric Aerosol' has been established and has quickly become the most essential and fastest growing area of aerosol research.[4] Comprehensive descriptions of AMS methods and their application to atmospheric science have been given in several recent reviews.[1-7]
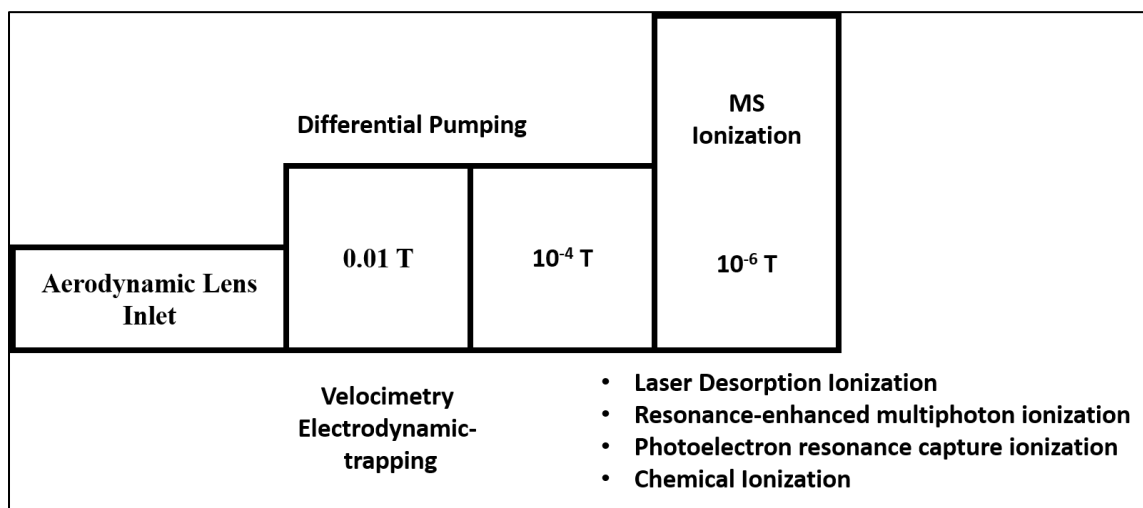


*Figure 3.1 Block diagram for Aerosol Mass Spectrometer[6]*

A generic block diagram of an aerosol mass spectrometer is shown in Figure 3.1. An AMS typically is comprised of a particle inlet and differential pumping system, a source region where desorption/ionization occurs (e.g., laser desorption/ionization and thermal desorption followed by electron impact or chemical ionization), and a mass analyzer (e.g., time-of-flight (TOF) and quadrupole).

The most critical component in AMS is the sample introduction system, where introduction of minute quantities of sample require a very efficient particle transport system from the inlet to the ionization region. Major advancement came through in 1995

with the development of an aerosol inlet, a so-called aerodynamic lens, which consists of a 100µm flow limiting orifice attached to a 1 cm inner diameter, 30 cm long tube.[8, 9] A series of carefully designed and machined apertures gently force the particles to the center of the tube by the time they reach the end of the lens where a 2mm nozzle accelerates the particles into the vacuum (Figure 3.2). In general, the aerodynamic lens system is used to focus aerosol ranging from 0.040 –1 µm into a very tight beam, though transmission efficiency is close to 100% only for particles in the 60–600-nm range. Efficiency drops off noticeably for smaller and larger particles (e.g., 25% efficiency for 1µm).[10] The aerodynamic lens system is definitely the most popular choice for particle-beam focusing (into a point where particle collection or desorption/ionization of a single particle will occur).
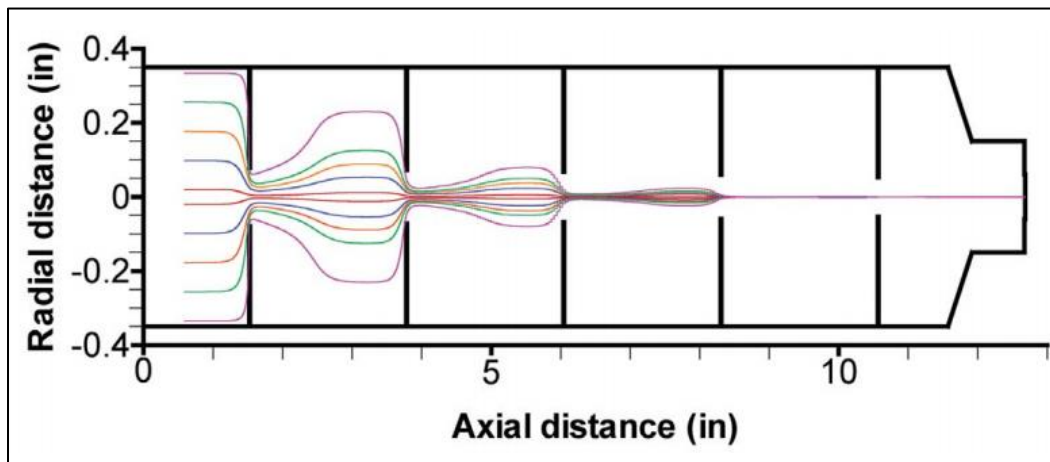


*Figure 3.2 Aerosol trajectory through an aerodynamic lens [11]*

AMS instruments are usually grouped into two categories based on their ionization mechanism, i.e., hard ionization AMS and soft ionization AMS. Methods that employ high energy ionization processes, which typically provide high ionization efficiencies at the expense of molecular information, are referred to as hard ionization AMS, whereas techniques specifically designed to prevent extensive fragmentation of molecules are

27

referred to as soft ionization AMS. The chemical composition of the particle plays a role in the choice of ionization methods. Salts, metals, and crustal particles are most efficiently desorbed and ionized by a strong UV laser pulse, whereas the more easily vaporized organic molecules are better ionized by electron impact, chemical ionization, electron attachment, or one-photon vacuum UV ionization.[2]

Instruments that employ hard ionization sources are the most widespread and have been used in both laboratory and field measurements throughout the world, resulting in many important advances in knowledge of atmospheric aerosols and their processing.[12-15] However, utilizing hard ionization methods makes mechanistic investigations of complex SOA extremely difficult as all the molecular information is lost due to fragmentation. Thus, a great emphasis has been given to development of soft ionization methods that impart less energy to the analyte molecule, resulting in little or no fragmentation.

Broadly, soft ionization methods (as applied to AMS to date) can be classified into two categories: chemical ionization (CI) and pulsed-laser methods. CI produces analyte ions via reaction of the gas-phase analyte molecule with a separately generated reagent gas ion. This low energy transfer often results in the formation of a single mass ion without any fragmentation.[16-18] Pulsed laser methods employ single or multi-photon ionization as well as use of low energy photoelectrons generated by directing photons onto a metallic surface resulting in analyte ions with little or no fragmentation. [19-21] A unique soft ionization custom built AMS system was developed in our lab that utilizes a low energy pulsed laser to desorb and ionize analyte molecules from a suitable collection surface.[21, 22] Details of the method are provided in the next section.

## 3.2 NIR-LDI-MS

NIR-LDI-AMS employs a single-wavelength of near-infrared radiation for both desorption and ionization of the organic component from a suitable collection surface. This method integrates the strategies of matrix-free LDI with AMS. Several types of nanostructured surfaces, such as silicon surface (DIOS)[23, 24], aluminum[25] , porous alumina[26] and stainless steel,[25] have been used successfully for matrix free LDI. Even though DIOS has received huge success, it is often tedious to obtain reproducible surfaces with the same nanostructures which often resulted in fragmentation. Moreover, storage of DIOS chips is problematic because the silicon surface tends to form an oxidized layer that reduces the signal intensity. It has been established that surface porosity, irrespective of the surface material, is a key factor for promoting signal intensity in LDI.[27] Formation of porous alumina structures by anodizing Al is a well-established technique which offers great reproducibility and has found several applications. In 2008, Hsu etal. demonstrated the use of inexpensive commercial Al foil to measure biomolecules with desorption ionization on metal (DIOM) without any surface modifications, generating great signal intensity with good signal to noise ratio and limited fragmentation.

The NIR-LDI-AMS instrument (Figure 3.3) consists of a Liu-type aerodynamic lens[8, 9] mounted on a modified high-vacuum flange to permit X-Y adjustments and supported by a Z-manipulator inside the first vacuum stage, pumped by a 500Lmin$^{-1}$ turbomolecular pump (TMH 521, Pfeiffer Vacuum, Nashua, NH). A ball valve is used to sample aerosol into the instrument through a 100μm diameter critical orifice (O'Keefe Controls, Monroe, CT) at the entrance of the inlet, which sets the aerosol sampling rate to 83 cm$^3$ min$^{-1}$. The particle beam is directed through a 5mm orifice (separating stages 1 and

2) into the high vacuum ionization region (pumped with a second 500Lmin$^{-1}$ turbomolecular pump) where it impinges upon a modified collection surface (discussed in detail below). This probe, mounted centrally in the ion extraction region of a reflectron time-of-flight mass spectrometer (R.M. Jordan Inc., Grass Valley, CA), is readily accessible via a high vacuum load lock (Nor-Cal Products Inc., CA). Alignment of the particle beam to the collection probe is aided by the use of a 150mW continuous wave (cw) 532 nm laser (Viasho VA-I-N-532, Beijing, China) focused to a spot in front of the probe, allowing visualization of high particle density beams; however, this is turned off during mass spectral measurements.
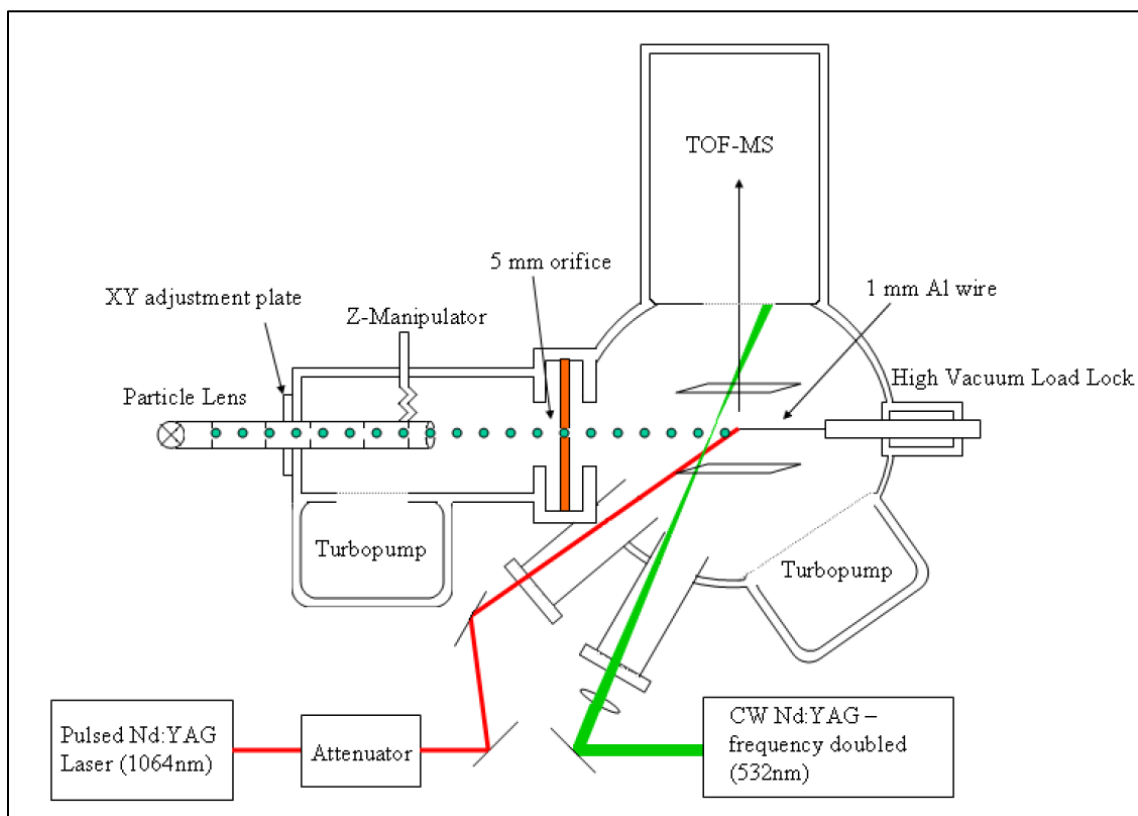


*Figure 3.3 Schematic diagram of the custom-built NIR-LDI-aerosol mass spectrometer.*

      Following particle deposition, laser desorption and ionization are performed with a 1064 nm laser pulse (5 ns) from a Nd:YAG laser (model Brio, Quantel, Big Sky, CO)

incident on the collection surface at approximately 30° from normal. The laser passes through a high energy beam attenuator (model 935-5-OPT, Newport, CA), offering fine control of the pulse energies, and is steered onto the collection probe with no additional focusing. Laser energy densities on the probe are ~4 mJ mm$^{-2}$ (80 MW cm$^{-2}$). The laser spot size covers the collection probe surface, ensuring small variations in the beam direction have a minimal effect on desorption /ionization process.

A pulse generator (DG535 from Stanford Research Instruments, Sunnyvale, CA) is used to control the delay time between laser Q-switch trigger and the ion extraction pulsed power supply (Model PVM-4210, Directed Energy, Inc., Fort Collins, CO). Typical delay times of 3-5 μs are employed in order to reduce the high energy ion signals observed to originate directly from the Al wire and obtain the pseudo-molecular ions of the adsorbed molecules. Mass spectral data is acquired at 1 GS/s with a digital oscilloscope (WavePro 7000, LeCroy, Chestnut Ridge, NY), which currently limits data acquisition to one mass spectrum (i.e., laser firing) per second. The mass spectrometer was configured to operate in negative ion mode, with all ions detected as [M-H]$^-$ anions. The working mass range of the instrument is 0−500 m/z. The measured mass spectral resolving power (m/Δm) is 1430 at 175 m/z and 2100 at 203 m/z. All mass spectra shown are averages of 4−6 laser shots (typically sufficient to vaporize all the collected SOA from the probe).

The current design of our NIR-LDI-AMS instrument has 2 main limitations. As mentioned in chapter 2, ambient SOA particles could exist as non-liquid particles (i.e., solid, semi-solid, amorphous) during part of their atmospheric residence time. For the sake of simplicity, in the remainder of the thesis, non-liquid particles will simply be referred to as "solid particles," without detailed regard of the actual phase or structure. Unlike liquid-

phase particles, solid particles can bounce off the collection probe within the AMS, which can a) significantly decrease collected aerosol and decrease overall instrumental sensitivity; b) bias AMS measurement of aerosol in favor of liquid-phase particles over those with a solid phase. Moreover, as will be shown in this chapter, the material of the collection surface can have a significant impact on the sensitivity and limit of detection (LOD) of the instrument while keeping the same signal to noise ratio.

The main aim of the work presented in this chapter is to overcome the stated limitations and to optimize the NIR-LDI-AMS analytical performance. Enhanced collection efficiency for solid particles was achieved by modification of the OA collection probe, which included physically modifying the surface (for example, roughening, changing overall shape of probe, etc.) and/or chemical modification to make the probe "stickier." To further increase the performance of NIR-LDI-AMS, a systematic variation of different collection surfaces/metal probe was performed. In each case, the limit of detection for oleic acid POA was used as the metric for analytical performance.

## 3.3 Experimental

### 3.3.1 Chemicals and metal probes

Phosphoric acid, acetic acid, nitric acid, sodium hydroxide and sodium carbonate, i.e., the chemicals needed for chemical modification of the collection probe, were purchased from Sigma Aldrich and used without further purification. Different metal probes (Magnesium, Aluminum, Silver, Copper, Lithium and Tungsten), were purchased from ESPI metal. All the probes were 0.125" diameter and 4N purity (i.e., guaranteed purity of atleast 99.99%).

### 3.3.2 Probe Modification methods

Since Aluminum had been the probe material of choice prior to my work on this project, all probe modifications were performed on an Al metal probe. Probes were modified by either dry etching or wet etching or a combination of both. For *dry etching,* an air gun (AEC-K air eraser kit, Paasche Airbrush company, IL) was used to roughen the Aluminum probe surface with a high velocity fast cutting compound: i.e $Al_2O_3$ particles (AEX-5, air eraser compound, average particle size of 50 microns, Paasche Airbrush company, IL). For *wet etching*, three different solutions were used (Table 3.1).[28, 29] Phosphoric acid is a common and recommended etching chemical for Al as it's easy to use and provides a fast and reproducible etch. Other etchants which utilize HF were not use due to the associated hazards. In each case, the probe was immersed in the solution for one hour. A combination of wet and dry etching was also used, where the probe was first wet etched for 1 hour followed by air gun etching.

*Table 3.1 Different etching solution for probe modification*

| Solution 1 | 16:1:1:2 (Phosphoric acid : Acetic acid : Nitric acid : Water ) Volume ratio |
|---|---|
| Solution 2 | 4:4:1:1 (Phosphoric acid : Acetic acid : Nitric acid : Water ) Volume ratio |
| Solution 3 | Equal volume each of Sodium Hydroxide , Sodium carbonate and water |

### 3.3.3 Generation of POA

Initial calibration and parameterization of the NIR-LDI-AMS instrument was carried out using OL particles as a proxy for organic aerosol and used to estimate the limit of detection (see section 3.3.6) of various metal probes. Particles were generated by homogeneous nucleation of oleic acid (Malinckrodt Chemicals, Phillipsburg, NJ) vapor generated in a small flask held at 110 °C and flushed through a condenser by a flow of zero

air (USP Medical Air, Airgas East, Williston, VT) into a small, 772L Teflon chamber. Aerosol particle number and mass size distributions (Figure 3.4) were measured with a scanning mobility particle sizer (SMPS: Model SMPS 3080, TSI Inc., Shoreview, MN). Aerosol (number) geometric mean diameter and standard deviation were typically on the order of 150 nm and 1.3, respectively.
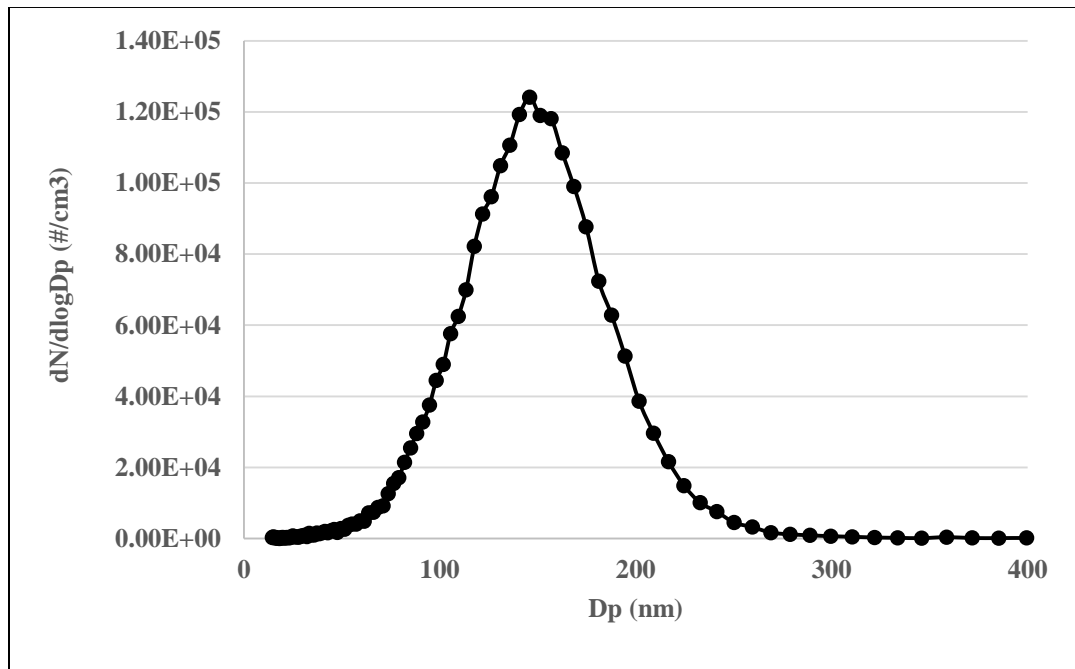


*Figure 3.4 Typical OL aerosol size distribution*

### 3.3.4 Relative Sensitivity Measurements

Oleic acid was also used as an internal standard to measure the instrumental response for different analytes of environmental interest. Internally mixed particles of the analyte(s) with oleic acid were generated by nebulization of ethanolic solutions. Solutions were typically prepared to be 50 ppmv oleic acid in ethanol and the concentration of the second analyte adjusted accordingly to yield ion signals of similar amplitude. The solution was then nebulized using a glass, concentric pneumatic nebulizer (J.E. Meinhard Associates, Santa Ana, CA) and the particles desolvated by passage through a diffusion

drier (length = 60 cm). Aerosol deposition times on the probe were typically on the order of a 10-30 seconds.

### 3.3.5 Generation of SOA

SOA was generated by introduction of VOC to the 772L Teflon chamber quantitatively by evaporating 10 µL of analyte of interest for 15 min from a three-neck flask over a warm water bath into a carrier flow of zero air. This resulted in a VOC mixing ratio in the chamber ranging from 200-500 ppb. Ozone, generated from dry, particle-free air by corona discharge (OL80A/DLS, Ozone Lab, Burton, BC, Canada), was then introduced to the chamber in a 30-60 s burst, until the desired concentration was attained. All the experiments in this chapter were performed using 1:1 mol ratios of VOC to Ozone.

### 3.3.6 Analytical figure of Merit

The signal response of the NIR-LDI-AMS was monitored at the m/z values corresponding to the pseudo molecular [M-H] $^-$ ion for each aerosol analyte. Calibration curves were generated for the pseudo molecular ion signals as a function of aerosol mass sampled into the aerodynamic lens. Using single-variable regression analysis (i.e., the method of least squares), linear regression equations were fitted to each calibration curve. The LOD for each analyte was defined as the sampled aerosol mass necessary to produce a blank-corrected pseudo molecular ion signal three times larger than the standard deviation of the blank signal ($3\sigma$). It should be noted that the calculated figures of merit refer to masses of aerosol particles sampled into the aerodynamic lens, and do not take into account potential sampling losses or non-unity particle collection efficiencies.

## 3.4 Results and Discussion

### 3.4.1 Modification of Aluminum probe

In order to overcome the first stated limitation of NIR-LDI-MS (i.e., improving the collection efficiency and sensitivity towards solid particles) it was necessary to modify the collection probe in such a way as to minimize particles bouncing off the probe upon impact. Visual inspection of the probe under the microscope (0.57mm * 0.28mm) after the modification (such as the probe with best pores and grooves) was used to choose the best surface.
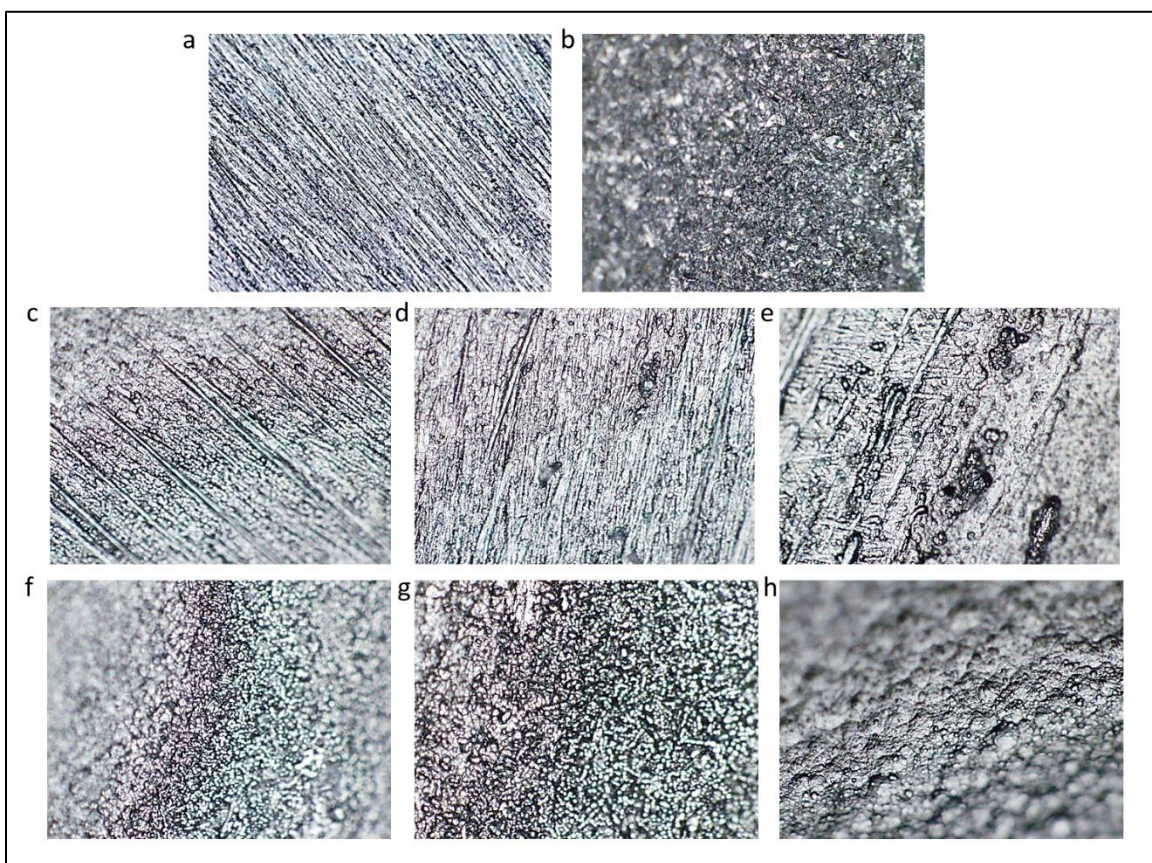


*Figure 3.5 Images for different probe modification a) no modification, b) air gun dry etch, c) solution 1 wet etch , d) solution 2 wet etch , e) solution 3 wet etch, f) solution 1 wet etch + air gun dry etch, g) solution 2 wet etch + air gun dry etch, h) solution 2  wet etch + air gun dry etch*

The first major modification, which was not actually directed at minimizing particle bounce, was to increase the diameter of the collection probe to 3mm from 1mm. AMS uses

an aerodynamic lens system to focus aerosol particles ranging from 0.040 –1 µm in diameter into a very tight beam. The transmission efficiency is close to 100% only for particles in the 60–600-nm range, with an assumption that particles are spherical in nature. However, the efficiency drops off noticeably for non-spherical particles. Hence for solid or non-liquid particles which are non –spherical, we can't expect a very tightly focused particle beam, suggesting formation of a broader particle beam. In order to effectively collect all the particles from the broader particle beam, it seemed obvious to use a bigger diameter collection probe. Moreover, the laser spot size is approximately 3 mm and would still cover the entire collection probe surface, ensuring small variations in the beam direction would have a minimal effect on the desorption /ionization process.

Next, the 3 mm probes were chemically modified to increase surface roughness, thereby potentially improving the collection efficiency for solid particles. Figure 3.5a-f shows images of the probe surface subjected to different solutions for wet etching. Figure 3.5a shows a freshly prepared aluminum metal probe with no modification, whereas figure 3.5b shows an air gun dry etched aluminum surface. Clearly, the etched surface seems uneven with tiny grooves or pores, which might aid to capture the solid particles. Furthermore, one of three different solutions was also used for wet etching with (Figure 3.5 f, g, h) and without (Figure 3.5 c, d, e) an initial dry etch step to see if surface topography can be further improved.

Aluminum was typically etched in a hot sodium hydroxide solution (solution 3) for an hour as shown in Figure 3.5e; however, this did not yield a surface better than the air gun etch. Even the combination of solution 3 with air gun etch (Figure 3.5h) didn't produce a highly porous grooved surface. Phosphoric acid solutions (solution 1, 2), which are

37

commonly used for steel etching, were also used as etchant for aluminum. Under natural conditions, aluminum and its alloys are coated with a thin layer of γ-AlOOH and bionite $Al_2O_3 \cdot H_2O$. When aluminum metal is dipped into the etchant bath (based on $H_3PO_4$), the oxide film is removed, and a part of Al dissolves into the solution by the reaction

$$2Al \qquad + \qquad 6H_3PO_4 \qquad \rightarrow \qquad Al_3^+ \quad + \qquad 6H_2PO_4^- \qquad + \qquad 3H_2\uparrow$$
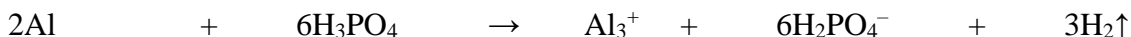
As shown in Figure 3.5 c,d,f,g, this method did yield a more porous and grooved surface as compared to Solution 3. However, it seemed shiny, which is opposite of what was desired. Hence, it was not better than the air gun etch by itself. It was decided, then to use the air gun etch method for modification of the probe surface. This same dry etching process was also applied to probes of different metals.

**3.4.2 LOD for different metal probes for different analytes**

Six different probe materials having vastly different properties (Table 3.2) were tested for optimization of NIR-LDI-AMS. Each of the metal probes was 3 mm in diameter and air gun etched. Again, OL was used as the proxy for organic aerosol to evaluate each of the probe materials. The signal response of NIR-LDI-AMS for pure OL particles, generated by homogeneous nucleation, was monitored for the 281 m/z [M-H]⁻ ion of OL, which was the base peak in all acquired mass spectra (Figure 3.6).

A linear response ($R^2 > 0.985$) was observed for the OL ion signal as a function of aerosol mass sampled into the NIR-LDI-MS. For these measurements, OL mass loadings in the 772L Teflon chamber ranged from 15 - 25 µg m⁻³, as measured by the SMPS, with particles being deposited onto the Al probe for periods of 10-150 s to achieve total aerosol mass depositions ranging from 0.30 - 6.0 ng.

*Table 3.2 Different test materials for metal probe*

| | Work Function | Electron Affinity (eV) | Ionization potential (eV) | Melting Point (ºC) | Density (g/cm³) | Specific Heat (J/gºC) | 1st Ionization energy (kJ/mol) |
|---|---|---|---|---|---|---|---|
| Lithium (Li) | 2.32 | 0.618 | 5.39 | 180 | 0.534 | 3.48 | 519.9 |
| Magnesium (Mg) | 3.61 | <0 | 7.65 | 649 | 1.738 | 1.025 | 737.3 |
| Aluminum (Al) | 4.28 | 0.441 | 5.98 | 660 | 2.69 | 0.9 | 577.2 |
| Silver (Ag) | 4.35 | 1.302 | 7.57 | 962 | 10.5 | 0.237 | 730.5 |
| Copper (Cu) | 4.51 | 1.228 | 7.72 | 1083 | 8.96 | 0.385 | 745 |
| Tungsten (W) | 4.55 | 0.815 | 7.98 | 3410 | 19.3 | 0.133 | 769 |
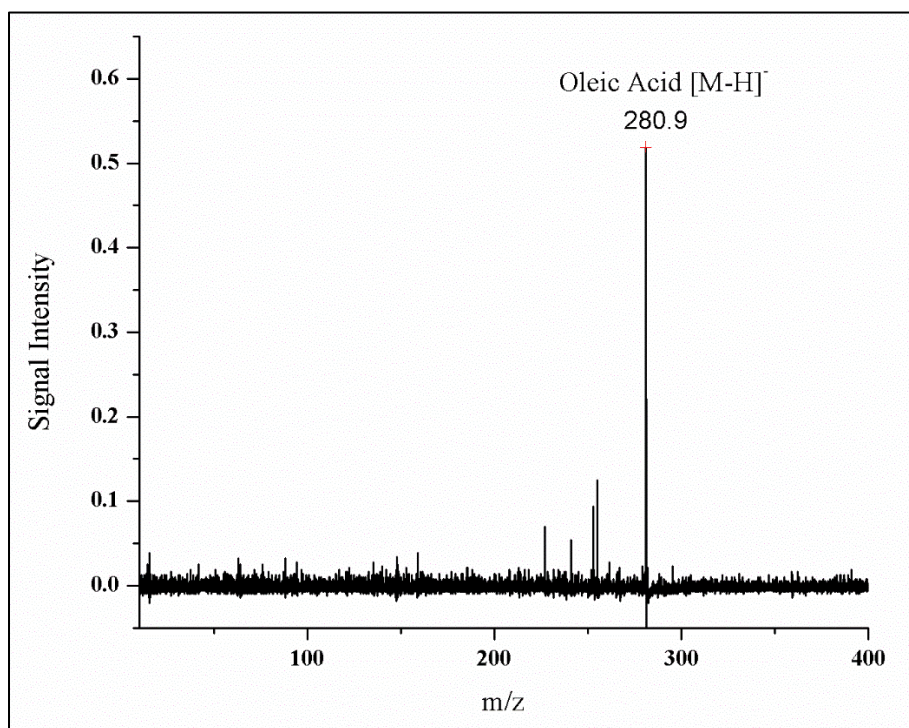


*Figure 3.6 Typical NIR-LDI-AMS spectrum of oleic acid particles i.e. the base peak in all acquired mass spectra sampled by the NIR-LDI-MS.*

Figure 3.7 shows the calibration curves obtained for the different metal probes studied. The analytical sensitivity and instrumental limits of detection for OL are summarized in Table 3.3. Among the tested probe materials, Al and Mg probes yielded the best, analogous LODs of about 1 pg, whereas the W and Li probes did not produce any signal. The Al probe is twice as more sensitive as compared to the Mg probe. The LDR for Mg was only 13 – 90 pg, whereas the Al probe has a much greater LDR of 60 – 600 pg. The Ag probe has an analytical sensitivity and LDR in the same order of magnitude as Al probe however the measured LOD was a factor of 2 worse than Al and the results were less reproducible, as evident from the error bars (Figure 3.7)
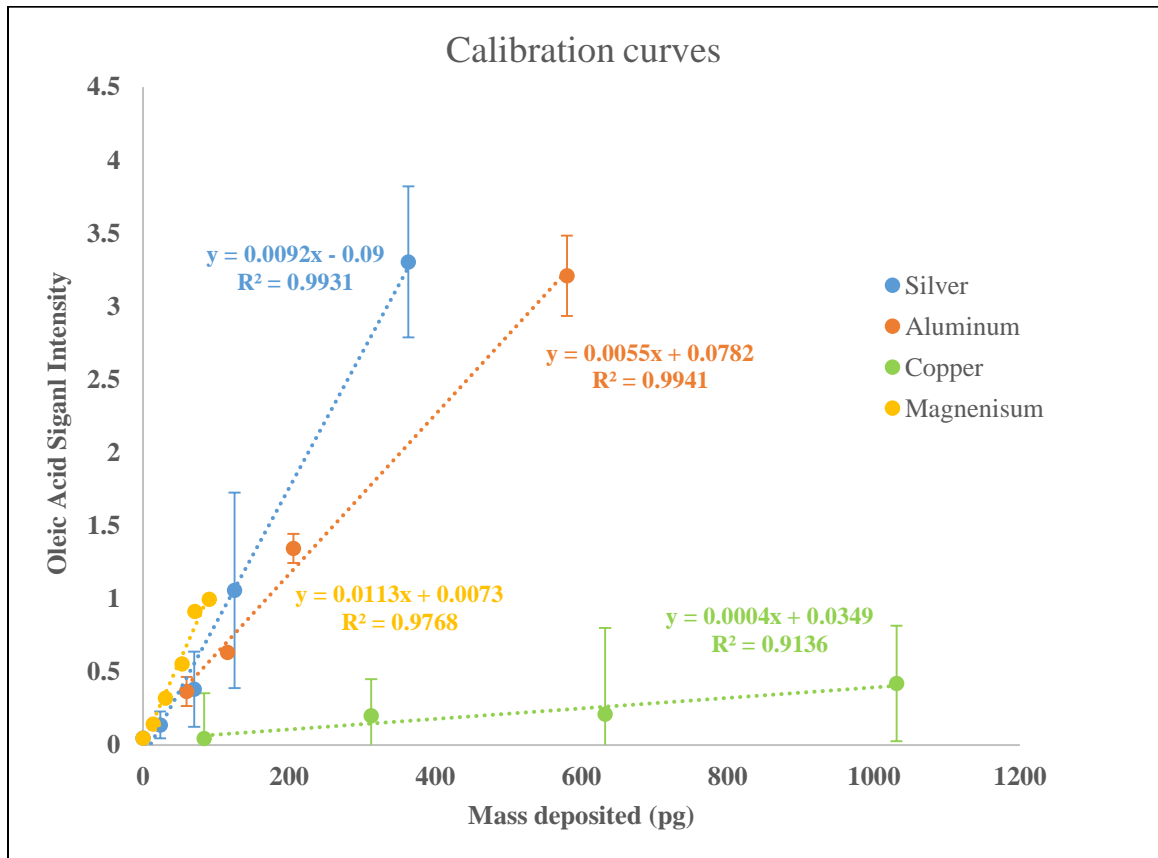


*Figure 3.7 Calibration curve for pure oleic acid particles (geometric mean diameter and standard deviation of 180 nm and 1.3, respectively). Error bar represents standard deviation of 3 replicate experiments.*

40

Al and Mg probes were also used for measurement of relative sensitivities for other analytes of interest to SOA. This is not straightforward due to difficulties with fractionation effects in the homogeneous nucleation process; therefore, the signal response of NIR-LDI-AMS for other organic analytes was determined by studies featuring internally mixed particles (generated by solution nebulization), where oleic acid served as an internal standard for comparison. The C9 dicarboxylic acid (azelaic acid, 188 u), which is a cooking emission and a chemical product resulting from oxidation of fatty acids, and nonanal, an oxidation product of α-pinene SOA, were used for these sensitivity studies. The mole ratios for AA and NL to OL was 2:1.

*Table 3.3 Summary of LOD and sensitivity of oleic acid by different metal probes*

| Metal Probe | Limit of detection (LOD), pg | Analytical Sensitivity V/pg |
|---|---|---|
| **Magnesium (Mg)** | **1.06** | **0.0113** |
| **Aluminum (Al)** | **1.09** | **0.0055** |
| **Silver (Ag)** | **2.40** | **0.0092** |
| **Copper (Cu)** | **23.1** | **0.0004** |

For the *Mg metal probe*, azelaic acid had a sensitivity relative to oleic acid, $S_{A/OL}$, of 0.35, corresponding to an instrumental LOD of 3 pg. The relative sensitivity for nonanal was 0.15, corresponding to an LOD of 6.8 pg. On the other hand, for the *Al metal probe*, azelaic acid was determined to have a sensitivity relative to oleic acid, $S_{A/OL}$, of 2.37, corresponding to an instrumental LOD of 0.458 pg and the relative sensitivity of nonanal was 0.108, corresponding to an LOD of 10.1 pg.

The enhanced performance of the Mg and Al probe over other probes is not immediately apparent but could have to do with the work function of each metal probe.

Oleic acid signal was measured only for metals having a work function ranging between 3.5 – 4.5. Lithium and tungsten, which have work functions < 3.5 and > 4.5 respectively, did not produce a signal. Also, Mg, which had the lowest work function among the group of selected metals, yielded the best LOD and an increase in work function resulted in a decrease in LOD.

Despite the analogous results obtained for Al, Mg and Ag probes, Al was chosen as the probe material for future experiments because it yielded higher relative sensitivities to carboxylic acids (of special relevance to SOA chemical studies) as compared to other metal probes, higher LDR, reproducibility and similar LODs to Mg and Ag. Once the probe material was selected, attempts were made to gain a nascent understanding of the mechanism(s) of ion generation in NIR-LDI-AMS by conducting power studies, as described in the next section.

### 3.4.3 Power study for metal probe

The phenomenon of ionization in LDI methods remains the most unclear as it has not yet been determined whether ionization takes place before or after the desorption step. First it is essential that photon absorption by the collection surface happens in the range of the laser wavelength which absorbs energy from a laser and then transfers the energy to the target sample to effectively desorb and ionize with little or no fragmentation. The mechanism of ionization for NIR-LDI-AMS has been shown to be functional group dependent.[21, 22] For acidic organic analytes (i.e., carboxylic acids, aldehydes, and alcohols), NIR-LDI-AMS reproducibly generates pseudo molecular anions at [M-H]⁻, hypothesized to occur through loss of an acidic proton. Generation of [M-H]⁻ via NIR-LDI-AMS was

rationalized in terms of a surface-assisted cleavage of the acidic O-H or C-H bond by the NIR laser pulse incident on the Al probe (as described below).
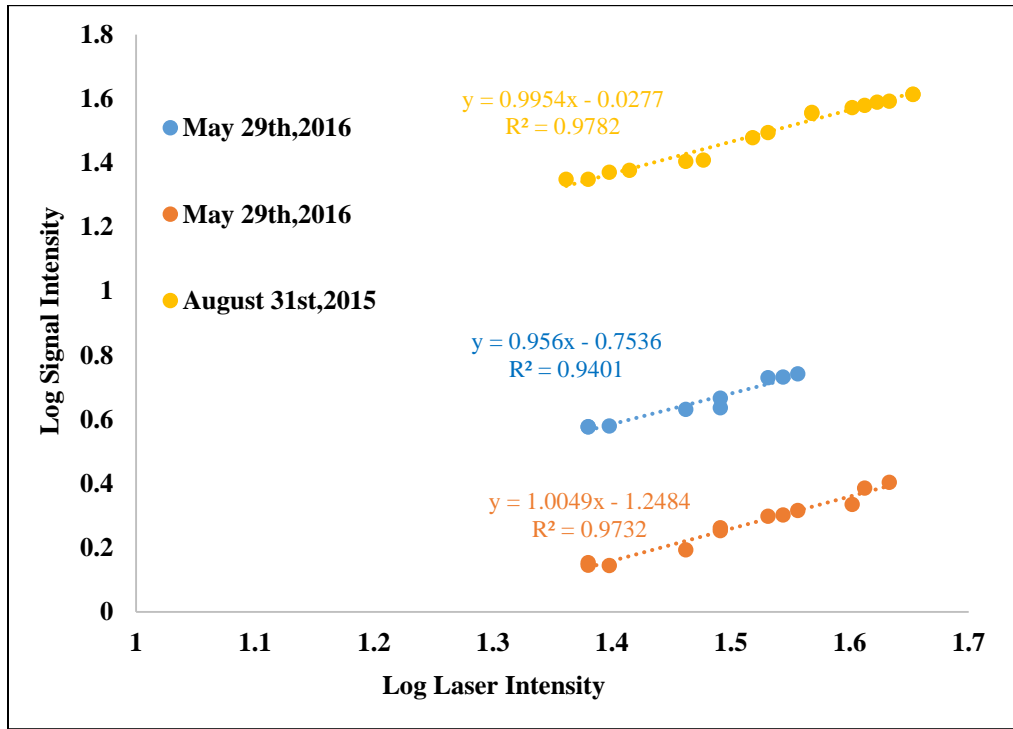


*Figure 3.8 log-log curve of the OL ion signal plotted as a function of incident laser energy*

To examine the dependence of the hypothesized ionization mechanism on the energy of the NIR laser pulse, the signal response was measured for a constant mass deposition of pure OL particles (generated by homogeneous nucleation). Based upon previous work by Petrucci *et.al.* [30], the dependence of the OL ion signal on the incident laser energy was represented by a simple power dependence:

$$S \propto L^k \qquad\qquad [1]$$

where S is the ion signal (V), L is the incident laser energy (mJ), and k is the number of photons per ionization event. From the slope of the log-log curve of the OL ion signal plotted as a function of incident laser energy (Figure 3.8), the signal intensity was found to exhibit a first-order dependence ($k = 0.9$ ; $R^2 = 0.97$).

Two potential mechanisms for the generation of ions in NIR-LDI-MS have been proposed in past i.e. photo ionization and surface assisted ionization. Direct photolysis of the O-H bond of OL would require simultaneous absorption of five photons at 1064 nm ($1.87 \times 10^{-19}$ J photon$^{-1}$) based on typical values for the O-H bond dissociation energy of organic acids at 298 K ($\Delta H$ 298 = 464 - 469 kJ mol-1).[31] This, however, is not occurring as indicated by the linear dependence of ion signal on laser intensity. Rather, contrary to this, it was found that another instrument operating in the same mode nominally, i.e., Bipolar NIR-LDI-AMS, exhibited a second-order dependence (k = 1.986; $R^2$ = 0.988), suggesting a simultaneous action of two 1064 nm photons for formation of ions. We do not have an explanation for this discrepancy, but work continues in this respect. Nonetheless, in spite of this discrepancy, results from both power studies suggest a surface assisted mechanism for ion formation.

### 3.4.4 Application to measurement of ambient organic aerosols

The utility of improved NIR-LDI-AMS to monitor chamber-based SOA at ambient levels of total organic particulate mass was demonstrated. Preliminary experiments validating the improved and modified instrument were conducted on chemical systems studied and reported on previously in the literature, such as limonene and α-pinene. As will be shown in subsequent chapters (Chapter 5, 6), both limonene and α-pinene upon oxidation generated SOA which is solid in phase.

Particle-phase oxidation products of α-pinene were measured directly with this modified NIR-LDI-AMS with high time resolution under atmospherically relevant aerosol mass loadings, $C_{OA}$, in the range of 1.5-8.7 μg m$^{-3}$. Also, NIR-LDI-AMS was used to study the oxidation of limonene, which, as a prevalent biogenic emission from vegetation, as well

as being a commonly added agent to household cleaners, is of importance to both atmospheric and indoor chemistry. Preliminary results show that at low $C_{OA}$ levels, the initial conditions of the aerosol-forming reactions result in strikingly diverse outcomes.

Limonene presents an interesting SOA precursor because it has two double bonds: an endocyclic trialkyl substituted double bond and a terminal exocyclic double bond (Figure 3.9). These contribute to limonene's high potential for SOA formation because both double bonds can be oxidized with little or no carbon loss. Moreover, studies[32] have shown that endocyclic double bond is 30 times more reactive than exocyclic double bond. In general the more substituted double bond is more reactive. Given this difference in reactivity, one might expect a clean separation in oxidation steps during ozonolysis. A mechanism for ozonolysis of limonene has been established previously.[22] This separation in oxidation step has been shown for a number of systems, leading to characteristic 'hooks' in growth curves [33] plotting SOA mass as a function of consumed terpene. Due to this separation one might expect that the order in which limonene and ozone are injected into the chamber can have an impact on the chemistry of SOA particle.

The improved NIR-LDI-AMS was used to perform some preliminary experiments to study the effect of order of introduction on SOA formation. If a VOC is injected first followed by oxidation by ozone, oxidation occurs in a VOC rich environment. On the other hand if ozone is injected first followed by injection of VOC, oxidation would occur in ozone rich environment. In order to get a better understanding, normalized ion signal intensity ratios of endo- and exo- oxidation products measured by NIR-LDI-ASM were plotted as a function of SOA mass loading.
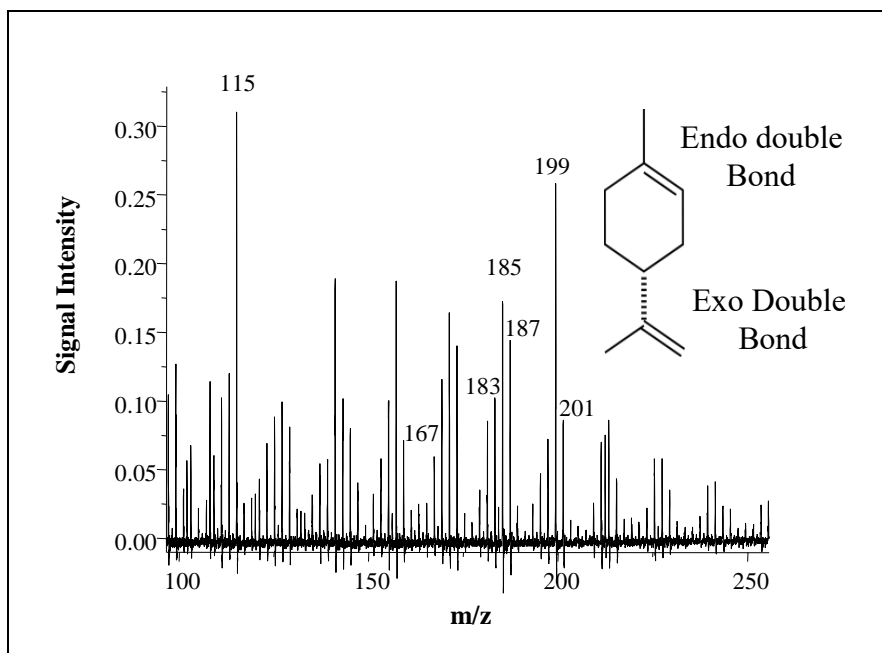
*Figure 3.9 NIR-LDI-AMS mass spectrum for Limonene SOA at $C_{OA}$ = 5.76μg/m³*

In the case of VOC rich environment, the more reactive endo bond is oxidized first in the initial stages of the reactions. As the reaction progresses, there is subsequent oxidation of the second double bond. This is supported by an increase in the ratio of exo-to-endo products as shown in Figure 3.10.
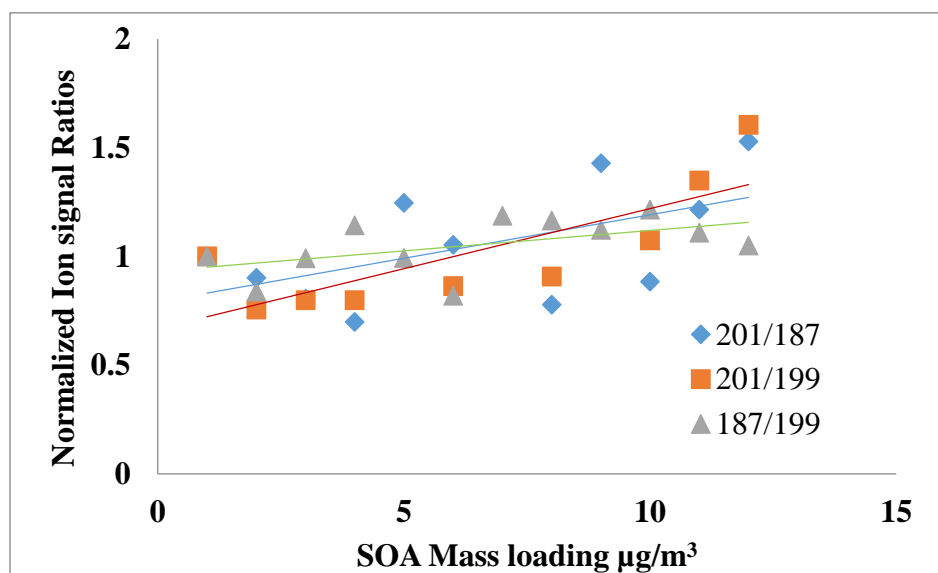


*Figure 3.10 Ratio of exo- to-endo products in case of VOC rich environment*

This implies that reaction products arising from oxidation of the endocyclic double bond are important in the early stages of SOA formation and that these products are subsequently consumed in the later stages of SOA formation and growth via oxidation of the remaining (exocyclic) double bond.[22]
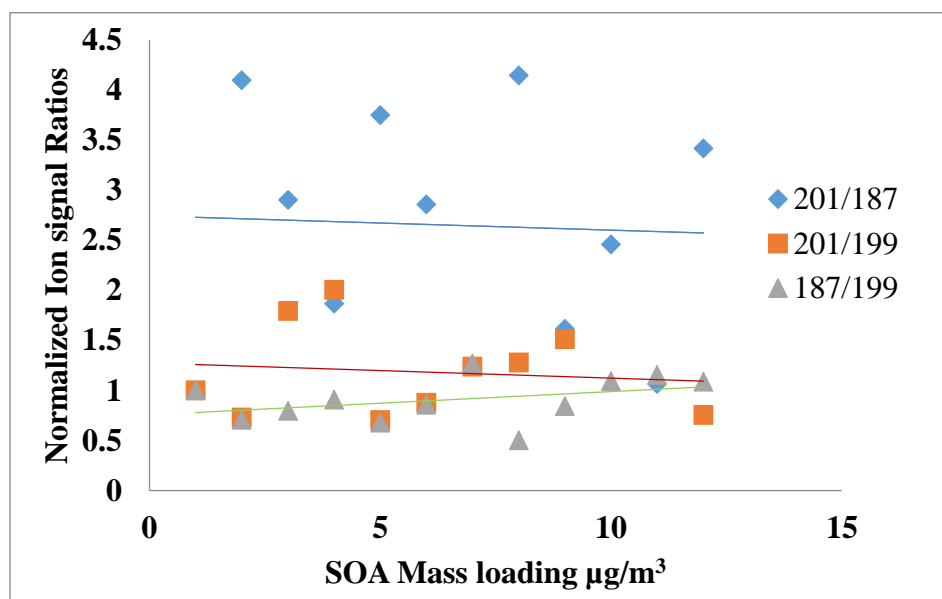


*Figure 3.11 Ratio of exo- to-endo products in case of ozone rich environment*

On the other hand, in the case of ozone rich environment, the ratio of the signal intensities between exo- and endo- products stays pretty constant (Figure 3.11). This could suggest that both double bonds are being oxidized simultaneously due to the high instantaneous ozone concentration. These experiments were not done quantitatively and trend lines are only added to show preliminary trends. The main objective of this work was to demonstrate the application of NIR-LDI-AMS for measurement of solid SOA. More elaborate work utilizing this improved methodology has been done for other chemical systems which are discussed in detail in chapter 4. These new chemical systems also form solid SOA, as will be shown in chapter 6 of this thesis. Detailed mechanisms for the oxidation of these chemical systems have also been proposed in chapter 4.

## 3.5 Conclusion

In this chapter, I described steps taken toward the instrumental optimization of an existing NIR-LDI-AMS instrument. I tested different probe metals and surface preparation methods to improve analytical performance. Ultimately, Al probes with only a dry etching were found to produce the best compromise between probe preparation and analytical performance. Finally, the use of the modified NIR-LDI-AMS for the analysis of SOA from different precursors and at atmospherically relevant levels was demonstrated.

## 3.6 References

1.      Lee, S. H.; Allen, H. C., Analytical Measurements of Atmospheric Urban Aerosol. *Analytical chemistry* **2012**, *84*, (3), 1196-1201.
2.      Nash, D. G.; Baer, T.; Johnston, M. V., Aerosol mass spectrometry: An introductory review. *International Journal of Mass Spectrometry* **2006,** *258*, (1-3), 2-12.
3.      Hartonen, K.; Laitinen, T.; Riekkola, M. L., Current instrumentation for aerosol mass spectrometry. *Trac-Trend Anal Chem* **2011**, *30*, (9), 1486-1496.
4.      Laskin, A.; Laskin, J.; Nizkorodov, S. A., Mass spectrometric approaches for chemical characterisation of atmospheric aerosols: critical review of the most recent advances. *Environ Chem* **2012,** *9*, (3), 163-189.
5.      Zahardis, J.; Geddes, S.; Petrucci, G. A., Improved understanding of atmospheric organic aerosols via innovations in soft ionization aerosol mass spectrometry. *Analytical chemistry* **2011,** *83*, (7), 2409-15.
6.      Pratt, K. A.; Prather, K. A., Mass spectrometry of atmospheric aerosolsuRecent developments and applications. Part II: On-line mass spectrometry techniques. *Mass Spectrom Rev* **2012**, *31*, (1), 17-48.
7.      Pratt, K. A.; Prather, K. A., Mass spectrometry of atmospheric aerosolsuRecent developments and applications. Part I: Off-line mass spectrometry techniques. *Mass Spectrom Rev* **2012,** *31*, (1), 1-16.
8.      Liu, P.; Ziemann, P. J.; Kittelson, D. B.; Mcmurry, P. H., Generating Particle Beams of Controlled Dimensions and Divergence .1. Theory of Particle Motion in Aerodynamic Lenses and Nozzle Expansions. *Aerosol Sci Tech* **1995,** *22*, (3), 293-313.
9.      Liu, P.; Ziemann, P. J.; Kittelson, D. B.; Mcmurry, P. H., Generating Particle Beams of Controlled Dimensions and Divergence .2. Experimental Evaluation of Particle Motion in Aerodynamic Lenses and Nozzle Expansions. *Aerosol Sci Tech* **1995,** *22*, (3), 314-324.
10.     Brands, M.; Kamphus, M.; Bottger, T.; Schneider, J.; Drewnick, F.; Roth, A.; Curtius, J.; Voigt, C.; Borbon, A.; Beekmann, M.; Bourdon, A.; Perrin, T.; Borrmann, S., Characterization of a Newly Developed Aircraft-Based Laser Ablation Aerosol Mass Spectrometer (ALABAMA) and First Field Deployment in Urban Pollution Plumes over Paris During MEGAPOLI 2009. *Aerosol Sci Tech* **2011,** *45*, (1), 46-64.
11.     Incorporated, T., Series 3800 Aerosol Time-of-Flight Mass Spectrometers with Aerodynamic Focusing Lens Technology. *Particle Instruments* **2004**.

12.      Canagaratna, M. R.; Jayne, J. T.; Jimenez, J. L.; Allan, J. D.; Alfarra, M. R.; Zhang, Q.; Onasch, T. B.; Drewnick, F.; Coe, H.; Middlebrook, A.; Delia, A.; Williams, L. R.; Trimborn, A. M.; Northway, M. J.; DeCarlo, P. F.; Kolb, C. E.; Davidovits, P.; Worsnop, D. R., Chemical and microphysical characterization of ambient aerosols with the aerodyne aerosol mass spectrometer. *Mass Spectrom Rev* **2007,** *26*, (2), 185-222.

13.      DeCarlo, P. F.; Slowik, J. G.; Worsnop, D. R.; Davidovits, P.; Jimenez, J. L., Particle morphology and density characterization by combined mobility and aerodynamic diameter measurements. Part 1: Theory (vol 38, pg 1185, 2004). *Aerosol Sci Tech* **2005,** *39*, (2), 184-184.

14.      Murphy, D. M., The design of single particle laser mass spectrometers. *Mass Spectrom Rev* **2007,** *26*, (2), 150-165.

15.      Noble, C. A.; Prather, K. A., Real-time single particle mass spectrometry: A historical review of a quarter century of the chemical analysis of aerosols. *Mass Spectrom Rev* **2000,** *19*, (4), 248-274.

16.      Hearn, J. D.; Smith, G. D., A chemical ionization mass spectrometry method for the online analysis of organic aerosols. *Analytical chemistry* **2004,** *76*, (10), 2820-2826.

17.      Smith, J. N.; Moore, K. F.; McMurry, P. H.; Eisele, F. L., Atmospheric measurements of sub-20 nm diameter particle chemical composition by thermal desorption chemical ionization mass spectrometry. *Aerosol Sci Tech* **2004,** *38*, (2), 100-110.

18.      Holzinger, R.; Williams, J.; Herrmann, F.; Lelieveld, J.; Donahue, N. M.; Rockmann, T., Aerosol analysis using a Thermal-Desorption Proton-Transfer-Reaction Mass Spectrometer (TD-PTR-MS): a new approach to study processing of organic aerosols. *Atmospheric Chemistry and Physics* **2010,** *10*, (5), 2257-2267.

19.      Oktem, B.; Tolocka, M. P.; Johnston, M. V., On-line analysis of organic components in fine and ultrafine particles by photoionization aerosol mass spectrometry. *Analytical chemistry* **2004,** *76*, (2), 253-261.

20.      Dreyfus, M. A.; Adou, K.; Zucker, S. M.; Johnston, M. V., Organic aerosol source apportionment from highly time-resolved molecular composition measurements. *Atmospheric Environment* **2009,** *43*, (18), 2901-2910.

21.      Geddes, S.; Nichols, B.; Todd, K.; Zahardis, J.; Petrucci, G. A., Near-infrared laser desorption/ionization aerosol mass spectrometry for measuring organic aerosol at atmospherically relevant aerosol mass loadings. *Atmos Measur Tech* **2010,** *3*, (4), 1175-1183.

22.      Geddes, S.; Nichols, B.; Flemer, S.; Eisenhauer, J.; Zahardis, J.; Petrucci, G. A., Near-Infrared Laser Desorption/Ionization Aerosol Mass Spectrometry for Investigating Primary and Secondary Organic Aerosols under Low Loading Conditions. *Analytical chemistry* **2010,** *82*, (19), 7915-7923.

23.      Shen, Z. X.; Thomas, J. J.; Averbuj, C.; Broo, K. M.; Engelhard, M.; Crowell, J. E.; Finn, M. G.; Siuzdak, G., Porous silicon as a versatile platform for laser desorption/ionization mass spectrometry. *Analytical chemistry* **2001,** *73*, (3), 612-619.

24.      Thomas, J. J.; Shen, Z. X.; Crowell, J. E.; Finn, M. G.; Siuzdak, G., Desorption/ionization on silicon (DIOS): A diverse mass spectrometry platform for protein characterization. *P Natl Acad Sci USA* **2001,** *98*, (9), 4932-4937.

25.      Hsu, N. F.; Tseng, S. Y.; Wu, C. Y.; Ren, C. T.; Lee, Y. C.; Wong, C. H.; Chen, C. H., Desorption ionization of biomolecules on metals. *Analytical chemistry* **2008,** *80*, (13), 5203-5210.

26.      Nayak, R.; Knapp, D. R., Effects of thin-film structural parameters on laser desorption/ionization from porous alumina. *Analytical chemistry* **2007,** *79*, (13), 4950-4956.

27.      Alimpiev, S.; Nikiforov, S.; Karavanskii, V.; Minton, T.; Sunner, J., On the mechanism of laser-induced desorption-ionization of organic compounds from etched silicon and carbon surfaces. *J Chem Phys* **2001,** *115*, (4), 1891-1901.

28.     Engineering, D. o. e. a. C. Wet Chemical Etching of metals and semiconductors. http://www.cleanroom.byu.edu/wet_etch.phtml

29.     Department of engineering, D. C., Etching Metal Films **2015**.

30.     Petrucci, G. A.; Winefordner, J. D., Use of the Optogalvanic Effect to Examine the Laser Power Dependency of Several Excitation Ionization Mechanisms in a Hollow-Cathode Discharge. *Appl Spectrosc* **1991,** *45*, (9), 1485-1490.

31.     Blanksby, S. J.; Ellison, G. B., Bond dissociation energies of organic molecules. *Acc. Chem. Res.* **2003,** *36*, 255-263.

32.     Zhang, J. Y.; Hartz, K. E. H.; Pandis, S. N.; Donahue, N. M., Secondary organic aerosol formation from limonene ozonolysis: Homogeneous and heterogeneous influences as a function of NOx. *J Phys Chem A* **2006,** *110*, (38), 11053-11063.

33.     Chen, X.; Hopke, P. K., A chamber study of secondary organic aerosol formation by limonene ozonolysis. *Indoor Air* **2010,** *20*, (4), 320-328.

# CHAPTER 4: SOFT IONIZATION CHEMICAL ANALYSIS OF SECONDARY ORGANIC AEROSOL FROM GREEN LEAF VOLATILES EMITTED BY TURF GRASS

The work described in this chapter was submitted and accepted for publication in the following two articles. The full references are as follows:

1) *Jain, S., Zahardis, J., Petrucci, G. A. (2014). Soft Ionization Chemical Analysis of Secondary Organic Aerosol from Green Leaf Volatiles Emitted by Turf Grass. Environ. Sci. Technol., 48 (9), pp 4835–4843*

2) *Harvey, R. M., Bateman, A. P., Jain, S., Li, Y. J., Martin, S., Petrucci, G. A. (2016). Optical Properties of Secondary Organic Aerosol from cis-3-Hexenol and cis-3-Hexenyl Acetate: Effect of Chemical Composition, Humidity, and Phase. Environ Sci Technol.*

## 4.1 Introduction

As stressed in Chapter 2, organic compounds are important components of atmospheric fine particles[1] and contribute significantly to the total fine aerosol mass at both continental mid-latitudes and tropical forested areas.[2] VOCs are ubiquitous in the troposphere, playing a key role in its chemistry and composition. Atmospheric oxidation of VOCs produces products that undergo gas-particle transfer, resulting in the formation of SOA.[2, 3] The formation and ageing of SOA has received considerable attention[2, 3] because of its potential impact on climate.[4]

Major classes of SOA precursors studied to date include alkanes, alkenes, aromatic hydrocarbons, and oxygenated compounds[2, 3] from both AVOC[5, 6] and BVOC sources.[7, 8] Biogenic VOC SOA precursors consist primarily of isoprene and monoterpenes (by mass), with the rest being other reactive (ORVOCs) and unidentified VOCs.[2, 3, 9] SOA yields from

BVOC precursors can approach 100% for some sesquiterpenes,[10] highlighting the importance of ORVOCs as a source of SOA. Recent top-down/bottom-up hybrid approaches to modeling SOA estimate a net BSOA production rate of approximately 80-90 TgC/year.[2, 4, 11]

Among BVOCs, a greater effort has been expended on SOA production from isoprene[12-14] and monoterpenes[15-17] as compared to ORVOCs, of which green leaf volatiles (GLVs) are a significant component. GLVs are unsaturated, oxygenated hydrocarbons emitted in large quantities by stressed plants (e.g., grass cutting, animal grazing or local weather changes[18-21]) by biochemical conversion of linoleic and linolenic acid within plant cells.[22-24] Grasslands emit[25, 26] up to 130 mg C $m^{-2}$ GLVs annually, with reactive lawn-GLV emissions estimated between 3.9 and 6.3 Gg C annually.[25] The GLV emission profiles[23, 27, 28] are dominated by *cis*-3-hexenylacetate (CHA) and *cis*-3-hexen-1-ol (HXL), both of which are susceptible to atmospheric oxidation. Current emission estimates[27] for CHA and HXL are in the range of 1.18 ($\pm$ 0.3) and 0.068 ($\pm$ 0.03) $\mu$g $m^{-2}$ of lawn area, respectively. These highly reactive compounds possess significant ozonolysis aerosol yields of approximately 1-10%.[23, 27] Several studies have considered the effect of GLVs on SOA formation.[21, 23] Significant progress has been made in understanding the oxidation pathways to SOA formation,[15] including for specific GLVs, such as CHA[23, 29], HXL[30] and 1-penten-3-ol.[31] Hamilton, et al. showed that the main condensed-phase products formed during ozonolysis of CHA were 3-acetoxypropanal, 3-acetoxypropanoic acid, and 3-acetoxypropane peroxoic acid.[30] These results were also supported by Li, et al. based on density functional theory.[29] There is evidence that the primary ozonolysis product of HXL is 3-hydroxypropanal, which can hydrate and undergo further reactions with aldehydes,

resulting in SOA dominated by oligomers.[23] These experiments[23, 31] have been run under a variety of conditions, but generally employ a single GLV SOA precursor. Such experiments have led to an improved understanding of SOA formation at the molecular level; however, results from experiments featuring a single precursor may not accurately describe atmospheric conditions, where multiple VOCs are susceptible to simultaneous oxidation. To the best of my knowledge, only one study[27] has been undertaken with mixed GLV systems, which, owing to the chemical complexity of mixed chemical precursors/oxidant systems, present a major challenge for state-of-the-art analytical techniques.[32-35] Only a small fraction of organic compounds are recovered using gas-chromatographic/mass spectrometric (GC/MS) techniques.[36] In order to reduce uncertainties in models predicting global and regional SOA levels, it is essential to better understand multi-component systems that are more representative of atmospheric conditions. At present, no study has attempted to describe condensed phase SOA formation from simple mixtures of GLVs, nor correlated the chemical profile of SOA generated from real mixtures (e.g., grass clippings) with that formed by these model systems.

Direct online soft ionization aerosol mass spectrometry (AMS) as described in chapter 3 is a sensitive technique to assess SOA formation at a molecular level.[37, 38] In this work metal-assisted near-infrared laser desorption/ionization (NIR-LDI) AMS[38, 39] was used to characterize the SOA generated from dominant GLVs, their mixtures, and GLVs directly emitted from grass clippings. Recently, Harvey, et al.[27] identified dominant GLVs from headspace analysis of grass clippings and quantified their relative emission rates. I used the chemical standards of these GLVs either individually or in concert to measure the resulting SOA composition. Also, I quantified the chemical similarity using Pearson's r[40]

between the various SOA systems based on the NIR-LDI data, showing that HXL-derived SOA most closely represented SOA from turf grass. The temporal evolution of selected products was also measured and used to deconvolute chemical mechanisms and elucidate later-generation products in the particle-phase. There is strong evidence that environmental conditions such as RH plays a strong role in determining chemical composition, hence some experiments were also done at varying environmental conditions in collaboration with the Harvard environmental chamber.

## 4.2 Experimental section

### 4.2.1 Reagents & equipment

All experiments involving grass clipping and standards were performed in a Teflon® (FEP, PFA) or Norton® (FEP) chamber with a volume of 775 L (Welch Fluorocarbon, Dover, NH) at ambient temperature (~ 298 (+/-2) K) and atmospheric pressure at University of Vermont. The Teflon chamber is equipped with ambient $O_3$ (Serinus $O_3$ model E020010, American Ecotech, Cincinnati, OH) and NOx (EC9041A NOx Analyzer, American Ecotech, Cincinnati, OH) analyzers. Between experiments, the chamber was passivated with $O_3$ (1-2 ppmv) overnight and then flushed with zero air until the background aerosol mass and number concentrations were below 0.1 µg/m$^3$ and 50 particles/cm$^3$, respectively. Dry, zero air was produced by passing compressed air sequentially through silica, activated carbon and HEPA filters.

Experiments concerning different environmental conditions (RH) were performed using the Harvard Environmental Chamber (HEC) operated under dark conditions and in continuous-flow mode.[41, 42] The HEC consists of a 4.7 m$^3$ PFA Teflon bag housed in a temperature and humidity-controlled room. Dry, clean, hydrocarbon-free air was produced

with a pure air generator (Aadco 737). A syringe pump was used to continuously introduce standards of CHA or HXL into a secondary chamber. A constant flow of zero air was used to sweep volatilized compounds from the secondary chamber into the HEC. Neither seed particles nor OH scavengers were used in these experiments. Ozone was produced by passing air around an ultraviolet lamp (Jelight 600) and then monitored in the chamber using a Teledyne 400 E. Humidity was controlled by passing zero air through a water bubbler (18 MΩ cm) followed by a HEPA filter and into the chamber, where it was monitored with a Rotronics humidity sensor (Hygroclip SC05). Bulk chemical properties (O:C, H:C) were measured using an Aerodyne high-resolution time of flight mass spectrometer (HR-ToF-AMS),[43, 44] according to Chen, et al. (2011).[45] The ozonolysis of CHA was performed under dry conditions only (10% relative humidity, RH) while that of HXL was performed under both dry and wet conditions (10% RH and 70% RH, respectively). Upon completion of dry-HXL ozonolysis experiments, RH was slowly increased from 10% to 70% over the course of 13 hours.

Aerosol particle number and mass size distributions were measured continuously with a scanning mobility particle sizer (SMPS, model SMPS 3080, TSI Inc., Shoreview, MN). Molecular level chemical characterization of SOA was accomplished by an improved and modified NIR-LDI-AMS[38, 39] as described briefly below, and in details in chapter 3. The vapor pressure of proposed ozonolysis products was predicted using the Estimation Programs Interface (EPI) Suite TM.[46] Estimates were made at 298K and are reported as an average of two values, as determined using the Antoine and Modified Grain methods.

CHA (>98%) and HXL (99%) were purchased from Sigma Aldrich and used without further purification. Propionaldehyde (99%) was purchased from Acros Chemicals

and also used without further purification. Grass clippings were obtained from a residential lawn in Essex Junction VT (44.487653, −73.09365), consisting primarily of *Festuca*, *Lolium* and *Poa*. Gas-phase oxidation products were measured with a thermal desorption gas chromatography mass spectrometer (TD-GC-MS), described in detail elsewhere.[27]

## 4.2.2 Near-Infrared Laser Desorption/Ionization Aerosol Mass Spectrometry (NIR-LDI-AMS)

Details of the NIR-LDI-AMS instrument are presented in chapter 3.[38, 39] Briefly, the system consists of a Liu-type aerodynamic lens[47] with a 100$\mu$m diameter critical orifice (O'Keefe Controls, Monroe, CT) that samples aerosols at 120 cm$^3$ min$^{-1}$. The resulting particle beam was directed through several stages of vacuum, before impinging on a 3mm diameter air gun etched aluminum probe (99.9% purity, ESPI metals) centered in the ionization region of the mass spectrometer. Details for alignment of the particle beam to the Al probe are described elsewhere.[39, 48] Typical aerosol masses sampled were in the range of 1 to 20 ng. Following particle collection, desorption and ionization were performed by a single 1064 nm laser pulse (5 ns) from a Nd-YAG laser (Brio, Quantel USA, Big Sky, CO) and a time of flight mass spectrometer was used for chemical analysis. The mass spectrometer was configured to operate in negative ion mode, with all ions detected as [M-H]$^−$ anions. The working mass range of the instrument is 0–500 *m/z*. The measured mass spectral resolving power (*m/Δm*) is 1430 at 175 *m/z* and 2100 at 203 *m/z*. All mass spectra shown are averages of 4-6 laser shots (typically sufficient to vaporize all the collected SOA from the probe). Individual mass spectra were collected at atmospherically relevant SOA mass loading. For grass clippings, the mass spectra were collected within the first 5 minutes of ozone injection, whereas for other chemical systems,

spectra were collected at close to the maximum SOA concentration, i.e., approximately 20 minutes into the reaction.

### 4.2.3 Grass clipping experiment

Grass clippings were obtained from a residential lawn consisting of primarily *Festuca, Lolium* and *Poa.* Sample acquisition and handling protocols are described in detail elsewhere.[27] Experiments were classified as either "headspace" or "grass clipping". Headspace experiments represent a simplified chemical system where only the volatile species emitted by cut grass were introduced into the reaction chamber and oxidized by ozone to generate SOA. For the headspace experiments, approximately 150 grams of grass clippings (wet weight) were placed in a 0.4L conical flask. Zero air was flushed through the conical flask for ~20 min into the reaction chamber, carrying the GLVs with it.

For the grass clipping experiments, approximately 0.5 kg of grass clippings (wet weight) was placed directly inside the experimental chamber, which was then filled with zero air and allowed to equilibrate for 10 minutes. Ozone was injected as a brief burst (~60 s) directly into the chamber. Grass clipping experiments were designed to more accurately represent environmentally relevant conditions, where ozone was allowed to interact with volatile species in the gas phase, along with any reactive species contained within or on the blades of grass.

### 4.2.4 GLV standard experiments

Single GLV standards were introduced in the chamber quantitatively by evaporation for 15 minutes from a three-neck pear flask over a warm water bath into a carrier flow of zero air. Ozone, generated from dry, particle-free air by corona discharge (OL80A/DLS, Ozone Lab, Burton, BC, Canada), was then introduced to the chamber in a

30-60 s burst, until the desired concentration was attained. All experiments were performed for 1:1 mole ratios of GLV to ozone. Details regarding each experiment are presented in Table 4.1. Relatively high GLV and ozone concentrations were used to ensure sufficient SOA mass and product evolution for analysis, especially for the temporal studies. SOA mass loadings ($C_{OA}$) ranged from $1 - 20$ µg/m$^3$. For a few experiments, an OH scrubber (cyclohexane) was used to scavenge OH radicals, in order to get a deeper understanding of the ozonolysis chemistry.

*Table 4.1 Summary of experimental conditions*

| Experiment | Precursor Concentration | | Ozone ppbv | $C_{OA}$ Max µg/m$^3$ | Relative Humidity (RH)% |
| --- | --- | --- | --- | --- | --- |
| | Kg | ppbv | | | |
| Grass clipping | 0.5 (wet weight) | NA | 450 | 120 | 20-25 |
| Head space | 0.15 (wet weight) | NA | 500 | 12 | 20-25 |
| CHA | NA | 5 µl ( 1000 ppbv) | 910 | 16 | 20-25 |
| HXL | NA | 5 µl ( 1000 ppbv) | 980 | 12 | 20-25 |
| HXL | NA | 2.5 µl ( 500 ppbv) | 200 | 80 | 10 |
| HXL | NA | 2.5 µl ( 500 ppbv) | 200 | 30 | 70 |
| HXL & propionaldehyde | NA | 5ul ( 1000 ppbv) & 5ul ( 2500ppbv) | 960 | 12.7 | 20-25 |
| Mixture of CHA & HXL | NA | 2.5 µl of each component (1000 ppbv) | 920 | 4.92 | 20/25 |

### 4.2.5 Statistical analysis of SOA

Correlation strengths between the chemical profiles of SOA generated from grass clippings with that from the model chemical systems were estimated using Pearson's 'r' coefficient to estimate if SOA production from the ozonolysis of grass could be modeled by a single SOA precursor or two-component mixtures of GLVs. Pearson's 'r' coefficient provides a quantitative measure of the similarity between two variables/systems. Pearson's 'r' coefficient falls between +1 and −1 inclusive, where 1 is total positive correlation, 0 is no correlation, and −1 is negative correlation. Typically $r > 0.60$ signifies strong correlation, $0.50 < r < 0.60$ signifies moderate to strong correlation and $0.30 < r < 0.50$ signifies low to moderate correlation. Prior to generation of correlation plots, each mass spectrum was normalized to the 185 m/z value, followed by plotting of relative intensity of the individual m/z values against each other.
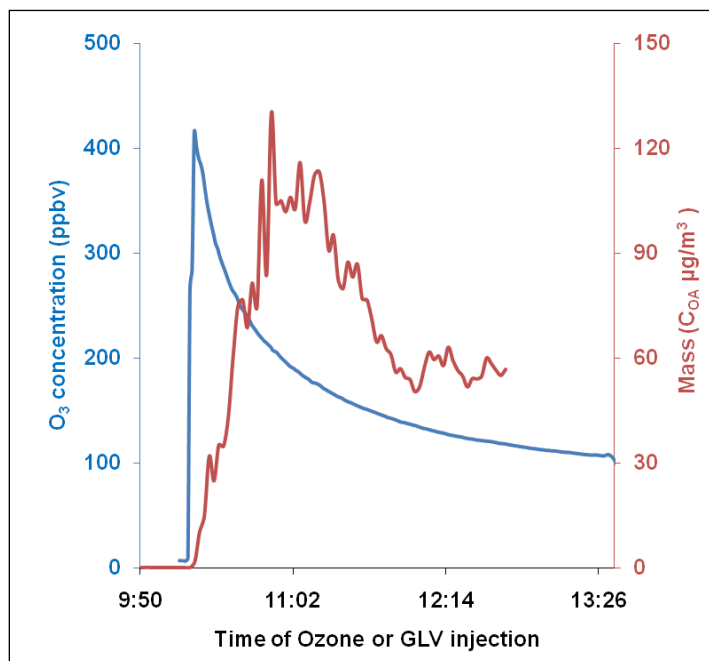


*Figure 4.1 Secondary organic aerosol (SOA) mass loading (COA) evolution and ozone concentration for SOA formation from grass clippings*

59

## 4.3 Results and Discussions

### 4.3.1 SOA from Grass Clippings

Previous studies[23, 25] have shown that reactive GLV emissions from cut grass are principally oxygenates, dominated by unsaturated C5-C6 compounds. When grass clippings were subjected to ozone, a nearly instantaneous burst of SOA (red trace) was produced (Figure 4.1) and ozone was consumed (blue trace). NIR-LDI-AMS analysis of this SOA revealed a complex mixture of highly oxygenated products (Figure 4.2a) ranging from 70 to > 300 *m/z*.
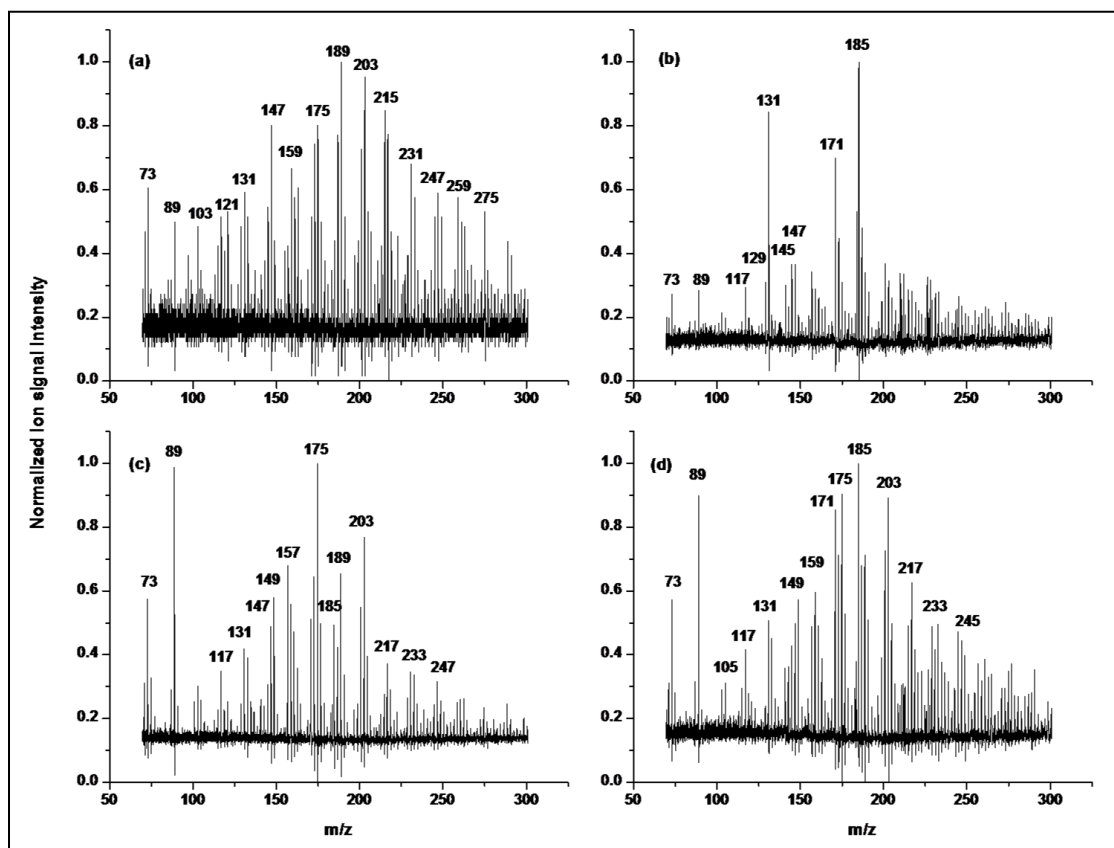


*Figure 4.2 NIR-LDI-AMS mass spectra for different chemical systems: SOA derived from (a) grass clippings at SOA mass loading (COA) = 16.3 μg/m3 sampled for 2 minutes (3.9 ng) (b) cis-3-hexenylacetate (CHA) at COA = 14.7 μg/m3 sampled for 6 minutes (10.6 ng) (c) cis- -3-hexen-1-ol (HXL) at COA = 10.3 μg/m3 sampled for 10 minutes (12.4 ng) and (d) CHA and HXL mixture at COA = 3.9 μg/m3 sampled for 5 minutes (2.3ng).*

The complex mixture of possible GLV contributors to the SOA makes complete chemical speciation challenging. In order to deconvolute the mass spectrum, SOA generated by individual dominant GLVs were first analyzed, and the primary oxidation products (ion signals >50% of base peak) proposed. Some general observations gleaned from the mass spectrum include: (1) ion signals in the range 70-150 *m/z* are representative of first-generation oxidation products; (2) higher mass products (150-300 *m/z*) result from second and later generation products, formed either by reactive uptake of gas-phase oxidation products or by formation of oligomers, dimers and trimers. A representative mass spectrum for headspace SOA is also shown in Figure 4.3.
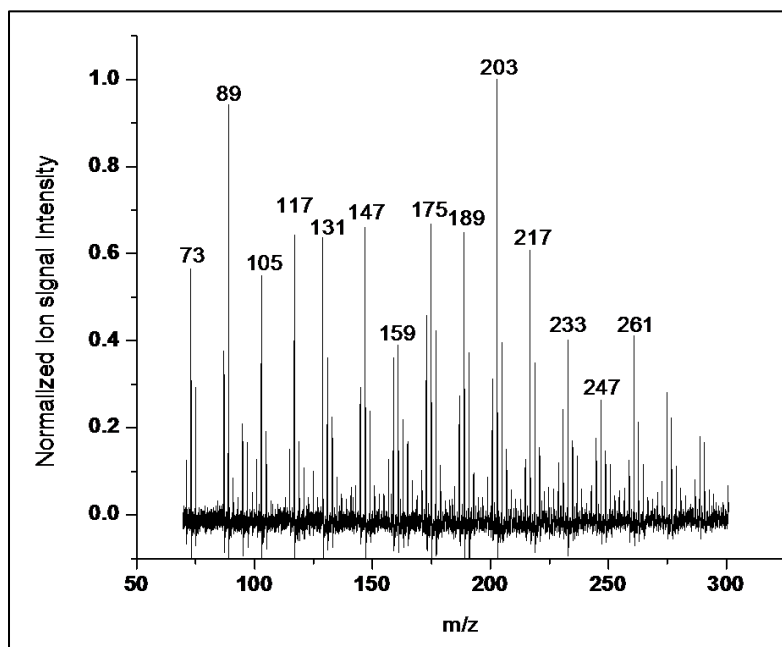


*Figure 4.3 Near Infrared Laser Desorption Ionization Aerosol Mass Spectrometer (NIR-LDI-AMS) mass spectra for headspace SOA.*

## 4.3.2 GLV standards

### 4.3.2.1 Cis-3-hexenylacetate

The basic chemical mechanism for ozonolysis of alkenes is described in chapter 2 and in detail elsewhere.[49-53] Briefly, oxidation of CHA is initiated by addition of ozone

across the double bond (Scheme 4.1) resulting in a primary ozonide that, upon cleavage, produces two products (3-oxopropyl acetate and propionaldehyde) and two Criegee Intermediates (**CI-1** and **CI-2**) that can rearrange to form low-volatility carboxylic acids as well as participate in multi-generational chemistry.
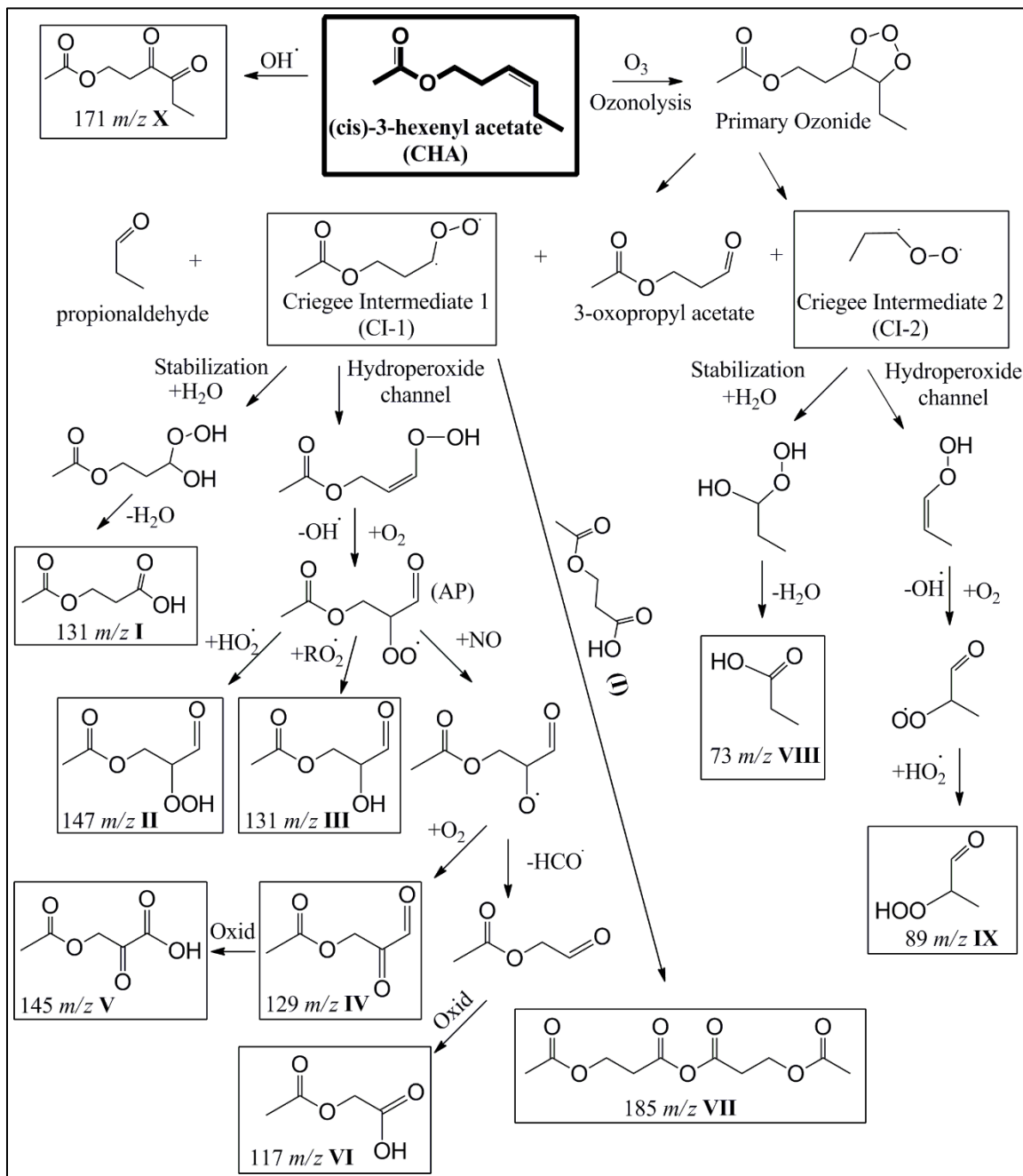


*Scheme 4.1 Abbreviated reaction mechanism for the ozonolysis of CHA*
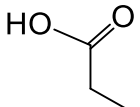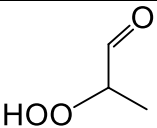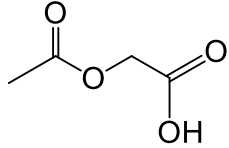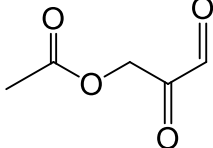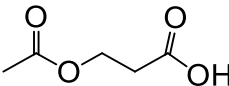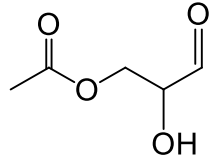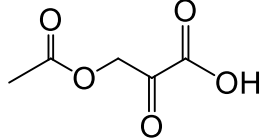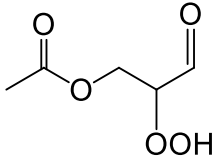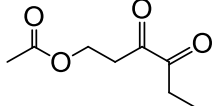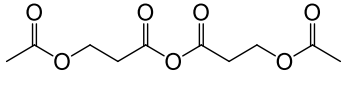
SOA forms almost immediately upon addition of ozone to CHA in the chamber (Figure 4.4). The NIR-LDI-AMS spectrum of the CHA-derived SOA (Figure 4.2b) is qualitatively simpler than that of the grass clippings, showing only a few common major ion peaks (i.e., oxidation products). Some of the products have been reported previously,[23, 29, 54] while others are assigned on the basis of a combined ozonolysis-radical mechanism (Scheme 4.1). Details of the major products are shown in Table 4.2.
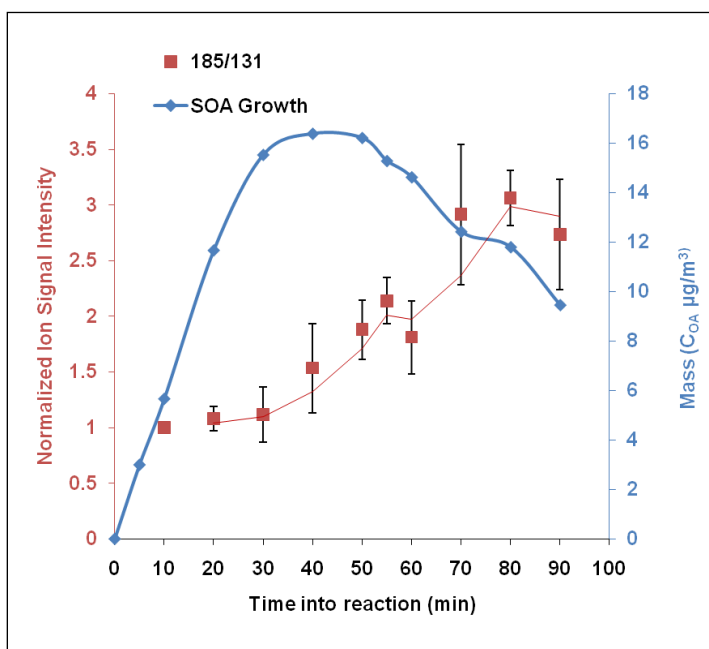


*Figure 4.4 cis-3-hexenylacetate secondary organic aerosol (SOA) mass loading (COA) evolution and oxidation product evolution (lines are included to aid the eye).*

The estimated vapor pressure[46] of 3-oxopropyl acetate ($3 \times 10^{-3}$ atm) suggests that, in the absence of reactive uptake, it will exist exclusively in the gas-phase and, therefore, this product was not observed with NIR-LDI-AMS. There are several major channels commonly evoked to describe the fate of the short-lived CI in the gas-phase, including rearrangement and bimolecular reactions with $H_2O$ and further reaction through the "hydroperoxide channel"[55], with the latter channel leading to the formation of OH-radicals.

*Table 4.2 Major products proposed for cis-3-hexenylacetate ozonolysis*

| Structure | IUPAC Nomenclature | Observed m/z | Abbreviation/ Number |
|---|---|---|---|
|  | propanoic acid | 73 | **VIII** |
|  | 2-hydroperoxy propanal | 89 | **IX** |
|  | 2-acetoxyacetic acid | 117 | **VI** |
|  | 2,3-dioxopropyl acetate | 129 | **IV** |
|  | 3-acetoxypropanoic acid | 131 | **I** |
|  | 2-hydroxy-3-oxopropyl acetate | 131 | **III** |
|  | 3-acetoxy-2-oxopropanoic acid | 145 | **V** |
|  | 2-hydroperoxy-3-oxopropyl acetate | 147 | **II** |
|  | 3,4-dioxohexyl acetate | 171 | **X** |
|  | 3-acetoxypropanoic anhydride | 185 | **VII** |

Rearrangement and bimolecular reactions between $H_2O$ and CI-1 and CI-2 result in formation of 3-acetoxypropanoic acid (**I**, 131 *m/z*) and propanoic acid (**VIII**, 73 *m/z*),

respectively, which have been observed in a prior study.[23] Although the estimated vapor pressure of **I** suggests that it would exist primarily in the gas-phase, a strong signal was measured by NIR-LDI-AMS in the particle-phase, suggesting partitioning between the gas-phase and aerosol particles (i.e., it is behaving as a semi-volatile organic compound, SVOC).

Evidence from chamber experiments suggests that the partitioning of SVOCs between gas and particle phases is highly dependent upon the organic aerosol mass. For typical atmospheric OA mass loading of between 0.1 and 100 $\mu$g m$^{-3}$ (consistent with SOA mass loading in our experiments, Figure 4.4), compounds with effective saturation concentrations between $1\times10^{-3}$ and $1\times10^{4}$ $\mu$g m$^{-3}$ are considered semi-volatile.[56-59]

Organic peroxides can be formed from the CIs through reactions with a variety of acidic species, such as water, alcohols, and carboxylic acids, to form α-hydroxy, α-alkoxy, and α-acyloxy hydroperoxides, respectively.[49, 55, 60] Briefly, in the hydroperoxide channel, the CI rearranges to a form a vinyl hydroperoxide that rapidly decomposes to generate hydroxyl and alkyl radicals (R•). The R• then reacts rapidly with molecular oxygen to form an alkylperoxy radical (RO$_2$•), which plays an important role in the production of lower-volatility products.[3, 15] As shown in Scheme 4.1 for CI-1, the alkylperoxy radical (AP) generated from 3-hydroperoxyallyl acetate can undergo three distinct reactions: (1) reaction with HO$_2$• to generate **II** (147 *m/z*); (2) reaction with other RO$_2$•, to form **III** (also at 131 *m/z*); and (3) reaction with NO to yield a wide array of products. For example, addition of O$_2$ can lead to formation of **IV** (129 *m/z*), which can further undergo oxidation to give a carboxylic acid (**V**, 145 *m/z*). Loss of HCO$^.$ followed by oxidation would result in formation of **VI** (117 *m/z*). Similarly, CI-2 can follow the hydroperoxide channel to yield

**IX** (89 *m/z*) and other higher volatility products like acetone and acetic acid observed in the gas-phase.[27]

As discussed above, ozonolysis of alkenes also results in the production of OH radicals,[61] which upon reaction with CHA can lead to direct formation of **X** (171 *m/z*). The absence of significantly higher molecular weight products from this GLV is explained by the presence of the acetate moiety, which prevents formation of oligomers and other highly oxygenated compounds, contrary to observations from ozonolysis of HXL.[23]
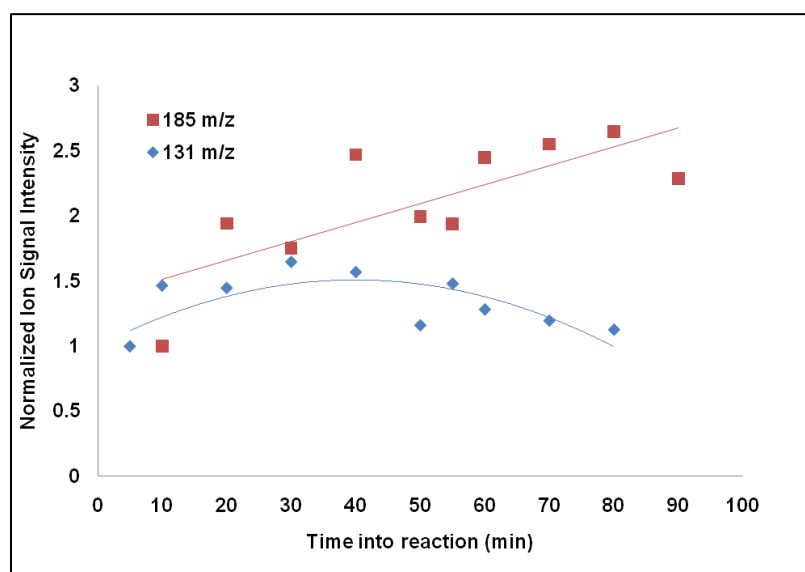


*Figure 4.5 Time evolution of select compounds for cis-3-hexenylacetate secondary organic aerosol (SOA).*

Criegee intermediates can react with carboxylic acid groups to form α-acyloxyalkyl hydroperoxides, which dehydrate *in situ* to form anhydride.[62] In this study, CI-1 reacts with 3-acetoxypropanoic acid to form **VII** (185 *m/z*). This hypothesis is supported by comparison of the profiles for the temporal evolution (Figure 4.4, 4.5) of product **I** (131 *m/z*) and the dehydrated hydroperoxide product (185 *m/z*). As the SOA grows and ages (blue curve), 131 *m/z* is consumed, while the hydroperoxide product **(VII)** is produced (i.e., the ion signal intensity ratio $I_{185}$:$I_{131}$ increases as a function of aging), suggesting that

product **VII** is formed from a precursor product with *m/z* 131. This implies that 3-acetoxypropanoic acid is important in the early stages of SOA formation and is subsequently consumed. These oxoacids may be a significant source of low-volatility, highly reactive oxygenated carbon in the atmosphere.

### 4.3.2.2 cis-3-hexen-1-ol

A previous study found that the emission rate of HXL is approximately one-fifth (by mass) that of CHA.[27] Upon exposure to ozone, HXL also immediately forms SOA (Figure 4.6). It is evident from the mass spectrum (Figure 4.2c) that HXL-derived SOA is of much greater chemical complexity than SOA derived from CHA. Contrary to CHA, here I observed a much wider range of chemical products, ranging from 50 *m/z* to greater than 300 *m/z*, suggesting the enhanced formation of oligomers, including ester-type products.[23]
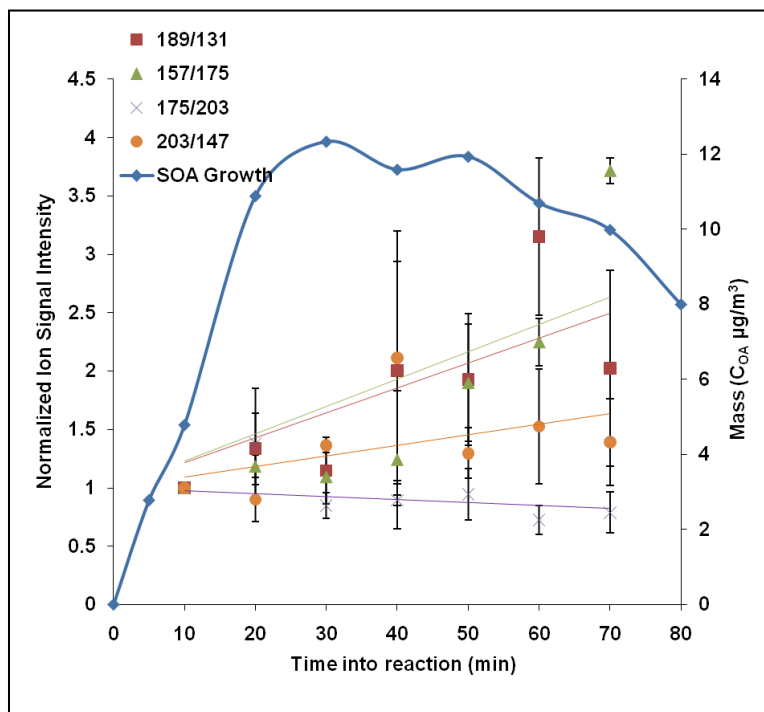


*Figure 4.6 cis-3-hexen-1-ol secondary organic aerosol (SOA) mass loading (COA) evolution and oxidation product evolution (lines are included to aid the eye)*

Similarly to CHA, ozonolysis of HXL (Scheme 4.2) is predicted to produce 3-hydroxypropanal (3HPA, 73 *m/z*) and propionaldehyde, along with two Criegee intermediates (**CI-3** and **CI-4**).
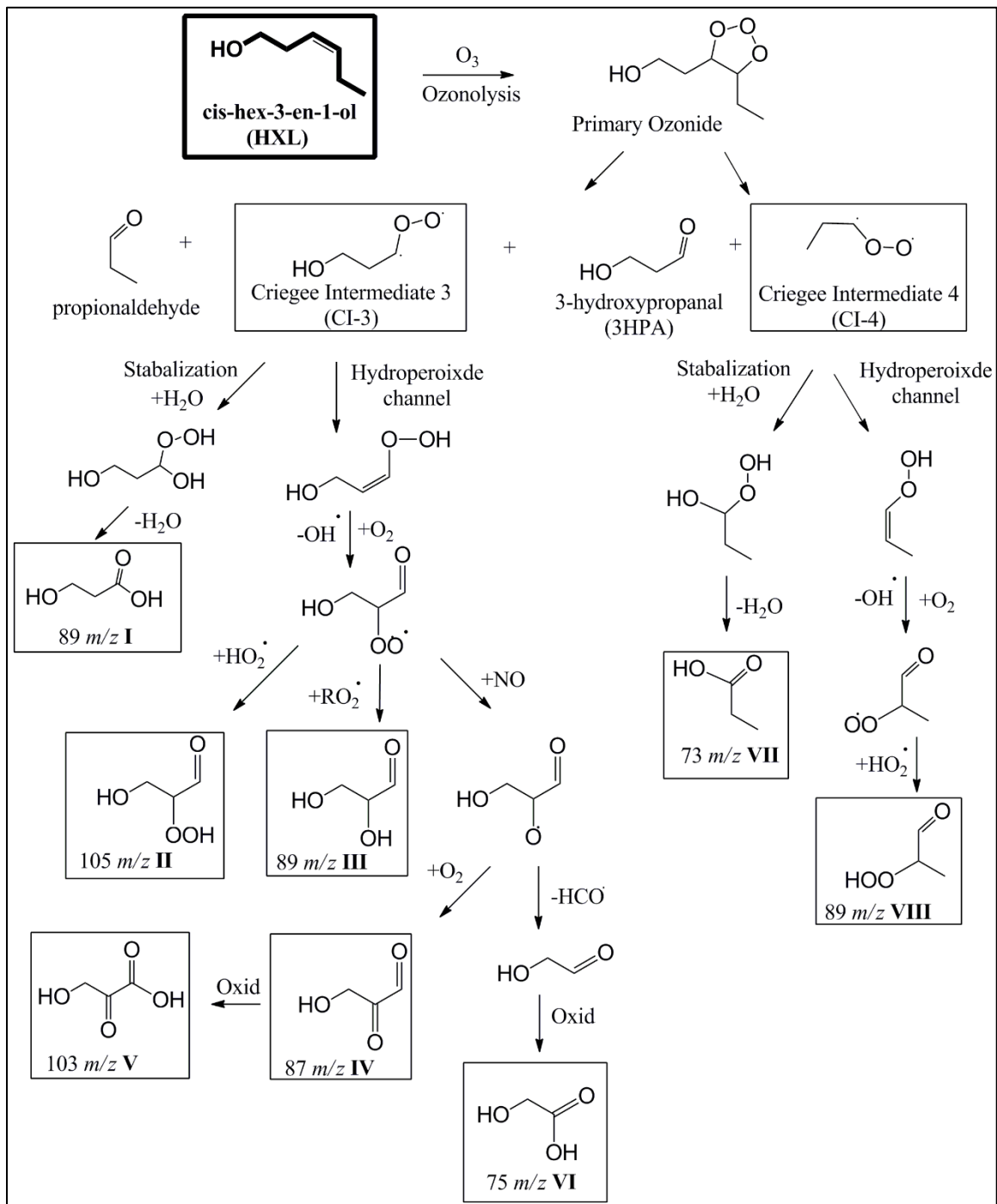


*Scheme 4.2 Abbreviated reaction mechanism for the ozonolysis of cis-3-hexen-1-ol*

Propionaldehyde is volatile and expected to reside exclusively in the gas-phase, whereas 3HPA, owing to its lower vapor pressure ($1.8 \times 10^{-3}$ atm), may enter the particle-phase, as suggested by the strong ion signal measured at 73 $m/z$. 3HPA has been identified previously as a major gas-phase product,[50] but has never been measured in the particle-phase. Details of major products are shown in Table 4.3.
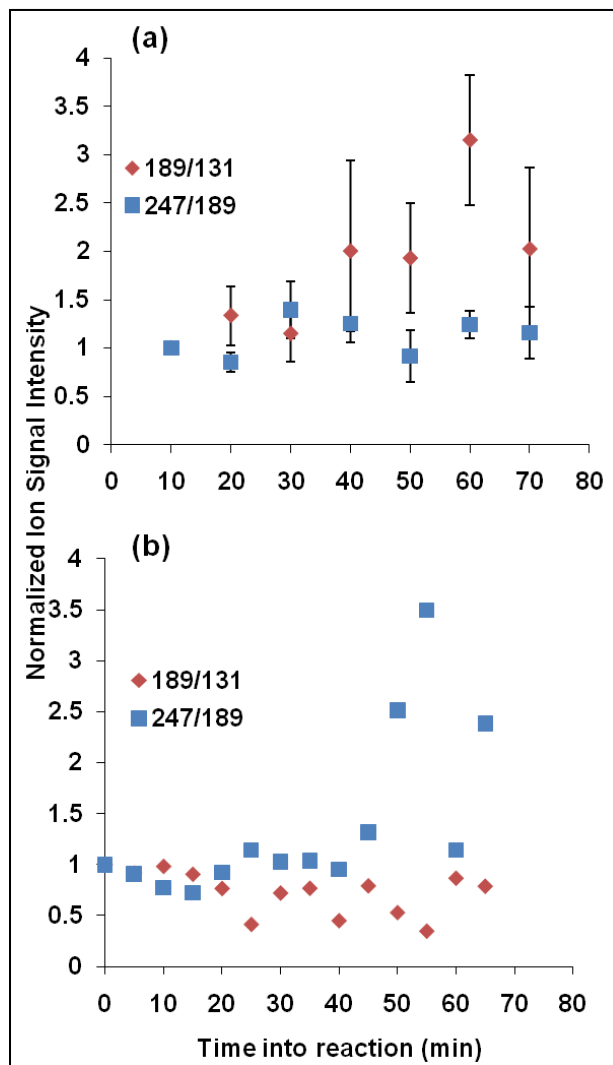


*Figure 4.7 Effect of propionaldehyde on the formation of SOA products in the (a) absence and (b) presence of excess propionaldehyde introduced extrinsically to the SOA-forming reaction.*

Criegee intermediates CI-3 and CI-4, upon stabilization and bimolecular reactions with $H_2O$, yield 3-hydroxypropanoic acid (3HPAA) (**I**, 89 $m/z$) and propanoic acid (**VII**,

73 *m/z*)**,** respectively. Owing to its lower estimated pressure of 2.5 x $10^{-5}$ atm, 3HPAA will reside, at least in part, in the particle-phase. Propanoic acid has the same mass and similar vapor pressure as 3HPA and hence is also assigned to 73 *m/z*. The hydroperoxide channel can also be invoked to predict other products observed, however neither branch adequately explains the origin of the higher mass peaks in the range 120-300 *m/z*.

Oligomer formation has been suggested as an important component driving SOA formation.[63-68] Ozonolysis of HXL may lead to significant oligomer formation by several mechanisms (Scheme 4.3). 3HPA has similar properties and structure to that of glyoxal and via an analogous mechanism[69] could undergo reversible hydration and dimerization, even at room temperature and humidity, to form low-volatility compounds,[69] for example polyols such as propane-1,1,3-triol.[23] This compound can further react either through reactive uptake of gas-phase products, such as propionaldehyde, or it can dimerize.

Reaction of propane-1,1,3-triol (Scheme 4.3) with the gas-phase product propionaldehyde results in formation of **X** (131 *m/z*), which can facilitate further reactive uptake of propionaldehyde to form **XI** (189 *m/z*) and **XII** (247 *m/z*). Products **XI** and **XII** have much lower vapor pressures compared to the monomeric precursor, suggesting they reside primarily in the particle-phase. To further test the hypothesis of the reactive uptake of propionaldehyde by **XI** and **XII**, I performed experiments comparing the ion signal intensity ratios of products **X, XI** and **XII** (as a function of SOA formation and aging) with and without additional propionaldehyde injected into the chamber during SOA formation (Figure 4.7). In the absence of extrinsic propionaldehyde, ion signal intensity ratios for $I_{189}$:$I_{131}$ (Fig. 4.7a, Scheme 4.3) increase as the SOA ages, whereas the $I_{247}$:$I_{189}$ ratio (Fig. 4.7a, Scheme 4.3) remains constant, suggesting that product **X** (131 *m/z*) is consumed to
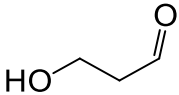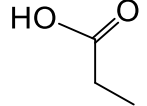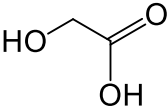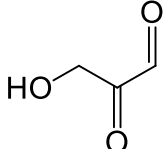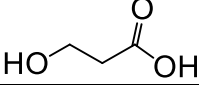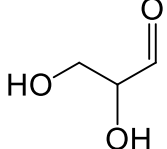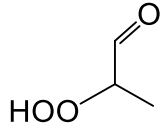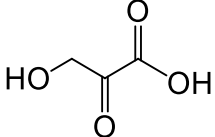
form product **XI** (189 *m/z*). However, this does not suggest anything about further uptake of propionaldehyde by product **XI** to form a new product. Conversely, in the presence of excess (extrinsic) propionaldehyde, we observe a reversal of these trends, i.e., the $I_{189}:I_{131}$ decreases as a function of aerosol aging, while the $I_{247}:I_{189}$ ratio (Fig 4.7b, Scheme 4.3) increases, suggesting consumption of product **XI** (by reactive uptake of extrinsic propionaldehyde) to form product **XII** (247 *m/z*). It seems that uptake of propionaldehyde occurs once product **XI** (189 *m/z*) reaches a threshold concentration.
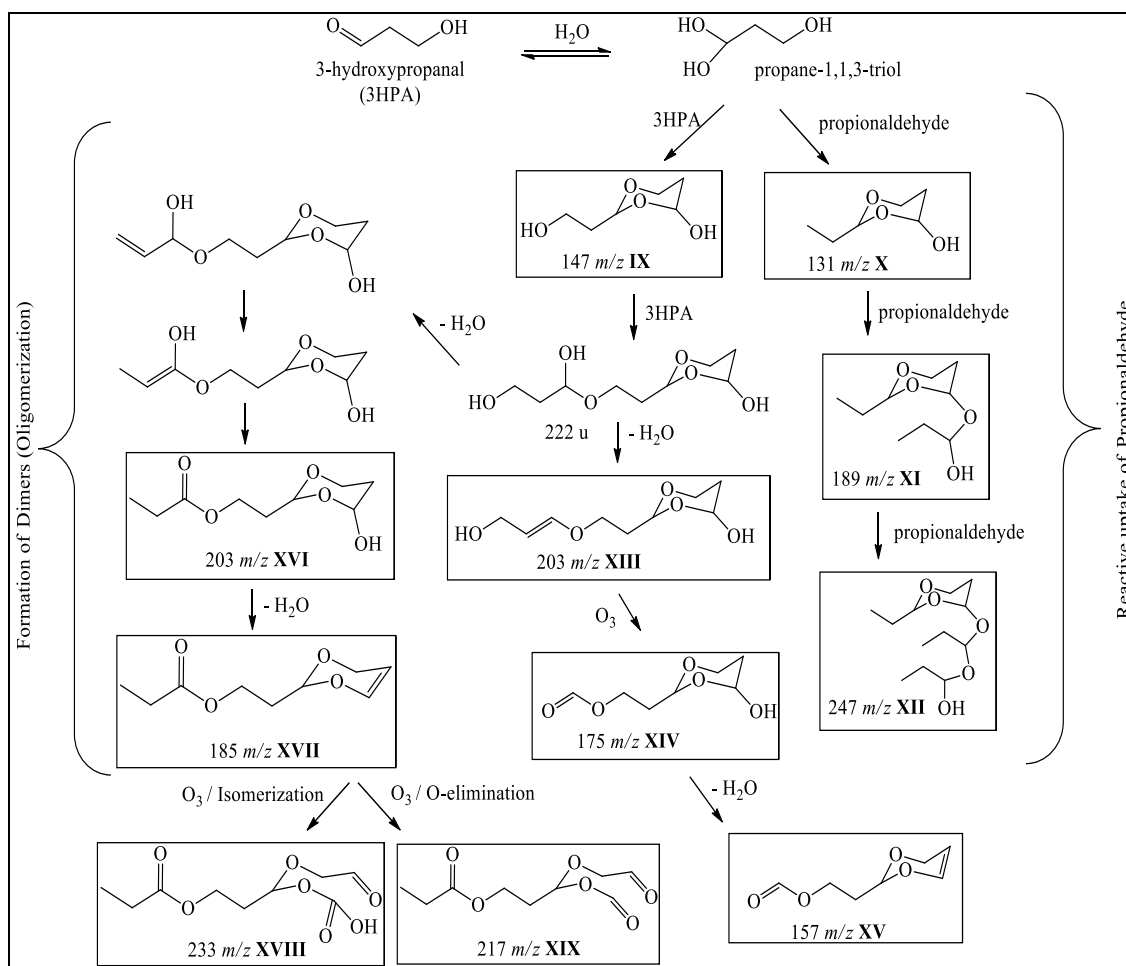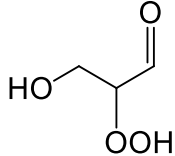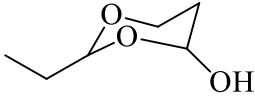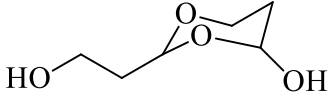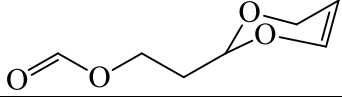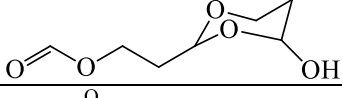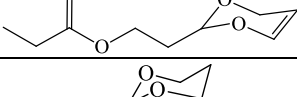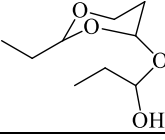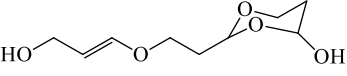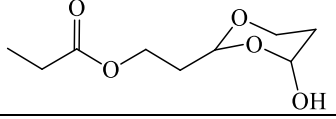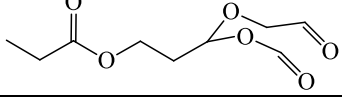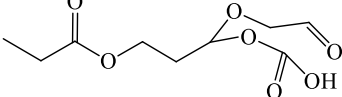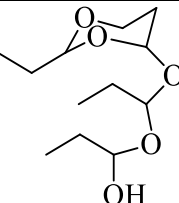


*Scheme 4.3 Proposed reaction mechanism for the formation of higher molecular weight products resulting from oxidation of HXL and reactive uptake of propionaldehyde.*

71

Furthermore, reaction of propane-1,1,3-triol (Scheme 3) with 3HPA results in the formation of the 3HPA dimer (**IX**, 147 *m/z*), which has been reported previously.[23] The estimated vapor pressure of this dimer is $1.9 \times 10^{-7}$ atm[46], which is a factor of $10^5$ lower than its monomer, suggesting it too will reside in the particle-phase. Attesting to its high reactivity, 3HPA dimer can further react to form higher molecular weight products, such as 3HPA trimer (222 amu, not observed) as shown, which can dehydrate by multiple pathways to give a wide array of products.

*Table 4.3 Major products proposed for cis-3-hexen-1-ol ozonolysis*

| Structure | IUPAC Nomenclature | Observed m/z | Abbreviation/ Number |
|---|---|---|---|
| | 3-hydroxypropanol | 73 | **3HPA** |
| | propionic acid | 73 | **VII** |
| | 2-hydroxyacetic acid | 75 | **VI** |
| | 3-hydroxy-2-oxopropanal | 87 | **IV** |
| | 3-hydroxypropanoic acid | 89 | **3HPAA (I)** |
| | 2,3-dihydroxypropanal | 89 | **III** |
| | 2-hydroperoxypropanal | 89 | **VIII** |
| | 3-hydroxy-2-oxopropanoic acid | 103 | **V** |

| Structure | Name | | |
|---|---|---|---|
| | 2-hydroperoxy-3-hydroxypropanal | 105 | **II** |
| | 2-ethyl-1,3-dioxan-4-ol | 131 | **X** |
| | 2-(2-hydroxyethyl)-1,3-dioxan-4-ol | 147 | **3HPA Dimer (IX)** |
| | 2-(1,3-dioxin-2-yl)ethylformate | 157 | **XV** |
| | 2-(4-hydroxy-1,3-dioxan-2-yl)ethyl formate | 175 | **XIV** |
| | 2-(1, 3-dioxin-2-yl) ethyl propionate | 185 | **XVII** |
| | 1-((2-ethyl-1,3-dioxan-4-yl)oxy)propan-1-ol | 189 | **XI** |
| | 2-(2-((3-hydroxyprop-1-en-1-yl)oxy)ethyl)-1,3-dioxan-4-ol | 203 | **XIII** |
| | 2-(4-hydroxy-1,3-dioxan-2-yl)ethyl propionate | 203 | **XVI** |
| | 3-(formyloxy)-3-(2-oxoethoxy) propyl propionate | 217 | **XIX** |
| | 3-(carboxyoxy)-3-(2-oxoethoxy) propyl propionate | 233 | **XVIII** |
| | 1-(1-((2-ethyl-1,3-dioxan-4-yl)oxy)propoxy)propan-1-ol | 247 | **XII** |

The presence of multiple hydroxyl groups on 3HPA trimer, suggests several pathways to dehydration that could help explain other peaks observed in the SOA envelope. Dehydration of alcohols usually requires a strong acid catalyst; however, organic acids, such as propanoic acid, acetic acid generated during the ozonolysis reaction, can also act

as catalysts to promote these dehydration reactions. Moreover, the dehydration may be promoted by the neighboring group atom[70] (Scheme 4.4). The hemi-acetal functionality favors dehydration as compared to the primary hydroxyl group. However, between linear and cyclic hemi-acetal functional groups, dehydration takes place preferentially at the linear group, as I do not observe any products formed from the cyclic analog. Dehydration of the linear hemi-acetal (Scheme 4.3) yields **XIII** (203 *m/z*), which may undergo further ozonolysis to yield **XIV** (175 *m/z*). In the absence of a linear hemi-acetal functionality (as is the case for product **XIV**), dehydration of **XIV** will give **XV** (157 *m/z*). The dehydration step is a slow step, which may occur in the sampling process. Further support of Scheme 4.3 is gained by measuring the different product ion ratios as a function of SOA formation and aging (Figure 4.6). There was an increase in the ion signal intensity ratio for $I_{157}{:}I_{175}$ **(XV: XIV)**, suggesting a slow consumption rate for product **XV** and that dehydration of **XIV** occurs at a much faster rate as compared to ozonolysis of product **XV**. I also observed an increase in the ratio $I_{203}{:}I_{147}$ (Fig. 4.6, **XIII: IX**) with aerosol aging, supporting our hypothesis that **XIII** results from dehydration of the trimer (222 u) formed by addition of 3HPA to **IX**.
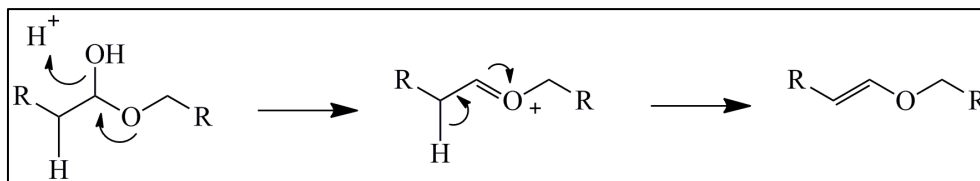


*Scheme 4.4 Abbreviated reaction mechanism for dehydration of alcohols in an acidic matrix*

Although less probable, the primary hydroxyl group on 3HPA trimer can also undergo dehydration and rearrange to give **XVI** (also at 203 *m/z*), as shown in Scheme 4.3. This suggests that there are multiple pathways that yield 203 *m/z* and, hence, this mass has been assigned to products **XVI** and **XIII**. Product **XVI** can undergo dehydration to yield

an alkene **XVII** (185 *m/z*). Ozonolysis of **XVII** yields **XVIII** (233 *m/z*). It should also be noted that O-atom elimination from the Criegee intermediate can lead to formation of **XIX** (217 *m/z*).[71, 72] The results discussed above suggest that HXL generates much more chemically complex SOA as compared to CHA. Ozonolysis of HXL results in formation of higher molecular weight compounds (e.g., oligomers) and preferential formation of ester-type linkages. In contrast, the hydroperoxide channel seems to be the dominant oxidation pathway for CHA, as oligomer formation is inhibited by the acetate functionality.

### *4.3.2.3 Mixture of GLVs*

To better understand the formation of SOA derived from GLVs, and to determine if either CHA or HXL could serve as a suitable proxy of SOA generated from grass clippings, we studied SOA generated by ozonolysis of standard GLV mixtures.

Not unexpectedly, upon inspection of the NIR-LDI-AMS mass spectrum (Figure 4.2d) of SOA generated from a 1:1 mole ratio mixture of CHA and HXL, I observed the same major product ion peaks as measured from ozonolysis of each GLV. However, isobaric signals can originate from ozonolysis of either GLV. While it is expected that various products of individual GLVs can react further (as discussed above), isobaric interferences from these later-generation reactions (e.g., subsequent oxidation, dehydration and decomposition) prevent the use of ion intensity ratios to develop detailed mechanisms for this higher-order chemistry.

Nonetheless, in order to assess the feasibility of using either a single SOA proxy or a mixture of dominant GLVs to predict SOA formation from grass clippings, I compared Pearson's 'r' coefficients[73] for SOA from grass clippings with that from the two individual

precursors and from their mixture. Prior to generation of the correlation plots (Figure 4.8), each mass spectrum was normalized to the 185 m/z value.
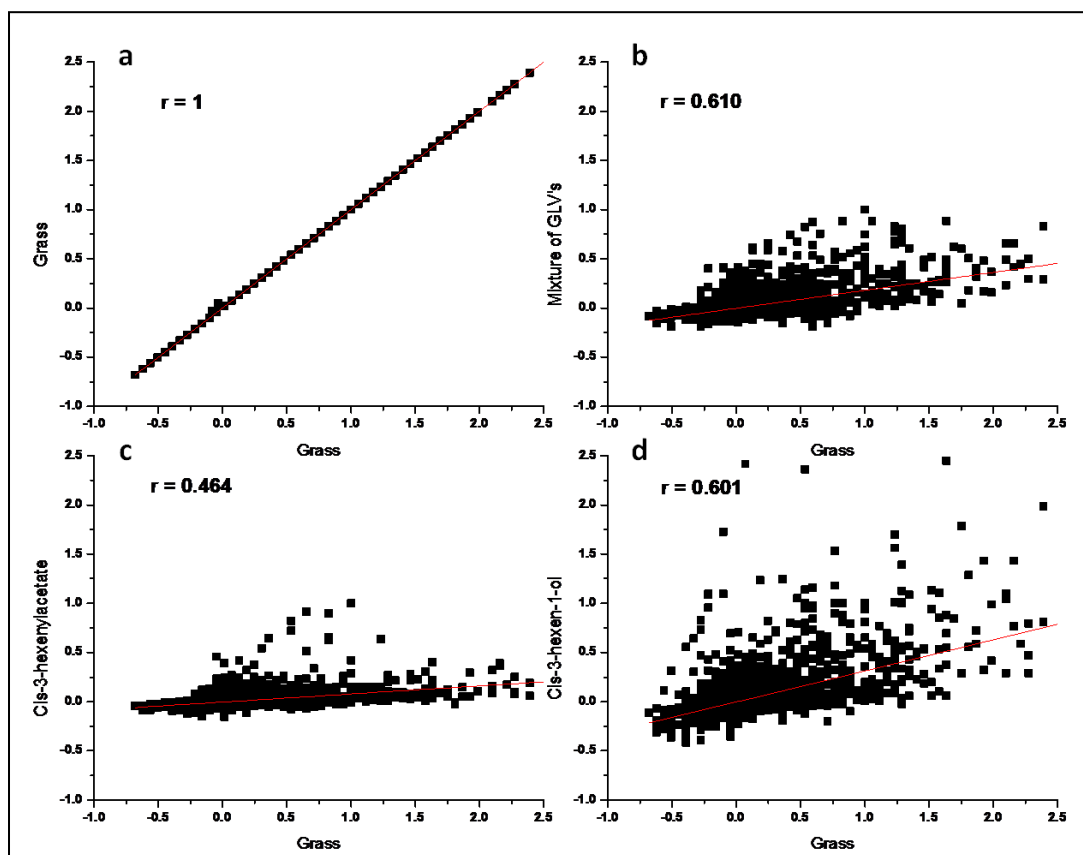


*Figure 4.8 Correlation plots of NIR-LDI-AMS mass spectra shown in Figures 1a-d. Pearson's 'r' coefficient is used as a measure of similarity between spectra. Plotted are the normalized intensities of individual m/z signals against each other where a) Grass vs Grass, (b) Grass vs Mixture of GLVs, (c) Grass vs CHA, and (d) Grass vs HXL.*

Perfect correlation between two mass spectra (Fig. 4.8 a), would result in a Pearson's 'r' coefficient equal to unity, with deviation from unity is a measure of dissimilarity. While the best correlation was found with the GLV mixture (0.610), a similar correlation was observed between SOA from grass and HXL alone (0.601), suggesting that HXL, in spite of its lower emission rates as compared to CHA, is the dominant contributor to SOA generated from grass clippings. This further suggests that HXL could be used as a chemical proxy for SOA generated from cut grass.

*Table 4.4 Area under the curve for each Near Infrared Laser Desorption Ionization Aerosol Mass Spectrometer (NIR-LDI-AMS) mass spectrum integrated from 70-300 m/z*

| Chemical System | Area under the Curve (Arbitrary units) | % Similarity (Compared to grass) |
|---|---|---|
| Grass | 37.65 | 100 |
| Mixture of 2 GLVs | 34.01 | 90 |
| Cis-3-hexen-1-ol (HXL) | 34.93 | 92 |
| Cis-3-hexenylacetate (CHA) | 28.34 | 70 |

Furthermore, comparison of the total ion current (i.e., the area under the curve of each mass spectrum) from 70 – 300 m/z (Table 4.4) reveals a 90% and 92% similarity between grass clippings and GLV mixture and HXL, respectively. However, there is only 70% similarity between the grass clippings and CHA, lending further support to our proposed use of HXL as a suitable proxy for SOA generated from grass clippings.

**4.3.3 Influence of OH scrubbers on SOA composition**

As previously mentioned, OH radicals are an important atmospheric oxidant and are also generated during the ozonolysis of alkenes. In order to isolate the SOA formation in ozone-alkene systems from the additional influence of hydroxyl (OH) radicals formed in the gas-phase ozone-alkene reaction, OH scavengers are employed. By doing so, we can understand the SOA formation due to ozonolysis even better and interpret the observed NIR-LDI-MS mass spectrum more effectively. The most commonly used OH-scavengers include cyclohexane, alcohol, and aldehydes. In this study a 10 fold excess of cyclohexane was used to scavenge the OH radicals.

### 4.3.3.1 CHA ozonolysis in presence of OH scrubbers

The mechanism for the oxidation of CHA by ozone is shown in scheme 4.1 and described in details in section 4.3.2.1. In order to understand the ozonolysis chemistry better and confirm the products formed due to OH radicals, CHA-derived SOA was formed in presence of excess of OH radical scrubbers to eliminate any OH radicals formed during ozonolysis. In doing so, ideally any product formed due to the reaction between CHA and OH radical would be eliminated and the products corresponding to those m/z should disappear from the NIR-LDI-MS mass spectrum.
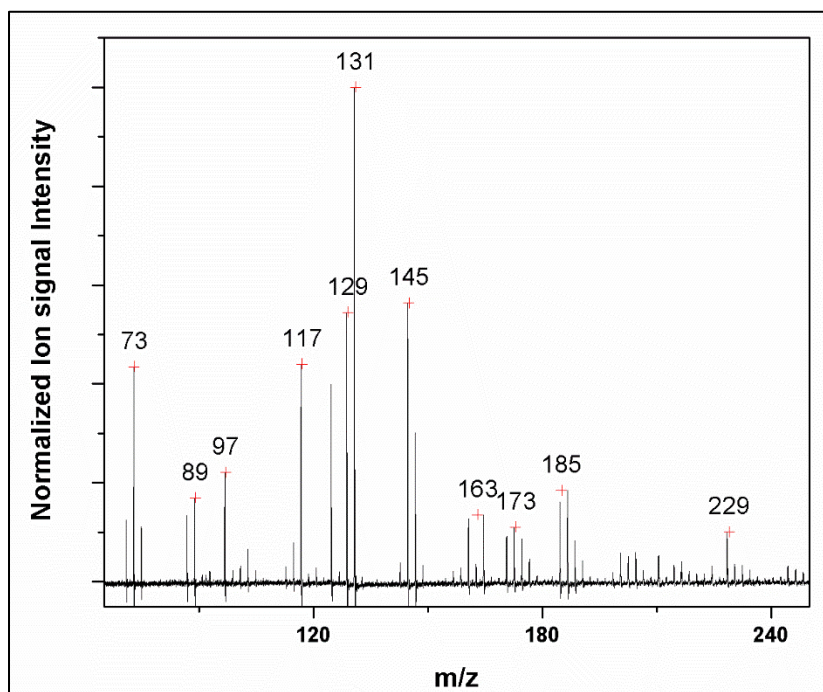


*Figure 4.9 CHA ozonolysis in presence of OH scrubber*

SOA forms almost immediately upon addition of ozone and OH scrubbers to CHA in the chamber. The NIR-LDI-AMS spectrum of the CHA-derived SOA in presence of OH scrubber (Figure 4.9) is similar to the CHA- derived SOA (Figure 4.2b) showing the same dominant peaks with one major exception. A peak at m/z 171 is missing in the mass spectrum of CHA-derived SOA in presence of OH scrubbers. Recall that, in section 4.3.2.1,

78

this peak was assigned to a product **X** which was formed by the direct reaction of CHA with the OH radicals produced during ozonolysis. Comparison of the profiles for the temporal evolution of m/z 185 and m/z 131 also revealed that the major peak in the NIR-LDI-MS shifted from 185 m/z **(VII)** to 131 m/z **(I).** I believe this is because we had effectively shut down a CHA consumption pathway (OH radical reacting with CHA) as a result of which more CHA is available to reach with ozone and form the first generation product at 131 m/z **(I)**. Profiles for the temporal evolution of other products stayed the same irrespective of the presence or absence of the OH scrubber. Based on the above observation, I was able to confirm our peak assignment for m/z 171 and showed that the OH radical plays a significant role in driving the chemistry of CHA derived SOA.

### *4.3.3.2 HXL ozonolysis in presence of OH scrubbers*

Similar experiments were performed with HXL and SOA was generated in the presence of an excess OH scrubber. The mechanism for the oxidation of HXL by ozone is shown earlier in this chapter (Scheme 4.2, 4.3) and described in details in section 4.3.2.2. Recall that, HXL SOA mainly consists of high molecular weight compounds which are formed by ester type linkages due to hydration and dehydration reactions.

In the presence of an excess of the OH scrubber, I did not observe any difference in the NIR-LDI-MS spectrum, suggesting that OH radicals have a very minimal or no effect on the SOA formation from HXL. Profiles for the temporal evolution of various predicted compounds also did not reveal any specific trend which were different from profiles obtained with no OH scrubber.

## 4.3.4 Influence of environmental conditions on SOA composition

Water plays an important role in the formation of $O_3$ and SOA, however, there are only a very limited number of studies that have addressed the impacts of relative humidity (RH) on chemical composition. It has been shown previously that environmental conditions such as temperature and relative humidity (RH) could have a significant impact on SOA chemical composition, phase and viscosity.[74-78] These few studies present inconsistent and conflicting results, reporting that high humidity levels significantly reduce SOA number concentration as well as that increasing liquid water led to increasing SOA formation.[79-81] Hence, in this collaborative work between Harvard and UVM, we decided to look at the effect of RH on the chemical composition of SOA formation by HXL by investigating the NIR-LDI-AMS spectra for SOA formed under either dry (10%) or wet (70%) RH conditions.
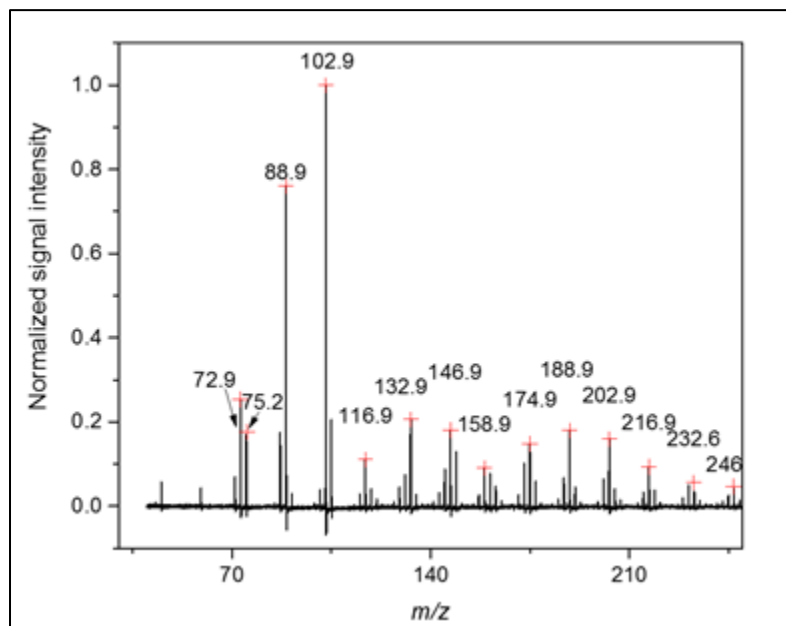


*Figure 4.10 Mass spectra of HXL-SOA (measured using NIR-LDI-AMS) formed under dry (10% RH)*

When HXL was oxidized under dry conditions (i.e., 10% RH), SOA formed almost immediately upon addition of ozone to HXL in the chamber. The NIR-LDI-AMS spectrum

of the HXL-derived SOA was similar to what we had observed earlier (Fig 4.2b, 4.10). It was observed that the HXL-derived SOA was of much greater chemical complexity than SOA derived from CHA and much wider range of chemical products were formed, ranging from 50 *m/z* to greater than 300 *m/z*, suggesting the enhanced formation of oligomers, including ester-type products. (Figure 4.10)

On the other hand when HXL was oxidized under wet conditions (i.e., 70% RH), we observed a very interesting difference. The NIR-LDI-AMS spectrum of the HXL-derived SOA under wet conditions generally showed the same dominant product peaks (73, 89, 103 m/z), yet their relative intensities differ, suggesting different relative product yields. (Figure 4.11)
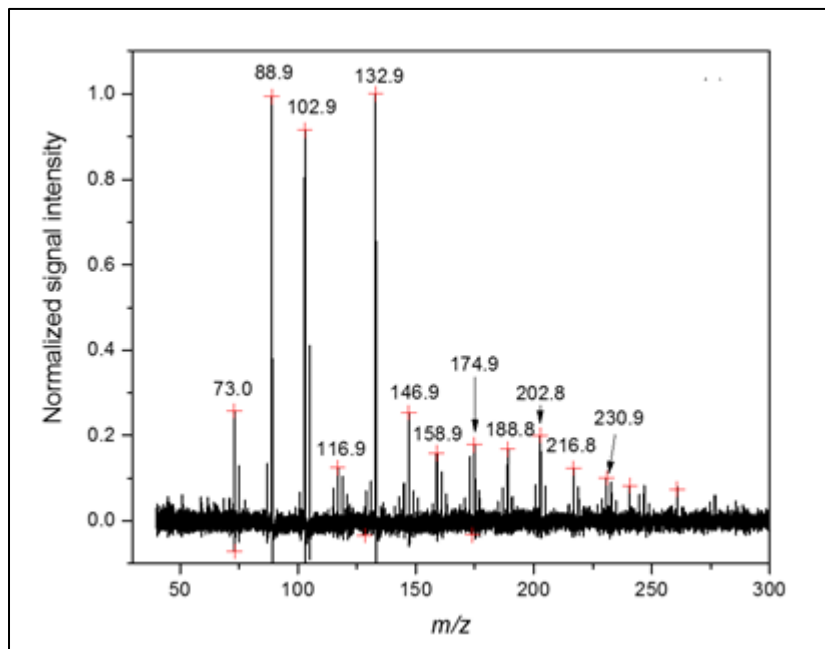


*Figure 4.11 Mass spectra of HXL-SOA (measured using NIR-LDI-AMS) formed under wet (70% RH)*

It was observed that, while peaks at 103 and 89 m/z dominate the spectrum for dry HXL-SOA, the peak at 133 m/z becomes dominant when SOA is formed under wet conditions. A detailed mechanism for formation of peak at 133 m/z under wet conditions

is presented  and discussed elsewhere.[82] Results from this work clearly demonstrate a changing chemical composition under different RH conditions which could have various atmospheric implications.

## 4.4 Conclusion

GLVs make a significant contribution to the atmospheric burden of SOA.[27] In this work, I reported the use of modified NIR-LDI-AMS to identify the primary precursors of SOA from grass clippings and elucidate the operative chemical mechanisms in SOA formation and aging. I also utilized NIR-LDI-MS to observe the effect of environmental conditions (RH) on the chemical composition of SOA.  The results of this study indicate that a single precursor cannot be used to quantitatively predict and determine the SOA formation for a complex chemical system; however, it may be possible to use HXL concentrations once a correction has been made for "missing SOA mass."[27] Although to-date, reported studies considered only single precursor systems to estimate SOA formation from GLVs, it is clear that while the chemistry appears adequately described by a single precursor, i.e., HXL, this is not the case for predicting aerosol mass yields.[27] I also show that the key difference in reactivity between these GLVs appears to be formation of polyols for ozonized HXL, which can undergo oligomerization by reversible hydration and dimerization. As a result, SOA derived from HXL contains a significant quantity of oligomers, which is not observed in CHA-derived SOA, further supporting our hypothesis that HXL is the better single-precursor model for GLV-derived SOA.

In the atmosphere, multiple VOCs are susceptible to simultaneous oxidation through different pathways. Due to their unsaturation, GLVs will likely react with oxidizing agents besides ozone, notably hydroxyl, $NO_3$, and $NO_x$ radicals, potentially

leading to enhanced SOA levels not accounted for by studies addressing the SOA forming potential of GLVs in the presence of ozone alone. In response to this, additional work should be done to characterize the SOA produced from the atmospherically relevant oxidizing systems on GLVs.

It is also important to realize that SOA derived from HXL contains a significant quantity of oligomers. High molecular weight oligomers/dimers are more viscous than smaller molecules due to the difficulty for larger molecules to arrange themselves into a crystal lattice structure. Therefore, particles containing oligomers have higher probability of forming glassy/semisolid compounds as compared to their monomeric units.[78, 83] As mentioned in chapter 2, the phase of the SOA can affect particulate phase chemical reactions, and thus the growth rates of newly formed atmospheric particles.[84, 85] Hence, understanding the physical state of SOA is especially important, as it can provide insight into its sources and formation, and also its subsequent growth, reactivity and atmospheric impacts. In-order to do so, a method was developed by me to estimate the phase state of SOA which is described in the next chapter (Chapter 5).

## 4.5 References

1. Seinfeld, J. H.; Pankow, J. F., Organic atmospheric particulate material. *Annual review of physical chemistry* **2003,** *54*, 121-40.
2. Hallquist, M.; Wenger, J. C.; Baltensperger, U.; Rudich, Y.; Simpson, D.; Claeys, M.; Dommen, J.; Donahue, N. M.; George, C.; Goldstein, A. H.; Hamilton, J. F.; Herrmann, H.; Hoffmann, T.; Iinuma, Y.; Jang, M.; Jenkin, M. E.; Jimenez, J. L.; Kiendler-Scharr, A.; Maenhaut, W.; McFiggans, G.; Mentel, T. F.; Monod, A.; Prevot, A. S. H.; Seinfeld, J. H.; Surratt, J. D.; Szmigielski, R.; Wildt, J., The formation, properties and impact of secondary organic aerosol: current and emerging issues. *Atmos Chem Phys* **2009,** *9*, (14), 5155-5236.
3. Kroll, J. H.; Seinfeld, J. H., Chemistry of secondary organic aerosol: Formation and evolution of low-volatility organics in the atmosphere. *Atmos Environ* **2008,** *42*, (16), 3593-3624.
4. Kanakidou, M.; Seinfeld, J. H.; Pandis, S. N.; Barnes, I.; Dentener, F. J.; Facchini, M. C.; Van Dingenen, R.; Ervens, B.; Nenes, A.; Nielsen, C. J.; Swietlicki, E.; Putaud, J. P.; Balkanski, Y.; Fuzzi, S.; Horth, J.; Moortgat, G. K.; Winterhalter, R.; Myhre, C. E. L.; Tsigaridis, K.; Vignati, E.; Stephanou, E. G.; Wilson, J., Organic aerosol and global climate modelling: a review. *Atmos Chem Phys* **2005,** *5*, 1053-1123.

5.      Farina, S. C.; Adams, P. J.; Pandis, S. N., Modeling global secondary organic aerosol formation and processing with the volatility basis set: Implications for anthropogenic secondary organic aerosol. *J Geophys Res-Atmos* **2010,** *115*.

6.      Volkamer, R.; Jimenez, J. L.; San Martini, F.; Dzepina, K.; Zhang, Q.; Salcedo, D.; Molina, L. T.; Worsnop, D. R.; Molina, M. J., Secondary organic aerosol formation from anthropogenic air pollution: Rapid and higher than expected. *Geophys Res Lett* **2006,** *33*, (17).

7.      Scott, C. E.; Rap, A.; Spracklen, D. V.; Forster, P. M.; Carslaw, K. S.; Mann, G. W.; Pringle, K. J.; Kivekas, N.; Kulmala, M.; Lihavainen, H.; Tunved, P., The direct and indirect radiative effects of biogenic secondary organic aerosol. *Atmos Chem Phys* **2014,** *14*, (1), 447-470.

8.      Kiendler-Scharr, A.; Zhang, Q.; Hohaus, T.; Kleist, E.; Mensah, A.; Mentel, T. F.; Spindler, C.; Uerlings, R.; Tillmann, R.; Wildt, J., Aerosol Mass Spectrometric Features of Biogenic SOA: Observations from a Plant Chamber and in Rural Atmospheric Environments. *Environ Sci Technol* **2009,** *43*, (21), 8166-8172.

9.      Guenther, A.; Hewitt, C. N.; Erickson, D.; Fall, R.; Geron, C.; Graedel, T.; Harley, P.; Klinger, L.; Lerdau, M.; Mckay, W. A.; Pierce, T.; Scholes, B.; Steinbrecher, R.; Tallamraju, R.; Taylor, J.; Zimmerman, P., A Global-Model of Natural Volatile Organic-Compound Emissions. *J Geophys Res-Atmos* **1995,** *100*, (D5), 8873-8892.

10.     Hoffmann, T.; Odum, J. R.; Bowman, F.; Collins, D.; Klockow, D.; Flagan, R. C.; Seinfeld, J. H., Formation of organic aerosols from the oxidation of biogenic hydrocarbons. *J Atmos Chem* **1997,** *26*, (2), 189-222.

11.     Goldstein, A.; Galbally, I., Known and unexplored organic constituents in the earth's atmosphere. *Environ Sci Technol* **2007,** *41*, (5), 1514–1521.

12.     Carlton, A. G.; Wiedinmyer, C.; Kroll, J. H., A review of Secondary Organic Aerosol (SOA) formation from isoprene. *Atmos Chem Phys* **2009,** *9*, (14), 4987-5005.

13.     Henze, D. K.; Seinfeld, J. H., Global secondary organic aerosol from isoprene oxidation. *Geophys Res Lett* **2006,** *33*, (9).

14.     Kroll, J. H.; Ng, N. L.; Murphy, S. M.; Flagan, R. C.; Seinfeld, J. H., Secondary organic aerosol formation from isoprene photooxidation. *Environ Sci Technol* **2006,** *40*, (6), 1869-1877.

15.     Ziemann, P. J.; Atkinson, R., Kinetics, products, and mechanisms of secondary organic aerosol formation. *Chem Soc Rev* **2012,** *41*, (19), 6582-6605.

16.     Lee, A.; Goldstein, A. H.; Kroll, J. H.; Ng, N. L.; Varutbangkul, V.; Flagan, R. C.; Seinfeld, J. H., Gas-phase products and secondary aerosol yields from the photooxidation of 16 different terpenes. *J Geophys Res-Atmos* **2006,** *111*, (D17).

17.     Kuhn, U.; Rottenberger, S.; Biesenthal, T.; Wolf, A.; Schebeske, G.; Ciccioli, P.; Brancaleoni, E.; Frattoni, M.; Tavares, T. M.; Kesselmeier, J., Isoprene and monoterpene emissions of Amazonian tree species during the wet season: Direct and indirect investigations on controlling environmental functions. *J Geophys Res-Atmos* **2002,** *107*, (D20).

18.     Konig, G.; Brunda, M.; Puxbaum, H.; Hewitt, C. N.; Duckham, S. C.; Rudolph, J., Relative Contribution of Oxygenated Hydrocarbons to the Total Biogenic Voc Emissions of Selected Mid-European Agricultural and Natural Plant-Species. *Atmos Environ* **1995,** *29*, (8), 861-874.

19.     Olofsson, M.; Ek-Olausson, B.; Ljungstrom, E.; Langer, S., Flux of organic compounds from grass measured by relaxed eddy accumulation technique. *J Environ Monitor* **2003,** *5*, (6), 963-970.

20.     Mentel, T. F.; Kleist, E.; Andres, S.; Dal Maso, M.; Hohaus, T.; Kiendler-Scharr, A.; Rudich, Y.; Springer, M.; Tillmann, R.; Uerlings, R.; Wahner, A.; Wildt, J., Secondary aerosol formation from stress-induced biogenic emissions and possible climate feedbacks. *Atmos Chem Phys* **2013,** *13*, (17), 8755-8770.

21.     Kleist, E.; Mentel, T. F.; Andres, S.; Bohne, A.; Folkers, A.; Kiendler-Scharr, A.; Rudich, Y.; Springer, M.; Tillmann, R.; Wildt, J., Irreversible impacts of heat on the emissions of monoterpenes, sesquiterpenes, phenolic BVOC and green leaf volatiles from several tree species. *Biogeosciences* **2012,** *9*, (12), 5111-5123.

22.     Croft, K. P. C.; Juttner, F.; Slusarenko, A. J., Volatile Products of the Lipoxygenase Pathway Evolved from Phaseolus-Vulgaris (L) Leaves Inoculated with Pseudomonas-Syringae Pv-Phaseolicola. *Plant Physiol* **1993,** *101*, (1), 13-24.

23.     Hamilton, J. F.; Lewis, A. C.; Carey, T. J.; Wenger, J. C.; Garcia, E. B. I.; Munoz, A., Reactive oxidation products promote secondary organic aerosol formation from green leaf volatiles. *Atmos Chem Phys* **2009,** *9*, (11), 3815-3823.

24.     Beauchamp, J.; Wisthaler, A.; Hansel, A.; Kleist, E.; Miebach, M.; Niinemets, U.; Schurr, U.; Wildt, J., Ozone induced emissions of biogenic VOC from tobacco: relationships between ozone uptake and emission of LOX products. *Plant Cell Environ* **2005,** *28*, (10), 1334-1343.

25.     Brilli, F.; Hortnagl, L.; Bamberger, I.; Schnitzhofer, R.; Ruuskanen, T. M.; Hansel, A.; Loreto, F.; Wohlfahrt, G., Qualitative and Quantitative Characterization of Volatile Organic Compound Emissions from Cut Grass. *Environ Sci Technol* **2012,** *46*, (7), 3859-3865.

26.     Joutsensaari, J.; Loivamaki, M.; Vuorinen, T.; Miettinen, P.; Nerg, A. M.; Holopainen, J. K.; Laaksonen, A., Nanoparticle formation by ozonolysis of inducible plant volatiles. *Atmos Chem Phys* **2005,** *5*, 1489-1495.

27.     Harvey, R. M.; Zahardis, J.; Petrucci, G. A., Establishing the contribution of lawn mowing to atmospheric aerosol levels in American suburbs. *Atmos. Chem. Phys.* **2014,** *14*, (2), 797-812.

28.     Karl, T.; Fall, R.; Jordan, A.; Lindinger, W., On-line analysis of reactive VOCs from urban lawn mowing. *Environ Sci Technol* **2001,** *35*, (14), 2926-2931.

29.     Li, J.; Sun, Y.; Cao, H.; Han, D.; He, M., Mechanisms and kinetics of the ozonolysis reaction of cis-3-hexenyl acetate and trans-2-hexenyl acetate in atmosphere: a theoretical study. *Struct Chem* **2013**, 1-13.

30.     Hamilton, J. F.; Lewis, A. C.; Carey, T. J.; Wenger, J. C., Characterization of polar compounds and oligomers in secondary organic aerosol using liquid chromatography coupled to mass spectrometry. *Analytical chemistry* **2008,** *80*, (2), 474-480.

31.     O'Dwyer, M. A.; Carey, T. J.; Healy, R. M.; Wenger, J. C.; Picquet-Varrault, B.; Doussin, J. F., The Gas-phase Ozonolysis of 1-Penten-3-ol, (Z)-2-Penten-1-ol and 1-Penten-3-one: Kinetics, Products and Secondary Organic Aerosol Formation. *Z Phys Chem* **2010,** *224*, (7-8), 1059-1080.

32.     Finessi, E.; Decesari, S.; Paglione, M.; Giulianelli, L.; Carbone, C.; Gilardoni, S.; Fuzzi, S.; Saarikoski, S.; Raatikainen, T.; Hillamo, R.; Allan, J.; Mentel, T. F.; Tiitta, P.; Laaksonen, A.; Petaja, T.; Kulmala, M.; Worsnop, D. R.; Facchini, M. C., Determination of the biogenic secondary organic aerosol fraction in the boreal forest by NMR spectroscopy. *Atmos Chem Phys* **2012,** *12*, (2), 941-959.

33.     Laskin, A.; Laskin, J.; Nizkorodov, S. A., Mass spectrometric approaches for chemical characterisation of atmospheric aerosols: critical review of the most recent advances. *Environ Chem* **2012,** *9*, (3), 163-189.

34.     Prather, K. A.; Hatch, C. D.; Grassian, V. H., Analysis of Atmospheric Aerosols. *Annu Rev Anal Chem* **2008,** *1*, 485-514.

35.     Sullivan, R. C.; Prather, K. A., Recent advances in our understanding of atmospheric chemistry and climate made possible by on-line aerosol analysis instrumentation. *Analytical chemistry* **2005,** *77*, (12), 3861-3885.

36.     Cahill, T. M.; Seaman, V. Y.; Charles, M. J.; Holzinger, R.; Goldstein, A. H., Secondary organic aerosols formed from oxidation of biogenic volatile organic compounds in the Sierra Nevada Mountains of California. *J Geophys Res-Atmos* **2006,** *111*, (D16).

37.     Holzinger, R.; Williams, J.; Herrmann, F.; Lelieveld, J.; Donahue, N. M.; Rockmann, T., Aerosol analysis using a Thermal-Desorption Proton-Transfer-Reaction Mass Spectrometer (TD-PTR-MS): a new approach to study processing of organic aerosols. *Atmos Chem Phys* **2010,** *10*, (5), 2257-2267.

38.     Geddes, S.; Nichols, B.; Flemer, S.; Eisenhauer, J.; Zahardis, J.; Petrucci, G. A., Near-Infrared Laser Desorption/Ionization Aerosol Mass Spectrometry for Investigating Primary and Secondary Organic Aerosols under Low Loading Conditions. *Analytical chemistry* **2010,** *82*, (19), 7915-7923.

39.     Geddes, S.; Nichols, B.; Todd, K.; Zahardis, J.; Petrucci, G. A., Near-infrared laser desorption/ionization aerosol mass spectrometry for measuring organic aerosol at atmospherically relevant aerosol mass loadings. *Atmos Measur Tech* **2010,** *3*, (4), 1175-1183.

40.     Danzer, K., *Analytical Chemistry: Theoretical and Metrological Fundamentals*. Springer: 2007.

41.     Seinfeld, J. H.; Kleindienst, T. E.; Edney, E. O.; Cohen, J. B., Aerosol Growth in a Steady-State, Continuous Flow Chamber: Application to Studies of Secondary Aerosol Formation. *Aerosol Sci Tech* **2003,** *37*, (9), 728-734.

42.     Shilling, J. E.; Chen, Q.; King, S. M.; Rosenoern, T.; Kroll, J. H.; Worsnop, D. R.; McKinney, K. A.; Martin, S. T., Particle mass yield in secondary organic aerosol formed by the dark ozonolysis of α-pinene. *Atmos. Chem. Phys.* **2008,** *8*, (7), 2073-2088.

43.     Jayne, J. T.; Leard, D. C.; Zhang, X.; Davidovits, P.; Smith, K. A.; Kolb, C. E.; Worsnop, D. R., Development of an Aerosol Mass Spectrometer for Size and Composition Analysis of Submicron Particles. *Aerosol Sci Tech* **2000,** *33*, (1-2), 49-70.

44.     DeCarlo, P. F.; Slowik, J. G.; Worsnop, D. R.; Davidovits, P.; Jimenez, J. L., Particle Morphology and Density Characterization by Combined Mobility and Aerodynamic Diameter Measurements. Part 1: Theory. *Aerosol Sci Tech* **2004,** *38*, (12), 1185-1205.

45.     Chen, Q.; Liu, Y. J.; Donahue, N. M.; Shilling, J. E.; Martin, S. T., Particle-Phase Chemistry of Secondary Organic Material: Modeled Compared to Measured O:C and H:C Elemental Ratios Provide Constraints. *Environ Sci Technol* **2011,** *45*, (11), 4763-4770.

46.     Agency, U. S. E. P. Exposure Assessment Tools and Models. http://www.epa.gov/oppt/exposure/pubs/episuite.htm (January 10th 2013),

47.     Liu, P.; Ziemann, P. J.; Kittelson, D. B.; McMurry, P. H., Generating particle beam of controlled dimensions and convergence: I. Theory of particle motion in aerodynamic lenses and nozzle expansions. *Aerosol Sci. Technol.* **1995,** *22*, 293-313.

48.     Geddes, S.; Zahardis, J.; Petrucci, G. A., Chemical transformations of peptide containing fine particles: oxidative processing, accretion reactions and implications to the atmospheric fate of cell-derived materials in organic aerosol. *J Atmos Chem* **2010,** *63*, (3), 187-202.

49.     Grosjean, E.; Grosjean, D., The gas-phase reaction of alkenes with ozone: formation yields of carbonyls from biradicals in ozone–alkene–cyclohexane experiments. *Atmos Environ* **1998,** *32*, (20), 3393-3402.

50.     Aschmann, S. M.; Shu, Y. H.; Arey, J.; Atkinson, R., Products of the gas-phase reactions of cis-3-hexen-1-ol with OH radicals and O-3. *Atmos Environ* **1997,** *31*, (21), 3551-3560.

51.     Horie, O.; Moortgat, G. K., Gas phase ozonolysis of alkenes. Recent advances in mechanistic investigations. *Accounts Chem Res* **1998,** *31*, (7), 387-396.

52.     Vereecken, L.; Francisco, J. S., Theoretical studies of atmospheric reaction mechanisms in the troposphere. *Chem Soc Rev* **2012,** *41*, (19), 6259-6293.

53.     Johnson, D.; Marston, G., The gas-phase ozonolysis of unsaturated volatile organic compounds in the troposphere. *Chem Soc Rev* **2008,** *37*, (4), 699-716.

54.      Atkinson, R.; Arey, J.; Aschmann, S. M.; Corchnoy, S. B.; Shu, Y. H., Rate Constants for the Gas-Phase Reactions of Cis-3-Hexen-1-Ol, Cis-3-Hexenylacetate, Trans-2-Hexenal, and Linalool with Oh and No3 Radicals and O-3 at 296+/-2 K, and Oh Radical Formation Yields from the O-3 Reactions. *Int J Chem Kinet* **1995,** *27*, (10), 941-955.

55.      Docherty, K. S.; Wu, W.; Lim, Y. B.; Ziemann, P. J., Contributions of organic peroxides to secondary aerosol formed from reactions of monoterpenes with O-3. *Environ Sci Technol* **2005,** *39*, (11), 4049-4059.

56.      Pankow, J. F., An Absorption-Model of Gas-Particle Partitioning of Organic-Compounds in the Atmosphere. *Atmos Environ* **1994,** *28*, (2), 185-188.

57.      Donahue, N. M.; Robinson, A. L.; Pandis, S. N.; Kroll, J. H.; Worsnop, D. L., Rethinking organic aerosols: Semivolatile emissions and photochemical aging. *Geochim Cosmochim Ac* **2009,** *73*, (13), A299-A299.

58.      Donahue, N. M.; Robinson, A. L.; Stanier, C. O.; Pandis, S. N., Coupled partitioning, dilution, and chemical aging of semivolatile organics. *Environ Sci Technol* **2006,** *40*, (8), 2635-2643.

59.      Robinson, A. L.; Donahue, N. M.; Shrivastava, M. K.; Weitkamp, E. A.; Sage, A. M.; Grieshop, A. P.; Lane, T. E.; Pierce, J. R.; Pandis, S. N., Rethinking organic aerosols: Semivolatile emissions and photochemical aging. *Science* **2007,** *315*, (5816), 1259-1262.

60.      Tobias, H. J.; Ziemann, P. J., Thermal Desorption Mass Spectrometric Analysis of Organic Aerosol Formed from Reactions of 1-Tetradecene and O3 in the Presence of Alcohols and Carboxylic Acids. *Environ SciTechnol* **2000,** *34*, (11), 2105-2115.

61.      Atkinson, R.; Aschmann, S. M.; Arey, J.; Shorees, B., Formation of Oh Radicals in the Gas-Phase Reactions of O3 with a Series of Terpenes. *J Geophys Res-Atmos* **1992,** *97*, (D5), 6065-6073.

62.      Zahardis, J.; LaFranchi, B. W.; Petrucci, G. A., Direct observation of polymerization in the oleic acid-ozone heterogeneous reaction system by photoelectron resonance capture ionization aerosol mass spectrometry. *Atmos Environ* **2006,** *40*, (9), 1661-1670.

63.      DePalma, J. W.; Horan, A. J.; Hall, W. A.; Johnston, M. V., Thermodynamics of oligomer formation: implications for secondary organic aerosol formation and reactivity. *Phys Chem Chem Phys* **2013,** *15*, (18), 6935-6944.

64.      Liggio, J.; Li, S. M., A new source of oxygenated organic aerosol and oligomers. *Atmos Chem Phys* **2013,** *13*, (6), 2989-3002.

65.      Hall, W. A.; Johnston, M. V., Oligomer Formation Pathways in Secondary Organic Aerosol from MS and MS/MS Measurements with High Mass Accuracy and Resolving Power. *Journal of the American Society for Mass Spectrometry* **2012,** *23*, (6), 1097-1108.

66.      Kroll, J. H.; Chan, A. W. H.; Ng, N. L.; Flagan, R. C.; Seinfeld, J. H., Reactions of semivolatile organics and their effects on secondary organic aerosol formation. *Environ Sci Technol* **2007,** *41*, (10), 3545-3550.

67.      Heaton, K. J.; Dreyfus, M. A.; Wang, S.; Johnston, M. V., Oligomers in the early stage of biogenic secondary organic aerosol formation and growth. *Environ Sci Technol* **2007,** *41*, (17), 6129-6136.

68.      Kalberer, M.; Paulsen, D.; Sax, M.; Steinbacher, M.; Dommen, J.; Prevot, A. S. H.; Fisseha, R.; Weingartner, E.; Frankevich, V.; Zenobi, R.; Baltensperger, U., Identification of polymers as major components of atmospheric organic aerosols. *Science* **2004,** *303*, (5664), 1659-1662.

69.      Hastings, W. P.; Koehler, C. A.; Bailey, E. L.; De Haan, D. O., Secondary organic aerosol formation by glyoxal hydration and oligomer formation: Humidity effects and equilibrium shifts during analysis. *Environ Sci Technol* **2005,** *39*, (22), 8728-8735.

70.	Gould, N. D.; Allen, C. L.; Nam, B. C.; Schepartz, A.; Miller, S. J., Combined Lewis acid and Bronsted acid-mediated reactivity of glycosyl trichloroacetimidate donors. *Carbohyd Res* **2013,** *382*, 36-42.

71.	Grosjean, E.; Grosjean, D., The gas phase reaction of unsaturated oxygenates with ozone: Carbonyl products and comparison with the alkene-ozone reaction. *J Atmos Chem* **1997,** *27*, (3), 271-289.

72.	Baker, J.; Aschmann, S. M.; Arey, J.; Atkinson, R., Reactions of stabilized Criegee intermediates from the gas-phase reactions of O-3 with selected alkenes. *Int J Chem Kinet* **2001,** *34*, (2), 73-85.

73.	Schneider, J.; Weimer, S.; Drewnick, F.; Borrmann, S.; Helas, G.; Gwaze, P.; Schmid, O.; Andreae, M. O.; Kirchner, U., Mass spectrometric analysis and aerodynamic properties of various types of combustion-related aerosol particles. *Int J Mass Spectrom* **2006,** *258*, (1-3), 37-49.

74.	Renbaum-Wolff, L.; Grayson, J. W.; Bateman, A. P.; Kuwata, M.; Sellier, M.; Murray, B. J.; Shilling, J. E.; Martin, S. T.; Bertram, A. K., Viscosity of alpha-pinene secondary organic material and implications for particle growth and reactivity. *P Natl Acad Sci USA* **2013,** *110*, (20), 8014-8019.

75.	Shiraiwa, M.; Ammann, M.; Koop, T.; Poschl, U., Gas uptake and chemical aging of semisolid organic aerosol particles. *P Natl Acad Sci USA* **2011,** *108*, (27), 11003-11008.

76.	Wang, B.; O'Brien, R. E.; Kelly, S. T.; Shilling, J. E.; Moffet, R. C.; Gilles, M. K.; Laskin, A., Reactivity of Liquid and Semisolid Secondary Organic Carbon with Chloride and Nitrate in Atmospheric Aerosols. *J. Phys. Chem. A* **2014**.

77.	Lignell, H.; Hinks, M. L.; Nizkorodov, S. A., Exploring matrix effects on photochemistry of organic aerosols. *P Natl Acad Sci USA* **2014,** *111*, (38), 13780-13785.

78.	Zobrist, B.; Marcolli, C.; Pedernera, D. A.; Koop, T., Do atmospheric aerosols form glasses? *Atmos Chem Phys* **2008,** *8*, (17), 5221-5244.

79.	Cocker, D. R.; Mader, B. T.; Kalberer, M.; Flagan, R. C.; Seinfeld, J. H., The effect of water on gas-particle partitioning of secondary organic aerosol: II. m-xylene and 1,3,5-trimethylbenzene photooxidation systems. *Atmospheric Environment* **2001,** *35*, (35), 6073-6085.

80.	Healy, R. M.; Temime, B.; Kuprovskyte, K.; Wenger, J. C., Effect of Relative Humidity on Gas/Particle Partitioning and Aerosol Mass Yield in the Photooxidation of p-Xylene. *Environ Sci Technol* **2009,** *43*, (6), 1884-1889.

81.	Zhou, Y.; Zhang, H. F.; Parikh, H. M.; Chen, E. H.; Rattanavaraha, W.; Rosen, E. P.; Wang, W. X.; Kamens, R. M., Secondary organic aerosol formation from xylenes and mixtures of toluene and xylenes in an atmospheric urban hydrocarbon mixture: Water and particle seed effects (II). *Atmospheric Environment* **2011,** *45*, (23), 3882-3890.

82.	Harvey, R. M.; Bateman, A. P.; Jain, S.; Li, Y. J.; Martin, S.; Petrucci, G. A., Optical Properties of Secondary Organic Aerosol from cis-3-Hexenol and cis-3-Hexenyl Acetate: Effect of Chemical Composition, Humidity, and Phase. *Environ Sci Technol* **2016**.

83.	Koop, T.; Bookhold, J.; Shiraiwa, M.; Poschl, U., Glass transition and phase state of organic compounds: dependency on molecular properties and implications for secondary organic aerosols in the atmosphere. *Phys Chem Chem Phys* **2011,** *13*, (43), 19238-19255.

84.	Virtanen, A.; Kannosto, J.; Kuuluvainen, H.; Arffman, A.; Joutsensaari, J.; Saukko, E.; Hao, L.; Yli-Pirila, P.; Tiitta, P.; Holopainen, J. K.; Keskinen, J.; Worsnop, D. R.; Smith, J. N.; Laaksonen, A., Bounce behavior of freshly nucleated biogenic secondary organic aerosol particles. *Atmos Chem Phys* **2011,** *11*, (16), 8759-8766.

85.	Kuwata, M.; Martin, S. T., Phase of atmospheric secondary organic material affects its reactivity. *P Natl Acad Sci USA* **2012,** *109*, (43), 17354-17359.

# CHAPTER 5: A NEW METHOD TO MEASURE AEROSOL PARTICLE BOUNCE USING A CASCADE ELECTRICAL LOW PRESSURE IMPACTOR

The work described in this chapter was submitted and accepted for publication in the following journal. The full reference is as follows:

*Jain, S. and Petrucci, G. A. (2015). A New Method to Measure Aerosol Particle Bounce Using a Cascade Electrical Low Pressure Impactor. Aerosol Sci. Technol. 49:390-399.*

## 5.1 Introduction

Organic aerosol is a ubiquitous component of atmospheric particulate that influences both human health[1] and global climate.[2] A large fraction of organic aerosol is secondary in nature (SOA), being produced by oxidation of volatile organic compounds (VOCs) emitted by biogenic and anthropogenic sources.[3] Estimates regarding global SOA formation suggest that SOA comprises of approximately 60-70% total organic aerosol mass, with 90% of this mass being in oxidized form.[4] Despite the integral role of SOA in atmospheric processes, there remains a limited understanding of the chemical and physical changes induced in SOA as it ages in the atmosphere. Understanding the physical state of SOA is especially important, as it can provide insight into its sources and formation, and also its subsequent growth, reactivity and atmospheric impacts.[5, 6]

A disparity exists between modeled and observed atmospheric SOA levels, which has stimulated several efforts to improve our understanding of SOA sources and formation yields.[7-9] Present models assume that SOA particles remain liquid-like throughout their lifetime and an equilibrium exists between the particle and gas phase due to rapid evaporation and condensation.[8, 10, 11] However, recent work suggests otherwise, where

researchers [8, 12, 13] found that evaporation of α-pinene SOA at room temperature was orders of magnitude slower than expected from well-mixed liquid droplets. Models further assume that SOA particles have low viscosity resulting in rapid diffusion and mixing throughout the homogeneous particles; however, recent studies provide surmounting evidence to challenge this long-held fundamental assumption.[13-15]

The physical state of particles can affect particulate phase chemical reactions and thus, the growth rates of newly formed atmospheric particles.[6, 16] The phase state may also increase the lifetime of organic aerosols markedly, as the oxidation caused by atmospheric ozone and other oxidants is confined to the surface.[5] Recent results suggest that biogenic SOA particles can adopt a solid, and most likely glassy state.[6, 13] Furthermore, it has been shown that for mixed compositions of isoprene- and α-pinene derived SOA, a significant number of particles bounce off (rather than adhere to) solid surfaces, suggesting a fraction of the particles are not in the liquid state.[17]

Several methods have been reported in the literature to access particle phase by measuring the "bounce factor (BF)". In the seminal work of Virtanen, et al. [6] a scanning mobility particle sizer (SMPS) and an electrical low pressure impactor (ELPI) were used in concert to calculate aerosol particle BF. Solid particles bounce in the ELPI cascade impactor, generating excess (i.e., erroneously high) current in the lower stages (i.e., larger particles are mistakenly counted as smaller particles). Particle BF is then calculated by comparing the bounce-affected ELPI measured currents with "ideal currents" (i.e., currents assuming no particle bounce) acquired by converting the SMPS number distribution to an ELPI current response function.[6] It is important to realize that ELPI and SMPS measure different physical properties; aerodynamic diameter and electro-mobility diameter,

respectively. In the ELPI, impaction is dependent upon the aerodynamic diameter, whereas the particle charging efficiency depends on the stokes diameter. Interconverting between diameters to obtain size and current distributions requires accurate knowledge of particle density ($\rho_p$) and shape, which in the case of polydisperse aerosols is dependent on the volume equivalent particle diameter.[18] Moreover, accurate conversion of an SMPS distribution to an ELPI "Ideal" current distribution requires accurate knowledge of kernel functions and charging efficiency, which are dependent on the effective density of the particle. Inaccurate estimation of particle density can result in deviations from the ideal current distribution, which will have a direct impact on the accuracy of the BF calculation. Moreover, charge transfer properties of the particles to the impaction substrate must be taken into account to accurately measure the BF. Saukko and co-workers [5] reported on the use of a single-stage impactor with optical particle detection to measure BF of monodisperse aerosols, requiring different impactor nozzles for each diameter. Recent work by Bateman and coworkers[19] extends the single-nozzle approach to elucidate polydisperse BF, while Kidd and co-workers [20] utilized an infrared-transmitting attenuated total reflectance (ATR) germanium crystal as the impaction surface to study the particle phase of SOA based on impaction pattern. The latter method, however, may be subject to bias due to either use of different size substrates, which could increase the collection efficiency, or use of varying flow rates, which would change the impaction pattern.

In this chapter, I describe a simplified method that eliminates the need for an SMPS and directly estimates BF of polydisperse SOA using only one multi-stage cascade ELPI. The method relies on comparison of absolute ion currents at each impactor stage under conditions that favor or eliminate particle bounce. I validated the proposed method with

solid and liquid aerosol, namely ammonium sulfate (AS), dioctyl sebacate (DOS), oleic acid (OA) and ozonized oleic acid and present BF evolution of aging α-pinene-derived SOA. This method allows for the real-time determination of SOA phase state for polydisperse aerosols, permitting studies of the relationship between SOA phase, oxidative formation and chemical aging. Furthermore, with the simultaneous use of two ELPI systems, the proposed method also provides the temporal resolution necessary to observe phase changes in a continuously evolving SOA parcel.

## 5.2 Experimental methods and measurements

### 5.2.1 Reagents & equipment

Oleic acid (OA, >98%), ammonium sulfate (AS, >99 %), dioctyl sebacate (DOS, 97%), α-pinene (>99%), CHA (>98%) and HXL (99%) were purchased from Sigma Aldrich and used without further purification. All experiments were performed in the $8m^3$ University of Vermont Environmental Chamber (UVMEC)[21] operated at ambient temperature (∼298 (± 2) K) and atmospheric pressure. The UVMEC is equipped with ambient $O_3$ (Serinus $O_3$ model E020010, American Ecotech, Cincinnati, OH) and NOx (EC9041A NOx Analyzer, American Ecotech, Cincinnati, OH) analyzers.

Current and aerosol particle number size distributions were measured continuously using an electrical low pressure impactor (ELPI+, Dekati, Finland) operating with either smooth or sintered plates (discussed in details below). Prior to initiating measurements, the ELPI charger was allowed to stabilize for one hour, followed by a zeroing of the instrument while flushing with particle-free air. ELPI measurements were made from time 0 i.e., the beginning of particle injection into the UVMEC. Time 0 in the figures represents the beginning of injection of particles to the UVMEC. Aerosol particle number size

distributions were also measured in parallel with a scanning mobility particle sizer (SMPS model 3080, TSI Inc., Shoreview, MN) to check for reproducibility and disparity between the ELPI and SMPS measurements.

## 5.2.2 Chamber experiments

Homogeneous nucleation was used to generate pure polydisperse particles of DOS and OA having geometric mean diameters of 80 nm and 140 nm respectively with a typical standard deviation of 1.3nm. Vapors generated in a 125-mL three-neck flask held at $125^{\circ}$C for DOS and $110^{\circ}$C for OA were flushed through a condenser ($10^{\circ}$C) by a flow of zero air (USP Medical Air, Airgas East, Williston, VT) into the UVMEC for 30 minutes followed by an equilibration period of one hour. Current distributions were measured throughout this time using the ELPI+ operating either with the sintered plates (to eliminate particle bounce) or smooth plates (to favor particle bounce). Polydisperse AS particles were produced by pneumatic nebulization (concentric nebulizer, J.E. Meinhard Associates, Santa Ana, CA) of a 500 ppm aqueous solution. Particles were dried by passage through a diffusion drier prior to introduction to the UVMEC. The RH of AS aerosol at the exit of the diffusion dryer was <10%. AS particles were introduced for 40 minutes followed by a one hour period of equilibration. There was no increase in the relative humidity within the UVMEC upon introduction of AS particles.  All experiments were conducted at a chamber relative humidity of 20 - 25 %.

The biogenic VOC α-pinene, HXL and CHA were introduced to the UVMEC quantitatively by evaporating 10 µl of analyte for 15 min from a three-neck flask over a warm water bath into a carrier flow of zero air. This resulted in a VOC mixing ratio in the UVMEC of 200 ppb. Ozone, generated from dry, particle-free air by corona discharge

(OL80A/DLS, Ozone Lab, Burton, BC, Canada), was then introduced to the chamber in a

30−60 s burst, until the desired concentration was attained.

*Table 5.1 Experimental conditions used to validate the newly developed BF analysis method*

| Sr. No | Aerosol/ VOC | Oxidant | Temp/% RH | Density (g/ml) | Viscosity* (Pa S) | ELPI impactor plates | Aerosol type |
|---|---|---|---|---|---|---|---|
| 1 | Ammonium Sulfate | NA | 25°C/ 19 | 1.769 | $> 10^{12}$ | Smooth | Solid |
| 2 | Ammonium Sulfate | NA | 23°C/ 20 | | | Sintered | |
| 3 | Dioctyl Sebacate | NA | 26°C/ 22 | 0.914 | 0.059-0.063*** | Smooth | Liquid |
| 4 | Dioctyl Sebacate | NA | 25°C/ 21 | | | Sintered | |
| 5 | Oleic Acid | NA | 23°C/ 20 | 0.895** | 0.026*** | Smooth | Liquid |
| 6 | Oleic Acid | NA | 24°C/ 19 | | | Sintered | |
| 7 | Oleic Acid | O₃ (200 ppb) | 23°C/ 20 | 0.895** | $\sim 10^2 - 10^{12}$ | Smooth | Non-liquid |
| 8 | Oleic Acid | O₃ (200 ppb) | 24°C/ 19 | | | Sintered | |
| 9 | α-pinene (200 ppb) | O₃ (157 ppb) | 25°C/ 23 | 1.2≠ | ~ 3.7E2 - 4.53E7**** | Smooth | Variable |
| 10 | α-pinene (200 ppb) | O₃ (168 ppb) | 26°C/ 20 | | | Sintered | |
| 11 | CHA (200 ppb) | O₃ (190 ppb) | 22°C/ 19 | 1.2 | Unknown | Smooth | Variable |
| 12 | CHA (200 ppb) | O₃ (187 ppb) | 24°C/ 22 | | | Sintered | |
| 13 | HXL (200 ppb) | O₃ (198 ppb) | 25°C/ 22 | 1.2 | Unknown | Smooth | Variable |
| 14 | HXL (200 ppb) | O₃ (196 ppb) | 26°C/ 21 | | | Sintered | |

Experimental details are given in Table 5.1. All experiments were carried out in duplicate. Between experiments, the chamber was passivated with $O_3$ (1-2 ppm) overnight and then flushed with zero air until the background aerosol mass and number concentrations were below 0.1 $\mu g/m^3$ and 50 particles/$cm^3$, respectively. Dry, zero air was produced by passing room air sequentially through silica, activated carbon and HEPA filters.

## 5.3 Theory

### 5.3.1 ELPI and particle bounce

Operational and calibration details of the electrical low pressure impactor (ELPI) are provided elsewhere.[22, 23] Briefly, the ELPI classifies particles based on their aerodynamic diameter. Operation of the ELPI can be divided into three main stages (Figure 5.1): (1) unipolar charging of the aerosols, (2) size classification of these charged aerosols in a Berners low-pressure cascade impactor and (3) electrical measurement of collected particles by a series of electrometers.

Aerosols are sampled at a flow rate of 10Lmin[-1] and after charging via corona discharge, are separated according to their aerodynamic diameter in a 14-stage cascade impactor. Both sintered and smooth impactor stages cover the size range of 6 nm to 10 $\mu$m. Each impactor stage is characterized by its cut-off diameter ($D_{50}$), the particle size with a 50% collection efficiency. Cut-point diameters for sintered and smooth impactor plates are given in Table 5.2.
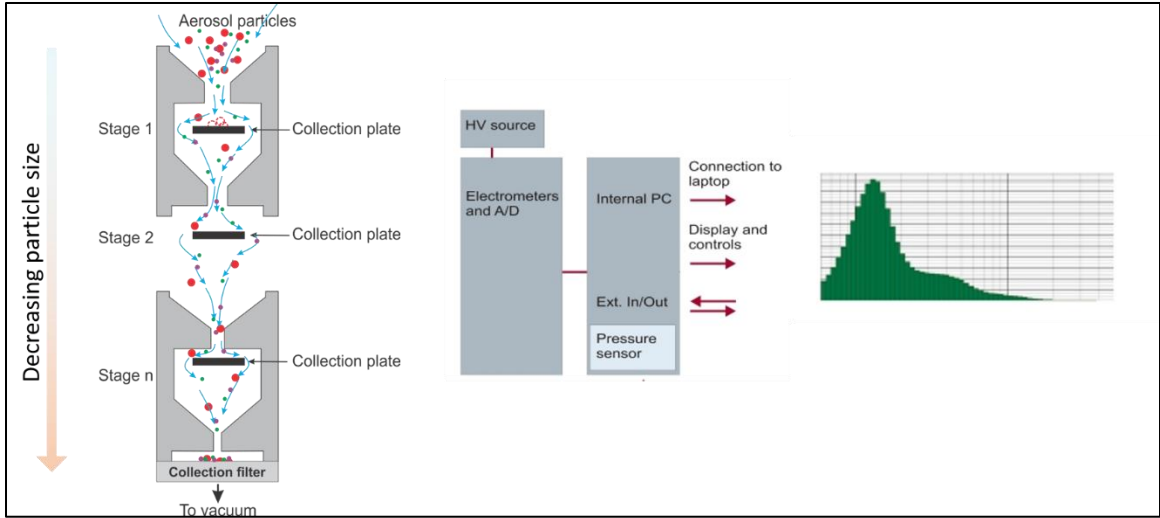
*Figure 5.1 Operation of electrical low pressure cascade impactor.*

Nominally, impaction of the charged particles results in an induced current, $I$ (A), at each stage (equation 1):

$$I = PneUN \qquad (1)$$

where P is the fraction of particles N (# cm$^{-3}$) penetrating through the corona charger, n is the average number of charges per particle, e is the elementary charge (C), and U is the volumetric flow rate (cm$^3$ s$^{-1}$). The induced current distribution is then converted to an input aerosol number distribution by correcting for the various efficiencies identified in equation (1).

A detailed treatment of the theory of particle impaction is described elsewhere.[24-26] Briefly, impaction of a particle with a surface results in loss of its incident kinetic energy, leading to either adhesion or bounce of the particle from the surface. After impaction, the incident kinetic energy is balanced by several energy relaxation terms, including dissipation energy, adhesion energy and rebound energy.[17, 19] A rebound energy that is greater than the sum of dissipation and adhesion energies, results in particle bounce. Hence,

particle bounce from a surface depends on the velocity of the particle, adhesion energy/kinetic energy, and energy loss mechanisms upon collision.[19, 27]

*Table 5.2 Aerodynamic cut point diameters (D₅₀) and downstream pressures for the ELPI+ using smooth and sintered impactor stages (from supplier).*

| Stage | Number of Jets | Smooth Impactor Plates | | Sintered Impactor plates | |
|---|---|---|---|---|---|
| | | $D_{50}$ (μm) | Pressure (KPa) | $D_{50}$ (μm) | Pressure (KPa) |
| 1 | Filter | 0.0060 | 4.00 | 0.0060 | 4.00 |
| 2 | 174 | 0.0168 | 4.48 | 0.0140 | 4.33 |
| 3 | 69 | 0.0271 | 9.73 | 0.0219 | 9.88 |
| 4 | 58 | 0.0545 | 21.86 | 0.0340 | 22.28 |
| 5 | 21 | 0.0933 | 38.44 | 0.0566 | 39.20 |
| 6 | 19 | 0.155 | 68.86 | 0.0932 | 68.13 |
| 7 | 27 | 0.260 | 88.80 | 0.178 | 88.92 |
| 8 | 50 | 0.380 | 97.21 | 0.299 | 97.23 |
| 9 | 48 | 0.610 | 99.59 | 0.491 | 99.63 |
| 10 | 20 | 0.944 | 100.50 | 0.855 | 100.50 |
| 11 | 17 | 1.59 | 101.01 | 1.44 | 101.01 |
| 12 | 14 | 2.38 | 101.19 | 2.16 | 101.19 |
| 13 | 3 | 3.98 | 101.25 | 3.60 | 101.25 |
| 14 | 1 | 6.66 | 101.30 | 6.03 | 101.30 |
| 15 | 1 | 9.87 | 101.32 | 8.94 | 101.32 |

Simple models for predicting particle collision dynamic and bounce assuming a spherical particle impacting on a smooth surface have been presented.[24, 28] According to

these models, the critical velocity, $V_c$, for which a particle could bounce from a surface[24, 28] depends on the surface material and particle aerodynamic diameter ($d_a$). Also, the minimum kinetic energy ($KE_b$)[29] required for particle bounce upon impaction with the surface [24] depends on x, the separation distance between individual particles (usually assumed to be 0.4 nm), A, the Hamaker constant [30] and e, the coefficient of restitution, which is the ratio of rebound velocity to the approach velocity.[24]

## 5.3.2 Charge transfer

As mentioned previously, in order to accurately measure particle bounce, particle charge transfer to the metal impaction surface cannot be ignored. The charge transfer [31] process is dependent upon multiple parameters. Briefly, the total charge transfer ($Q_t$) upon impaction of a particle with a surface includes contact charge ($Q_c$), defined as the charge transferred by a neutral particle and transfer of pre-charge ($Q_o$), defined as the initial charge of the particle entering the impactor. The role of charge transfer on particle bounce in general has been discussed in the literature.[14, 27] Below, I discuss specifically the impact of charge transfer on our approach to calculate BF.

## 5.3.3 Approach & Bounce analysis

Two separate cascade impactors were used to perform bounce analysis and calculate BF. One cascade impactor was equipped with smooth impaction plates (Figure 5.2a), favoring particle bounce. The second cascade impactor used sintered impaction plates (Figure 5.2b) coated with a thin layer of vacuum grease to minimize (ideally shut down) bounce. The method was characterized using liquid and solid reference aerosols of DOS and AS, respectively.

*Figure 5.2 (Left) ELPI smooth plates (right) ELPI sintered plates*

When using smooth impaction plates, particles with sufficient kinetic energy can overcome the adhesion energy at the surface and bounce to lower impactor stages (Figure 5.3), resulting in a systematic bias of the number distribution toward lower channels and smaller particle diameters. The presence of bounce therefore, generates an erroneously high current in the lower stages (i.e., larger particles are mistakenly counted as smaller particles). Recently, this phenomenon was utilized to calculate the BF of atmospheric aerosol.[32] In order to calculate the BF however, simultaneous mobility size distributions had to be made with a scanning mobility particle sizer. In this manner, the SMPS distribution was assumed to be the "true" size distribution and comparison with the measured "biased" ELPI distribution would be used to derive the BF.
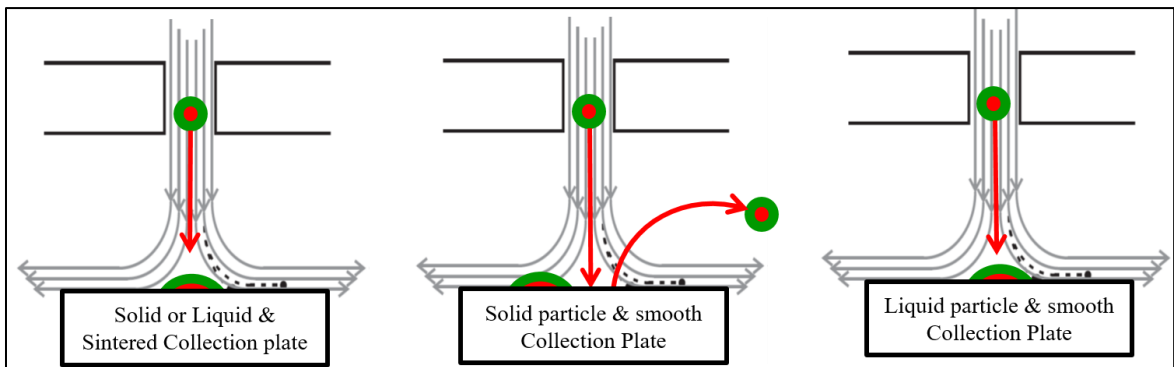


*Figure 5.3 Solid and liquid particles impacting on the sintered and smooth collection plates*

99

In the method proposed herein, the BF is calculated by analyzing the raw current measured with the ELPI+ operating sequentially with smooth and sintered plates according to Equation 2:

$$BF = \frac{I_{Filter\,(smooth)}^{(Bounce)} - I_{Filter\,(sintered)}^{(No\,Bounce)}}{\sum I_{(impactor\,Stage > filter)}^{(no\,Bounce)}} \qquad (2)$$

where $I_{Filter(smooth)}^{(bounce)}$ and, $I_{Filter\,(sintered)}^{(no\,bounce)}$ are the raw currents measured at the back up filter (i.e., smallest diameter channel) of the smooth and sintered plates, respectively. $\sum I_{impactor\,stage\,>filter}^{(no\,bounce)}$ is the sum of the raw currents obtained from all stages of the sintered plates except the backup filter. Use of equation 2 requires that for each aerosol system, the particle size distribution be measured using both smooth and sintered impactor plates. The cut-size of the last impactor stage (filter) is 6 nm and hence, BF can be calculated for particles sizes as low as 6 nm.
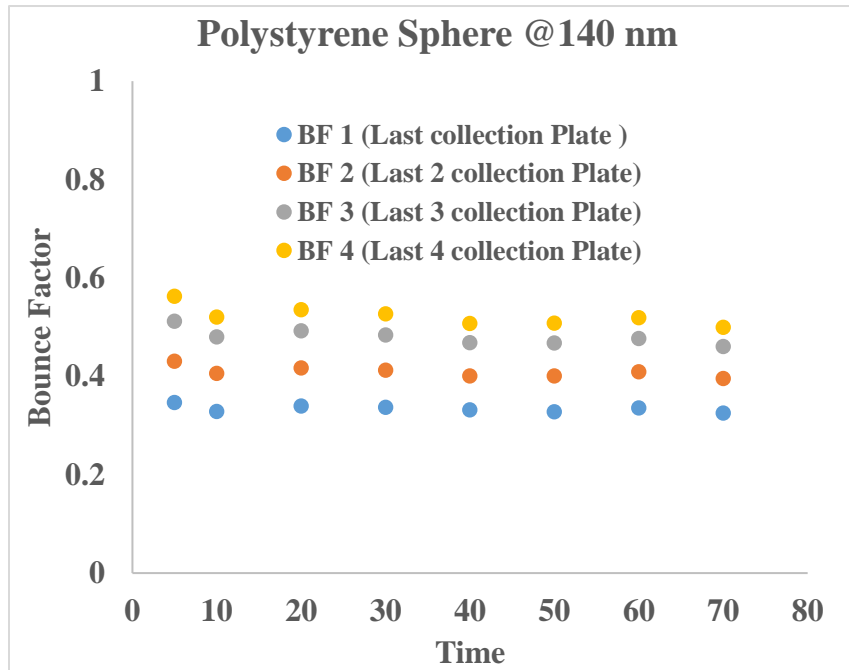


Figure 5.4 BF calculated for different impaction stages for polystyrene Spheres (140 nm)

Bounce factor estimation using equation 2 assumes that all the particles that bounce at stage n (n = 2-14) will continue to bounce at all subsequent stages until they reach the filter stage. If this simplifying assumption holds true, then the values for BF for stages preceding the filter stage (i.e., n > 1) should be negligible. However, as shown previously by Kannosto, et al. [14] and experimentally confirmed in this work (Figure 5.4), this is not necessarily true in all cases. I observed that, for all test samples, BF at stages 2, 3 and 4 were slightly higher than BF at the filter stage (less than 15% difference between stages), suggesting that all particle bounce does not necessarily terminate at the filter stage. Figure 5.4 shows BF results for polystyrene spheres of 140 nm at different channels. Therefore, the calculated BF should be considered as a lower limit of the bounce factor. It should also be noted that the current measured in the filter stage depends on the various charge transfer processes.[27] The final charge of particles entering the filter stage depends on the charge transfer process that takes place every time a particle bounces in an upper stage.

Furthermore, as the ideal and bounce affected currents are measured directly with the same ELPI instrument, as well as impactor cascades with analogous cutoff diameters, the assumption is made that similar charge transfer properties are operable for all measurements involving the same aerosol. It is further shown (Section 5.4.1) that the sum of raw currents across all channels when measured by the smooth and sintered plates is equivalent, supporting the assumption that the overall charge transfer effects are analogous for the two impactor cascades. Hence, the proposed method minimizes the need to know the charge transfer effects quantitatively. Keeping this assumption in mind, calculation of BF using Equation 2 results in reduction of charge transfer effects in the subtracted raw currents.

101

## 5.4 Results and Discussions

In validating the proposed method, it is essential that generation of pure test particles by homogeneous nucleation and pneumatic nebulization does not produce significant numbers of particles below 20 nm, because these primary particles cannot be distinguished from larger particles that have bounced. Figure 5.5 shows a comparison of particle size distributions for AS as measured by the SMPS (20-400 nm) and a nano SMPS (4 – 200 nm). The presence of smaller diameter particles would contribute to the current measured in the filter channel of the ELPI and would erroneously be attributed to particle bounce. As shown in Fig. 5.5 however, analogous particle size distributions were measured by the two instruments, indicating that no native sub-20 nm particles resulted directly from the aerosolization process. Therefore, elevated currents in the filter channel could be correctly attributed to particle bounce from upper (larger diameter) stages.
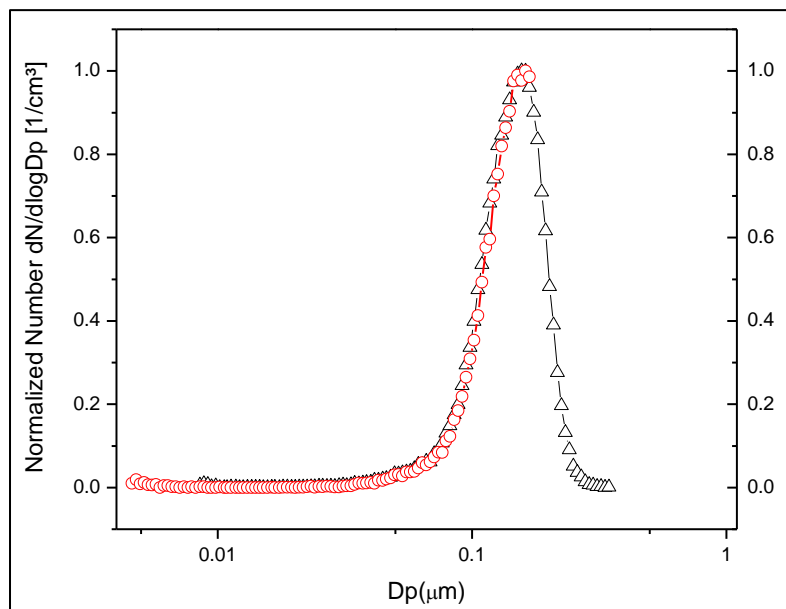


*Figure 5.5 Comparison of particle number distributions for AS aerosol as measured by (O) NanoSMPS and (△) SMPS.*

Multiple phases and different particle morphologies in atmospheric organic and inorganic aerosol reflect the complex interplay between chemical composition and particle

102

phase. Hence, the proposed method was validated with ammonium sulfate and dioctyl sebacate as the crystalline solid and liquid test substances, respectively. These standard materials are readily available and their phase states in aerosol form have been described previously.[6, 14, 32, 33] Additionally, oleic acid was used as a test aerosol, which starts as a liquid and transitions to a non-liquid state (changes viscosity) under conditions of ozonolysis.[34] Results from these experiments were also used to understand the phase characteristics of α-pinene, CHA and HXL derived SOA.

### 5.4.1 Ammonium Sulfate (AS) & Dioctyl Sebacate (DOS)

At relative humidity less than 20%, AS particles exist as a crystalline solid[33, 35] and are therefore expected to exhibit significant bounce. Figure 5.6a shows the sum of raw currents, (fA), measured by the ELPI across all impactor stages, $\sum_{n=1}^{15} fA$. Summed raw currents represent an accurate estimate of the total number of particles measured from all ELPI stages irrespective of particle size and bounce. Hence, Fig 5.6a suggests that the total number concentration of test aerosols as a function of time is the same across the two experiments (i.e., sintered and smooth plates). However, a different picture emerges if we consider the raw currents only on the filter channel (Channel 1, dp < 6nm) (Fig. 5.6b). Both the smooth and sintered filter stages have a $D_{50}$ cut-off of 6nm (see Table 5.2); however, the smooth plate response on Channel 1 is approximately 40 times greater than that of the sintered plates, which, given analogous input aerosol distributions, implies that for the smooth plates, a significant fraction of the larger AS particles are bouncing to and being counted on the filter stage. It has been shown [36] that the RH is reduced at each subsequent stage of the ELPI cascade. Based on previous results,[23] an RH of 25% at the inlet of the ELPI would be reduced to 2.5% downstream of the last ELPI stage, before the filter.
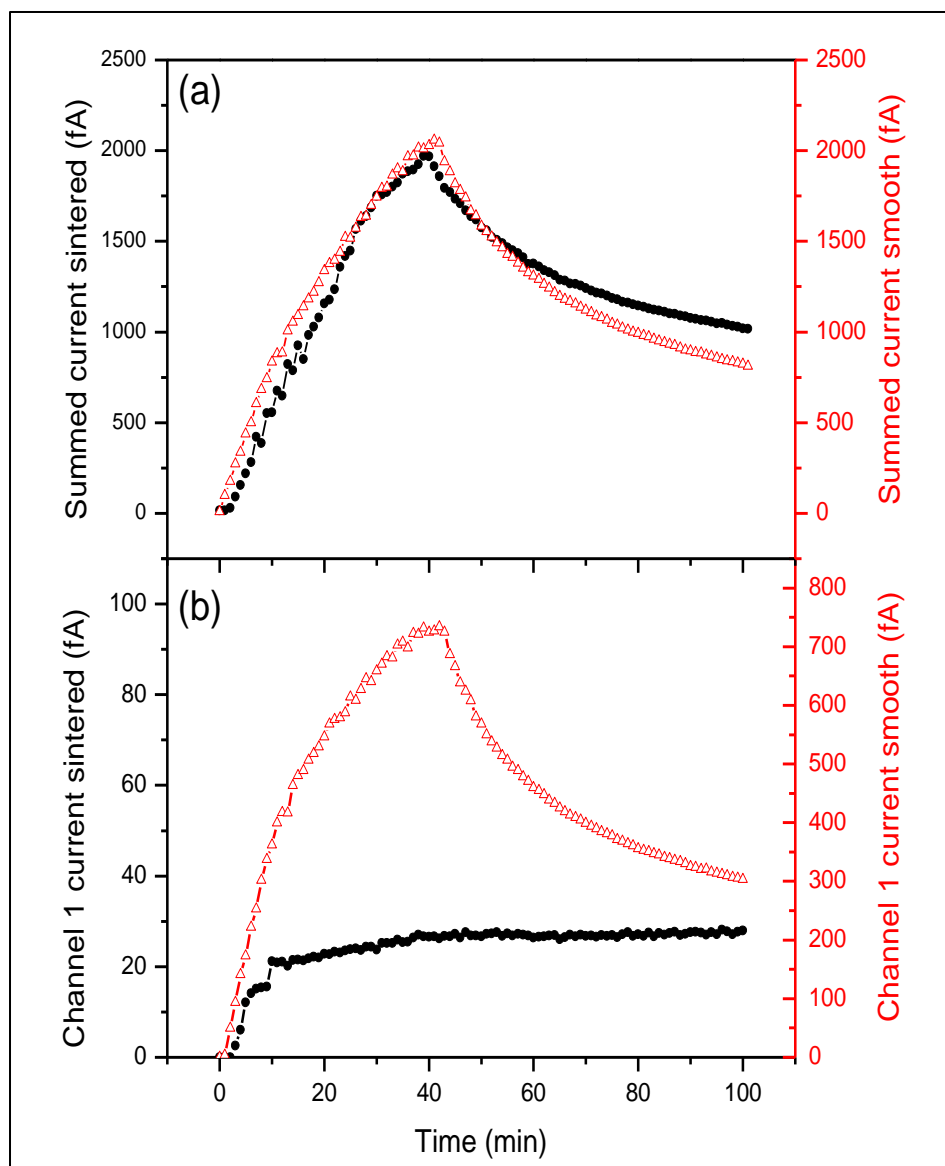
*Figure 5.6 AS aerosol (a) summed and (b) filter stage currents measured by ELPI with ( △) smooth and ( ●) sintered impaction plates.*

It is possible that this significant pressure and RH drop to which the particles are subjected could have an impact on the properties and phase of the aerosol. This could produce a positive error in the measured BF when operating at relatively high RH conditions. However, all experiments in the present work were conducted at relatively low RH (i.e., initial RH of about 20%) which does not induce any change in the aerosol phase in the chamber. Hence, by further reduction of RH as the aerosol reaches the last ELPI

stage, I do not anticipate any significant interference or positive error in my results (i.e., initially solid AS particles will remain solid at subsequent stages). Moreover, the $D_{50}$ for the filter channel is the same for both types of impaction plates, i.e., 6nm. To calculate the BF, we only take into account the excess current on the filter channel and total current measured across all sintered plates (i.e., the ideal distribution). Hence, the difference in cut point diameters for Channels 2-14 should have minimal impact on the BF measurement.
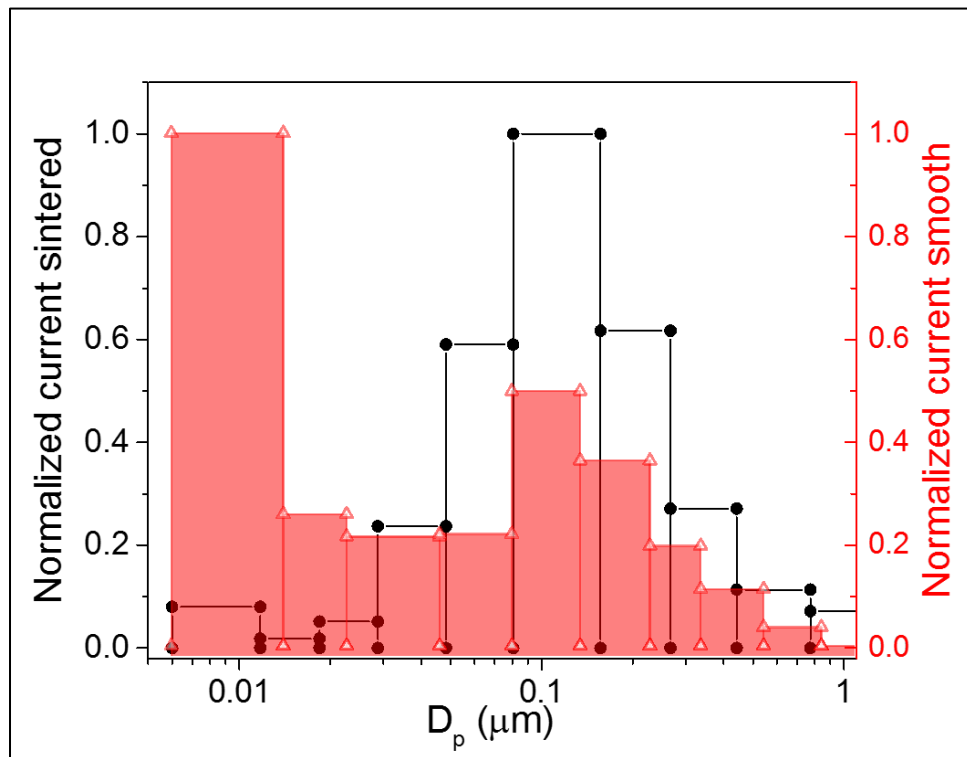


*Figure 5.7 Normalized current distribution when measured with (△) smooth and (●) sintered plates for AS*

Figure 5.7 shows typical normalized "current distributions" for AS when measured with smooth and sintered plates. When AS is sampled with sintered plates, the aerosol GMD and standard deviation are 100nm and 1.4nm, respectively, and less than 4% of the measured current resides in Channels 1-3. When using smooth plates however, the current distribution is shifted to lower diameters and the current fraction in Channels 1-3 has

increased to 53%, suggesting significant particle bounce. Previous studies[6] have suggested that bounce of sub-30 nm particles decreases with decreasing particle size. Therefore, the excess current measured with the smooth plates on channels 1-3, as compared to the sintered plates, is likely due to bounce of larger particles (i.e., from channels $\geq$ 4).
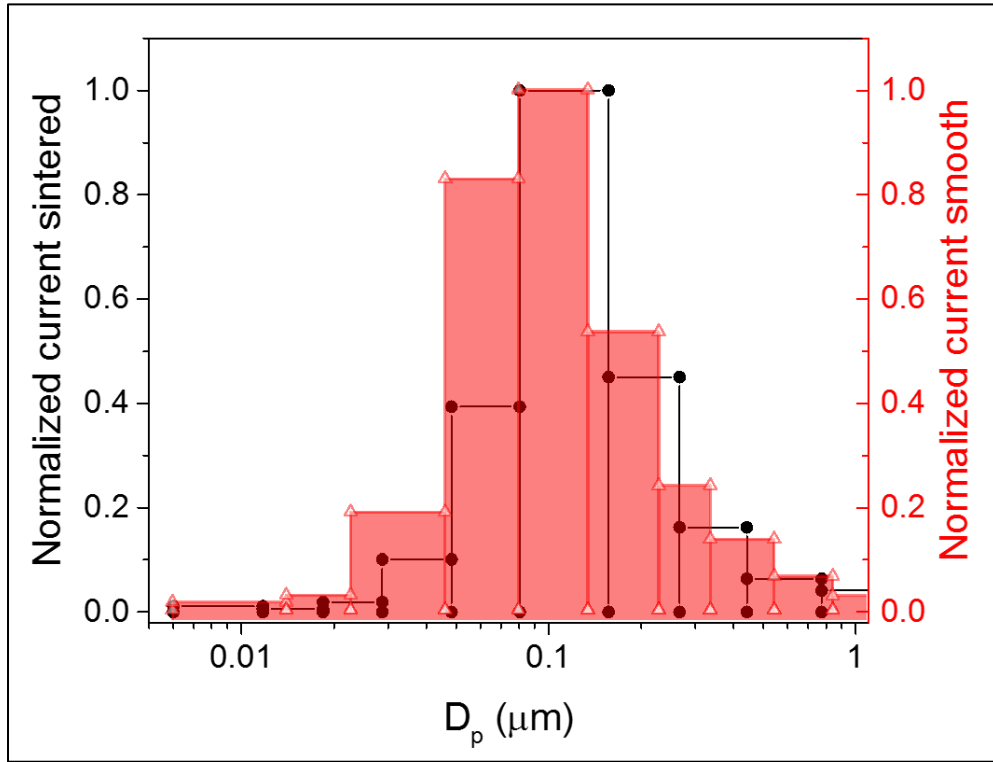


*Figure 5.8 Normalized current distribution when measured with ( △ ) smooth and ( ● ) sintered plates for DOS*

Dioctyl sebacate (DOS) is a liquid particle and under our experimental conditions, served as the negative control for method validation. Figure 5.8 shows a typical normalized "current distributions" for DOS when measured with smooth and sintered plates. Being liquid (i.e., suffering significant deformation upon impact) DOS particles should suffer minimal bounce on both smooth and sintered plates. As such, current distributions for analogous input aerosol distributions should be nearly identical, as supported by the

equivalent GMD of the two curves and the lack of any measurable excess current on the filter channel (Fig. 5.8).

The BF, as calculated from Equation (2), is plotted for the two reference particle types in Figure 5.9. As expected for liquid DOS particles, no bounce was observed and, hence, the calculated BF is 0. For AS particles, on the other hand, I measured a significant particle BF that initially decays with time and then stabilizes at a value of 0.5, despite experimental conditions being well below the deliquescence point for AS particles (RH > 80%). The reason for such a decay is not clear, however, it is possible that this reduction in BF from 0.7 to 0.5 as a function of time is due to the loading effect on the impaction plates which could result in initial changes in the charging efficiency.[37] Once the surface has been modified and reaches a state of equilibrium (20-70 minutes), the BF stabilizes. Previously, it has been shown that water-soluble inorganic salts can reversibly take up atmospheric water vapor without reaching deliquescence and efflorescence phase transition points.[38, 39] In this scenario, a decrease in BF could be explained by the formation of a water layer on the particle surface (Saukko, et al. 2012a). My results are in accord with reported BF values for AS particles below deliquescence, which range from 0.8 to 0.3 depending on the experimental conditions.[5, 6, 19]

### 5.4.2 Oleic Acid

Oleic acid is commonly recognized as a liquid primary organic aerosol and considered a proxy for meat-cooking aerosol.[40-42] In analogy to DOS, it is not expected to exhibit particle bounce. This is also in accord with recent observations that organic aerosols that have not been extensively processed oxidatively (i.e., particles with relatively low

degree of oxidation) are associated with the less solid nature of atmospheric particulate matter.[6]
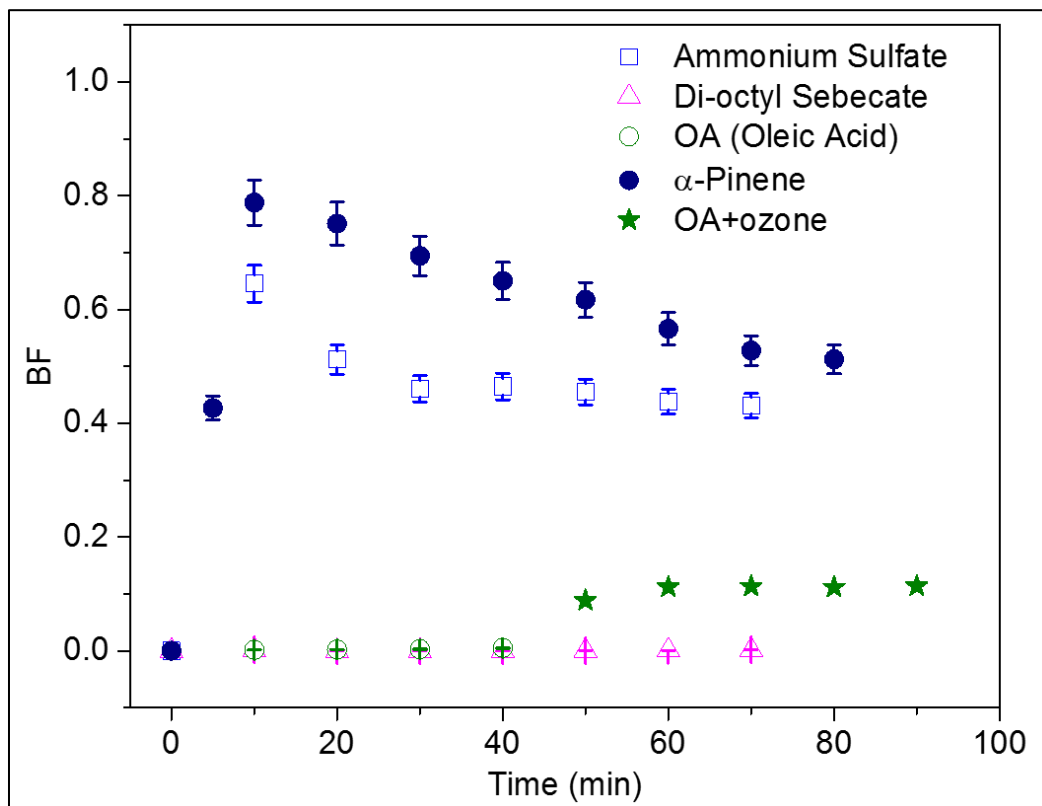


*Figure 5.9 BF of (□) AS, (△) DOS, (O) OA and ( ●) α-pinene derived SOA as a function of particle age.*

As expected (Fig. 5.9, 0-45 min), no significant bounce was measured for pure OA particles under low RH and no-ozone conditions. However, when subjected to ozone at time = 45 min, a particle BF of about 0.15 was reached, indicating the now oxidized OA particles had become non-liquid. The increase in BF for OA may be due, in part, to the formation of higher molecular weight oligomers upon ozonolysis.[43] The main factors affecting the bounce behavior of SOA particles are likely their viscosity, elasticity and surface adhesion properties.[36] These properties depend on glass transition temperatures, which can be affected by various factors such as humidity, oxidative extent and oligomer formation. High molecular weight oligomers are more viscous than smaller molecules due

to the difficulty for larger molecules to arrange themselves into a crystal lattice structure.[44,][45] Also, oligomers have much higher glass transition temperatures, resulting in a higher probability of forming glassy/semisolid compounds as compared to their monomeric units.[44]

Owing to the observed behavior where oleic acid particles act as a liquid and transition to non-liquid upon ozonolysis, it is likely that many atmospheric SOA exhibit this transition behavior during their atmospheric lifetime, necessitating an improved understanding of the conditions requisite for these particles to undergo the transition from liquid to non-liquid.

### 5.4.3 α-Pinene

There exists considerable evidence in the literature to suggest that α-pinene-derived SOA exists in a solid/glassy state in nature.[6, 14, 20] Results from our chamber experiments shows that α-pinene SOA demonstrated considerable bounce from the outset of SOA formation (Fig. 5.9), suggesting a non-liquid state.

Again, comparison of the summed raw currents from the smooth and sintered impaction plates shows good general agreement between the two SOA experiments (Figure 5.10a). On the other hand, the cumulative current measured as a function of particle diameter for the duration of each experiment suggests a difference in "current distribution" with diameter over time. For the case of the smooth plates (Figure 5.10b), we see a significant current (ca. 60%) in the lowest channels (i.e., smallest diameters) that is not present when the sintered plates are used, suggesting that excess current with the smooth impactor plates is due to particle bounce.

The calculated BF of SOA particles generated by α-pinene as a function of aging is shown in Fig 5.9. The particles start bouncing right from the inception of particle growth and have a BF of 0.8, indicative of the non-liquid phase state of the newly formed, highly oxidized SOA. These results are in agreement with those of Saukko and co-workers[36], who found that for $20\% < RH < 50\%$, the BF of biogenic SOA particles is between 0.9 and 0.65.
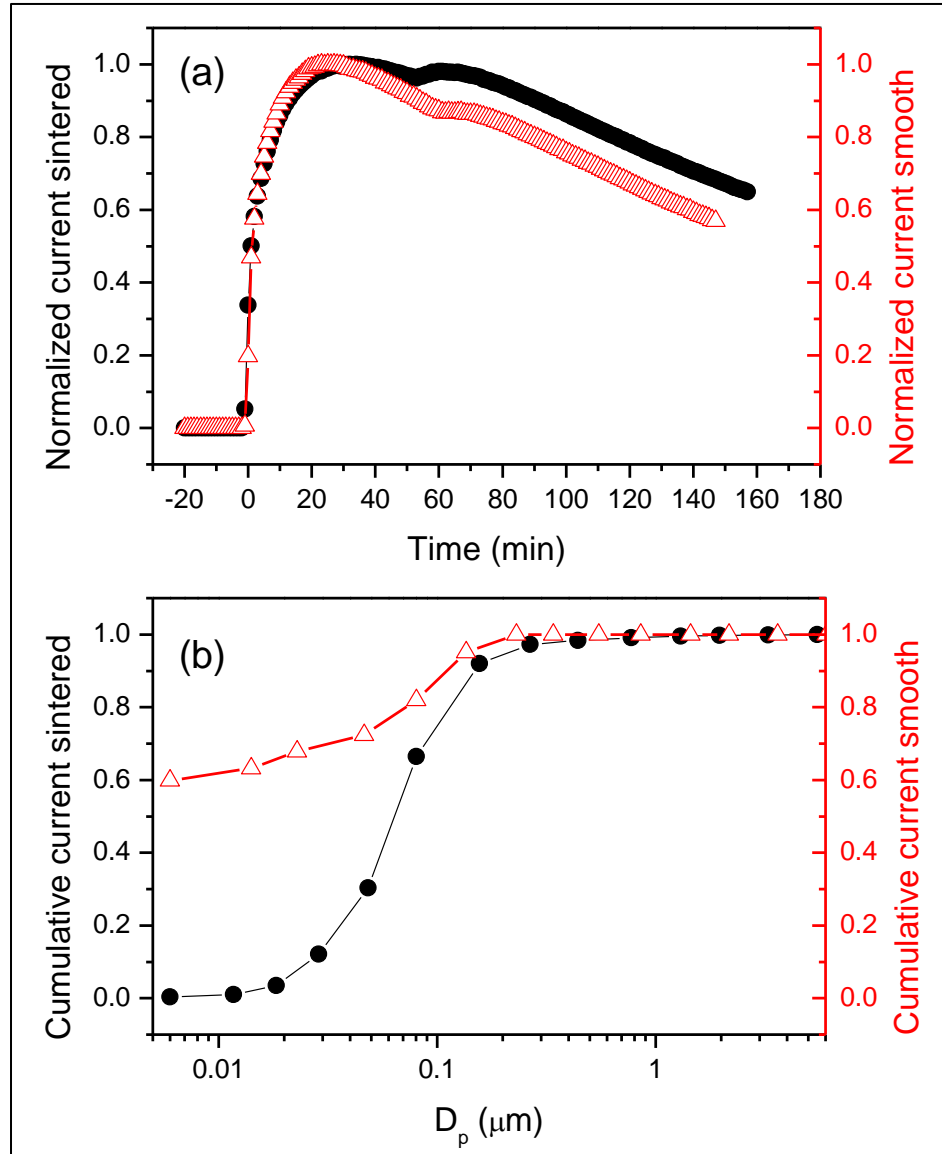


*Figure 5.10 (a) Normalized total current and (b) cumulative current distribution for α-pinene derived SOA as measured with the ELPI operating with ( △ ) smooth and ( ● ) sintered plates. The cumulative current distributions are the average of two hours of ageing.*

In the present study, it was also observed that as the particles aged, the BF decreased to 0.55, suggesting a continuously evolving phase as biogenic SOA ages. The reason for the decreased BF is not immediately apparent, although it may be due to a decrease in SOA viscosity brought about by the formation of a liquid surface layer produced by water adsorption.[36] Although the effect of water vapor on SOA composition is not well understood [46, 47], I may anticipate that formation of such a layer would not only yield a more adhesive particle surface, but also hamper formation of higher molecular weight oligomers and, hence, lead to decreased viscosity [15, 20], making the particles less susceptible to bounce.

Interestingly, the BF of α-pinene SOA is greater than that for AS, i.e., solid particle reference. Such a difference in bounce factor could be attributed to differences in the elastic properties of amorphous SOA and crystalline AS particles. Amorphous material eliminates the possibility of slip planes (dislocation) upon interaction with a surface and hence can be thought of as an atomic gridlock. This means that the initial kinetic energy of amorphous SOA upon impaction is not lost easily, suggesting higher rebound energy as compared to the adhesion energy. Higher rebound energy would result in amorphous SOA having a higher BF as compared to crystalline AS particles.

### 5.4.4 *cis*-3-hexen-1-ol (HXL)

Results from chapter 4 show that HXL-SOA is comprised primarily of higher molecular weight products such as oligomers, dimers which are formed by hydration/dehydration reactions. Results shown above for ozonized oleic acid and α-Pinene SOA demonstate that higher molecular weight products are responsible for non-liquid nature of SOA. Hence, it is obvious to expect HXL-SOA to be non-liquid in nature.
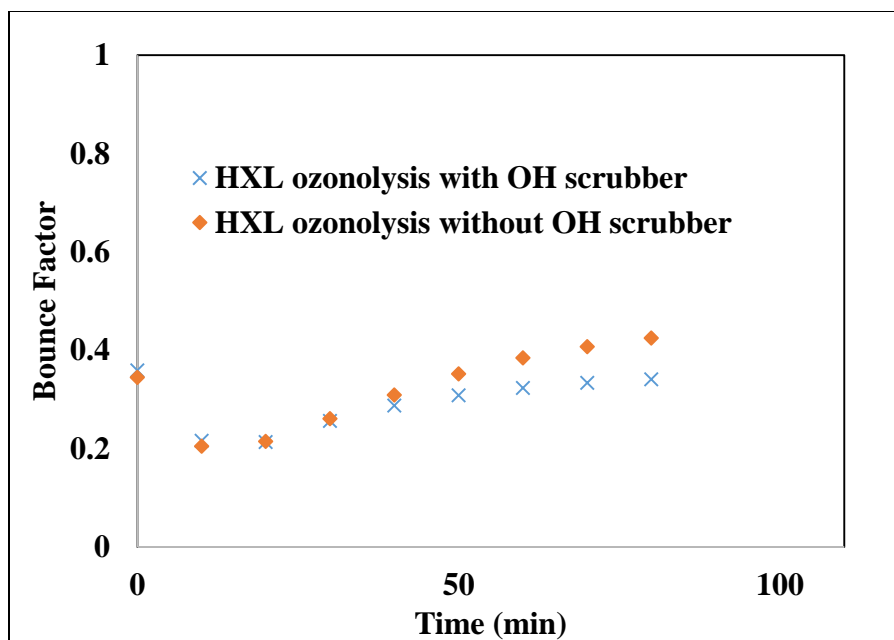
*Figure 5.11 BF for HXL-derived SOA as a function of particle age.*

As shown in Figure 5.11, HXL-derived SOA exhibits a significant particle bounce, suggesting a non-liquid phase state of SOA. It is interesting to note that the BF initially decreases and then starts increasing, which implies a continuous evolving and changing chemical composition. The reason for the initial decrease in BF is not immediately apparent but this could be due to the loading effect on the impaction plates which results in an initial change in the charging efficiency[37] and modification of the impaction surface, thereby creating a new state of equilibrium. On the other hand, the increase in BF as the SOA ages could be attributed to second and third generation higher molecular weight products. This is consistent with the relative signal intensities ratios reported in Chapter 4 i.e., generation of higher molecular products with the ageing of SOA.

Also it was shown in Chapter 4 that OH radicals do not play any significant role in driving the chemistry of HXL-derived SOA. This was shown by performing experiments in the presence of an excess of OH radical scrubber and comparing the chemical composition by NIR-LDI-AMS mass spectrum. Similar experiments were performed, i.e.,

generation of HXL-derived SOA in the presence of excess OH scrubber and BF of the resulting SOA was calculated. As expected, and shown in Figure 5.11, there was no difference in the BF of SOA generated with or without the presence of OH scrubber, further supporting our hypothesis that OH radicals do not drive the chemistry in case of HXL derived SOA.

### 5.4.5 *cis*-3-hexenylacetate (CHA)

Chemical composition analysis for the SOA generated by ozonolysis of CHA, as discussed in Chapter 4, shows a simpler chemical profile dominated by small molecular weight products produced mainly by hydroperoxide channel. Formation of higher molecular weight products is inhibited due to the acetate functionality. Hence, I did not expect any significant particle bounce from the CHA-derived SOA.
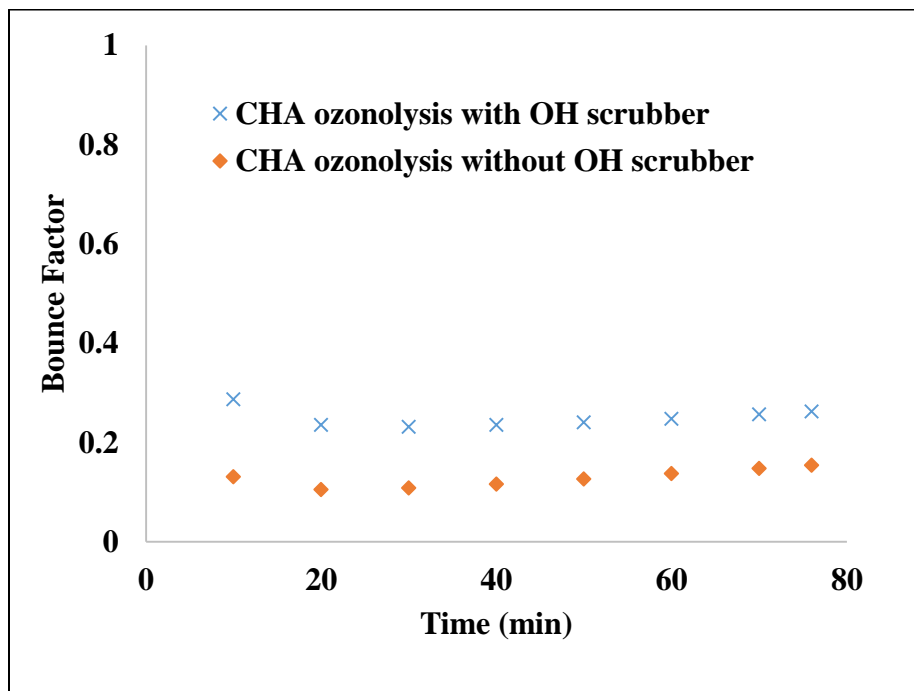


*Figure 5.12 BF for CHA derived SOA as a function of particle age*

To my surprise, I observed some particle bounce from CHA generated SOA as shown in Figure 5.12. However, as expected, BF = 0.2 is much lower than HXL or α-pinene

BF. Looking at the BF trend, it also seems like the chemical composition does not change much as the SOA ages. Similar to HXL, experiments were performed with an OH radical scrubber to isolate the any OH radical chemistry. Recall from Chapter 4, that the OH radical plays a significant role in the chemical composition of CHA-derived SOA. Interestingly, I observed that the OH radical also affects the phase of CHA – SOA. As shown in Figure 5.12, BF increases to 0.3 for experiments conducted in the presence of the OH scrubber, suggesting that product **X (**which was observed at m/z 171) was present in the liquid phase, upon elimination of which, the overall phase of SOA changed.

**5.5 Conclusion**

The bounce of particles from an impactor surface is used to elucidate the phase state of aerosol particles. Herein, I present a new SMPS-free method for studying the phase state of polydisperse aerosols under atmospherically relevant conditions. This method is based on comparing the current measured by an ELPI when polydisperse aerosols are sampled by smooth and sintered impaction plates. The reported method also permits measurement of bounce factors for polydisperse SOA, as well as studies of the effects of aerosol ageing on its physical properties, with the temporal resolution necessary to observe phase changes in a continuously evolving SOA. The utilization of a commercially available instrument with no special modifications makes this method easy to adopt. To validate the method and demonstrate its applicability, we measured the phase behavior of four test substances that represent solid (ammonium sulfate), liquid (dioctyl sebacate), liquid (oleic acid), non-liquid (ozonized oleic acid) and SOA particles (ozonolysis of α-pinene, CHA and HXL).

This method will advance the understanding of the relationship between SOA phase and reactivity, which will ultimately speak to the fate of SOA in the atmosphere. The

proposed method has the potential to be used with both monodisperse and polydisperse aerosols and could be used to determine relationships between fractions of bounced particles, diameters and their chemical identity. It can also be used to make quantitative connections between bounce factor and the physical properties of various classes of particles.

Work done in this chapter made me think what other parameters can potentially impact the phase state of SOA. Though there were plans of expanding this work to evaluate bounce factors and improve our understanding of the impact that some parameters, such as SOA precursor, relative humidity, oxidation type and mixing ratio, have on the phase of atmospheric aerosols, there was one factor, i.e., SOA mass loading which made me curious. Mass loading affects chemical composition and chemical composition affects viscosity. Hence, it seems obvious that mass loading should impact the phase state of aerosol. Therefore, the next chapter of this thesis addresses the influence of SOA mass loading on the phase state of aerosol.

## 5.6 References

1.      Pope, C. A.; Dockery, D. W., Health effects of fine particulate air pollution: Lines that connect. *J Air Waste Manage* **2006,** *56*, (6), 709-742.
2.      Poschl, U., Atmospheric aerosols: Composition, transformation, climate and health effects. *Angew Chem Int Edit* **2005,** *44*, (46), 7520-7540.
3.      Kroll, J. H.; Seinfeld, J. H., Chemistry of secondary organic aerosol: Formation and evolution of low-volatility organics in the atmosphere. *Atmos Environ* **2008,** *42*, (16), 3593-3624.
4.      Hallquist, M.; Wenger, J. C.; Baltensperger, U.; Rudich, Y.; Simpson, D.; Claeys, M.; Dommen, J.; Donahue, N. M.; George, C.; Goldstein, A. H.; Hamilton, J. F.; Herrmann, H.; Hoffmann, T.; Iinuma, Y.; Jang, M.; Jenkin, M. E.; Jimenez, J. L.; Kiendler-Scharr, A.; Maenhaut, W.; McFiggans, G.; Mentel, T. F.; Monod, A.; Prevot, A. S. H.; Seinfeld, J. H.; Surratt, J. D.; Szmigielski, R.; Wildt, J., The formation, properties and impact of secondary organic aerosol: current and emerging issues. *Atmos Chem Phys* **2009,** *9*, (14), 5155-5236.
5.      Saukko, E.; Kuuluvainen, H.; Virtanen, A., A method to resolve the phase state of aerosol particles. *Atmos Meas Tech* **2012,** *5*, (1), 259-265.
6.      Virtanen, A.; Kannosto, J.; Kuuluvainen, H.; Arffman, A.; Joutsensaari, J.; Saukko, E.; Hao, L.; Yli-Pirila, P.; Tiitta, P.; Holopainen, J. K.; Keskinen, J.; Worsnop, D. R.; Smith, J. N.; Laaksonen,

A., Bounce behavior of freshly nucleated biogenic secondary organic aerosol particles. *Atmos Chem Phys* **2011,** *11*, (16), 8759-8766.

7.      Robinson, A. L.; Donahue, N. M.; Shrivastava, M. K.; Weitkamp, E. A.; Sage, A. M.; Grieshop, A. P.; Lane, T. E.; Pierce, J. R.; Pandis, S. N., Rethinking organic aerosols: Semivolatile emissions and photochemical aging. *Science* **2007,** *315*, (5816), 1259-1262.

8.      Vaden, T. D.; Imre, D.; Beranek, J.; Shrivastava, M.; Zelenyuk, A., Evaporation kinetics and phase of laboratory and ambient secondary organic aerosol. *Proc. Natl. Acad. Sci. USA* **2011,** *108*, (6), 2190-2195.

9.      Pye, H. O. T.; Seinfeld, J. H., A global perspective on aerosol from low-volatility organic compounds. *Atmos Chem Phys* **2010,** *10*, (9), 4377-4401.

10.     Pankow, J. F., An Absorption-Model of Gas-Particle Partitioning of Organic-Compounds in the Atmosphere. *Atmos Environ* **1994,** *28*, (2), 185-188.

11.     Chan, A. W. H.; Kroll, J. H.; Ng, N. L.; Seinfeld, J. H., Kinetic modeling of secondary organic aerosol formation: effects of particle- and gas-phase reactions of semivolatile products. *Atmos Chem Phys* **2007,** *7*, (15), 4135-4147.

12.     Abramson, E.; Imre, D.; Beranek, J.; Wilson, J.; Zelenyuk, A., Experimental determination of chemical diffusion within secondary organic aerosol particles. *Phys Chem Chem Phys* **2013,** *15*, (8), 2983-2991.

13.     Cappa, C. D.; Wilson, K. R., Evolution of organic aerosol mass spectra upon heating: implications for OA phase and partitioning behavior. *Atmos Chem Phys* **2011,** *11*, (5), 1895-1911.

14.     Kannosto, J.; Yli-Pirila, P.; Hao, L. Q.; Leskinen, J.; Jokiniemi, J.; Makela, J. M.; Joutsensaari, J.; Laaksonen, A.; Worsnop, D. R.; Keskinen, J.; Virtanen, A., Bounce characteristics of alpha-pinene-derived SOA particles with implications to physical phase. *Boreal Environ Res* **2013,** *18*, (3-4), 329-340.

15.     Renbaum-Wolff, L.; Grayson, J. W.; Bateman, A. P.; Kuwata, M.; Sellier, M.; Murray, B. J.; Shilling, J. E.; Martin, S. T.; Bertram, A. K., Viscosity of alpha-pinene secondary organic material and implications for particle growth and reactivity. *P Natl Acad Sci USA* **2013,** *110*, (20), 8014-8019.

16.     Kuwata, M.; Martin, S. T., Phase of atmospheric secondary organic material affects its reactivity. *P Natl Acad Sci USA* **2012,** *109*, (43), 17354-17359.

17.     Bateman, A. P.; Bertram, A. K.; Martin, S. T., Hygroscopic Influence on the Semisolid-to-Liquid Transition of Secondary Organic Materials. *J. Phys. Chem. A* **2014**.

18.     DeCarlo, P. F.; Slowik, J. G.; Worsnop, D. R.; Davidovits, P.; Jimenez, J. L., Particle morphology and density characterization by combined mobility and aerodynamic diameter measurements. Part 1: Theory (vol 38, pg 1185, 2004). *Aerosol Sci Tech* **2005,** *39*, (2), 184-184.

19.     Bateman, A. P.; Belassein, H.; Martin, S. T., Impactor Apparatus for the Study of Particle Rebound: Relative Humidity and Capillary Forces. *Aerosol Sci. Technol.* **2014,** *48*, (1), 42-52.

20.     Kidd, C.; Perraud, V.; Wingen, L. M.; Finlayson-Pitts, B. J., Integrating phase and composition of secondary organic aerosol from the ozonolysis of α-pinene. *P Natl Acad Sci* **2014**.

21.     Geddes, S.; Nichols, B.; Flemer, S.; Eisenhauer, J.; Zahardis, J.; Petrucci, G. A., Near-Infrared Laser Desorption/Ionization Aerosol Mass Spectrometry for Investigating Primary and Secondary Organic Aerosols under Low Loading Conditions. *Analytical chemistry* **2010,** *82*, (19), 7915-7923.

22.     Keskinen, J.; Marjamaki, M.; Virtanen, A.; Makela, T.; Hillamo, R., Electrical calibration method for cascade impactors. *J Aerosol Sci* **1999,** *30*, (1), 111-116.

23.     Marjamaki, M.; Keskinen, J.; Chen, D. R.; Pui, D. Y. H., Performance evaluation of the electrical low-pressure impactor (ELPI). *J Aerosol Sci* **2000,** *31*, (2), 249-261.

24.	Dahneke, B., The capture of aerosol particles by surfaces. *J Colloid Interf Sci* **1971,** *37*, (2), 342-353.

25.	Rogers, L. N.; Reed, J., The Adhesion of Particles Undergoing an Elastic Plastic Impact with a Surface. *J Phys D Appl Phys* **1984,** *17*, (4), 677-689.

26.	Dahneke, B., Particle Bounce or Capture - Search for an Adequate Theory .1. Conservation-of-Energy Model for a Simple Collision Process. *Aerosol Sci Tech* **1995,** *23*, (1), 25-39.

27.	Kuuluvainen, H.; Arffman, A.; Saukko, E.; Virtanen, A.; Keskinen, J., A new method for characterizing the bounce and charge transfer properties of nanoparticles. *J Aerosol Sci* **2013,** *55*, 104-115.

28.	Wall, S.; John, W.; Wang, H.-C.; Goren, S. L., Measurements of Kinetic Energy Loss for Particles Impacting Surfaces. *Aerosol Sci Tech* **1990,** *12*, (4), 926-946.

29.	Hinds, W. C., *Aerosol Technology: Properties, Behavior, and Measurement of Airborne Particles*. John Wiley & Sons: 1982.

30.	Bergström, L., Hamaker constants of inorganic materials. *Adv Colloid Interfac* **1997,** *70*, (0), 125-169.

31.	John, W.; Reischl, G.; Devor, W., Charge-Transfer to Metal-Surfaces from Bouncing Aerosol-Particles. *J Aerosol Sci* **1980,** *11*, (2), 115-138.

32.	Virtanen, A.; Joutsensaari, J.; Koop, T.; Kannosto, J.; Yli-Pirila, P.; Leskinen, J.; Makela, J. M.; Holopainen, J. K.; Poschl, U.; Kulmala, M.; Worsnop, D. R.; Laaksonen, A., An amorphous solid state of biogenic secondary organic aerosol particles. *Nature* **2010,** *467*, (7317), 824-827.

33.	Martin, S. T., Phase transitions of aqueous atmospheric particles. *Chem Rev* **2000,** *100*, (9), 3403-3453.

34.	Hosny, N. A.; Fitzgerald, C.; Tong, C. L.; Kalberer, M.; Kuimova, M. K.; Pope, F. D., Fluorescent lifetime imaging of atmospheric aerosols: a direct probe of aerosol viscosity. *Faraday Discuss* **2013,** *165*, 343-356.

35.	Smith, M. L.; Kuwata, M.; Martin, S. T., Secondary Organic Material produced by the dark ozonolysis of alpha-pinene minimally affects the deliquescence and efflorescence of ammonium sulfate. *Aerosol Sci Tech* **2011,** *45*, (2), 244-261.

36.	Saukko, E.; Lambe, A. T.; Massoli, P.; Koop, T.; Wright, J. P.; Croasdale, D. R.; Pedernera, D. A.; Onasch, T. B.; Laaksonen, A.; Davidovits, P.; Worsnop, D. R.; Virtanen, A., Humidity-dependent phase state of SOA particles from biogenic and anthropogenic precursors. *Atmos Chem Phys* **2012,** *12*, (16), 7517-7529.

37.	Wang, H.-C.; John, W., Comparative Bounce Properties of Particle Materials. *Aerosol Sci Tech* **1987,** *7*, (3), 285-299.

38.	Romakkaniemi, S.; Hameri, K.; Vakeva, M.; Laaksonen, A., Adsorption of water on 8-15 nm NaCl and (NH4)(2)SO4 aerosols measured using an ultrafine tandem differential mobility analyzer. *J Phys Chem A* **2001,** *105*, (35), 8183-8188.

39.	Svenningsson, B.; Rissler, J.; Swietlicki, E.; Mircea, M.; Bilde, M.; Facchini, M. C.; Decesari, S.; Fuzzi, S.; Zhou, J.; Monster, J.; Rosenorn, T., Hygroscopic growth and critical supersaturations for mixed aerosol particles of inorganic and organic compounds of atmospheric relevance. *Atmos Chem Phys* **2006,** *6*, 1937-1952.

40.	Robinson, A. L.; Subramanian, R.; Donahue, N. M.; Bernardo-Bricker, A.; Rogge, W. F., Source apportionment of molecular markers and organic aerosol. 3. Food cooking emissions. *Environ Sci Technol* **2006,** *40*, (24), 7820-7827.

41.	Zheng, M.; Cass, G. R.; Schauer, J. J.; Edgerton, E. S., Source apportionment of PM2.5 in the southeastern United States using solvent-extractable organic compounds as tracers. *Environ Sci Technol* **2002,** *36*, (11), 2361-2371.

42.	Fraser, M. P.; Yue, Z. W.; Tropp, R. J.; Kohl, S. D.; Chow, J. C., Molecular composition of organic fine particulate matter in Houston, TX. *Atmos Environ* **2002,** *36*, (38), 5751-5758.

43.	Zahardis, J.; LaFranchi, B. W.; Petrucci, G. A., Direct observation of polymerization in the oleic acid–ozone heterogeneous reaction system by photoelectron resonance capture ionization aerosol mass spectrometry. *Atmos Environ* **2006,** *40*, (9), 1661-1670.

44.	Koop, T.; Bookhold, J.; Shiraiwa, M.; Poschl, U., Glass transition and phase state of organic compounds: dependency on molecular properties and implications for secondary organic aerosols in the atmosphere. *Phys Chem Chem Phys* **2011,** *13*, (43), 19238-19255.

45.	Zobrist, B.; Marcolli, C.; Pedernera, D. A.; Koop, T., Do atmospheric aerosols form glasses? *Atmos Chem Phys* **2008,** *8*, (17), 5221-5244.

46.	Warscheid, B.; Hoffmann, T., On-line measurements of a-pinene ozonolysis products using an atmospheric pressure chemical ionisation ion-trap mass spectrometer. *Atmos Environ* **2001,** *35*, (16), 2927-2940.

47.	Ma, Y.; Luciani, T.; Porter, R. A.; Russell, A. T.; Johnson, D.; Marston, G., Organic acid formation in the gas-phase ozonolysis of alpha-pinene. *Phys Chem Chem Phys* **2007,** *9*, (37), 5084-5087.

**CHAPTER 6: THE INFLUENCE OF ABSOLUTE MASS LOADING OF SECONDARY ORGANIC AEROSOLS ON THEIR PHASE STATE**

The work described in this chapter is submitted and is under review for publication in the following journal. The full reference is as follows:

*Jain, S. and Petrucci, G. A. (2016). The influence of absolute mass loading of secondary organic aerosols on their phase state. Aerosol Sci. Technol.*

## 6.1 Introduction

Organic aerosols (OA) are an important component of atmospheric particulate, often contributing 20–90% of the fine particle mass worldwide.[1, 2] These OA are emitted from the earth's surface by human and natural sources influencing both human health[3] and global climate.[4] Studies suggest that 90% of these OA are from secondary sources, termed secondary organic aerosol (SOA), due to oxidation of volatile compounds in the atmosphere.[2]

There is growing evidence that SOA influences the earth's energy budget both directly and indirectly either by scattering/absorption of solar radiation[5] or by acting as cloud condensation/ice nuclei.[6] SOA can also alter atmospheric gas and condensed phase species concentrations through multiphase reactions.[7] Despite the integral role of SOA in atmospheric processes, there remains a limited understanding of the chemical and physical changes induced in SOA as it is formed and subsequently aged. Understanding the physical state of SOA is especially important, as it can provide insight into SOA formation[8] and growth[9], gas–particle partitioning[10], reactive uptake on particle surfaces[11] and atmospheric impacts.[12]

Recent attention on the phase state of atmospheric particles has motivated several questions regarding parameters/conditions that influence the phase state and physical properties of SOA. Current models assume that SOA particles remain liquid-like throughout their lifetime and an equilibrium exists between the particle and gas phase due to rapid evaporation and condensation.[13-16] However, recent measurements have provided strong evidence to challenge this assumption[17, 18] showing that SOA can adopt liquid, semisolid (viscous) and solid phase states depending on its composition and ambient conditions.[7, 19, 20]

It has been shown previously that environmental conditions such as temperature and relative humidity (RH) could have a significant impact on SOA phase and viscosity.[7, 21-24] Lingnell, et al. showed that a decrease in temperature from 20 $^{0}$C to 0 $^{0}$C decreases the viscosity of α-pinene/$O_3$ SOA by roughly two orders of magnitude. They hypothesize that SOA viscosity is altered either by slowing down unimolecular decomposition and bimolecular reactions of photo-excited molecules or by physically changing the SOA matrix.[23] Furthermore, results from Renbaum-Wolff, et al. suggest that viscosity of α-pinene/$O_3$ SOA is comparable to that of honey at 90% RH, similar to that of peanut butter at 70%RH, and at least as viscous as bitumen at ≤30% RH. [21]

In addition to RH and temperature, the phase state of SOA may also be impacted by the absolute SOA mass loading ($C_{SOA}$). It has been shown recently that the aerosol composition of SOA generated from the ozonolysis of α-pinene changes as a function of total organic aerosol mass loading.[25, 26] Results from two independent studies have shown that for α-pinene/$O_3$ SOA, the aerosol mass spectrometry (AMS) signal intensity at m/z 44 (which includes fragments of oxo- and di-carboxylic acids) increases at low mass loading,

suggesting that more polar components appear to dominate the aerosol at low loading, while other products become more prevalent at higher loadings.[25, 27] These studies also showed that as SOA mass loading increases, particle mass yield and H:C ratio increase, while O:C ratio decreases. These seminal studies, however, did not provide insight with regard to changes in phase as a function of absolute mass loading.

Mass loading affects chemical composition and chemical composition affects viscosity/phase. However, to the best of my knowledge, no reports have been published elucidating the impact of absolute SOA mass loading upon the SOA phase state. I report herein, for the first time, the results of a systematic study investigating the influence of $C_{SOA}$ on the phase state of SOA formed by ozonolysis of several atmospherically relevant SOA precursors, i.e., α-pinene, limonene, *cis*-3-hexenyl acetate (CHA) and *cis*-3-hexen-1-ol (HXL). These chemical systems were selected to represent both cyclic and linear analogues of atmospheric VOCs. α-pinene is arguably the most important precursor to global SOA and limonene is the most important indoor SOA precursor. Green leaf volatiles such as CHA and HXL are unsaturated, oxygenated hydrocarbons emitted in large quantities by stressed plants and are susceptible to atmospheric oxidation, possessing significant ozonolysis aerosol yields of approximately 1−10%.[28] Experiments were performed with each of the precursors by either varying the VOC or ozone concentration to obtain a different maximum $C_{SOA}$. Phase state was inferred by measuring the maximum bounce factor (BF) of the generated polydisperse SOA using a previously established method.[29] Reported here are the BF results for each chemical system as a function of $C_{SOA}$ ranging for 0.2 µg m$^{-3}$ to 160 µg m$^{-3}$. Understanding the influence of $C_{SOA}$ on phase state

is important to better understand atmospheric processes, such as gas–particle partitioning and chemical reactive uptake by SOA.

## 6.2 Experimental methods and measurements

### 6.2.1 Reagents & equipment

α-pinene (>99%), limonene (>99%), CHA (>98%) and HXL (>99%), were purchased from Sigma Aldrich and used without further purification. All experiments were performed in the $8m^3$ University of Vermont Environmental Chamber (UVMEC)[30] operated at ambient temperature (~298 (±2) K) and atmospheric pressure. Dry, zero air was produced by passing compressed air sequentially through silica, activated carbon and HEPA filters. This zero air was also used to generate ozone using a commercial corona discharge ozone generator (OL80A/DLS, Ozone Lab, Burton, BC, Canada). The UVMEC is equipped with ambient $O_3$ (Serinus $O_3$ model E020010, American Ecotech, Cincinnati, OH, USA) and $NO_x$ (EC9041A NOx Analyzer, American Ecotech, Cincinnati, OH, USA) analyzers.

Current distributions to estimate the bounce factor and aerosol particle number size distributions were measured continuously using an electrical low pressure impactor (ELPI+, Dekati, Finland) operating either with sintered plates (to eliminate particle bounce) or smooth plates (to favor particle bounce).[29] Aerosol particle number size distributions were also measured in parallel with a scanning mobility particle sizer (SMPS model 3080, TSI Inc., Shoreview, MN, USA) to check for reproducibility and any disparity between the ELPI and SMPS measurements.

### 6.2.2 Chamber experiments (generation of SOA)

Experiments using different SOA precursors (Table 6.1) were carried out in the UVMEC[30]. During experiments, ozonolysis of all the SOA precursors led to SOA formation and subsequent growth. SOA was formed in the absence of seed particles and no OH scavenger was used. Experimental conditions and details are provided in Table 6.1. All experiments were carried out in duplicate. Between experiments, the chamber was passivated with $O_3$ (1–2 ppm) overnight and then flushed with zero air until the background aerosol mass and number concentrations were below 0.1 $\mu g/m^3$ and 50 particles/$cm^3$, respectively.

SOA precursors were introduced into the UVMEC quantitatively by evaporating different aliquots of analyte for 15 min from a three-neck flask over a warm water bath into a carrier flow of zero air. This resulted in a desired, theoretical maximum VOC mixing ratio in the UVMEC. Ozone was then introduced to the chamber in a 30 - 60 s burst, until the desired concentration was attained. Injection of ozone was previously calibrated in the absence of VOC for the environmental chamber such that a 30 s injection of ozone corresponded to a 100 ppb mixing ratio in the chamber. Identical injection times were used for replicate experiments. Ozone concentrations shown in Table 6.1 correspond to the measured value of ozone in the presence of VOC. All experiments were conducted at a relative humidity of 20–25 %. The particles were assumed to have a density of 1.2 $\mu g/m^3$. The aerosol mass loading in the chamber for these experiments varied from 0.2 to 160 $\mu g/m^3$. The environmental chamber was at a minimally higher pressure relative to its surroundings. No steps were taken to estimate wall losses, as they should have limited or no impact on the phase state of the aerosols. Each data point on the figures represents the

maximum bounce factor reached during an independent experiment done at a different

$C_{SOA}$.

*Table 6.1 Summary of experimental Conditions*

| Parent VOC | Code | VOC (μl) | VOC (ppbv) | Ozone (ppbv) | RH | $C_{OA}$ Max (μg/m$^3$) |
|---|---|---|---|---|---|---|
| **α-Pinene** | AP1 | 1 | 20 | 25 | 23 | 0.25 |
| | AP2 | 1 | 20 | 58 | 22 | 2 |
| | AP3 | 3 | 60 | 58 | 21 | 4.5 |
| | AP4 | 5 | 100 | 89 | 21 | 8 |
| | AP5 | 3 | 60 | 57 | 22 | 10 |
| | AP6 | 5 | 100 | 58 | 23 | 28 |
| | AP7 | 10 | 200 | 77 | 21 | 36 |
| | AP8 | 10 | 200 | 200 | 21 | 70 |
| | AP9 | 10 | 200 | 550 | 23 | 82 |
| **Limonene** | L1 | 1 | 20 | 12 | 23 | 5 |
| | L2 | 2.5 | 50 | 13 | 23 | 10 |
| | L3 | 5 | 100 | 13 | 23 | 20 |
| | L4 | 2.5 | 50 | 47 | 25 | 25 |
| | L5 | 2.5 | 50 | 160 | 24 | 65 |
| | L6 | 5 | 100 | 235 | 23 | 163 |
| *cis*-**3-hexenyl acetate (CHA)** | CHA1 | 40 | 750 | 280 | 20 | 1.6 |
| | CHA2 | 50 | 1000 | 280 | 22 | 3 |
| | CHA3 | 40 | 750 | 420 | 21 | 10.5 |
| | CHA4 | 50 | 1000 | 990 | 22 | 25 |
| | CHA5 | 40 | 750 | 620 | 21 | 41 |
| *cis*-**3-hexen-1-ol (HXL)** | HXL1 | 13 | 350 | 195 | 22 | 3 |
| | HXL2 | 25 | 670 | 200 | 20 | 12 |
| | HXL3 | 13 | 350 | 350 | 21 | 15 |
| | HXL4 | 25 | 670 | 350 | 22 | 37 |
| | HXL5 | 25 | 670 | 600 | 19 | 82 |

### 6.2.3 Atomic Force Microscopy Imaging

Aerosol samples were deposited directly from the UVMEC onto a 0.5" diameter mica substrate using an electrostatic particulate dosage and exposure system described in detail elsewhere.[31] Prior to deposition, the mica surface was cleaned using sonication in acetone, and methanol. New surfaces of mica were produced by cleaving the outermost surface using adhesive tape.

Atomic force microscopy (AFM) imaging was performed on the mica substrate with an Asylum Research MFP-3D-BIO (Asylum Research, an Oxford Instruments company; Santa Barbara, CA) in contact mode in air. For imaging, a SHOCONG probe (Appnano, SPM probes, Mountain View, CA) with a gold coating on the reflex side was used having a tip radius of 6 nm and a spring constant of 0.140 N/m. A scan rate of 0.3 Hz with 512 lines per image was used for imaging. Topographical dimensions of raw data were further analyzed off-line using Igor Pro 6.34 software (Wave Metrics, Portland OR).

### 6.2.4 Bounce Analysis

Details of the approach and method used to estimate the phase state of generated SOA is discussed in Chapter 5.[29] Briefly, two separate cascade impactors are used to perform bounce analysis and calculate BF. One cascade impactor was equipped with smooth impaction plates, favoring particle bounce. The second cascade impactor used sintered impaction plates coated with a thin layer of vacuum grease to minimize (ideally, eliminate) bounce. When using smooth impaction plates, particles with sufficient kinetic energy can overcome the adhesion energy at the surface and bounce to lower impactor stages, resulting in a systematic bias of the current distribution toward lower channels and smaller particle diameters. The presence of bounce, therefore, generates an erroneously

high current in the lower stages (i.e., larger particles are mistakenly counted as smaller particles). BF is then calculated by analyzing the raw current measured with the ELPI+ operating sequentially with smooth and sintered plates according to Equation 1, described in Chapter 5.

## 6.3 Results and Discussions

The impact of absolute $C_{SOA}$ upon the phase state of SOA remains a question of considerable importance to the atmospheric sciences community. The volatility of α-pinene SOA is mostly independent of the SOA mass loading over several orders of magnitude (1 – 800 μg/m$^3$).[26] Comparison of this result with various kinetic models suggests that SOA from the ozonolysis of α-pinene is composed of a large fraction of effectively non-volatile, but thermally unstable species, which are likely dimers or higher-order oligomers, but could also be exceptionally low-volatility monomers.[26] Somewhat contradictory, a separate study[32] found that, for mixed organic-sulfate particles, the observed CCN activity increased beyond predicted values at low mass loading, implying differences in the physico-chemical properties of the organic component, such as surface tension, effective molecular weight, and effective density, at low mass loading.

Below, I describe the results of a systematic study, utilizing several key SOA precursors, to better understand the important role of absolute $C_{SOA}$ on phase. In the ensuing discussion, the particle bounce fraction (BF) is measured and used as a surrogate for particle viscosity or phase. No quantitative absolute measure of viscosity has been made. Rather, the BF is used to provide information regarding the relative particle viscosity between different SOA systems.

### 6.3.1 α-Pinene

A simple cursory analysis of the BF of SOA generated from α-pinene ozonolysis under different absolute mass loadings (Figure 6.1) clearly illustrates a strong dependence between the BF and the mass loading. Additional important general conclusions that may be gleaned from these data include 1) an initial increase in the BF immediately following SOA particle inception to reach the most non-liquid state and 2) a general reduction in BF as the SOA ages.
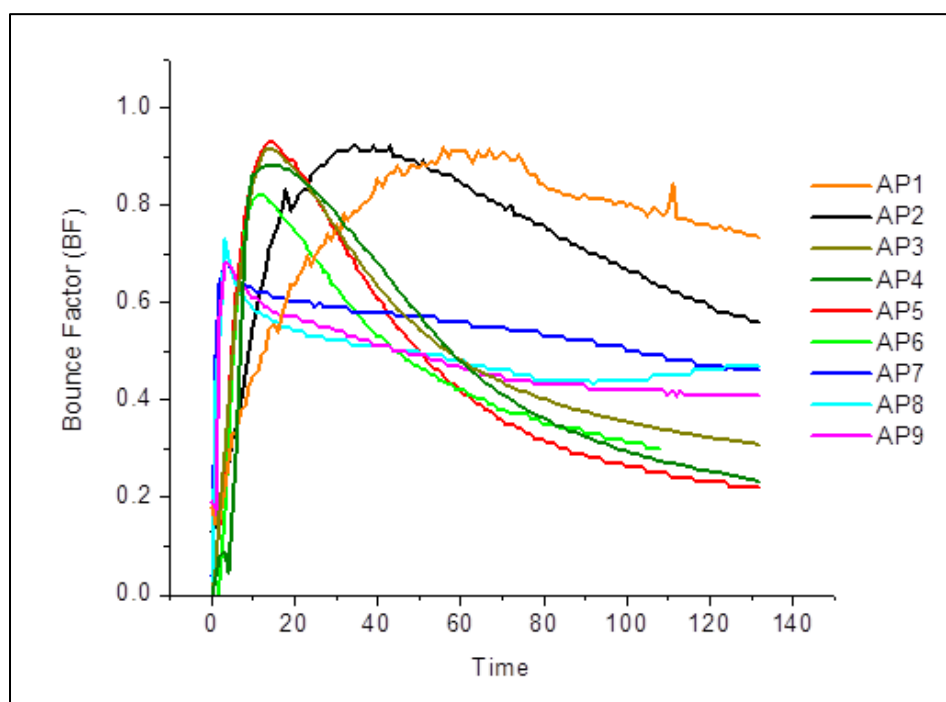


*Figure 6.1 Calculated BF for α-pinene derived SOA as a function of particle age done at different mass loadings.*

While there is some degree of similarity in BF trends at different mass loadings, Figure 6.2 illustrates that the maximum BF (i.e., most non-liquid state), and time to reach such a state ($t_{maxBF}$), change substantially with $C_{SOA}$. For example, at the lowest mass loading (2 μg/m$^3$), I measured the greatest BF (0.92), which was reached in approximately 60 minutes. As successively greater $C_{SOA}$ was used, I observed a very steep change in BF

and $t_{maxBF}$. It was seen that higher mass loadings not only require less time to reach the most non-liquid state (20 mins for 10 μg/m$^3$ and 10 mins for 28 μg/m$^3$) but the maximum BF also decreases, from 0.88 at 8 μg/m$^3$ to 0.82 at 28 μg/m$^3$). Beyond a $C_{SOA}$ of approximately 40 μg/m$^3$, further increases in $C_{SOA}$ do not result in changes in BF or $t_{maxBF}$.
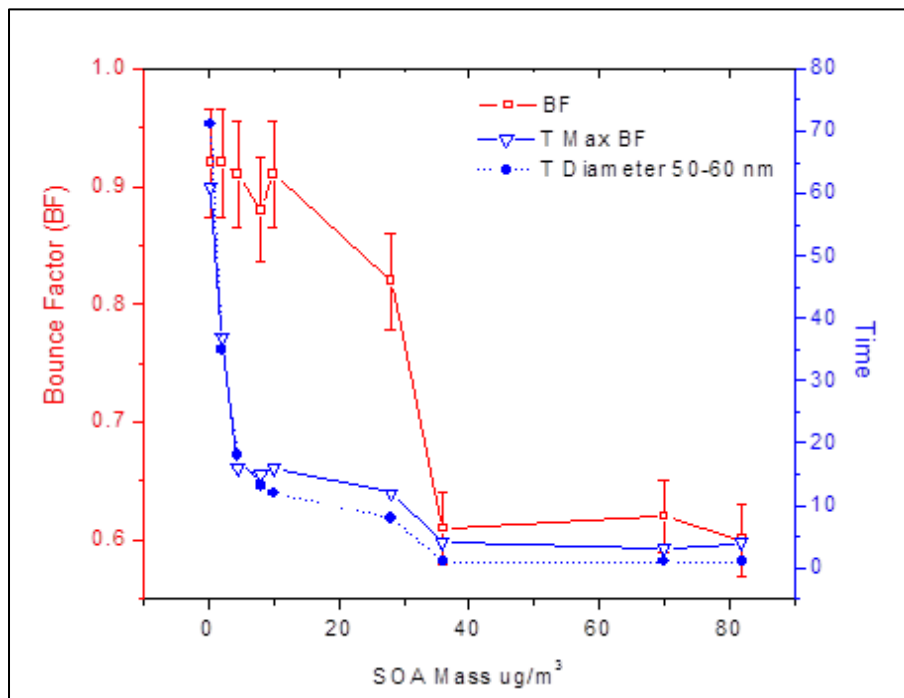


*Figure 6.2 Calculated BF and tmaxBF for a-pinene derived SOA at different CSOA. Error bars represent 1 standard deviation.*

These results suggest that at low mass loading, which more closely approximate atmospherically relevant conditions, α-pinene SOA is more non-liquid in state, further suggesting that dimers, lower volatility and highly viscous products form the majority of the SOA chemical composition. These results can also be used to rationalize observations reported in the literature previously. For example, Shilling, et al.[25] showed that for α-pinene SOA, elemental composition, O:C ratio and H:C ratio vary more at low mass loading as compared to high mass loading. When taken together with this work, it seems plausible that both chemical composition and mass loading play significant roles in determining the

128

phase state of SOA. Additionally, Gao, et.al [33] reported that formation of a dimer of pinic acid and terpenylic acid, was enhanced substantially as $C_{SOA}$ decreased. If my reasoning is correct then, the greater BF I observed at the lowest mass loadings may be indicative of an increased oligomeric content. This is in keeping with the present understanding that high molecular weight oligomers/dimers are more viscous than smaller molecules due to the difficulty for larger molecules to arrange themselves into a crystal lattice structure.[20, 24] Therefore, particles containing oligomers have higher probability of forming glassy/semisolid compounds as compared to their monomeric units.[20, 24] Finally, it has been shown[34] that α-pinene SOA is more oxygenated at low organic mass loading, a condition which can also produce non-liquid particles.
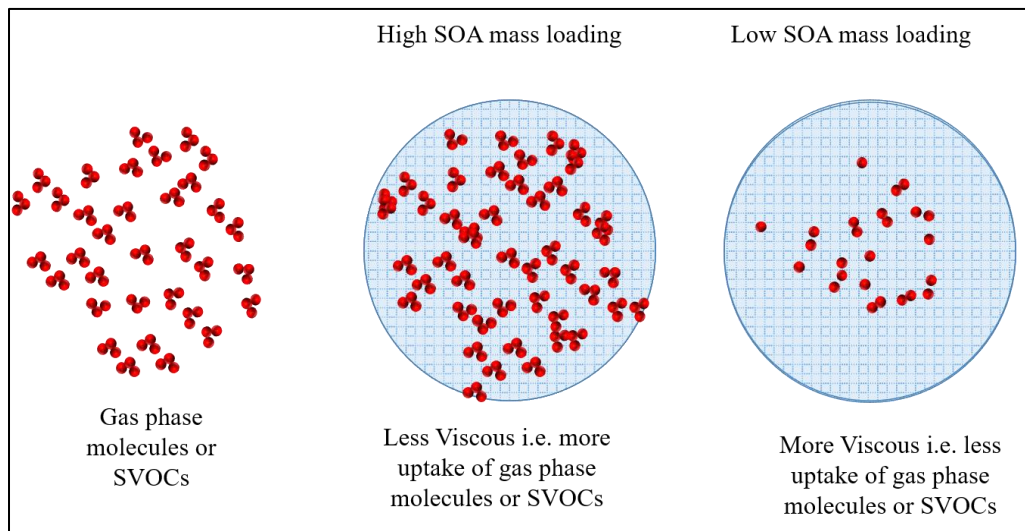


*Figure 6.3 Uptake of gas phase molecules at different SOA mass loading*

Recent work has shown that, at relative humidity less than 30%, partitioning of organic molecules between gas and particle phases may be confined to the top few surface monolayers of the particle.[21] At this RH, it is not unreasonable to expect that instantaneous equilibrium partitioning within the particle bulk cannot take place. As a result, models that assume equilibrium partitioning at ≤30% RH may over-predict SOA particle mass.[21, 35]The

same would hold true for SOA at different mass loadings, which, as shown above, has an effect on the phase state of α-pinene SOA. Therefore, at lower mass loading, where SOA is more non-liquid (more viscous), one can expect that the particles will take up fewer SVOCs compared to a higher mass loading where SOA is relatively less viscous (Figure 6.3).
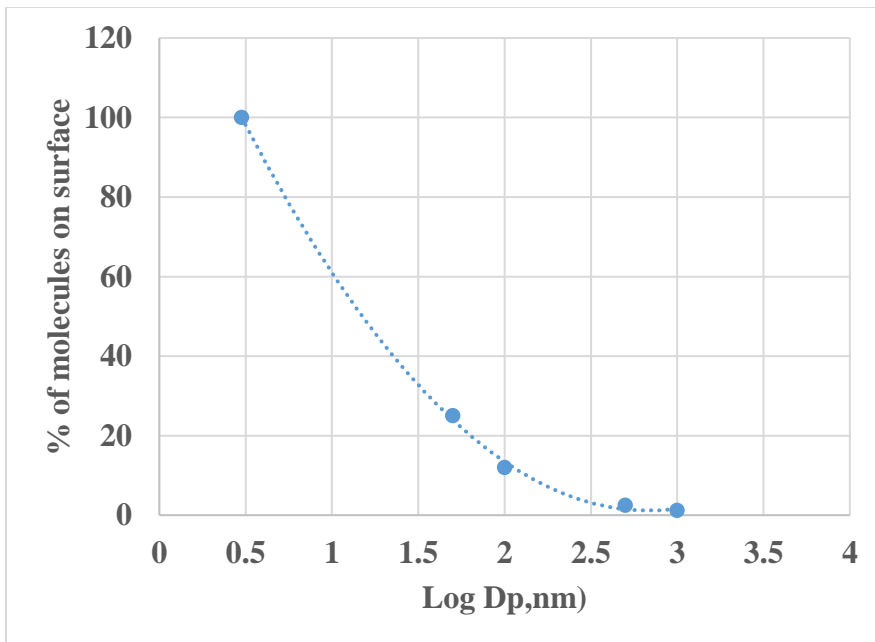


*Figure 6.4 Particle diameter vs % of molecules in a particle on surface*

Interestingly it was also observed that, at all $C_{SOA}$ studied, the most non-liquid state (i.e., maximum BF) was achieved invariably when particles reach a geometric mean diameter (GMD) of 50-60 nm. As shown in fig 6.2, the time for a particle to reach a GMD of 50-60 nm follows the same trend as the time needed for a particle to be in its most non-liquid state. It is well established that the physical properties of a particle can play a crucial role in their interaction with gases.[11, 22, 36, 37] An accurate description of reactions and interactions at the surface is important to understand the fate and role of SOA in the atmosphere. Reactions at the interface between gas and condensed phase become

increasingly important as particle size decreases. A decrease in the particle size causes an increase in the effective surface area and, hence, the reaction rates.

As shown in Figure 6.4 (adapted from[36]), the percentage of molecules in the particle that are on the surface for a typical particle density of 1.2 g/cm$^3$ and a chemical composition with average molecular mass of 300 g/mol, increases as the particle diameter decreases. For a 50nm particle, 25% of the molecules are on the surface of the particle. It's the surface of the particle which first interacts and uptakes gases. Based on my results, a particle with a GMD of 50 nm is in its most non-liquid state. That being the case, even though the surface area is greater for a 50 nm particle, the mixing within the particle bulk will be kinetically limited and the gas–particle partitioning cannot be well represented by an equilibrium process. Hence, I can expect that at low $C_{SOA}$ during the initial stages of SOA formation, reactions and gas uptake would be limited primarily to the thin layers at the particle surface as shown in Figure 6.5.



High SOA mass loading      Low SOA mass loading

Gas phase molecules or SVOCs      Less Viscous i.e. interaction of molecules to the bulk of particle      More Viscous i.e. interaction of molecules to the surface layer of particle
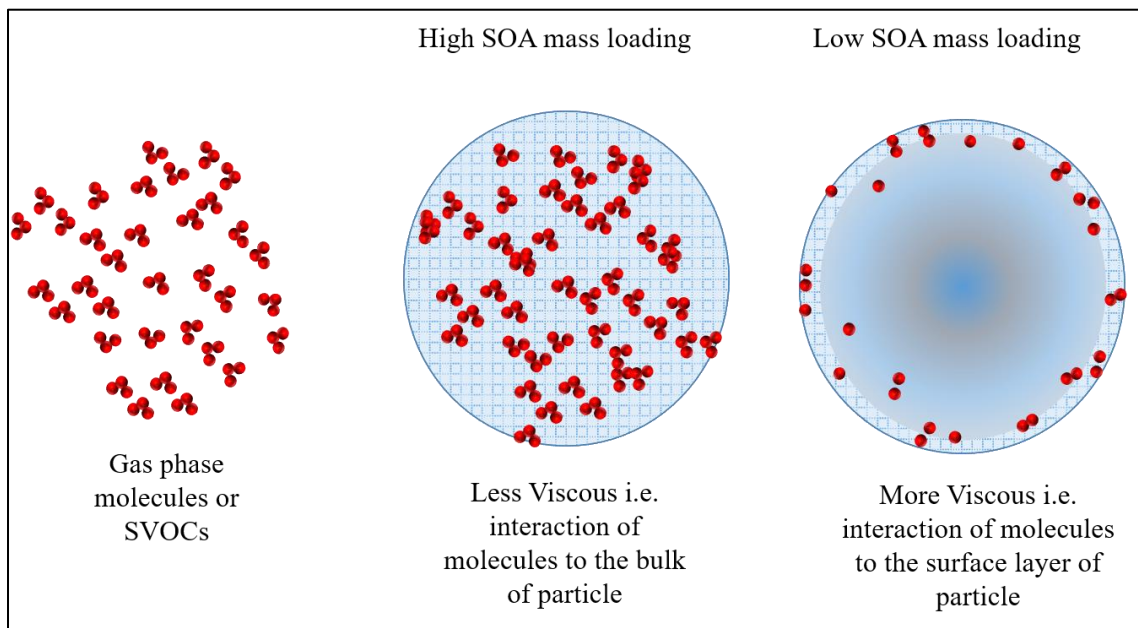
*Figure 6.5 Interaction of gas phase molecules with the particles at different SOA mass loading*

### 6.3.2 Limonene

Some literature reports suggest that limonene SOA could exist as non-liquid, but no concrete evidence has yet been presented to support this supposition. Kundu, et al. provided a detailed molecular analysis of limonene SOA, generated by ozonolysis, using ultrahigh-resolution Fourier transform ion cyclotron resonance (FT-ICR) mass spectrometry and identified over 1200 molecular formulas over the mass range of 140 to 850 Da.[38] The high molecular weight compounds ($m/z$>300) were found to constitute a significant number fraction of the identified SOA components, consisting primarily of oligomers formed by the reactive uptake of gas-phase carbonyls during the ozonolysis reaction.[38, 39] As stated earlier, oligomers have much higher glass transition temperatures, resulting in a higher probability of forming glassy/semisolid compounds. In another study, evaporation kinetics of limonene-generated SOA particles show different behaviors at <5% RH and 90% RH.  It was shown that for SOA at 90% RH, a slightly larger fraction of the particle mass evaporated as compared to SOA at lower RH, suggesting that the SOA may be non-liquid/solid at lower RH.[40]

Figure 6.6 shows an AFM image of limonene SOA particles collected by electrostatic precipitation onto a mica surface. Close examination of the AFM image reveals two interesting observations: (1) the distribution of the particle sizes was quite broad and (2) the collected particles are not spherical in shape as one would expect in the case of liquid particles.  A non-spherical shape suggests that the collected particles are likely non-liquid and therefore, would exhibit, as I confirmed experimentally, significant particle bounce when measured by ELPI+ (Figure 6.7) at the same nominal mass loading

($5\ \mu g/m^3$). These results present the first direct evidence of limonene SOA likely being non-liquid in phase at atmospherically relevant conditions.
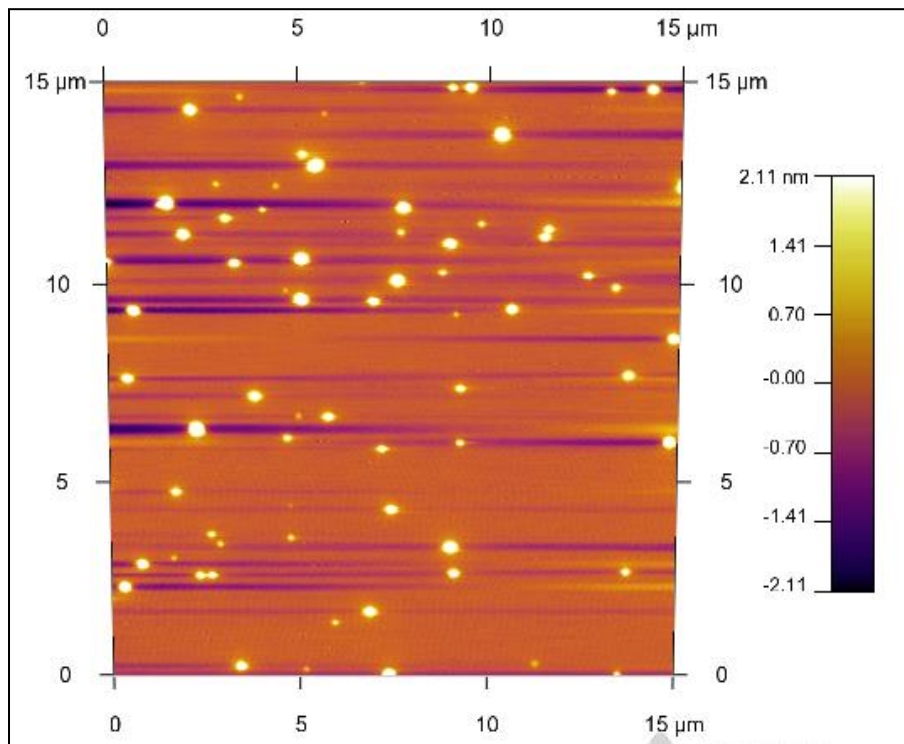


*Figure 6.6 AFM analysis of Limonene ozonolysis SOA collected over mica surface for 1.5 hours by electrostatic precipitation*

I also investigated the influence of $C_{SOA}$ on the phase state of SOA generated by limonene oxidation. Unlike α-pinene, which has only one endocyclic double bond, limonene possesses both an endocyclic and exocyclic double bond. In the case of limonene, the endocyclic double bond is oxidized first, followed by heterogeneous ozonolysis of the terminal double bond in the first-generation condensed-phase products.[30, 41] The presence of multiple double bonds would result in highly oxygenated species and are expected to produce products with a wider range of volatilities.
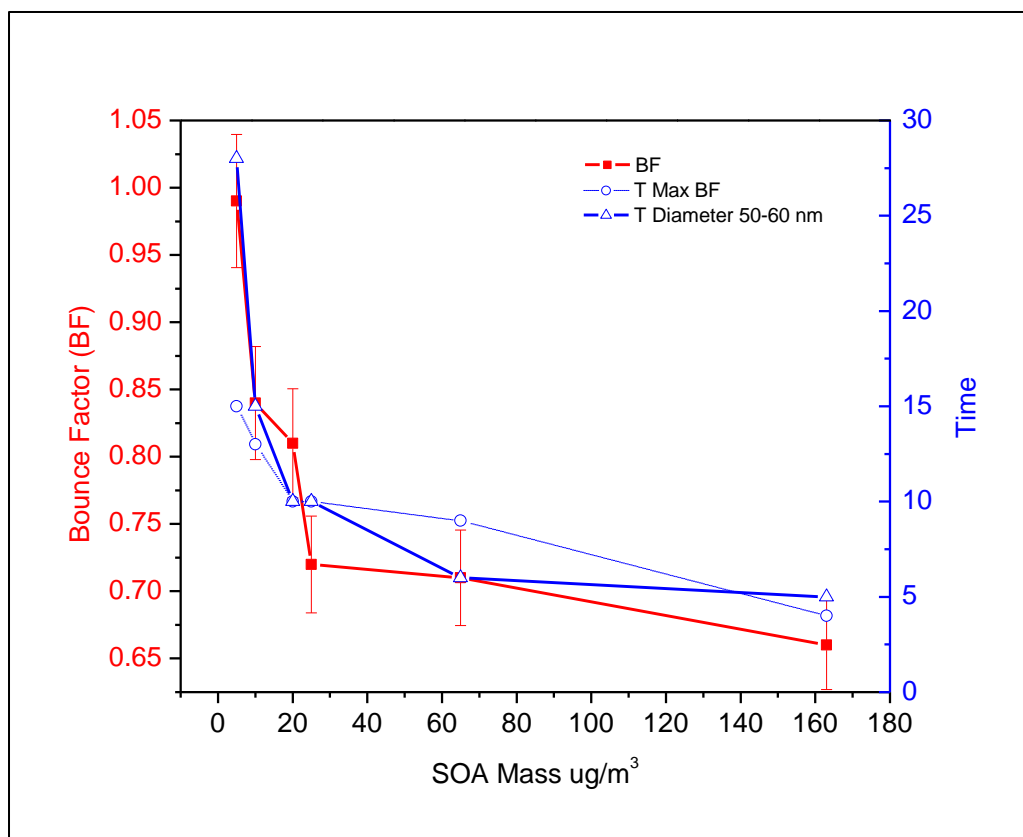
*Figure 6.7 Calculated BF and tmaxBF for limonene derived SOA at different CSOA. Error bars represent 1 standard deviation.*

Results from the chamber experiments show that limonene SOA demonstrated considerable bounce from the outset of SOA formation (Figure 6.7) suggesting a non-liquid state. Also, as was the case with α-pinene SOA, I see a significant mass loading dependence of the measured BF. Analogous to α-pinene SOA, the highest BF (0.98) is also measured at the lowest mass loading (5 μg/m$^3$) and takes approximately 15 minutes to reach the most non-liquid state. It was also observed that as C$_{SOA}$ increases, the BF decreases very quickly only to a certain mass loading and then remains constant. For instance, I observed a 26.5 % reduction in the maximum BF as C$_{SOA}$ increased to 25 μg/m$^3$ (i.e., BF=0.98 at 5 μg/m$^3$ to BF=0.72 at 25 μg/m$^3$), while only an 8 % decrease is measured upon further increasing C$_{SOA}$ to 163 μg/m$^3$ (i.e., BF=0.72 at 25 μg/m$^3$ to BF=0.66 at 163 μg/m$^3$). Moreover, the

134

maximum BF for limonene SOA also was achieved when the geometric mean diameter of the SOA distribution reached 50-60 nm, irrespective of the $C_{SOA}$.

Interestingly, it was observed that the BF in general was higher for limonene SOA as compared to the α-pinene SOA across the range of mass loadings studied. The overall greater BF for limonene SOA may be attributed to the relative volatility of α-pinene and limonene SOA, which has been measured in previous studies.[42] The lower volatility of limonene SOA may be indicative of higher oligomeric content[43] and particle hardening,[17, 40] both of which would produce greater bounce.

### 6.3.3 Cis-3-Hexenyl Acetate (CHA) and Cis-3-Hexen-1-ol (HXL)

Several studies have considered the effect of GLVs on SOA formation[28, 44, 45] and progress has been made in understanding the oxidation pathways to SOA formation from CHA and HXL.[46, 47] Previous NIR-LDI-MS[46] studies have shown that SOA from these GLVs consists of a complex mixture of oxygenated compounds ranging from 70 to >300 *m/z*. It has been shown that HXL-SOA is formed primarily by oligomerization via ester-type linkages. HXL-SOA can undergo hydration / dehydration reactions and reactive uptake of gas-phase products, such as propionaldehyde, to form higher MW compounds such as dimers and trimers. Contrary to HXL, CHA-derived SOA is formed primarily through the hydroperoxide channel, as oligomer formation is inhibited by the lower reactivity of the acetate functionality. The greater oligomeric content in the HXL-SOA would suggest particles of greater viscosity than pure liquid, yet no studies thus far have reported on the phase and physical properties of SOA formed from these GLVs.
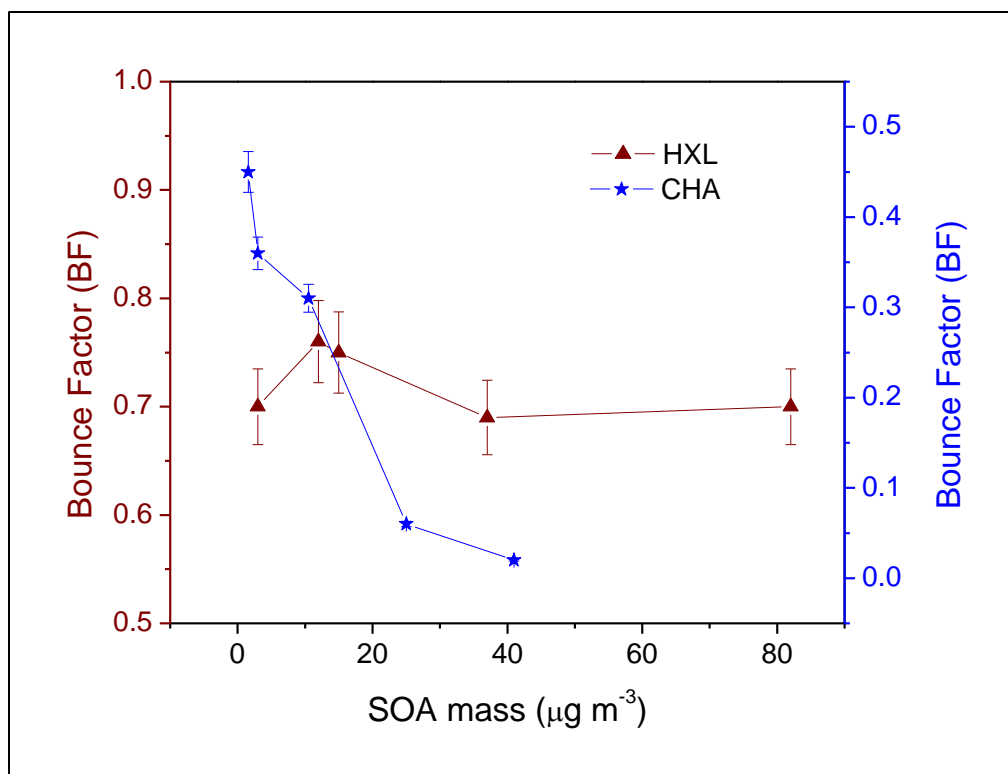
*Figure 6.8 (Primary Y axis) BF for HXL derived SOA as a function of CSOA, (Secondary Y axis) BF for CHA derived SOA as a function of CSOA. Note the different y-scales for the two GLVs.*

In this work, I demonstrate a strong dependence of the phase of GLV-derived SOA on the absolute SOA mass loading ($C_{SOA}$, Figure 6.8). While both HXL- and CHA-derived SOA exhibit non-liquid behavior, HXL-SOA appears more viscous (or less liquid-like) (maximum BF = 0.7) than CHA-derived SOA (maximum BF = 0.45). It was also observed (Figure 6.8) that the BF of HXL-SOA was independent of $C_{SOA}$, unlike other SOA precursors in this study. Independence of BF from absolute $C_{SOA}$ suggests that the chemical composition for HXL-SOA does not change significantly with SOA mass loading. Unlike limonene and α-pinene SOA, I did not observe any relation between the most non-liquid state (i.e., maximum BF) and the geometric mean diameter.

Interestingly, for the case of CHA-SOA, I observed significant particle bounce (BF = 0.45) at low mass loading (1.6 µg/m³), despite a hypothesized lack of oligomeric content.

136

However, at slightly higher SOA mass loadings (25 µg/m$^3$), the BF quickly decreased to 0.06, indicating a transition to a liquid SOA. The evolution of the BF for this system suggests a continuous changing chemical composition of CHA - SOA with mass loading. Clearly these results call for further studies to understand what classes of chemical compounds, besides oligomers such as aldehydes, ketones, alcohols etc., may impact the phase state of SOA. Also, similar to HXL and unlike limonene and α-pinene, I did not observe any correlation between the most non-liquid state (i.e., maximum BF) and the geometric mean diameter.

## 6.4 Conclusion

The results presented in this chapter demonstrate that SOA absolute mass loading may have a significant influence on the phase state of atmospheric aerosols. My results provide new insights into parameters influencing the phase state of atmospheric aerosols. I provided evidence that besides α-pinene, other SOA precursors can form SOA which is non-liquid in phase. My findings show that under ambient environmental conditions i.e. ( < 10 µg/m$^3$), α-pinene, limonene, CHA and HXL SOA is not a pure liquid as has been previously assumed, which could have important implications as discussed below on the ultimate fate of SOA in the atmosphere. Based on my results, I suggest and highly recommend that chamber studies must be performed at atmospherically relevant SOA levels to accurately simulate the chemical properties, reactions and phase of ambient organic aerosol.

Persistent disparity between the measured and modelled SOA level is a question of considerable importance to the atmospheric sciences community. Attempts thus far, to close the gap between model and data, have focused primarily on finding additional SOA

precursors and refining methods of estimating the aerosol yield from precursors, while leaving the fundamental assumptions about SOA properties mostly unchallenged. My findings show that phase of atmospheric aerosols changes with SOA mass loading, which may help to constrain the discrepancy between measured and modelled SOA levels.

Semi-solid, non-liquid or glassy particles can have an impact on atmospheric reactions and uptake. Molecular diffusion in the condensed phase, which largely depends on SOA viscosity, can affect the gas uptake and chemical transformation of organic particles. Estimation of the SOA phase and viscosity at specific, relevant SOA mass loadings would help to better estimate the gas uptake. Hence, the results of this study can improve model estimates of gas uptake into particles. Moreover, a decrease in diffusion rates within the particles results in an increase in the chemical lifetime of reactive compounds in atmospheric particles from seconds to days.[22] An improved understanding of the parameters that result in a phase change would thereby improve model accuracy of particle growth rates and reactive processes.

Current models of atmospheric aerosol assume that various properties of the aerosol are governed by equilibrium thermodynamics. However, the presence of non-liquid aerosol in the atmosphere highlights the importance of quantifying the rates of change of these properties. Studies suggest that non-liquid particles can kinetically inhibit the partitioning of semi volatile components, in contrast to the traditional assumption that organic compounds exist in quasi-instantaneous gas–particle equilibrium.[10] Studies also demonstrate that the timescale for particle equilibration correlates with bulk viscosity/phase.[48, 49] So if absolute SOA mass loading can influence the phase state by up to 30%, it could very well have a significant impact on various properties such as

partitioning, water and gas uptake, condensation and evaporation kinetics. For example, a 100nm particle, which is in a non-liquid phase at organic mass loadings of 1 $\mu g/m^3$, can have an equilibration time scale of SOA partitioning ($T_{eq}$) of approximately 1 hour.[50] On the other hand, that same particle at a much higher organic mass loading of say 15 $\mu g/m^3$ (which according to my results should now be slightly less non-liquid), would have $T_{eq}$ of only 1 min. My results add support to the hypothesis of kinetic inhibition of the partitioning by non-liquid particles, suggesting that accounting for the additional parameters such as SOA mass loading influencing the phase can be important for accurately modelling the behavior of atmospheric aerosols. Clearly more work needs to be done to improve our understanding of the impact that various other parameters, such as SOA precursor, oxidation type ($O_3$ Vs OH Vs $NO_x$), mixing ratio and chamber surface area to volume ratio can have on the phase of atmospheric aerosols.

## 6.5 References

1.      Jimenez, J. L.; Canagaratna, M. R.; Donahue, N. M.; Prevot, A. S. H.; Zhang, Q.; Kroll, J. H.; DeCarlo, P. F.; Allan, J. D.; Coe, H.; Ng, N. L.; Aiken, A. C.; Docherty, K. S.; Ulbrich, I. M.; Grieshop, A. P.; Robinson, A. L.; Duplissy, J.; Smith, J. D.; Wilson, K. R.; Lanz, V. A.; Hueglin, C.; Sun, Y. L.; Tian, J.; Laaksonen, A.; Raatikainen, T.; Rautiainen, J.; Vaattovaara, P.; Ehn, M.; Kulmala, M.; Tomlinson, J. M.; Collins, D. R.; Cubison, M. J.; Dunlea, E. J.; Huffman, J. A.; Onasch, T. B.; Alfarra, M. R.; Williams, P. I.; Bower, K.; Kondo, Y.; Schneider, J.; Drewnick, F.; Borrmann, S.; Weimer, S.; Demerjian, K.; Salcedo, D.; Cottrell, L.; Griffin, R.; Takami, A.; Miyoshi, T.; Hatakeyama, S.; Shimono, A.; Sun, J. Y.; Zhang, Y. M.; Dzepina, K.; Kimmel, J. R.; Sueper, D.; Jayne, J. T.; Herndon, S. C.; Trimborn, A. M.; Williams, L. R.; Wood, E. C.; Middlebrook, A. M.; Kolb, C. E.; Baltensperger, U.; Worsnop, D. R., Evolution of Organic Aerosols in the Atmosphere. *Science* **2009,** *326*, (5959), 1525-1529.
2.      Hallquist, M.; Wenger, J. C.; Baltensperger, U.; Rudich, Y.; Simpson, D.; Claeys, M.; Dommen, J.; Donahue, N. M.; George, C.; Goldstein, A. H.; Hamilton, J. F.; Herrmann, H.; Hoffmann, T.; Iinuma, Y.; Jang, M.; Jenkin, M. E.; Jimenez, J. L.; Kiendler-Scharr, A.; Maenhaut, W.; McFiggans, G.; Mentel, T. F.; Monod, A.; Prevot, A. S. H.; Seinfeld, J. H.; Surratt, J. D.; Szmigielski, R.; Wildt, J., The formation, properties and impact of secondary organic aerosol: current and emerging issues. *Atmos Chem Phys* **2009,** *9*, (14), 5155-5236.
3.      Pope, C. A.; Dockery, D. W., Health effects of fine particulate air pollution: Lines that connect. *J Air Waste Manage* **2006,** *56*, (6), 709-742.
4.      Poschl, U., Atmospheric aerosols: Composition, transformation, climate and health effects. *Angew Chem Int Edit* **2005,** *44*, (46), 7520-7540.

5.      Yu, H.; Kaufman, Y. J.; Chin, M.; Feingold, G.; Remer, L. A.; Anderson, T. L.; Balkanski, Y.; Bellouin, N.; Boucher, O.; Christopher, S.; DeCola, P.; Kahn, R.; Koch, D.; Loeb, N.; Reddy, M. S.; Schulz, M.; Takemura, T.; Zhou, M., A review of measurement-based assessments of the aerosol direct radiative effect and forcing. *Atmos Chem Phys* **2006,** *6*, 613-666.

6.      Berkemeier, T.; Shiraiwa, M.; Poschl, U.; Koop, T., Competition between water uptake and ice nucleation by glassy organic aerosol particles. *Atmos Chem Phys* **2014,** *14*, (22), 12513-12531.

7.      Wang, B.; O'Brien, R. E.; Kelly, S. T.; Shilling, J. E.; Moffet, R. C.; Gilles, M. K.; Laskin, A., Reactivity of Liquid and Semisolid Secondary Organic Carbon with Chloride and Nitrate in Atmospheric Aerosols. *J. Phys. Chem. A* **2014**.

8.      Perraud, V.; Bruns, E. A.; Ezell, M. J.; Johnson, S. N.; Yu, Y.; Alexander, M. L.; Zelenyuk, A.; Imre, D.; Chang, W. L.; Dabdub, D.; Pankow, J. F.; Finlayson-Pitts, B. J., Nonequilibrium atmospheric secondary organic aerosol formation and growth. *P Natl Acad Sci USA* **2012,** *109*, (8), 2836-2841.

9.      Power, R. M.; Simpson, S. H.; Reid, J. P.; Hudson, A. J., The transition from liquid to solid-like behaviour in ultrahigh viscosity aerosol particles. *Chem. Sci.* **2013,** *4*, (6), 2597-2604.

10.     Shiraiwa, M.; Zuend, A.; Bertram, A. K.; Seinfeld, J. H., Gas-particle partitioning of atmospheric aerosols: interplay of physical state, non-ideal mixing and morphology. *Phys Chem Chem Phys* **2013,** *15*, (27), 11441-11453.

11.     Kuwata, M.; Martin, S. T., Phase of atmospheric secondary organic material affects its reactivity. *P Natl Acad Sci USA* **2012,** *109*, (43), 17354-17359.

12.     Virtanen, A.; Kannosto, J.; Kuuluvainen, H.; Arffman, A.; Joutsensaari, J.; Saukko, E.; Hao, L.; Yli-Pirila, P.; Tiitta, P.; Holopainen, J. K.; Keskinen, J.; Worsnop, D. R.; Smith, J. N.; Laaksonen, A., Bounce behavior of freshly nucleated biogenic secondary organic aerosol particles. *Atmos Chem Phys* **2011,** *11*, (16), 8759-8766.

13.     Pankow, J. F., An Absorption-Model of Gas-Particle Partitioning of Organic-Compounds in the Atmosphere. *Atmos Environ* **1994,** *28*, (2), 185-188.

14.     Chan, A. W. H.; Kroll, J. H.; Ng, N. L.; Seinfeld, J. H., Kinetic modeling of secondary organic aerosol formation: effects of particle- and gas-phase reactions of semivolatile products. *Atmos Chem Phys* **2007,** *7*, (15), 4135-4147.

15.     Vaden, T. D.; Imre, D.; Beranek, J.; Shrivastava, M.; Zelenyuk, A., Evaporation kinetics and phase of laboratory and ambient secondary organic aerosol. *Proc. Natl. Acad. Sci. USA* **2011,** *108*, (6), 2190-2195.

16.     Loza, C. L.; Coggon, M. M.; Nguyen, T. B.; Zuend, A.; Flagan, R. C.; Seinfeld, J. H., On the Mixing and Evaporation of Secondary Organic Aerosol Components. *Environ Sci Technol* **2013,** *47*, (12), 6173-6180.

17.     Abramson, E.; Imre, D.; Beranek, J.; Wilson, J.; Zelenyuk, A., Experimental determination of chemical diffusion within secondary organic aerosol particles. *Phys Chem Chem Phys* **2013,** *15*, (8), 2983-2991.

18.     Cappa, C. D.; Wilson, K. R., Evolution of organic aerosol mass spectra upon heating: implications for OA phase and partitioning behavior. *Atmos Chem Phys* **2011,** *11*, (5), 1895-1911.

19.     Virtanen, A.; Joutsensaari, J.; Koop, T.; Kannosto, J.; Yli-Pirila, P.; Leskinen, J.; Makela, J. M.; Holopainen, J. K.; Poschl, U.; Kulmala, M.; Worsnop, D. R.; Laaksonen, A., An amorphous solid state of biogenic secondary organic aerosol particles. *Nature* **2010,** *467*, (7317), 824-827.

20.     Koop, T.; Bookhold, J.; Shiraiwa, M.; Poschl, U., Glass transition and phase state of organic compounds: dependency on molecular properties and implications for secondary organic aerosols in the atmosphere. *Phys Chem Chem Phys* **2011,** *13*, (43), 19238-19255.

21.     Renbaum-Wolff, L.; Grayson, J. W.; Bateman, A. P.; Kuwata, M.; Sellier, M.; Murray, B. J.; Shilling, J. E.; Martin, S. T.; Bertram, A. K., Viscosity of alpha-pinene secondary organic material and implications for particle growth and reactivity. *P Natl Acad Sci USA* **2013,** *110*, (20), 8014-8019.

22.     Shiraiwa, M.; Ammann, M.; Koop, T.; Poschl, U., Gas uptake and chemical aging of semisolid organic aerosol particles. *P Natl Acad Sci USA* **2011,** *108*, (27), 11003-11008.

23.     Lignell, H.; Hinks, M. L.; Nizkorodov, S. A., Exploring matrix effects on photochemistry of organic aerosols. *P Natl Acad Sci USA* **2014,** *111*, (38), 13780-13785.

24.     Zobrist, B.; Marcolli, C.; Pedernera, D. A.; Koop, T., Do atmospheric aerosols form glasses? *Atmos Chem Phys* **2008,** *8*, (17), 5221-5244.

25.     Shilling, J. E.; Chen, Q.; King, S. M.; Rosenoern, T.; Kroll, J. H.; Worsnop, D. R.; DeCarlo, P. F.; Aiken, A. C.; Sueper, D.; Jimenez, J. L.; Martin, S. T., Loading-dependent elemental composition of alpha-pinene SOA particles. *Atmos Chem Phys* **2009,** *9*, (3), 771-782.

26.     Kolesar, K. R.; Chen, C.; Johnson, D.; Cappa, C. D., The influences of mass loading and rapid dilution of secondary organic aerosol on particle volatility. *Atmos Chem Phys* **2015,** *15*, (16), 9327-9343.

27.     Grieshop, A. P.; Donahue, N. M.; Robinson, A. L., Is the gas-particle partitioning in alpha-pinene secondary organic aerosol reversible? *Geophys Res Lett* **2007,** *34*, (14).

28.     Harvey, R. M.; Zahardis, J.; Petrucci, G. A., Establishing the contribution of lawn mowing to atmospheric aerosol levels in American suburbs. *Atmos. Chem. Phys.* **2014,** *14*, (2), 797-812.

29.     Jain, S.; Petrucci, G. A., A New Method to Measure Aerosol Particle Bounce Using a Cascade Electrical Low Pressure Impactor. *Aerosol Sci. Technol.* **2015,** *49*, (6), 390-399.

30.     Geddes, S.; Nichols, B.; Flemer, S.; Eisenhauer, J.; Zahardis, J.; Petrucci, G. A., Near-Infrared Laser Desorption/Ionization Aerosol Mass Spectrometry for Investigating Primary and Secondary Organic Aerosols under Low Loading Conditions. *Analytical chemistry* **2010,** *82*, (19), 7915-7923.

31.     Stevens, J. P.; Zahardis, J.; MacPherson, M.; Mossman, B. T.; Petrucci, G. A., A new method for quantifiable and controlled dosage of particulate matter for in vitro studies: The electrostatic particulate dosage and exposure system (EPDExS). *Toxicology in Vitro* **2008,** *22*, (7), 1768-1774.

32.     King, S. M.; Rosenoern, T.; Shilling, J. E.; Chen, Q.; Martin, S. T., Increased cloud activation potential of secondary organic aerosol for atmospheric mass loadings. *Atmos Chem Phys* **2009,** *9*, (9), 2959-2971.

33.     Gao, Y. Q.; Hall, W. A.; Johnston, M. V., Molecular Composition of Monoterpene Secondary Organic Aerosol at Low Mass Loading. *Environ Sci Technol* **2010,** *44*, (20), 7897-7902.

34.     Pfaffenberger, L.; Barmet, P.; Slowik, J. G.; Praplan, A. P.; Dommen, J.; Prevot, A. S. H.; Baltensperger, U., The link between organic aerosol mass loading and degree of oxygenation: an alpha-pinene photooxidation study. *Atmos Chem Phys* **2013,** *13*, (13), 6493-6506.

35.     Booth, A. M.; Murphy, B.; Riipinen, I.; Percival, C. J.; Topping, D. O., Connecting Bulk Viscosity Measurements to Kinetic Limitations on Attaining Equilibrium for a Model Aerosol Composition. *Environ Sci Technol* **2014,** *48*, (16), 9298-9305.

36.     Finlayson-Pitts, B. J., Reactions at surfaces in the atmosphere: integration of experiments and theory as necessary (but not necessarily sufficient) for predicting the physical chemistry of aerosols. *Phys Chem Chem Phys* **2009,** *11*, (36), 7760-7779.

37.     Shiraiwa, M.; Yee, L. D.; Schilling, K. A.; Loza, C. L.; Craven, J. S.; Zuend, A.; Ziemann, P. J.; Seinfeld, J. H., Size distribution dynamics reveal particle-phase chemistry in organic aerosol formation. *P Natl Acad Sci USA* **2013,** *110*, (29), 11746-11750.

38.     Kundu, S.; Fisseha, R.; Putman, A. L.; Rahn, T. A.; Mazzoleni, L. R., High molecular weight SOA formation during limonene ozonolysis: insights from ultrahigh-resolution FT-ICR mass spectrometry characterization. *Atmos Chem Phys* **2012,** *12*, (12), 5523-5536.

39.     Bateman, A. P.; Nizkorodov, S. A.; Laskin, J.; Laskin, A., Time-resolved molecular characterization of limonene/ozone aerosol using high-resolution electrospray ionization mass spectrometry. *Phys Chem Chem Phys* **2009,** *11*, (36), 7931-7942.

40.     Wilson, J.; Imre, D.; Beranek, J.; Shrivastava, M.; Zelenyuk, A., Evaporation Kinetics of Laboratory-Generated Secondary Organic Aerosols at Elevated Relative Humidity. *Environ Sci Technol* **2015,** *49*, (1), 243-249.

41.     Maksymiuk, C. S.; Gayahtri, C.; Gil, R. R.; Donahue, N. M., Secondary organic aerosol formation from multiphase oxidation of limonene by ozone: mechanistic constraints via two-dimensional heteronuclear NMR spectroscopy. *Phys Chem Chem Phys* **2009,** *11*, (36), 7810-7818.

42.     Kim, H.; Paulson, S. E., Real refractive indices and volatility of secondary organic aerosol generated from photooxidation and ozonolysis of limonene, alpha-pinene and toluene. *Atmos Chem Phys* **2013,** *13*, (15), 7711-7723.

43.     Vaden, T. D.; Imre, D.; Beranek, J.; Shrivastava, M.; Zelenyuk, A., Evaporation kinetics and phase of laboratory and ambient secondary organic aerosol. *P Natl Acad Sci USA* **2011,** *108*, (6), 2190-2195.

44.     Hamilton, J. F.; Lewis, A. C.; Carey, T. J.; Wenger, J. C.; Garcia, E. B. I.; Munoz, A., Reactive oxidation products promote secondary organic aerosol formation from green leaf volatiles. *Atmos Chem Phys* **2009,** *9*, (11), 3815-3823.

45.     Kleist, E.; Mentel, T. F.; Andres, S.; Bohne, A.; Folkers, A.; Kiendler-Scharr, A.; Rudich, Y.; Springer, M.; Tillmann, R.; Wildt, J., Irreversible impacts of heat on the emissions of monoterpenes, sesquiterpenes, phenolic BVOC and green leaf volatiles from several tree species. *Biogeosciences* **2012,** *9*, (12), 5111-5123.

46.     Jain, S.; Zahardis, J.; Petrucci, G. A., Soft Ionization Chemical Analysis of Secondary Organic Aerosol from Green Leaf Volatiles Emitted by Turf Grass. *Environ. Sci. Technol.* **2014**.

47.     Hamilton, J. F.; Lewis, A. C.; Carey, T. J.; Wenger, J. C., Characterization of polar compounds and oligomers in secondary organic aerosol using liquid chromatography coupled to mass spectrometry. *Analytical chemistry* **2008,** *80*, (2), 474-480.

48.     Bones, D. L.; Reid, J. P.; Lienhard, D. M.; Krieger, U. K., Comparing the mechanism of water condensation and evaporation in glassy aerosol. *P Natl Acad Sci USA* **2012,** *109*, (29), 11613-11618.

49.     Hodas, N.; Zuend, A.; Mui, W.; Flagan, R. C.; Seinfeld, J. H., Influence of particle-phase state on the hygroscopic behavior of mixed organic-inorganic aerosols. *Atmos Chem Phys* **2015,** *15*, (9), 5027-5045.

50.     Shiraiwa, M.; Seinfeld, J. H., Equilibration timescale of atmospheric secondary organic aerosol partitioning. *Geophys Res Lett* **2012,** *39*.

# CHAPTER 7: SUMMARY AND OUTLOOK

## 7.1 Summary

Atmospheric aerosol have been the focus of researchers for over 2 decades now. Many organic aerosol precursors are known, but still the chemical composition of the overall organic aerosol mass cannot yet be accounted for, suggesting a lot is missing from our knowledge and understanding. What unifies the work presented in this thesis is that each chapter, either directly or indirectly, works towards the goal of better understanding the chemical composition and phase-state of atmospheric aerosol, either by establishing a chemical mechanism or by improving instrumentation or developing new methodology. The work presented will increase the knowledge of processes and properties of atmospherically relevant secondary organic aerosol (SOA) from biogenic origin.

Building upon the previous work done in the Petrucci Group[1, 2], some of the challenges of the innovative home-built NIR-LDI-AMS were addressed in Chapter 3 of this thesis. Previously, sampling via NIR-LDI-AMS was biased towards liquid aerosol, resulting in reduced collection efficiency and sensitivity towards solid aerosols. This main limitation was overcome by making three significant modifications to the collection probe in the NIR-LDI-AMS: a) increasing the diameter of the collection probe from 1mm to 3mm, b) air gun etching the front surface of the probe to make it uneven with tiny grooves in order to improve the collection efficiency and c) utilizing different metal probes to see which metal provides an improved sensitivity and collection efficiency.

This improved NIR-LDI-AMS was utilized to identify the primary precursors of SOA from grass clippings and elucidate the operative chemical mechanisms in SOA formation and aging (Chapter 4 of this thesis). Results from this work [3] showed that HXL-

derived SOA contains a significant quantity of oligomers formed by reversible hydration and dimerization reactions, whereas CHA-derived SOA is dominated by smaller molecular weight products formed mainly via the hydroperoxide channel. It was also found that a single precursor cannot be used to quantitatively predict and determine the SOA formation for a complex chemical system; however, it may be possible to use HXL concentrations once a correction has been made for "missing SOA mass."[4] The presence of high molecular weight oligomers/dimers in HXL- SOA begged the question "what is the phase state of such a SOA." Particles containing oligomers have higher probability of forming glassy/semisolid compounds as compared to their monomeric units due to higher viscosity.[5, 6] This necessitated the need for a simple method to estimate the phase state of SOA, which was the focus of the next project and chapter of this thesis.

A 10-100-fold disparity exists between modeled and observed atmospheric SOA levels because present models assume that SOA particles remain liquid-like throughout their lifetime, which might not be the case.[7-9] Hence, I worked on designing a method to estimate the phase state of aerosol by measuring the "bounce factor (BF)." This work is described in Chapter 5 of this thesis.[10] The bounce factor method is based on comparing the current measured by an ELPI when polydisperse aerosols are sampled by smooth and sintered impaction plates. This technique is advantageous as it overcomes almost all of the limitations of the existing methods described in the literature. The newly developed method does not require multiple instruments, complex calculations or mathematical modelling to estimate the phase. This method can be utilized for both monodisperse and polydisperse aerosol and does not require different impactor nozzles for different diameter particles. The proposed method was validated by measuring the phase behavior of four test substances

that represent solid (ammonium sulfate), liquid (dioctyl sebacate), liquid (oleic acid), non-liquid (ozonized oleic acid) and SOA particles (ozonolysis of α-pinene). I also demonstrated its applicability to the measurement of the BF of SOA originating from the ozonolysis of GLV's, such as CHA and HXL. This method was limited to relatively low RH conditions and hence the obvious next step was to study the potential impact that different experimental parameters might have on the phase state of SOA.

Recent attention on the phase state of atmospheric particles has motivated several questions regarding parameters/conditions that influence the phase state and physical properties of SOA. Hence, I performed a series of laboratory chamber measurements to elucidate the influence of absolute SOA mass loading ($C_{SOA}$), ranging from 1 to 160 µg/m$^3$, on the phase state of SOA formed by ozonolysis of various precursors, including α-pinene, limonene, cis-3-hexenyl acetate (CHA) and cis-3-hexen-1-ol (HXL). To my surprise, results suggested that under nominally identical conditions, the maximum BF decreases by approximately 30% at higher $C_{SOA}$, suggesting a more liquid phase state. With the exception of HXL-SOA, the phase state for all studied SOA precursors varied as a function of $C_{SOA}$. Furthermore, the BF was found to be the maximum when SOA particle distributions reached a geometric mean particle diameter of 50-60 nm. I found that $C_{SOA}$ is an important parameter impacting the phase state of SOA, suggesting that extrapolation of experiments not conducted at atmospherically relevant SOA levels to simulate the chemical properties may not yield results that are relevant to our natural environment.

## 7.2 Outlook

The work carried out in this thesis helps in establishing chemical mechanisms and estimating phase states of secondary organic aerosols from atmospherically relevant

organic precursors. It helps to fill some of the missing gaps in our knowledge but further experimental and theoretical studies are needed to close this gap in our understanding of SOA formation and composition. This work presents many new opportunities to expand on in various directions, some of which are discussed below.

### 7.2.1 Instrumentation development

Chapter 3 of the thesis presents some of the preliminary results for the optimization of NIR-LDI-AMS. Even though I was successfully able to improve the collection efficiency of the instrument, there is still more to be done.

Presently, NIR-LDI-AMS uses a 3mm air etched Al probe and is highly sensitive towards carboxylic acids. However, its sensitivity towards other functional groups such as aldehyde, ketones, alcohols, esters, etc. is limited. Hence, the first task should be to improve this sensitivity, which could be achieved by doing systematic sensitivity studies using different metal probes for each analyte class. It is possible that the Al probe is sensitive towards carboxylic acids, whereas Mg may be better suited for alcohols or other functional groups. This would largely depend on the ionization mechanism in NIR-LDI-AMS. This brings us to the next essential task, i.e., understanding the mechanism of ion formation in NIR-LDI-AMS.

Preliminary experiments suggest that NIR-LDI-AMS utilizes a surface assisted ionization mechanism, where one photon is used to generate ions. However, similar studies conducted in the Petrucci group on analogous instrumentation indicate that the ionization process occurs through the simultaneous action of two photons. Hence, it becomes imperative to narrow down to one mechanism to further improve the sensitivity of NIR-LDI-AMS towards different functional groups and further reducing the LOD.

146

**7.2.2 Method Development**

In this work, I was successfully able to utilize ELPI and develop a method to estimate the phase state of aerosol. It has been shown[11] that the RH is reduced at each subsequent stage of the ELPI cascade. Based on previous results,[12] an RH of 25% at the inlet of the ELPI would be reduced to 2.5% downstream of the last ELPI stage, before the filter. Hence, in order to perform experiments at higher RH, it is essential to first measure the inlet and outlet RH for our instrument, which can later be used as a correction factor to get an accurate estimation of BF. In the present state, this method can only be used to accurately identify phase state for aerosol at RH of 25% or lower. Therefore, the next obvious step is to perform a systematic study with a reference aerosol (polystyrene sphere) at different RH conditions and compare the inlet RH, outlet RH and the change in BF as a function of humidity. By doing so, we can generate a calibration graph between BF and RH and obtain the accurate RH for the measured BF. While doing so, it is also important to keep a close eye on other parameters which changes at higher RH such as particle size due to particle hygroscopicity and temperature due to pressure difference. This will allow us to perform experiments at different RH conditions which have shown to impact the chemistry and phase state of atmospheric aerosols.

In Chapter 6 of this thesis, I utilized the measured particle bounce fraction (BF) as a surrogate for particle viscosity. However, using this method, we cannot make a quantitative measure of viscosity. Hence, if a method could be developed to estimate the viscosity in real time, which can then be correlated to the measured BF, we can get both quantitative and qualitative measure of the phase state of aerosols. One possible way to do so could be to collect the aerosols on AFM grids and use tapping mode AFM to measure

the force needed to deform the collected particle. This force can later be correlated with the measured BF.

### 7.2.3 Laboratory chamber experiments

Better understanding of SOA formation from BVOC can contribute to a reduction of the uncertainties in chemical transport, air quality, weather and climate models, and improve our understanding of the global problems of human-induced climate change and the impact of atmospheric particulate matter.

In Chapter 4 of this thesis, I presented a comprehensive ozonolysis mechanism for SOA generation from various GLVs. This being said, other atmospherically relevant oxidants such as hydroxyl radicals, NOx and photo oxidation were ignored. This leads to the obvious next set of chamber experiments, i.e., the incorporation of these atmospherically relevant oxidants to understand the chemical mechanism of SOA formation. Hydroxyl radicals (OH) are much more reactive than ozone and oxidation by OH has the potential to impact the chemical composition of GLV-derived SOA. I have already presented some evidence in support of this by analyzing the chemical composition of SOA in the presence and absence of an OH radical scrubber. Yet the chemistry of this radical oxidation has not yet received much attention mainly because OH is difficult to generate and quantify at atmospherically relevant concentrations in the laboratory. NOx is also another important oxidant that is prevalent during night time, which should be considered via describing the SOA formation mechanism by various GLVs.

In Chapter 6 of this thesis, I presented one of the many parameters that could have potential to impact the phase state of aerosols. Other parameters, such as the surface area to volume ratio of the environmental chamber and VOC to oxidant ratio, could also have a

significant impact on the chemical composition, which would result in impacting the phase state of the aerosol. As described in Chapter 3, changing the ratios of VOC to oxidant could result in either a VOC rich or an oxidant rich environment which have shown to impact the chemical composition of SOA. It seems obvious that such a change in chemical composition would also impact the phase state and the reactivity of generated SOA. Hence, a study involving various mixing ratios such as 1:1, 2:1, 4:1, 8:1 (VOC: Oxidant) and vice versa should be performed. Simultaneous NIR-LDI-AMS and ELPI measurements should be taken to obtain molecular level chemical composition and phase state of the generated SOA. There is some evidence[13] showing that chemical composition, particle size and reactivity changes for limonene derived SOA as a function of chamber volume and surface area ratio. Therefore, it seems obvious, again, that such a change would also impact the phase state. Hence a study involving variation of UVMEC surface area to volume ratio is required to obtain a better understanding of chemical and physical changes in the generated SOA. This could potentially be done by change the surface area of UVMEC by spreading rolls of Teflon sheet inside the chamber and keeping the volume of UVMEC constant.

Another parameter, which has never been investigated, is the effect of different functional groups and structures on the phase state of aerosol. Decades of careful investigations of the oxidation products have produced a large body of information on various functional groups and structures out there in the environment. Different functional groups would have different reactivity with different structured compounds and hence would have varying effect on the physical properties of the products. Therefore, understanding the effects of functional groups and structures on the phase state should be

an important research topic for atmospheric chemistry in addition to being of fundamental

scientific interest.

## 7.3 References

1.      Geddes, S.; Nichols, B.; Todd, K.; Zahardis, J.; Petrucci, G. A., Near-infrared laser desorption/ionization aerosol mass spectrometry for measuring organic aerosol at atmospherically relevant aerosol mass loadings. *Atmos Measur Tech* **2010,** *3*, (4), 1175-1183.
2.      Geddes, S.; Nichols, B.; Flemer, S.; Eisenhauer, J.; Zahardis, J.; Petrucci, G. A., Near-Infrared Laser Desorption/Ionization Aerosol Mass Spectrometry for Investigating Primary and Secondary Organic Aerosols under Low Loading Conditions. *Analytical chemistry* **2010,** *82*, (19), 7915-7923.
3.      Jain, S.; Zahardis, J.; Petrucci, G. A., Soft Ionization Chemical Analysis of Secondary Organic Aerosol from Green Leaf Volatiles Emitted by Turf Grass. *Environ. Sci. Technol.* **2014**.
4.      Harvey, R. M.; Zahardis, J.; Petrucci, G. A., Establishing the contribution of lawn mowing to atmospheric aerosol levels in American suburbs. *Atmos. Chem. Phys.* **2014,** *14*, (2), 797-812.
5.      Koop, T.; Bookhold, J.; Shiraiwa, M.; Poschl, U., Glass transition and phase state of organic compounds: dependency on molecular properties and implications for secondary organic aerosols in the atmosphere. *Phys Chem Chem Phys* **2011,** *13*, (43), 19238-19255.
6.      Zobrist, B.; Marcolli, C.; Pedernera, D. A.; Koop, T., Do atmospheric aerosols form glasses? *Atmos Chem Phys* **2008,** *8*, (17), 5221-5244.
7.      Vaden, T. D.; Imre, D.; Beranek, J.; Shrivastava, M.; Zelenyuk, A., Evaporation kinetics and phase of laboratory and ambient secondary organic aerosol. *Proc. Natl. Acad. Sci. USA* **2011,** *108*, (6), 2190-2195.
8.      Pankow, J. F., An Absorption-Model of Gas-Particle Partitioning of Organic-Compounds in the Atmosphere. *Atmos Environ* **1994,** *28*, (2), 185-188.
9.      Chan, A. W. H.; Kroll, J. H.; Ng, N. L.; Seinfeld, J. H., Kinetic modeling of secondary organic aerosol formation: effects of particle- and gas-phase reactions of semivolatile products. *Atmos Chem Phys* **2007,** *7*, (15), 4135-4147.
10.     Jain, S.; Petrucci, G. A., A New Method to Measure Aerosol Particle Bounce Using a Cascade Electrical Low Pressure Impactor. *Aerosol Sci. Technol.* **2015,** *49*, (6), 390-399.
11.     Saukko, E.; Lambe, A. T.; Massoli, P.; Koop, T.; Wright, J. P.; Croasdale, D. R.; Pedernera, D. A.; Onasch, T. B.; Laaksonen, A.; Davidovits, P.; Worsnop, D. R.; Virtanen, A., Humidity-dependent phase state of SOA particles from biogenic and anthropogenic precursors. *Atmos Chem Phys* **2012,** *12*, (16), 7517-7529.
12.     Marjamaki, M.; Keskinen, J.; Chen, D. R.; Pui, D. Y. H., Performance evaluation of the electrical low-pressure impactor (ELPI). *J Aerosol Sci* **2000,** *31*, (2), 249-261.
13.     Waring, M. S.; Siegel, J. A., Indoor Secondary Organic Aerosol Formation Initiated from Reactions between Ozone and Surface-Sorbed D-Limonene. *Environ Sci Technol* **2013,** *47*, (12), 6341-6348.

# CHAPTER 8: COMPREHENSIVE BIBLIOGRAPHY

Abramson, E., Imre, D., Beranek, J., Wilson, J., & Zelenyuk, A. (2013). Experimental determination of chemical diffusion within secondary organic aerosol particles. *Physical Chemistry Chemical Physics, 15*(8), 2983-2991. doi: Doi 10.1039/C2cp44013j

Agency, U. S. E. P. (2012, November 2012). Exposure Assessment Tools and Models. 4.11. Retrieved January 10th 2013, 2013, from http://www.epa.gov/oppt/exposure/pubs/episuite.htm

Alimpiev, S., Nikiforov, S., Karavanskii, V., Minton, T., & Sunner, J. (2001). On the mechanism of laser-induced desorption-ionization of organic compounds from etched silicon and carbon surfaces. *Journal of Chemical Physics, 115*(4), 1891-1901. doi: Doi 10.1063/1.1381531

Andreae, M. O., & Crutzen, P. J. (1997). Atmospheric aerosols: Biogeochemical sources and role in atmospheric chemistry. *Science, 276*(5315), 1052-1058. doi: DOI 10.1126/science.276.5315.1052

Anenberg, S. C., West, J. J., Horowitz, L. W., & Tong, D. Q. (2010). The Global Burden of Air Pollution on Mortality response. *Environmental Health Perspectives, 118*(10), A424-A425. doi: 10.1289/ehp.1002397R

Aschmann, S. M., Shu, Y. H., Arey, J., & Atkinson, R. (1997). Products of the gas-phase reactions of cis-3-hexen-1-ol with OH radicals and O-3. *ATMOS ENVIRON, 31*(21), 3551-3560. doi: Doi 10.1016/S1352-2310(97)00205-7

Atkinson, R., Arey, J., Aschmann, S. M., Corchnoy, S. B., & Shu, Y. H. (1995). Rate Constants for the Gas-Phase Reactions of Cis-3-Hexen-1-Ol, Cis-3-Hexenylacetate, Trans-2-Hexenal, and Linalool with Oh and No3 Radicals and O-3 at 296+/-2 K, and Oh Radical Formation Yields from the O-3 Reactions. *International Journal of Chemical Kinetics, 27*(10), 941-955. doi: DOI 10.1002/kin.550271002

Atkinson, R., Aschmann, S. M., Arey, J., & Shorees, B. (1992). Formation of Oh Radicals in the Gas-Phase Reactions of O3 with a Series of Terpenes. *Journal of Geophysical Research-Atmospheres, 97*(D5), 6065-6073.

Baker, J., Aschmann, S. M., Arey, J., & Atkinson, R. (2001). Reactions of stabilized Criegee intermediates from the gas-phase reactions of O-3 with selected alkenes. *International Journal of Chemical Kinetics, 34*(2), 73-85.

Baltensperger, U., Kalberer, M., Dommen, J., Paulsen, D., Alfarra, M. R., Coe, H., . . . Zenobi, R. (2005). Secondary organic aerosols from anthropogenic and biogenic precursors. *Faraday Discussions, 130*, 265-278. doi: Doi 10.1039/B417367h

Bateman, A. P., Belassein, H., & Martin, S. T. (2014). Impactor Apparatus for the Study of Particle Rebound: Relative Humidity and Capillary Forces. *Aerosol Sci. Technol., 48*(1), 42-52. doi: 10.1080/02786826.2013.853866

Bateman, A. P., Bertram, A. K., & Martin, S. T. (2014). Hygroscopic Influence on the Semisolid-to-Liquid Transition of Secondary Organic Materials. *J. Phys. Chem. A*. doi: 10.1021/jp508521c

Bateman, A. P., Nizkorodov, S. A., Laskin, J., & Laskin, A. (2009). Time-resolved molecular characterization of limonene/ozone aerosol using high-resolution electrospray ionization mass spectrometry. *Physical Chemistry Chemical Physics, 11*(36), 7931-7942. doi: 10.1039/b905288g

Beauchamp, J., Wisthaler, A., Hansel, A., Kleist, E., Miebach, M., Niinemets, U., . . . Wildt, J. (2005). Ozone induced emissions of biogenic VOC from tobacco: relationships between ozone uptake and emission of LOX products. *Plant Cell and Environment, 28*(10), 1334-1343. doi: DOI 10.1111/j.1365-3040.2005.01383.x

Bergström, L. (1997). Hamaker constants of inorganic materials. *Advances in Colloid and Interface Science, 70*(0), 125-169. doi: http://dx.doi.org/10.1016/S0001-8686(97)00003-1

Berkemeier, T., Shiraiwa, M., Poschl, U., & Koop, T. (2014). Competition between water uptake and ice nucleation by glassy organic aerosol particles. *Atmos Chem Phys, 14*(22), 12513-12531. doi: 10.5194/acp-14-12513-2014

Blanksby, S. J., & Ellison, G. B. (2003). Bond dissociation energies of organic molecules. *Acc. Chem. Res., 36*, 255-263.

Bones, D. L., Reid, J. P., Lienhard, D. M., & Krieger, U. K. (2012). Comparing the mechanism of water condensation and evaporation in glassy aerosol. *Proceedings of the National Academy of Sciences of the United States of America, 109*(29), 11613-11618. doi: 10.1073/pnas.1200691109

Booth, A. M., Murphy, B., Riipinen, I., Percival, C. J., & Topping, D. O. (2014). Connecting Bulk Viscosity Measurements to Kinetic Limitations on Attaining Equilibrium for a Model Aerosol Composition. *Environmental Science & Technology, 48*(16), 9298-9305. doi: Doi 10.1021/Es501705c

Brands, M., Kamphus, M., Bottger, T., Schneider, J., Drewnick, F., Roth, A., . . . Borrmann, S. (2011). Characterization of a Newly Developed Aircraft-Based

Laser Ablation Aerosol Mass Spectrometer (ALABAMA) and First Field Deployment in Urban Pollution Plumes over Paris During MEGAPOLI 2009. *Aerosol Science and Technology, 45*(1), 46-64. doi: 10.1080/02786826.2010.517813

Brilli, F., Hortnagl, L., Bamberger, I., Schnitzhofer, R., Ruuskanen, T. M., Hansel, A., . . . Wohlfahrt, G. (2012). Qualitative and Quantitative Characterization of Volatile Organic Compound Emissions from Cut Grass. *Environmental Science & Technology, 46*(7), 3859-3865. doi: Doi 10.1021/Es204025y

Brook, R. D., & Rajagopalan, S. (2010). Particulate Matter Air Pollution and Atherosclerosis. *Current Atherosclerosis Reports, 12*(5), 291-300. doi: 10.1007/s11883-010-0122-7

Brown, S. S., & Stutz, J. (2012). Nighttime radical observations and chemistry. *Chemical Society Reviews, 41*(19), 6405-6447. doi: 10.1039/C2CS35181A

Cahill, T. M., Seaman, V. Y., Charles, M. J., Holzinger, R., & Goldstein, A. H. (2006). Secondary organic aerosols formed from oxidation of biogenic volatile organic compounds in the Sierra Nevada Mountains of California. *Journal of Geophysical Research-Atmospheres, 111*(D16). Doi 10.1029/2006jd007178

Canagaratna, M. R., Jayne, J. T., Jimenez, J. L., Allan, J. D., Alfarra, M. R., Zhang, Q., . . . Worsnop, D. R. (2007). Chemical and microphysical characterization of ambient aerosols with the aerodyne aerosol mass spectrometer. *Mass Spectrometry Reviews, 26*(2), 185-222. doi: 10.1002/mas.20115

Cappa, C. D., & Wilson, K. R. (2011). Evolution of organic aerosol mass spectra upon heating: implications for OA phase and partitioning behavior. *Atmos Chem Phys, 11*(5), 1895-1911. doi: 10.5194/acp-11-1895-2011

Carlton, A. G., Wiedinmyer, C., & Kroll, J. H. (2009). A review of Secondary Organic Aerosol (SOA) formation from isoprene. *Atmos Chem Phys, 9*(14), 4987-5005.

Chan, A. W. H., Kroll, J. H., Ng, N. L., & Seinfeld, J. H. (2007). Kinetic modeling of secondary organic aerosol formation: effects of particle- and gas-phase reactions of semivolatile products. *Atmos Chem Phys, 7*(15), 4135-4147.

Chen, X., & Hopke, P. K. (2010). A chamber study of secondary organic aerosol formation by limonene ozonolysis. *Indoor Air, 20*(4), 320-328. doi: DOI 10.1111/j.1600-0668.2010.00656.x

Claeys, M., Graham, B., Vas, G., Wang, W., Vermeylen, R., Pashynska, V., . . . Maenhaut, W. (2004). Formation of secondary organic aerosols through photooxidation of isoprene. *Science, 303*(5661), 1173-1176. doi: DOI 10.1126/science.1092805

Cocker, D. R., Mader, B. T., Kalberer, M., Flagan, R. C., & Seinfeld, J. H. (2001). The effect of water on gas-particle partitioning of secondary organic aerosol: II. m-xylene and 1,3,5-trimethylbenzene photooxidation systems. *Atmospheric Environment, 35*(35), 6073-6085. doi: Doi 10.1016/S1352-2310(01)00405-8

Croft, K. P. C., Juttner, F., & Slusarenko, A. J. (1993). Volatile Products of the Lipoxygenase Pathway Evolved from Phaseolus-Vulgaris (L) Leaves Inoculated with Pseudomonas-Syringae Pv-Phaseolicola. *Plant Physiology, 101*(1), 13-24.

Dahneke, B. (1971). The capture of aerosol particles by surfaces. *Journal of Colloid and Interface Science, 37*(2), 342-353. doi: http://dx.doi.org/10.1016/0021-9797(71)90302-X

Dahneke, B. (1995). Particle Bounce or Capture - Search for an Adequate Theory .1. Conservation-of-Energy Model for a Simple Collision Process. *Aerosol Science and Technology, 23*(1), 25-39. doi: Doi 10.1080/02786829508965292

Danzer, K. (2007). *Analytical Chemistry: Theoretical and Metrological Fundamentals*: Springer.

De Gouw, J., & Jimenez, J. L. (2009). Organic Aerosols in the Earth's Atmosphere. *Environmental Science & Technology, 43*(20), 7614-7618. doi: 10.1021/es9006004

DeCarlo, P. F., Slowik, J. G., Worsnop, D. R., Davidovits, P., & Jimenez, J. L. (2005). Particle morphology and density characterization by combined mobility and aerodynamic diameter measurements. Part 1: Theory (vol 38, pg 1185, 2004). *Aerosol Science and Technology, 39*(2), 184-184. doi: Doi 10.1080/02786820590928897

DePalma, J. W., Horan, A. J., Hall, W. A., & Johnston, M. V. (2013). Thermodynamics of oligomer formation: implications for secondary organic aerosol formation and reactivity. *Physical Chemistry Chemical Physics, 15*(18), 6935-6944. doi: Doi 10.1039/C3cp44586k

Department of engineering, D. C. (2015). Etching Metal Films

Docherty, K. S., Wu, W., Lim, Y. B., & Ziemann, P. J. (2005). Contributions of organic peroxides to secondary aerosol formed from reactions of monoterpenes with O-3. *Environmental Science & Technology, 39*(11), 4049-4059. doi: Doi 10.1021/Es050228s

Donahue, N. M., Robinson, A. L., Pandis, S. N., Kroll, J. H., & Worsnop, D. L. (2009). Rethinking organic aerosols: Semivolatile emissions and photochemical aging. *Geochimica Et Cosmochimica Acta, 73*(13), A299-A299.

Donahue, N. M., Robinson, A. L., Stanier, C. O., & Pandis, S. N. (2006). Coupled partitioning, dilution, and chemical aging of semivolatile organics. *Environmental Science & Technology, 40*(8), 2635-2643. doi: Doi 10.1021/Es052297c

Dreyfus, M. A., Adou, K., Zucker, S. M., & Johnston, M. V. (2009). Organic aerosol source apportionment from highly time-resolved molecular composition measurements. *Atmospheric Environment, 43*(18), 2901-2910. doi: 10.1016/j.atmosenv.2009.03.008

Engineering, D. o. e. a. C. (2015). Wet Chemical Etching of metals and semiconductors. 2016, from http://www.cleanroom.byu.edu/wet_etch.phtml

Farina, S. C., Adams, P. J., & Pandis, S. N. (2010). Modeling global secondary organic aerosol formation and processing with the volatility basis set: Implications for anthropogenic secondary organic aerosol. *Journal of Geophysical Research-Atmospheres, 115*. Doi 10.1029/2009jd013046

Finessi, E., Decesari, S., Paglione, M., Giulianelli, L., Carbone, C., Gilardoni, S., . . . Facchini, M. C. (2012). Determination of the biogenic secondary organic aerosol fraction in the boreal forest by NMR spectroscopy. *Atmos Chem Phys, 12*(2), 941-959. doi: DOI 10.5194/acp-12-941-2012

Finlayson-Pitts, B. J. (2009). Reactions at surfaces in the atmosphere: integration of experiments and theory as necessary (but not necessarily sufficient) for predicting the physical chemistry of aerosols. *Physical Chemistry Chemical Physics, 11*(36), 7760-7779. doi: Doi 10.1039/B906540g

Finlayson-Pitts, B. J., & Pitts Jr, J. N. (2000a). CHAPTER 5 - Kinetics and Atmospheric Chemistry *Chemistry of the Upper and Lower Atmosphere* (pp. 130-178). San Diego: Academic Press.

Finlayson-Pitts, B. J., & Pitts Jr, J. N. (2000b). Preface *Chemistry of the Upper and Lower Atmosphere* (pp. xvii-xviii). San Diego: Academic Press.

Fraser, M. P., Yue, Z. W., Tropp, R. J., Kohl, S. D., & Chow, J. C. (2002). Molecular composition of organic fine particulate matter in Houston, TX. *ATMOS ENVIRON, 36*(38), 5751-5758. Doi 10.1016/S1352-2310(02)00725-2

Gao, Y. Q., Hall, W. A., & Johnston, M. V. (2010). Molecular Composition of Monoterpene Secondary Organic Aerosol at Low Mass Loading. *Environmental Science & Technology, 44*(20), 7897-7902. doi: Doi 10.1021/Es101861k

Gaschen, A., Lang, D., Kalberer, M., Savi, M., Geiser, T., Gazdhar, A., . . . Geiser, M. (2010). Cellular Responses after Exposure of Lung Cell Cultures to Secondary Organic Aerosol Particles. *Environmental Science & Technology, 44*(4), 1424-1430. doi: 10.1021/es902261m

Geddes, S., Nichols, B., Flemer, S., Eisenhauer, J., Zahardis, J., & Petrucci, G. A. (2010). Near-Infrared Laser Desorption/Ionization Aerosol Mass Spectrometry for Investigating Primary and Secondary Organic Aerosols under Low Loading Conditions. *Anal Chem, 82*(19), 7915-7923. doi: Doi 10.1021/Ac1013354

Geddes, S., Nichols, B., Todd, K., Zahardis, J., & Petrucci, G. A. (2010). Near-infrared laser desorption/ionization aerosol mass spectrometry for measuring organic aerosol at atmospherically relevant aerosol mass loadings. *Atmos Measur Tech, 3*(4), 1175-1183. doi: 10.5194/amt-3-1175-2010

Geddes, S., Zahardis, J., & Petrucci, G. A. (2010). Chemical transformations of peptide containing fine particles: oxidative processing, accretion reactions and implications to the atmospheric fate of cell-derived materials in organic aerosol. *J Atmos Chem, 63*(3), 187-202. doi: 10.1007/s10874-010-9161-2

Ginzburg, A. S., Gubanova, D. P., & Minashkin, V. M. (2009). Influence of natural and anthropogenic aerosols on global and regional climate. *Russian Journal of General Chemistry, 79*(9), 2062-2070. doi: 10.1134/S1070363209090382

Goldstein, A., & Galbally, I. (2007). Known and unexplored organic constituents in the earth's atmosphere. *Environmental Science & Technology, 41*(5), 1514–1521. doi: 10.1021/es072476p

Gould, N. D., Allen, C. L., Nam, B. C., Schepartz, A., & Miller, S. J. (2013). Combined Lewis acid and Bronsted acid-mediated reactivity of glycosyl trichloroacetimidate donors. *Carbohydrate Research, 382*, 36-42. doi: DOI 10.1016/j.carres.2013.09.011

Grieshop, A. P., Donahue, N. M., & Robinson, A. L. (2007). Is the gas-particle partitioning in alpha-pinene secondary organic aerosol reversible? *Geophysical Research Letters, 34*(14). doi: Artn L1481010.1029/2007gl029987

Grosjean, E., DeAndrade, J. B., & Grosjean, D. (1996). Carbonyl products of the gas-phase reaction of ozone with simple alkenes. *Environmental Science & Technology, 30*(3), 975-983. doi: Doi 10.1021/Es950442o

Grosjean, E., & Grosjean, D. (1997). The gas phase reaction of unsaturated oxygenates with ozone: Carbonyl products and comparison with the alkene-ozone reaction. *J Atmos Chem, 27*(3), 271-289. doi: Doi 10.1023/A:1005868119515

Grosjean, E., & Grosjean, D. (1998). The gas-phase reaction of alkenes with ozone: formation yields of carbonyls from biradicals in ozone–alkene–cyclohexane experiments. *ATMOS ENVIRON, 32*(20), 3393-3402. doi: http://dx.doi.org/10.1016/S1352-2310(98)80005-8

Guenther, A., Hewitt, C. N., Erickson, D., Fall, R., Geron, C., Graedel, T., . . . Zimmerman, P. (1995). A Global-Model of Natural Volatile Organic-Compound Emissions. *Journal of Geophysical Research-Atmospheres, 100*(D5), 8873-8892. doi: Doi 10.1029/94jd02950

Hall, W. A., & Johnston, M. V. (2012). Oligomer Formation Pathways in Secondary Organic Aerosol from MS and MS/MS Measurements with High Mass Accuracy and Resolving Power. *J Am Soc Mass Spectrom, 23*(6), 1097-1108. doi: DOI 10.1007/s13361-012-0362-6

Hallquist, M., Wenger, J. C., Baltensperger, U., Rudich, Y., Simpson, D., Claeys, M., . . . Wildt, J. (2009). The formation, properties and impact of secondary organic aerosol: current and emerging issues. *Atmos Chem Phys, 9*(14), 5155-5236.

Hamilton, J. F., Lewis, A. C., Carey, T. J., & Wenger, J. C. (2008). Characterization of polar compounds and oligomers in secondary organic aerosol using liquid chromatography coupled to mass spectrometry. *Anal Chem, 80*(2), 474-480. doi: Doi 10.1021/Ac701852t

Hamilton, J. F., Lewis, A. C., Carey, T. J., Wenger, J. C., Garcia, E. B. I., & Munoz, A. (2009). Reactive oxidation products promote secondary organic aerosol formation from green leaf volatiles. *Atmos Chem Phys, 9*(11), 3815-3823. doi: DOI 10.5194/acp-9-3815-2009

Hartonen, K., Laitinen, T., & Riekkola, M. L. (2011). Current instrumentation for aerosol mass spectrometry. *Trac-Trends in Analytical Chemistry, 30*(9), 1486-1496. doi: 10.1016/j.trac.2011.06.007

Harvey, R. M., Bateman, A. P., Jain, S., Li, Y. J., Martin, S., & Petrucci, G. A. (2016). Optical Properties of Secondary Organic Aerosol from cis-3-Hexenol and cis-3-Hexenyl Acetate: Effect of Chemical Composition, Humidity, and Phase. *Environmental Science & Technology*. doi: 10.1021/acs.est.6b00625

Harvey, R. M., Zahardis, J., & Petrucci, G. A. (2014). Establishing the contribution of lawn mowing to atmospheric aerosol levels in American suburbs. *Atmos. Chem. Phys., 14*(2), 797-812. doi: 10.5194/acp-14-797-2014

Hastings, W. P., Koehler, C. A., Bailey, E. L., & De Haan, D. O. (2005). Secondary organic aerosol formation by glyoxal hydration and oligomer formation: Humidity effects and equilibrium shifts during analysis. *Environmental Science & Technology, 39*(22), 8728-8735. doi: Doi 10.1021/Es0504461

Heald, C. L., Kroll, J. H., Jimenez, J. L., Docherty, K. S., DeCarlo, P. F., Aiken, A. C., . . . Artaxo, P. (2010). A simplified description of the evolution of organic aerosol composition in the atmosphere. *Geophysical Research Letters, 37*. Doi 10.1029/2010gl042737

Healy, R. M., Temime, B., Kuprovskyte, K., & Wenger, J. C. (2009). Effect of Relative Humidity on Gas/Particle Partitioning and Aerosol Mass Yield in the Photooxidation of p-Xylene. *Environmental Science & Technology, 43*(6), 1884-1889. doi: 10.1021/es802404z

Hearn, J. D., & Smith, G. D. (2004). A chemical ionization mass spectrometry method for the online analysis of organic aerosols. *Anal Chem, 76*(10), 2820-2826. doi: Doi 10.1021/Ac049948s

Heaton, K. J., Dreyfus, M. A., Wang, S., & Johnston, M. V. (2007). Oligomers in the early stage of biogenic secondary organic aerosol formation and growth. *Environmental Science & Technology, 41*(17), 6129-6136. doi: Doi 10.1021/Es070314n

Henze, D. K., & Seinfeld, J. H. (2006). Global secondary organic aerosol from isoprene oxidation. *Geophysical Research Letters, 33*(9). Doi 10.1029/2006gl025976

Hinds, W. C. (1982). *Aerosol Technology: Properties, Behavior, and Measurement of Airborne Particles*: John Wiley & Sons.

Hinds, W. C. (1999). *Aerosol Technology: Properties, Behavior, and Measurements or Airborne Particles* (2 ed.). New york: John Wiley & Sons, Inc.

Hodas, N., Zuend, A., Mui, W., Flagan, R. C., & Seinfeld, J. H. (2015). Influence of particle-phase state on the hygroscopic behavior of mixed organic-inorganic aerosols. *Atmos Chem Phys, 15*(9), 5027-5045. doi: 10.5194/acp-15-5027-2015

Hoffmann, T., Odum, J. R., Bowman, F., Collins, D., Klockow, D., Flagan, R. C., & Seinfeld, J. H. (1997). Formation of organic aerosols from the oxidation of biogenic hydrocarbons. *J Atmos Chem, 26*(2), 189-222. doi: Doi 10.1023/A:1005734301837

Holzinger, R., Williams, J., Herrmann, F., Lelieveld, J., Donahue, N. M., & Rockmann, T. (2010a). Aerosol analysis using a Thermal-Desorption Proton-Transfer-Reaction Mass Spectrometer (TD-PTR-MS): a new approach to study processing of organic aerosols. *Atmos Chem Phys, 10*(5), 2257-2267.

Holzinger, R., Williams, J., Herrmann, F., Lelieveld, J., Donahue, N. M., & Rockmann, T. (2010b). Aerosol analysis using a Thermal-Desorption Proton-Transfer-Reaction Mass Spectrometer (TD-PTR-MS): a new approach to study processing of organic aerosols. *Atmospheric Chemistry and Physics, 10*(5), 2257-2267. doi: 10.5194/acp-10-2257-2010

Horie, O., & Moortgat, G. K. (1998). Gas phase ozonolysis of alkenes. Recent advances in mechanistic investigations. *Accounts of Chemical Research, 31*(7), 387-396. doi: Doi 10.1021/Ar9702740

Hosny, N. A., Fitzgerald, C., Tong, C. L., Kalberer, M., Kuimova, M. K., & Pope, F. D. (2013). Fluorescent lifetime imaging of atmospheric aerosols: a direct probe of aerosol viscosity. *Faraday Discussions, 165*, 343-356. doi: Doi 10.1039/C3fd00041a

Hsu, N. F., Tseng, S. Y., Wu, C. Y., Ren, C. T., Lee, Y. C., Wong, C. H., & Chen, C. H. (2008). Desorption ionization of biomolecules on metals. *Anal Chem, 80*(13), 5203-5210. doi: 10.1021/ac800435r

Incorporated, T. (2004). Series 3800 Aerosol Time-of-Flight Mass Spectrometers with Aerodynamic Focusing Lens Technology. *Particle Instruments*.

Jain, S., & Petrucci, G. A. (2015). A New Method to Measure Aerosol Particle Bounce Using a Cascade Electrical Low Pressure Impactor. *Aerosol Sci. Technol., 49*(6), 390-399. doi: 10.1080/02786826.2015.1036393

Jain, S., Zahardis, J., & Petrucci, G. A. (2014). Soft Ionization Chemical Analysis of Secondary Organic Aerosol from Green Leaf Volatiles Emitted by Turf Grass. *Environ. Sci. Technol.* doi: 10.1021/es405355d

Jimenez, J. L., Canagaratna, M. R., Donahue, N. M., Prevot, A. S. H., Zhang, Q., Kroll, J. H., . . . Worsnop, D. R. (2009). Evolution of Organic Aerosols in the Atmosphere. *Science, 326*(5959), 1525-1529. doi: DOI 10.1126/science.1180353

John, W., Reischl, G., & Devor, W. (1980). Charge-Transfer to Metal-Surfaces from Bouncing Aerosol-Particles. *Journal of Aerosol Science, 11*(2), 115-138. doi: Doi 10.1016/0021-8502(80)90029-4

Johnson, D., & Marston, G. (2008). The gas-phase ozonolysis of unsaturated volatile organic compounds in the troposphere. *Chemical Society Reviews, 37*(4), 699-716. doi: Doi 10.1039/B704260b

Joutsensaari, J., Loivamaki, M., Vuorinen, T., Miettinen, P., Nerg, A. M., Holopainen, J. K., & Laaksonen, A. (2005). Nanoparticle formation by ozonolysis of inducible plant volatiles. *Atmos Chem Phys, 5*, 1489-1495.

Kalberer, M., Paulsen, D., Sax, M., Steinbacher, M., Dommen, J., Prevot, A. S. H., . . . Baltensperger, U. (2004). Identification of polymers as major components of atmospheric organic aerosols. *Science, 303*(5664), 1659-1662. doi: DOI 10.1126/science.1092185

Kamens, R., Jang, M., Chien, C. J., & Leach, K. (1999). Aerosol formation from the reaction of alpha-pinene and ozone using a gas-phase kinetics aerosol partitioning model. *Environmental Science & Technology, 33*(9), 1430-1438. doi: Doi 10.1021/Es980725r

Kanakidou, M., Seinfeld, J. H., Pandis, S. N., Barnes, I., Dentener, F. J., Facchini, M. C., . . . Wilson, J. (2005a). Organic aerosol and global climate modelling: a review. *Atmospheric Chemistry and Physics, 5*, 1053-1123.

Kanakidou, M., Seinfeld, J. H., Pandis, S. N., Barnes, I., Dentener, F. J., Facchini, M. C., . . . Wilson, J. (2005b). Organic aerosol and global climate modelling: a review. *Atmos Chem Phys, 5*, 1053-1123.

Kannosto, J., Yli-Pirila, P., Hao, L. Q., Leskinen, J., Jokiniemi, J., Makela, J. M., . . . Virtanen, A. (2013). Bounce characteristics of alpha-pinene-derived SOA particles with implications to physical phase. *Boreal Environment Research, 18*(3-4), 329-340.

Karl, T., Fall, R., Jordan, A., & Lindinger, W. (2001). On-line analysis of reactive VOCs from urban lawn mowing. *Environmental Science & Technology, 35*(14), 2926-2931. doi: Doi 10.1021/Es010637y

Keskinen, J., Marjamaki, M., Virtanen, A., Makela, T., & Hillamo, R. (1999). Electrical calibration method for cascade impactors. *Journal of Aerosol Science, 30*(1), 111-116. doi: Doi 10.1016/S0021-8502(98)00026-3

Kidd, C., Perraud, V., Wingen, L. M., & Finlayson-Pitts, B. J. (2014). Integrating phase and composition of secondary organic aerosol from the ozonolysis of α-pinene. *P Natl Acad Sci*. doi: 10.1073/pnas.1322558111

Kiendler-Scharr, A., Zhang, Q., Hohaus, T., Kleist, E., Mensah, A., Mentel, T. F., . . . Wildt, J. (2009). Aerosol Mass Spectrometric Features of Biogenic SOA: Observations from a Plant Chamber and in Rural Atmospheric Environments. *Environmental Science & Technology, 43*(21), 8166-8172. doi: Doi 10.1021/Es901420b

Kim, H., & Paulson, S. E. (2013). Real refractive indices and volatility of secondary organic aerosol generated from photooxidation and ozonolysis of limonene, alpha-pinene and toluene. *Atmos Chem Phys, 13*(15), 7711-7723. doi: 10.5194/acp-13-7711-2013

King, S. M., Rosenoern, T., Shilling, J. E., Chen, Q., & Martin, S. T. (2009). Increased cloud activation potential of secondary organic aerosol for atmospheric mass loadings. *Atmos Chem Phys, 9*(9), 2959-2971.

Kleist, E., Mentel, T. F., Andres, S., Bohne, A., Folkers, A., Kiendler-Scharr, A., . . . Wildt, J. (2012). Irreversible impacts of heat on the emissions of monoterpenes, sesquiterpenes, phenolic BVOC and green leaf volatiles from several tree species. *Biogeosciences, 9*(12), 5111-5123. doi: DOI 10.5194/bg-9-5111-2012

Kolesar, K. R., Chen, C., Johnson, D., & Cappa, C. D. (2015). The influences of mass loading and rapid dilution of secondary organic aerosol on particle volatility. *Atmos Chem Phys, 15*(16), 9327-9343. doi: 10.5194/acp-15-9327-2015

Konig, G., Brunda, M., Puxbaum, H., Hewitt, C. N., Duckham, S. C., & Rudolph, J. (1995). Relative Contribution of Oxygenated Hydrocarbons to the Total Biogenic Voc Emissions of Selected Mid-European Agricultural and Natural Plant-Species. *ATMOS ENVIRON, 29*(8), 861-874. doi: Doi 10.1016/1352-2310(95)00026-U

Koop, T., Bookhold, J., Shiraiwa, M., & Poschl, U. (2011). Glass transition and phase state of organic compounds: dependency on molecular properties and implications for secondary organic aerosols in the atmosphere. *Physical Chemistry Chemical Physics, 13*(43), 19238-19255. doi: Doi 10.1039/C1cp22617g

Krejci, R., Strom, J., de Reus, M., Williams, J., Fischer, H., Andreae, M. O., & Hansson, H. C. (2005). Spatial and temporal distribution of atmospheric aerosols in the lowermost troposphere over the Amazonian tropical rainforest. *Atmospheric Chemistry and Physics, 5*, 1527-1543.

Kroll, J. H., Chan, A. W. H., Ng, N. L., Flagan, R. C., & Seinfeld, J. H. (2007). Reactions of semivolatile organics and their effects on secondary organic aerosol formation. *Environmental Science & Technology, 41*(10), 3545-3550. doi: Doi 10.1021/Es062059x

Kroll, J. H., Ng, N. L., Murphy, S. M., Flagan, R. C., & Seinfeld, J. H. (2006). Secondary organic aerosol formation from isoprene photooxidation. *Environmental Science & Technology, 40*(6), 1869-1877. doi: Doi 10.1021/Es0524301

Kroll, J. H., & Seinfeld, J. H. (2008). Chemistry of secondary organic aerosol: Formation and evolution of low-volatility organics in the atmosphere. *ATMOS ENVIRON, 42*(16), 3593-3624. doi: 10.1016/j.atmosenv.2008.01.003

Kuhn, U., Rottenberger, S., Biesenthal, T., Wolf, A., Schebeske, G., Ciccioli, P., . . . Kesselmeier, J. (2002). Isoprene and monoterpene emissions of Amazonian tree species during the wet season: Direct and indirect investigations on controlling environmental functions. *Journal of Geophysical Research-Atmospheres, 107*(D20). Doi 10.1029/2001jd000978

Kundu, S., Fisseha, R., Putman, A. L., Rahn, T. A., & Mazzoleni, L. R. (2012). High molecular weight SOA formation during limonene ozonolysis: insights from ultrahigh-resolution FT-ICR mass spectrometry characterization. *Atmos Chem Phys, 12*(12), 5523-5536. doi: 10.5194/acp-12-5523-2012

Kuuluvainen, H., Arffman, A., Saukko, E., Virtanen, A., & Keskinen, J. (2013). A new method for characterizing the bounce and charge transfer properties of

nanoparticles. *Journal of Aerosol Science, 55*, 104-115. doi: DOI 10.1016/j.jaerosci.2012.08.007

Kuwata, M., & Martin, S. T. (2012). Phase of atmospheric secondary organic material affects its reactivity. *Proceedings of the National Academy of Sciences of the United States of America, 109*(43), 17354-17359. doi: DOI 10.1073/pnas.1209071109

Laskin, A., Laskin, J., & Nizkorodov, S. A. (2012a). Mass spectrometric approaches for chemical characterisation of atmospheric aerosols: critical review of the most recent advances. *Environmental Chemistry, 9*(3), 163-189. doi: 10.1071/EN12052

Laskin, A., Laskin, J., & Nizkorodov, S. A. (2012b). Mass spectrometric approaches for chemical characterisation of atmospheric aerosols: critical review of the most recent advances. *Environmental Chemistry, 9*(3), 163-189. doi: Doi 10.1071/En12052

Lee, A., Goldstein, A. H., Kroll, J. H., Ng, N. L., Varutbangkul, V., Flagan, R. C., & Seinfeld, J. H. (2006). Gas-phase products and secondary aerosol yields from the photooxidation of 16 different terpenes. *Journal of Geophysical Research-Atmospheres, 111*(D17). Doi 10.1029/2006jd007050

Lee, S. H., & Allen, H. C. (2012). Analytical Measurements of Atmospheric Urban Aerosol. *Anal Chem, 84*(3), 1196-1201. doi: Doi 10.1021/Ac201338x

Lesins, G., Chylek, P., & Lohmann, U. (2002). A study of internal and external mixing scenarios and its effect on aerosol optical properties and direct radiative forcing. *Journal of Geophysical Research-Atmospheres, 107*(D10). doi: Artn 409410.1029/2001jd000973

Li, J., Sun, Y., Cao, H., Han, D., & He, M. (2013). Mechanisms and kinetics of the ozonolysis reaction of cis-3-hexenyl acetate and trans-2-hexenyl acetate in atmosphere: a theoretical study. *Structural Chemistry*, 1-13. doi: 10.1007/s11224-013-0226-0

Liggio, J., & Li, S. M. (2013). A new source of oxygenated organic aerosol and oligomers. *Atmos Chem Phys, 13*(6), 2989-3002. doi: DOI 10.5194/acp-13-2989-2013

Lignell, H., Hinks, M. L., & Nizkorodov, S. A. (2014). Exploring matrix effects on photochemistry of organic aerosols. *Proceedings of the National Academy of Sciences of the United States of America, 111*(38), 13780-13785. doi: 10.1073/pnas.1322106111

Liu, P., Ziemann, P. J., Kittelson, D. B., & McMurry, P. H. (1995a). Generating particle beam of controlled dimensions and convergence: I. Theory of particle motion in aerodynamic lenses and nozzle expansions. *Aerosol Sci. Technol., 22*, 293-313.

Liu, P., Ziemann, P. J., Kittelson, D. B., & Mcmurry, P. H. (1995b). Generating Particle Beams of Controlled Dimensions and Divergence .1. Theory of Particle Motion in Aerodynamic Lenses and Nozzle Expansions. *Aerosol Science and Technology, 22*(3), 293-313. doi: Doi 10.1080/02786829408959748

Liu, P., Ziemann, P. J., Kittelson, D. B., & Mcmurry, P. H. (195c). Generating Particle Beams of Controlled Dimensions and Divergence .2. Experimental Evaluation of Particle Motion in Aerodynamic Lenses and Nozzle Expansions. *Aerosol Science and Technology, 22*(3), 314-324. doi: Doi 10.1080/02786829408959749

Loza, C. L., Coggon, M. M., Nguyen, T. B., Zuend, A., Flagan, R. C., & Seinfeld, J. H. (2013). On the Mixing and Evaporation of Secondary Organic Aerosol Components. *Environmental Science & Technology, 47*(12), 6173-6180. doi: 10.1021/es400979k

Ma, Y., Luciani, T., Porter, R. A., Russell, A. T., Johnson, D., & Marston, G. (2007). Organic acid formation in the gas-phase ozonolysis of alpha-pinene. *Physical Chemistry Chemical Physics, 9*(37), 5084-5087. doi: Doi 10.1039/B709880d

Maksymiuk, C. S., Gayahtri, C., Gil, R. R., & Donahue, N. M. (2009). Secondary organic aerosol formation from multiphase oxidation of limonene by ozone: mechanistic constraints via two-dimensional heteronuclear NMR spectroscopy. *Physical Chemistry Chemical Physics, 11*(36), 7810-7818. doi: 10.1039/b820005j

Marjamaki, M., Keskinen, J., Chen, D. R., & Pui, D. Y. H. (2000). Performance evaluation of the electrical low-pressure impactor (ELPI). *Journal of Aerosol Science, 31*(2), 249-261. doi: Doi 10.1016/S0021-8502(99)00052-X

Martin, S. T. (2000). Phase transitions of aqueous atmospheric particles. *Chemical Reviews, 100*(9), 3403-3453. doi: Doi 10.1021/Cr990034t

McDonald, J. D., Doyle-Eisele, M., Campen, M. J., Seagrave, J., Holmes, T., Lund, A., . . . Knipping, E. M. (2010). Cardiopulmonary response to inhalation of biogenic secondary organic aerosol. *Inhalation Toxicology, 22*(3), 253-265. doi: 10.3109/08958370903148114

Mentel, T. F., Kleist, E., Andres, S., Dal Maso, M., Hohaus, T., Kiendler-Scharr, A., . . . Wildt, J. (2013). Secondary aerosol formation from stress-induced biogenic emissions and possible climate feedbacks. *Atmos Chem Phys, 13*(17), 8755-8770. doi: DOI 10.5194/acp-13-8755-2013

Murphy, D. M. (2007). The design of single particle laser mass spectrometers. *Mass Spectrometry Reviews, 26*(2), 150-165. doi: 10.1002/mas.20113

Myhre, G., Samset, B. H., Schulz, M., Balkanski, Y., Bauer, S., Berntsen, T. K., . . . Zhou, C. (2013). Radiative forcing of the direct aerosol effect from AeroCom Phase II simulations. *Atmospheric Chemistry and Physics, 13*(4), 1853-1877. doi: 10.5194/acp-13-1853-2013

Nash, D. G., Baer, T., & Johnston, M. V. (2006). Aerosol mass spectrometry: An introductory review. *International Journal of Mass Spectrometry, 258*(1-3), 2-12. doi: 10.1016/j.ijms.2006.09.017

Nayak, R., & Knapp, D. R. (2007). Effects of thin-film structural parameters on laser desorption/ionization from porous alumina. *Anal Chem, 79*(13), 4950-4956. doi: 10.1021/ac062289u

Noble, C. A., & Prather, K. A. (2000). Real-time single particle mass spectrometry: A historical review of a quarter century of the chemical analysis of aerosols. *Mass Spectrometry Reviews, 19*(4), 248-274. doi: Doi 10.1002/1098-2787(200007)19:4<248::Aid-Mas3>3.3.Co;2-9

O'Dwyer, M. A., Carey, T. J., Healy, R. M., Wenger, J. C., Picquet-Varrault, B., & Doussin, J. F. (2010). The Gas-phase Ozonolysis of 1-Penten-3-ol, (Z)-2-Penten-1-ol and 1-Penten-3-one: Kinetics, Products and Secondary Organic Aerosol Formation. *Zeitschrift Fur Physikalische Chemie-International Journal of Research in Physical Chemistry & Chemical Physics, 224*(7-8), 1059-1080. doi: DOI 10.1524/zpch.2010.6141

Oberdorster, G., Oberdorster, E., & Oberdorster, J. (2005). Nanotoxicology: An emerging discipline evolving from studies of ultrafine particles. *Environmental Health Perspectives, 113*(7), 823-839. doi: 10.1289/ehp.7339

Oktem, B., Tolocka, M. P., & Johnston, M. V. (2004). On-line analysis of organic components in fine and ultrafine particles by photoionization aerosol mass spectrometry. *Anal Chem, 76*(2), 253-261. doi: 10.1021/ac0350559

Olofsson, M., Ek-Olausson, B., Ljungstrom, E., & Langer, S. (2003). Flux of organic compounds from grass measured by relaxed eddy accumulation technique. *Journal of Environmental Monitoring, 5*(6), 963-970. doi: Doi 10.1039/B303329e

Pankow, J. F. (1994). An Absorption-Model of Gas-Particle Partitioning of Organic-Compounds in the Atmosphere. *ATMOS ENVIRON, 28*(2), 185-188. doi: Doi 10.1016/1352-2310(94)90093-0

Perraud, V., Bruns, E. A., Ezell, M. J., Johnson, S. N., Yu, Y., Alexander, M. L., . . . Finlayson-Pitts, B. J. (2012). Nonequilibrium atmospheric secondary organic

aerosol formation and growth. *Proceedings of the National Academy of Sciences of the United States of America, 109*(8), 2836-2841. doi: DOI 10.1073/pnas.1119909109

Petrucci, G. A., & Winefordner, J. D. (1991). Use of the Optogalvanic Effect to Examine the Laser Power Dependency of Several Excitation Ionization Mechanisms in a Hollow-Cathode Discharge. *Applied Spectroscopy, 45*(9), 1485-1490. doi: Doi 10.1366/0003702914335454

Pfaffenberger, L., Barmet, P., Slowik, J. G., Praplan, A. P., Dommen, J., Prevot, A. S. H., & Baltensperger, U. (2013). The link between organic aerosol mass loading and degree of oxygenation: an alpha-pinene photooxidation study. *Atmos Chem Phys, 13*(13), 6493-6506. doi: 10.5194/acp-13-6493-2013

Pope, C. A., & Dockery, D. W. (2006). Health effects of fine particulate air pollution: Lines that connect. *Journal of the Air & Waste Management Association, 56*(6), 709-742.

Poschl, U. (2005a). Atmospheric aerosols: Composition, transformation, climate and health effects. *Angewandte Chemie-International Edition, 44*(46), 7520-7540. doi: 10.1002/anie.200501122

Poschl, U. (2005b). Atmospheric aerosols: Composition, transformation, climate and health effects. *Angewandte Chemie-International Edition, 44*(46), 7520-7540. doi: DOI 10.1002/anie.200501122

Power, R. M., Simpson, S. H., Reid, J. P., & Hudson, A. J. (2013). The transition from liquid to solid-like behaviour in ultrahigh viscosity aerosol particles. *Chem. Sci., 4*(6), 2597-2604. doi: 10.1039/C3SC50682G

Prather, K. A., Hatch, C. D., & Grassian, V. H. (2008a). Analysis of Atmospheric Aerosols. *Annual Review of Analytical Chemistry, 1*, 485-514. doi: DOI 10.1146/annurev.anchem.1.031207.113030

Prather, K. A., Hatch, C. D., & Grassian, V. H. (2008b). Analysis of Atmospheric Aerosols. *Annual Review of Analytical Chemistry, 1*, 485-514. doi: DOI 10.1146/annurev.anchem.1.031207.113030

Pratt, K. A., & Prather, K. A. (2012a). Mass spectrometry of atmospheric aerosolsuRecent developments and applications. Part I: Off-line mass spectrometry techniques. *Mass Spectrometry Reviews, 31*(1), 1-16. doi: Doi 10.1002/Mas.20322

Pratt, K. A., & Prather, K. A. (2012b). Mass spectrometry of atmospheric aerosolsuRecent developments and applications. Part II: On-line mass

spectrometry techniques. *Mass Spectrometry Reviews, 31*(1), 17-48. doi: Doi 10.1002/Mas.20330

Putaud, J.-P., Raes, F., Van Dingenen, R., Brüggemann, E., Facchini, M. C., Decesari, S., . . . Wiedensohler, A. (2004). A European aerosol phenomenology—2: chemical characteristics of particulate matter at kerbside, urban, rural and background sites in Europe. *ATMOS ENVIRON, 38*(16), 2579-2595. doi: http://dx.doi.org/10.1016/j.atmosenv.2004.01.041

Pye, H. O. T., & Seinfeld, J. H. (2010). A global perspective on aerosol from low-volatility organic compounds. *Atmos Chem Phys, 10*(9), 4377-4401. doi: DOI 10.5194/acp-10-4377-2010

Raes, F., Van Dingenen, R., Vignati, E., Wilson, J., Putaud, J. P., Seinfeld, J. H., & Adams, P. (2000). Formation and cycling of aerosols in the global troposphere. *Atmospheric Environment, 34*(25), 4215-4240. doi: Doi 10.1016/S1352-2310(00)00239-9

Renbaum-Wolff, L., Grayson, J. W., Bateman, A. P., Kuwata, M., Sellier, M., Murray, B. J., . . . Bertram, A. K. (2013). Viscosity of alpha-pinene secondary organic material and implications for particle growth and reactivity. *Proceedings of the National Academy of Sciences of the United States of America, 110*(20), 8014-8019. doi: DOI 10.1073/pnas.1219548110

Robinson, A. L., Donahue, N. M., Shrivastava, M. K., Weitkamp, E. A., Sage, A. M., Grieshop, A. P., . . . Pandis, S. N. (2007). Rethinking organic aerosols: Semivolatile emissions and photochemical aging. *Science, 315*(5816), 1259-1262. doi: DOI 10.1126/science.1133061

Robinson, A. L., Subramanian, R., Donahue, N. M., Bernardo-Bricker, A., & Rogge, W. F. (2006). Source apportionment of molecular markers and organic aerosol. 3. Food cooking emissions. *Environmental Science & Technology, 40*(24), 7820-7827. doi: Doi 10.1021/Es060781p

Rogers, L. N., & Reed, J. (1984). The Adhesion of Particles Undergoing an Elastic Plastic Impact with a Surface. *Journal of Physics D-Applied Physics, 17*(4), 677-689. doi: Doi 10.1088/0022-3727/17/4/007

Rohr, A. C. (2013). The health significance of gas- and particle-phase terpene oxidation products: A review. *Environment International, 60*, 145-162. doi: 10.1016/j.envint.2013.08.002

Romakkaniemi, S., Hameri, K., Vakeva, M., & Laaksonen, A. (2001). Adsorption of water on 8-15 nm NaCl and (NH4)(2)SO4 aerosols measured using an ultrafine tandem differential mobility analyzer. *Journal of Physical Chemistry A, 105*(35), 8183-8188. doi: Doi 10.1021/Jp010647l

Ruckerl, R., Schneider, A., Breitner, S., Cyrys, J., & Peters, A. (2011). Health effects of particulate air pollution: A review of epidemiological evidence. *Inhalation Toxicology, 23*(10), 555-592. doi: 10.3109/08958378.2011.593587

Saukko, E., Kuuluvainen, H., & Virtanen, A. (2012). A method to resolve the phase state of aerosol particles. *Atmos Meas Tech, 5*(1), 259-265. doi: DOI 10.5194/amt-5-259-2012

Saukko, E., Lambe, A. T., Massoli, P., Koop, T., Wright, J. P., Croasdale, D. R., . . . Virtanen, A. (2012). Humidity-dependent phase state of SOA particles from biogenic and anthropogenic precursors. *Atmos Chem Phys, 12*(16), 7517-7529. doi: DOI 10.5194/acp-12-7517-2012

Schneider, J., Weimer, S., Drewnick, F., Borrmann, S., Helas, G., Gwaze, P., . . . Kirchner, U. (2006). Mass spectrometric analysis and aerodynamic properties of various types of combustion-related aerosol particles. *International Journal of Mass Spectrometry and Ion Processes, 258*(1-3), 37-49. doi: DOI 10.1016/j.ijms.2006.07.008

Scott, C. E., Rap, A., Spracklen, D. V., Forster, P. M., Carslaw, K. S., Mann, G. W., . . . Tunved, P. (2014). The direct and indirect radiative effects of biogenic secondary organic aerosol. *Atmos Chem Phys, 14*(1), 447-470. doi: DOI 10.5194/acp-14-447-2014

Scott, C. E., Rap, A., Spracklen, D. V., Forster, P. M., Carslaw, K. S., Mann, G. W., . . . Tunved, P. (2013). The direct and indirect radiative effects of biogenic secondary organic aerosol. *Atmos. Chem. Phys. Discuss., 13*(6), 16961-17019. doi: 10.5194/acpd-13-16961-2013

Seinfeld, J. H., & Pandis, S. N. (1998). *Atmospheric chemistry and physics: from air pollution to climate change*: Wiley.

Seinfeld, J. H., & Pandis, S. N. (2006). *Atmospheric Chemistry and Physics: From Air Pollution to Climate Change*: Wiley.

Seinfeld, J. H., & Pankow, J. F. (2003). Organic atmospheric particulate material. *Annu Rev Phys Chem, 54*, 121-140. doi: 10.1146/annurev.physchem.54.011002.103756

Shen, Z. X., Thomas, J. J., Averbuj, C., Broo, K. M., Engelhard, M., Crowell, J. E., . . . Siuzdak, G. (2001). Porous silicon as a versatile platform for laser desorption/ionization mass spectrometry. *Anal Chem, 73*(3), 612-619. doi: 10.1021/ac000746f

Shilling, J. E., Chen, Q., King, S. M., Rosenoern, T., Kroll, J. H., Worsnop, D. R., . . . Martin, S. T. (2009). Loading-dependent elemental composition of alpha-pinene SOA particles. *Atmos Chem Phys, 9*(3), 771-782.

Shiraiwa, M., Ammann, M., Koop, T., & Poschl, U. (2011). Gas uptake and chemical aging of semisolid organic aerosol particles. *Proceedings of the National Academy of Sciences of the United States of America, 108*(27), 11003-11008. doi: DOI 10.1073/pnas.1103045108

Shiraiwa, M., & Seinfeld, J. H. (2012). Equilibration timescale of atmospheric secondary organic aerosol partitioning. *Geophysical Research Letters, 39*. Doi 10.1029/2012gl054008

Shiraiwa, M., Yee, L. D., Schilling, K. A., Loza, C. L., Craven, J. S., Zuend, A., . . . Seinfeld, J. H. (2013). Size distribution dynamics reveal particle-phase chemistry in organic aerosol formation. *Proceedings of the National Academy of Sciences of the United States of America, 110*(29), 11746-11750. doi: DOI 10.1073/pnas.1307501110

Shiraiwa, M., Zuend, A., Bertram, A. K., & Seinfeld, J. H. (2013). Gas-particle partitioning of atmospheric aerosols: interplay of physical state, non-ideal mixing and morphology. *Physical Chemistry Chemical Physics, 15*(27), 11441-11453. doi: Doi 10.1039/C3cp51595h

Sindelarova, K., Granier, C., Bouarar, I., Guenther, A., Tilmes, S., Stavrakou, T., . . . Knorr, W. (2014). Global data set of biogenic VOC emissions calculated by the MEGAN model over the last 30 years. *Atmospheric Chemistry and Physics, 14*(17), 9317-9341. doi: 10.5194/acp-14-9317-2014

Smith, J. N., Moore, K. F., McMurry, P. H., & Eisele, F. L. (2004). Atmospheric measurements of sub-20 nm diameter particle chemical composition by thermal desorption chemical ionization mass spectrometry. *Aerosol Science and Technology, 38*(2), 100-110. doi: 10.1080/02786820490249036

Smith, M. L., Kuwata, M., & Martin, S. T. (2011). Secondary Organic Material produced by the dark ozonolysis of alpha-pinene minimally affects the deliquescence and efflorescence of ammonium sulfate. *Aerosol Science and Technology, 45*(2), 244-261. doi: Doi 10.1080/02786826.2010.532178

Stevens, J. P., Zahardis, J., MacPherson, M., Mossman, B. T., & Petrucci, G. A. (2008). A new method for quantifiable and controlled dosage of particulate matter for in vitro studies: The electrostatic particulate dosage and exposure system (EPDExS). *Toxicology in Vitro, 22*(7), 1768-1774. doi: 10.1016/j.tiv.2008.05.013

Sullivan, R. C., & Prather, K. A. (2005). Recent advances in our understanding of atmospheric chemistry and climate made possible by on-line aerosol analysis instrumentation. *Anal Chem, 77*(12), 3861-3885. doi: Doi 10.1021/Ac050716i

Svenningsson, B., Rissler, J., Swietlicki, E., Mircea, M., Bilde, M., Facchini, M. C., . . . Rosenorn, T. (2006). Hygroscopic growth and critical supersaturations for mixed

aerosol particles of inorganic and organic compounds of atmospheric relevance. *Atmos Chem Phys, 6*, 1937-1952.

Thomas, J. J., Shen, Z. X., Crowell, J. E., Finn, M. G., & Siuzdak, G. (2001). Desorption/ionization on silicon (DIOS): A diverse mass spectrometry platform for protein characterization. *Proceedings of the National Academy of Sciences of the United States of America, 98*(9), 4932-4937. doi: DOI 10.1073/pnas.081069298

Tobias, H. J., & Ziemann, P. J. (2000). Thermal Desorption Mass Spectrometric Analysis of Organic Aerosol Formed from Reactions of 1-Tetradecene and O3 in the Presence of Alcohols and Carboxylic Acids. *Environ SciTechnol, 34*(11), 2105-2115. doi: 10.1021/es9907156

Vaden, T. D., Imre, D., Beranek, J., Shrivastava, M., & Zelenyuk, A. (2011a). Evaporation kinetics and phase of laboratory and ambient secondary organic aerosol. *Proceedings of the National Academy of Sciences of the United States of America, 108*(6), 2190-2195. doi: 10.1073/pnas.1013391108

Vaden, T. D., Imre, D., Beranek, J., Shrivastava, M., & Zelenyuk, A. (2011b). Evaporation kinetics and phase of laboratory and ambient secondary organic aerosol. *Proc. Natl. Acad. Sci. USA, 108*(6), 2190-2195. doi: DOI 10.1073/pnas.1013391108

Vereecken, L., & Francisco, J. S. (2012). Theoretical studies of atmospheric reaction mechanisms in the troposphere. *Chemical Society Reviews, 41*(19), 6259-6293. doi: Doi 10.1039/C2cs35070j

Vingarzan, R. (2004). A review of surface ozone background levels and trends. *Atmospheric Environment, 38*(21), 3431-3442. doi: 10.1016/j.atmosenv.2004.03.030

Virtanen, A., Joutsensaari, J., Koop, T., Kannosto, J., Yli-Pirila, P., Leskinen, J., . . . Laaksonen, A. (2010). An amorphous solid state of biogenic secondary organic aerosol particles. *Nature, 467*(7317), 824-827. doi: Doi 10.1038/Nature09455

Virtanen, A., Kannosto, J., Joutsensaari, J., Saukko, E., Kuuluvainen, H., Hao, L., . . . Laaksonen, A. (2011). Bounce behavior of freshly nucleated biogenic secondary organic aerosol particles. *Atmospheric Chemistry and Physics Discussions, 11*(3), 9313-9334. doi: 10.5194/acpd-11-9313-2011

Virtanen, A., Kannosto, J., Kuuluvainen, H., Arffman, A., Joutsensaari, J., Saukko, E., . . . Laaksonen, A. (2011). Bounce behavior of freshly nucleated biogenic secondary organic aerosol particles. *Atmos Chem Phys, 11*(16), 8759-8766. doi: DOI 10.5194/acp-11-8759-2011

Volkamer, R., Jimenez, J. L., San Martini, F., Dzepina, K., Zhang, Q., Salcedo, D., . . . Molina, M. J. (2006). Secondary organic aerosol formation from anthropogenic air pollution: Rapid and higher than expected. *Geophysical Research Letters, 33*(17).Doi 10.1029/2006gl026899

Wall, S., John, W., Wang, H.-C., & Goren, S. L. (1990). Measurements of Kinetic Energy Loss for Particles Impacting Surfaces. *Aerosol Science and Technology, 12*(4), 926-946. doi: 10.1080/02786829008959404

Wang, B., O'Brien, R. E., Kelly, S. T., Shilling, J. E., Moffet, R. C., Gilles, M. K., & Laskin, A. (2014). Reactivity of Liquid and Semisolid Secondary Organic Carbon with Chloride and Nitrate in Atmospheric Aerosols. *J. Phys. Chem. A*. doi: 10.1021/jp510336q

Wang, H.-C., & John, W. (1987). Comparative Bounce Properties of Particle Materials. *Aerosol Science and Technology, 7*(3), 285-299. doi: 10.1080/02786828708959165

Waring, M. S., & Siegel, J. A. (2013). Indoor Secondary Organic Aerosol Formation Initiated from Reactions between Ozone and Surface-Sorbed D-Limonene. *Environmental Science & Technology, 47*(12), 6341-6348. doi: Doi 10.1021/Es400846d

Warscheid, B., & Hoffmann, T. (2001). On-line measurements of a-pinene ozonolysis products using an atmospheric pressure chemical ionisation ion-trap mass spectrometer. *ATMOS ENVIRON, 35*(16), 2927-2940. doi: Doi 10.1016/S1352-2310(00)00513-6

Wexler, A. S., & Clegg, S. L. (2002). Atmospheric aerosol models for systems including the ions H+, NH4+, Na+, SO42-, NO3-,Cl-, Br-, and H2O. *Journal of Geophysical Research-Atmospheres, 107*(D14). doi: Artn 4207 10.1029/2001jd000451

Wilson, J., Imre, D., Beranek, J., Shrivastava, M., & Zelenyuk, A. (2015). Evaporation Kinetics of Laboratory-Generated Secondary Organic Aerosols at Elevated Relative Humidity. *Environmental Science & Technology, 49*(1), 243-249. doi: 10.1021/es505331d

Yu, H., Kaufman, Y. J., Chin, M., Feingold, G., Remer, L. A., Anderson, T. L., . . . Zhou, M. (2006). A review of measurement-based assessments of the aerosol direct radiative effect and forcing. *Atmos Chem Phys, 6*, 613-666.

Yu, J. Z. (2012). Editorial: mass spectrometric approaches for chemical characterisation of atmospheric aerosols. *Environmental Chemistry, 9*(3), I-Ii. doi: 10.1071/Env9n3_Ed

Zahardis, J., Geddes, S., & Petrucci, G. A. (2011). Improved understanding of atmospheric organic aerosols via innovations in soft ionization aerosol mass spectrometry. *Anal Chem, 83*(7), 2409-2415. doi: 10.1021/ac102737k

Zahardis, J., LaFranchi, B. W., & Petrucci, G. A. (2006). Direct observation of polymerization in the oleic acid-ozone heterogeneous reaction system by photoelectron resonance capture ionization aerosol mass spectrometry. *ATMOS ENVIRON, 40*(9), 1661-1670. doi: DOI 10.1016/j.atmosenv.2005.10.065

Zahardis, J., LaFranchi, B. W., & Petrucci, G. A. (2006). Direct observation of polymerization in the oleic acid–ozone heterogeneous reaction system by photoelectron resonance capture ionization aerosol mass spectrometry. *ATMOS ENVIRON, 40*(9), 1661-1670. doi: 10.1016/j.atmosenv.2005.10.065

Zhang, J. Y., Hartz, K. E. H., Pandis, S. N., & Donahue, N. M. (2006). Secondary organic aerosol formation from limonene ozonolysis: Homogeneous and heterogeneous influences as a function of NOx. *Journal of Physical Chemistry A, 110*(38), 11053-11063. doi: Doi 10.1021/Jp062836f

Zheng, M., Cass, G. R., Schauer, J. J., & Edgerton, E. S. (2002). Source apportionment of PM2.5 in the southeastern United States using solvent-extractable organic compounds as tracers. *Environmental Science & Technology, 36*(11), 2361-2371. doi: Doi 10.1021/Es011275x

Zhou, Y., Zhang, H. F., Parikh, H. M., Chen, E. H., Rattanavaraha, W., Rosen, E. P., . . . Kamens, R. M. (2011). Secondary organic aerosol formation from xylenes and mixtures of toluene and xylenes in an atmospheric urban hydrocarbon mixture: Water and particle seed effects (II). *Atmospheric Environment, 45*(23), 3882-3890. doi: 10.1016/j.atmosenv.2010.12.048

Ziemann, P. J., & Atkinson, R. (2012). Kinetics, products, and mechanisms of secondary organic aerosol formation. *Chemical Society Reviews, 41*(19), 6582-6605. doi: Doi 10.1039/C2cs35122f

Zobrist, B., Marcolli, C., Pedernera, D. A., & Koop, T. (2008). Do atmospheric aerosols form glasses? *Atmos Chem Phys, 8*(17), 5221-5244.

# APPENDIX I

Abstract of first published article "Soft Ionization Chemical Analysis of Secondary Organic Aerosol from Green Leaf Volatiles Emitted by Turf Grass"

Globally, biogenic volatile organic compound (BVOC) emissions contribute 90% of the overall VOC emissions. Green leaf volatiles (GLVs) are an important component of plant-derived BVOCs, including cis-3-hexenylacetate (CHA) and cis-3-hexen-1-ol (HXL), which are emitted by cut grass. In this study we describe secondary organic aerosol (SOA) formation from the ozonolysis of dominant GLVs, their mixtures and grass clippings. Near-infrared laser desorption/ionization aerosol mass spectrometry (NIR-LDI-AMS) was used for chemical analysis of the aerosol. The chemical profile of SOA generated from grass clippings was correlated with that from chemical standards of CHA and HXL. We found that SOA derived from HXL most closely approximated SOA from turf grass, in spite of the approximately 5x lower emission rate of HXL as compared to CHA. Ozonolysis of HXL results in formation of low volatility, higher molecular weight compounds, such as oligomers, and formation of ester-type linkages. This is in contrast to CHA, where the hydroperoxide channel is the dominant oxidation pathway, as oligomer formation is inhibited by the acetate functionality.

# APPENDIX II

Abstract of Second published article "A New Method to Measure Aerosol Particle Bounce Using a Cascade Electrical Low Pressure Impactor"

The phase state of secondary organic aerosol (SOA) in the atmosphere is of scientific interest as it can impact SOA growth and reactivity. For this purpose, a simplified method is described herein to estimate SOA bounce factor to gain an improved understanding of the phase state of atmospheric aerosols. This new method involves the use of a multi-stage electrical low pressure cascade impactor operating with either smooth or sintered impaction plates. Measurement of the raw current on smooth and sintered plates allows one to calculate the bounce factor, eliminating the need for a scanning mobility particle sizer to independently measure the SOA aerodynamic size distribution. The proposed method provides the temporal resolution necessary to measure phase changes in a continuously evolving SOA parcel.

We validate our method by measuring the bounce factor of solid and liquid aerosols, namely ammonium sulfate (AS), dioctyl sebacate (DOS), oleic acid (OA) and ozonized OA, and also present bounce factor evolution of aging α-pinene-derived aerosols. The results suggest that the new method can be used to understand the phase state of amorphous and crystalline substances, as well as distinguish between liquid and non-liquid particles.

# APPENDIX III

Abstract of Third published article "Optical Properties of Secondary Organic Aerosol from Cis-3-Hexenol and Cis-3-Hexenyl Acetate: Effect of Chemical Composition, Humidity and Phase"

Atmospheric aerosols play an important role in Earth's radiative balance directly, by scattering and absorbing radiation, and indirectly by acting as cloud condensation nuclei (CCN). Atmospheric aerosol is dominated by secondary organic aerosol (SOA) formed by the oxidation of biogenic volatile organic compounds (BVOCs). Green leaf volatiles (GLVs) are a class of BVOCs that contribute to SOA, yet their role in the Earth's radiative budget is poorly understood. In this work we measured the scattering efficiency (at 450 nm, 525 nm and 635 nm), absorption efficiency (between 190-900 nm), particle phase, bulk chemical properties (O:C, H:C) and molecular-level composition of SOA formed from the ozonolysis of two GLVs; cis-3-hexenol (HXL) and cis-3-hexenyl acetate (CHA). Both HXL and CHA produced SOA that was weakly absorbing, yet CHA-SOA was a more efficient absorber than HXL-SOA. The scatter efficiency of SOA from both systems was wavelength-dependent, with the stronger dependence exhibited by HXL-SOA, likely due to differences in particle size. HXL-SOA formed under both dry (10% RH) and wet (70% RH) conditions had the same bulk chemical properties (O:C), yet significantly different optical properties, which was attributed to differences in molecular-level composition. We have found that SOA derived from green leaf volatiles has the potential to affect the Earth's radiative budget, and also that bulk chemical properties can be insufficient to predict SOA optical properties.

# APPENDIX IIIV

Abstract of submitted article "The influence of absolute mass loading of secondary organic aerosols on their phase state"

Understanding the phase state of secondary organic aerosol (SOA) in the atmosphere is important as it can impact SOA growth and reactivity. Due to various uncertainties in defining and measuring SOA components, atmospheric models underestimate measured SOA mass concentrations by a factor of up to 10 or more. This underestimation is due, in part, to a still incomplete understanding of SOA formation mechanisms and sources, as well as the absence of consideration of the phase state of atmospheric aerosols.

In this study, we performed systematic laboratory chamber measurements to elucidate the influence of absolute SOA mass loading (CSOA), ranging from 1 to 160 µg/m3, on the phase state of SOA formed by ozonolysis of various precursors, including α-pinene, limonene, cis-3-hexenyl acetate (CHA) and cis-3-hexen-1-ol (HXL). A previously established method to estimate SOA bounce factor (BF, a surrogate for particle viscosity) was utilized to infer particle viscosity as a function of CSOA. Results show that under nominally identical conditions, the maximum BF decreases by approximately 30% at higher CSOA, suggesting a more liquid phase state. With the exception of HXL-SOA, the phase state for all studied SOA precursors varied as a function of CSOA. Furthermore, the BF was found to be the maximum when SOA particle distributions reached a geometric mean particle diameter of 50-60 nm. We have found that CSOA is an important parameter

impacting the phase state of SOA, suggesting that extrapolation of experiments not conducted at atmospherically relevant SOA levels to simulate the chemical properties may not yield results that are relevant to our natural environment.